Doctoral thesis

Doctoral theses at NTNU, 2021:342

Line Aanerud Omtvedt

Combining Functionality of Polysaccharides for Drug Delivery Applications

A Study of CyD-Grafted Alginates

NTNU
Norwegian University of Science and Technology
Thesis for the Degree of
Philosophiae Doctor
Faculty of Natural Sciences
Department of Biotechnology and Food Science

NTNU
Norwegian University of
Science and Technology

Line Aanerud Omtvedt

Combining Functionality of Polysaccharides for Drug Delivery Applications

A Study of CyD-Grafted Alginates

Thesis for the Degree of Philosophiae Doctor

Trondheim, November 2021

Norwegian University of Science and Technology
Faculty of Natural Sciences
Department of Biotechnology and Food Science

NTNU
Norwegian University of
Science and Technology

NTNU
Norwegian University of Science and Technology

Thesis for the Degree of Philosophiae Doctor

Faculty of Natural Sciences
Department of Biotechnology and Food Science

ISBN 978-82-326-5704-9 (printed ver.)
ISBN 978-82-326-5681-3 (electronic ver.)
ISSN 1503-8181 (printed ver.)
ISSN 2703-8084 (online ver.)

Doctoral theses at NTNU, 2021:342

Printed by NTNU Grafisk senter

Acknowledgements

First, I would like to express my gratitude to both my supervisors, Berit L. Strand and Finn L. Aachmann. Your support, enthusiasm, and friendly discussions have been highly valued, as well as your vast knowledge and insights. My professional development has hugely benefited from your thoughtful guidance and helpful advice. I also want to thank you Berit for our many Teams-meetings and your continuous encouragement and guidance after I left Trondheim, which gave me stamina and courage to finish my thesis.

I would furthermore like to thank all the co-authors in the papers included in this thesis for their excellent contributions and good discussions.

Daria S. Zaytseva-Zotova, both your insight and knowledge about drug delivery, as well as your kindness have been much appreciated these past years.

I would also like to thank Thorbjørn T. Nielsen, Kim L. Larsen, and Reinhard Wimmer. You ensured I felt welcome when I first came to Aalborg, and your advice and assistance have been very much appreciated.

Marianne Ø. Dalheim I want to thank for first teaching me about chemical modification of alginate and for our further good discussions.

I also want to thank Ingrid V. Mo and Amalie Solberg for excellent insight and discussions about modification of oligosaccharides, as well as their friendship.

Kåre A. Kristiansen I would like to thank for help with the MS analysis, your expertise was highly appreciated.

Wenche I. Strand, Ann-Sissel T. Ulset and Gerd Inger Sætrom I would like to thank for excellent technical expertise, and for creating a warm and nourishing lab environment.

To my fellow PhD-candidates and other coworkers at the Department of Biotechnology and Food Science, a large thank you also needs to be said for providing friendship and an overall good place to work in. Georg, Annalucia, Susan, Yiming, Olha, Isabel, Abba,

Joachim, Olav, Eva, and Morten are some of the many people that have made this journey so memorable.

I would also like to thank my friends outside of work, especially Ingvild, Gurminder, Mari, Kjersti, Einar Johan, Ane and Torje for support, fun times, long talks, and dinners.

Lastly, I want to thank my family for all your care, support, and help. My brother Erik and his wife Christine I want to thank for making me laugh. I would also like to thank my grandparents for their enthusiasm and interest throughout this journey. I especially want to thank my parents, Lone and Jon Petter, for always supporting me, encouraging me, and believing in me. As my mother Lone once dedicated her thesis to my brother and me, I now dedicate this thesis to my parents, Lone and Jon Petter.

Preface

This thesis is submitted in partial fulfillment of the requirements for the academic title *Philosophiae Doctor* at the Norwegian University of Science and Technology (NTNU). The work was carried out at the Department of Biotechnology and Food Science under the supervision of Professor Berit Løkensgard Strand and Professor Finn Lillelund Aachmann. The project was financed by the MARPOL project 221576 funded by the Research Council of Norway.

This thesis consists of an introduction, the scope of the work, a summary of the results and discussion based on the four papers listed in the “List of Papers” section.

Summary

The biopolymer alginate has a vast potential for use within biomedical applications largely due to its ability to form ionically crosslinked hydrogels under gentle conditions. Furthermore, the versatile ways the polymer can be tailored give rise to the possibility of altering the alginates for specific needs and functions. In this thesis, the main focus was to explore how the alginate hydrogel could be tailored for use in drug delivery, and how the subsequent modification otherwise alters the properties and behavior of the gel. The hydrophilic environment of the alginate hydrogel can be problematic for delivery of both hydrophilic and hydrophobic drugs. For hydrophilic drugs, the compound may be released too fast, while for hydrophobic drugs both load and release may be difficult due to problems dissolving the compound. Cyclodextrins (CyDs) are cyclic oligosaccharides that are capable of forming inclusion complexes with various hydrophobic molecules and moieties. The CyDs can therefore help dissolve drugs that are otherwise difficult to dissolve in an aqueous environment. On the other hand, if a drug is easily dissolved in water, but has a moiety able to interact with the CyD cavity, this can prolong the release of drugs that would otherwise give a too fast release profile.

To combine the hydrogel forming properties of the alginate with the ability of the CyDs to form inclusion complexes with various drugs, β-CyDs were grafted to alginate. This was done using a three-step procedure where alginates first are oxidized followed by linker attachment using reductive amination and finally attachment of CyD to the linker via Cu(I)-catalyzed click chemistry. M- and MG-blocks were also terminally functionalized with both β- and γ-CyDs by using first hydrazide and then click chemistry. In contrast, the reducing end of G-blocks were not successfully attached with CyDs, likely due to the G-blocks affinity towards the catalyst used in the click-chemistry reaction. In addition to this, alginate was also functionalized with either the RGD-peptide GRGDSP commonly used for cell attachment, or L-Tyrosine methyl ester (MeOTyr) used as a model small-size substitute.

As the properties of the alginate hydrogel is closely linked to the structure of the biopolymer, the mechanical properties and stability of CyD-functionalized Ca-alginate hydrogels were examined. Alginate modified with other molecules, such as peptides with cell-binding motifs were also studied. Generally, the modified hydrogels formed less stable and weaker gels than their unmodified counterparts. However, this could be controlled to a certain degree by creating hydrogels from mixtures of both functionalized and non-modified alginate, as well as controlling the degree of oxidation for the grafted alginates. A strategy using chemoenzymatic modification was also compared to using purely chemical modifications. This showed a potential to slightly increase the mechanical properties of the modified gels as seen for stress needed to rupture the gels. However, non-modified Ca-alginate hydrogels still showed markedly higher stiffness and stability in the form of resistance to breakage and dissolution. Leakage studies of the grafted Ca-hydrogels in saline treatment solutions showed that grafted material leaked out of the hydrogels.

Finally, the CyD-grafted alginate was tested as a drug delivery system for a partially water-soluble molecule, methyl orange, and the hydrophobic anti-cancer drug, paclitaxel. Grafted alginate gel-beads were able to take up and release more methyl orange compared to non-grafted beads. For paclitaxel, the grafted material helped dissolve the hydrophobic drug in the aqueous hydrogel environment and facilitated release. The released paclitaxel and degradation products were shown to have a cytotoxic effect on prostate cancer cells. To conclude, the CyD-grafted alginate can aid alginate hydrogels in delivering both partially hydrophilic molecules with hydrophobic moieties and hydrophobic drugs.

Symbols and abbreviations

Alg	Alginate
API	Active pharmaceutical ingredient
CuAAC	Cu(I)-catalyzed alkyne-azide cycloaddition reaction
CyD	Cyclodextrin
DOSY	Diffusion ordered spectroscopy
DP_n	Degree of polymerization
DS	Degree of substitution
E	Young’s modulus / Elastic modulus
Epim	Epimerized
F_G	Fraction of guluronic acid residues in an alginate sample
F_M	Fraction of mannuronic acid residues in an alginate sample
G’	Storage modulus
GDL	Glucono-δ-lactone
GRGDSP	Peptide sequence: Glycine-Arginine-Glycine-Aspartic acid-Serine-Proline
MeOTyr	L-tyrosine methyl ester
MO	Methyl orange
M_w	Molecular weight
NMR	Nuclear magnetic resonance
P_0	Periodate/monomer molar ratio. Expressed as for example 2% or 0.02.
POA	Partially oxidized alginate
POM	Partially oxidized mannuronan
pK_a	Acid dissociation constant
Ptx	Paclitaxel
SEC-MALS	Size exclusion chromatography with multi angle light scattering

List of Papers

Paper I:

Omtvedt, L. Aa.∗, Dalheim, M. Ø.∗, Nielsen, T. T., Larsen, K. L., Strand, B. L., Aachmann, F. L. Efficient Grafting of Cyclodextrin to Alginate and Performance of the Hydrogel for Release of Model Drug. Sci. Rep. 2019, 9 (9325).

Paper II:

Dalheim, Ø. M.∗; Omtvedt, Aa. L.∗; Bjørge, M. I.; Akbarzadeh, A.; Mano, F. J.; Aachmann, L. F.; Strand, L. B. Mechanical Properties of Ca-Saturated Hydrogels with Functionalized Alginate. Gels. 2019.

Paper III:

Omtvedt, L. Aa.; Kristiansen K. A.; Strand, W. I.; Aachmann, F. L.; Strand, B. L.; Zaytseva-Zotova, D. S. Alginate hydrogels functionalized with β-cyclodextrin as a local paclitaxel delivery system. J Biomed Mater Res A. 2021 Jun 30. doi: 10.1002/jbm.a.37255. Epub ahead of print. PMID: 34190416.

Paper IV:

Alginate Oligomers Terminally Functionalized with β- and γ-Cyclodextrins

Line Aa. Omtvedt, Amalie Solberg, Ingrid V. Mo, Bjørn E. Christensen, Berit L. Strand, and Finn L. Aachmann. Manuscript in preparation.

∗The authors contributed equally to these papers.

Table of Contents

1. Background

A vast number of compounds in the form of drugs or active pharmaceutical ingredients have been found and utilized to solve various health issues. However, appropriate delivery of these molecules to the correct place in the body, at the correct time and concentration remains challenging. Problems include poor solubility of the drug, adverse side-effects, poor bioavailability and non-specific targeting [1,2]. To ensure that a drug has the optimal effect in a desired location, a carrier vehicle is often needed for delivery [3]. For example, to ensure delivery to specific target sites, stimuli-responsible systems using for example pH, light, enzymes, magnetic or temperature triggers have been investigated [4,5]. Drug delivery vehicles can be formed by many different materials and with many different techniques, examples include delivery via micelles, organic or inorganic nanoparticles, hydrogels, emulsions, microspheres, drug-eluting stents, solid dispersions and supramolecular chemistry [1,2,5,6]. Delivery routes can be done with injections, surgical implantation, ocular, inhalation, transdermal, mucosal or oral administration [5]. The anti-cancer drug paclitaxel has for example traditionally been delivered by intravenous injection in Cremophor EL (Taxol), which can cause adverse effects such as hypersensitivity reactions. New drug delivery systems for paclitaxel have therefore been developed, for example Abraxane where paclitaxel is bound to human serum albumin, delivered as a nanoparticle colloidal suspension [7]. A more thorough and in-depth discussion of general drug delivery systems can be found in references as for example [1,2,5,6,8–14]. The work presented here focus on how to functionalize alginates, how this influences hydrogel properties and how the modified alginate hydrogels can be utilized as a drug delivery system.

Alginates, a polymer mainly harvested from marine algae, shows good potential for use as a drug delivery system due to its ability to form 3D structured water-swollen hydrophilic networks with divalent cations at physiological conditions, as well as its general biocompatibility and possibility for tailoring the polymer with different functionalities [15–17]. These properties also make alginates good candidates for encapsulating cells and constructing artificial extracellular matrixes for tissue engineering [16,18,19].

However, challenges remain for fully unlocking the potential of using alginates as a drug delivery system and for tissue engineering. While alginate hydrogels have good potential to be used as a localized drug delivery system, load and release of bioactive compounds from the hydrogel can be challenging [20,21]: For small hydrophilic molecules, release from the gel can happen too fast. On the other hand, hydrophobic drugs may not be soluble in the hydrogel and subsequently not released in a proper manner to the target site.

Modifying the alginate to suit load and release of specific drugs may thus be necessary for creating an optimal drug delivery system. Likewise, if the purpose of the alginate hydrogel is for creating an artificial extracellular matrix, the polymer may need to be altered so that for example cells can attach to the network. Changing the structure of the alginate can alter fundamental properties such as the structural integrity, mechanical strength, and stability of the hydrogel. Hence, these properties need to be studied and optimized for the intended use.

2. Aim

The overarching aim of this work was to better understand how alginates can be tailored for use in drug delivery application of both small partially hydrophilic molecules and very hydrophobic molecules, and how the altered alginate structure influences hydrogel properties. The topic was motivated based on the gentle and excellent hydrogel-forming ability of alginate on one side, and the hydrophilic characteristics of the gel on the other side. As cyclodextrins (CyDs) are well known for forming inclusion complexes with a large variety of molecules [22,23], shielding hydrophobic moieties from a hydrophilic bulk phase, it was hypothesized that covalently binding CyDs to alginate would facilitate load and release of different compounds into and from the modified alginate hydrogel.

This thesis therefore investigates three main topics: First, the possibility of grafting CyDs to partially oxidized alginate was investigated (Paper I). This was followed up (Paper IV) by examining if the CyDs could also be attached to the reducing end of alginate block-oligomers. The resulting structural changes in the alginate molecule led to studying the second topic of this thesis: How modified alginates affected the mechanical properties of the alginate hydrogel (Paper I, II and III). Here, also L-tyrosine methyl ester (MeOTyr) and the cell adhesion peptide GRGDSP was included as chemical modifications to compare the mechanical properties to the CyD grafted alginate. Lastly, the capacity of the CyD-functionalized alginate hydrogel for controlling load and release of the color compound methyl-orange and anti-cancer drug paclitaxel was examined (Paper I and III).

3. Introduction

Alginate is a polymer mainly found in brown algae where it gives structural support to the plant [24]. The biopolymer is also produced by certain bacteria where it is excreted and can be used in for example biofilm formation [25–27]. The compound was first described by Stanford [28], and has since been used for a wide range of products ranging from additives in the food industry to biomaterials for medical applications [16,18,19,24,29–32]: In the food industry alginate is for instance used as a thickener and stabilizing agent. Dentists can use alginate to make a mold of teeth, and the polymer is also used in the cosmetic industry (in for example toothpaste), in the textile printing industry and in the surface treatment of paper. Alginates have been chemically modified with cell adhesion-ligands (for example RGD-motif) to function as extracellular matrix for tissue engineering purposes [33–35], and been explored for delivery of various molecules such as anti-cancer agents and insulin [36,37]. Examples for the use of alginate in drug delivery systems will be further outlined in section 3.4.

Alginate is well suited for a variety of applications largely due to its ability to form a hydrogel at physiological conditions, its general biocompatibility, versatile nature and possibility for tailoring the functionality using chemical or enzymatic modification [15,16,18,19]. To fully comprehend why alginates are useful, it is important to understand the fundamental characteristics of the biopolymer.

3.1 Structure and Molecular Weight of Alginate

Alginate is an unbranched (1 → 4)-linked polysaccharide made from two types of monomers: β-D-mannuronic acid (M) and its C5-epimer α-L-guluronic acid (G) [38], see Figure 1 for chemical structure. The monomers can be arranged as sequential M-monomers (M-block), sequential G-monomers (G-block) and alternating M- and G-monomers (MG-block) as illustrated in Figure 1 [39–42]. G-units have $^1C_4$ chair conformation and M-units have $^4C_1$ [43,44], while the glycosidic bond between the G-monomers is axial-axial and equatorial-equatorial between the M-monomers. The pKa of β-D-mannuronic acid and α-L-guluronic acid is 3.38 and 3.65 [45], respectively.

Hence, at physiological pH (7.4 [18]) the carboxyl-group on the alginate monomers are negatively charged.

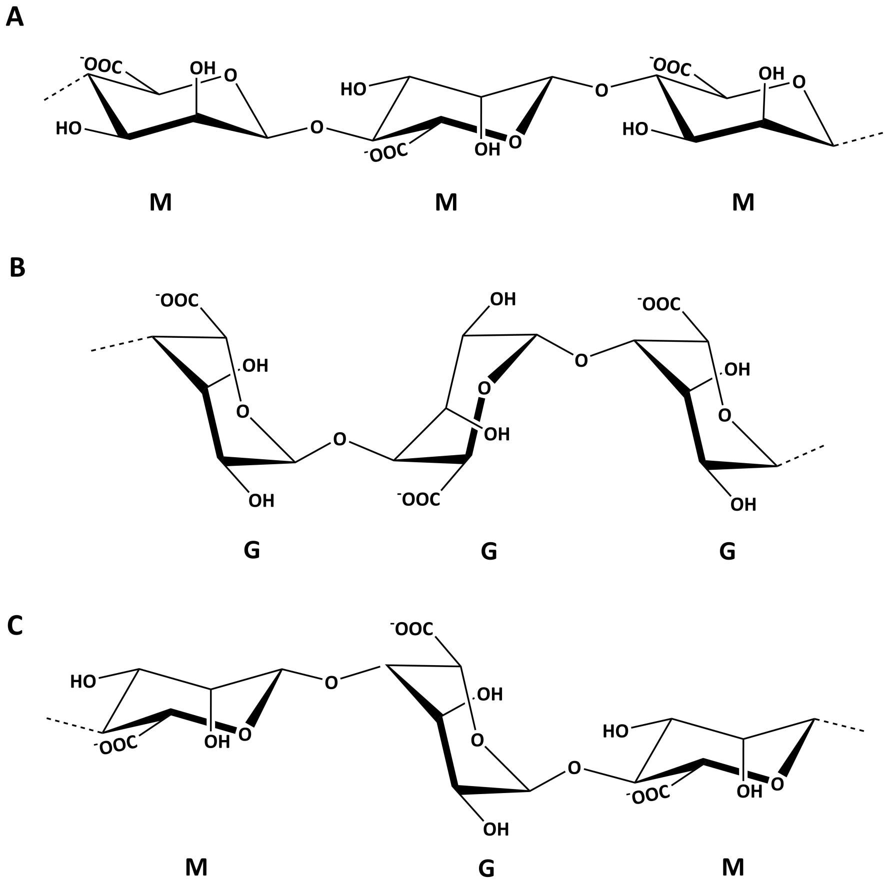

Figure 1. Alginate structures. A: Example of M-block consisting of β-D-mannuronate. B: Example of G-block consisting of α-L-guluronate. C: Example of MG-block consisting of alternating β-D-mannuronate and α-L-guluronate. Constructed in ChemDraw 20.0, based on [24].

The alginate functionality is closely linked to the sequence and composition of the two monomers it is made from, which varies for different types of alginates [24,40,46]: Alginates isolated from different types of seaweed for instance, varies in sequence and composition. E.g. alginates from *Laminaria hyperborea* contains more G than alginates from *Lessonia* or *Macrocystis* species [47]. Furthermore, variation can be seen for alginate harvested from different tissues of the same plant, and due to seasonal changes. Bacterial alginates are more extreme in composition than the seaweed alginates with G ranging from 5 % to 85 %, but the alginates are acetylated on the M [47,48]. The fraction of M (F_M) or G (F_G) units can be elucidated with ^{13}C- or ^{1}H-nuclear magnetic resonance (NMR) spectroscopy [39,44,49,50]. The anomeric region between 4.0 and 5.5 ppm reveals structural differences between H-1 and H-5 for the uronic acids and allows the calculation of F_M and F_G. Diads (F_{MM}, F_{GG}, F_{MG}, F_{GM},) and triads (F_{GGM}, F_{MGM}, F_{GGG}, F_{MGG},) can also be found, and average G-block length can be calculated. Details on alginate block structure has lately been elucidated using specific lyases and chromatography on the digested fractions [51–53]. The very long G-blocks found in seaweed alginates has been shown to heavily influence the properties of the biopolymer with regards to its functionality [51,52].

Alginate chains can vary in length, and thus in molecular weight. For alginate samples the average molecular weight is therefore used for characterization. This average is often given as either the weight average ($\overline{\mathrm{M_w}}$) or the number average ($\overline{\mathrm{M_n}}$) as shown in equations 1 and 2, where w_i is the weight of the molecules with molecular weight M_i, and N_i the number of molecules with molecular weight M_i [38]. The molecular weight distribution and average molecular weight of an alginate sample can be determined with Size-Exclusion Chromatography with Multi Angle Light-Scattering (SEC-MALS) [38].

$$\overline{M_w} = \frac{\sum_i w_i M_i}{\sum_i w_i} \tag{1}$$

$$\overline{M_n} = \frac{\sum_i N_i M_i}{\sum_i N_i} \tag{2}$$

Viscosity describes a liquids’ resistance to flow [38]. The viscosity of alginate solutions can be important for aspects such as ease of handling, homogeneity of alginate hydrogels, how easy it will be to inject an alginate drug delivery system and the distribution of molecules in the solution/gel state [10,16,54,55]. The viscosity of an aqueous alginate solution will depend on the concentration and molecular weight of the alginate. Generally, increasing these two parameters increases the viscosity of the solution [56]. The viscosity of an alginate solution will also depend on the ionic strength of the solution and how this balance the negatively charged alginate chains [56–58].

3.2 Chemical and Enzymatic Modification of Alginate

The alginate has different functional groups that can be used to chemically modify the alginate, such as the hydroxyl- and carboxyl-groups. Grafting to the carboxyl-groups can be done using for example carbodiimide chemistry. However, carbodiimide chemistry has previously been shown to give low substitution degree for primary amines, such as for the cell adhesive RGD-peptide [35]. In addition, the reaction gives the by-product N-acylurea. Esterification is another example of modification that can be done due to the carboxyl-groups [59]. For the hydroxyl-groups, alginates have been modified by sulfation to achieve interaction with proteins [60]. Periodate oxidation allows opening of the sugar ring and the formation of reactive aldehyde groups that are accessible to reductive amination [33]. Hydrazides are also good candidates for functionalizing of partially oxidized alginate, due to their reactivity to aldehyde groups [61–65]. Here, hydrophobic groups were covalently attached to the alginate with the goal to incorporate both hydrophilic and hydrophobic drugs in the alginate hydrogel. A comprehensive discussion of the chemical modifications is given in Section 4 and introduction to the methods used in the thesis given in the following sections.

3.2.1 Partial Oxidation

Partial oxidation of alginate is yet another way functional groups can be incorporated into the biopolymer chain. Partial oxidation of alginate with sodium (meta)periodate cleaves the bond between C2 and C3 of the alginate monomer [50,56,66]. As the periodate reacts with vicinal diols both the reducing end and non-reducing end may also be cleaved [67]. The reaction stoichiometry was shown to be 1:1 up to an oxidation limit of about 50% where formation of inter-residue hemiacetals hinders the reaction [66,68,69]. When working with alginate oligomers periodate consumed by the end groups should also be considered when performing the reaction [67].

In addition to creating reactive groups for further modification, partially oxidized alginate also creates hydrogels with decreased mechanical properties compared to non-modified alginate gels [50,68]. This can be explored to tailor the mechanical stability of the alginate. Chemically, such reactions cleave the monomer ring-structure. As a consequence, the oxidized monomers cannot contribute to the gel network as normal (see section 3.3). In addition, partially oxidized alginate is more prone to degradation [67,70,71]. Partial oxidation of alginate has also been observed to give decreased molecular weight and a more flexible polymer chain, and thus decreased intrinsic viscosity [56]. Hence, partially oxidized alginate can be used to tailor both the mechanical properties and degradability of the alginate hydrogel.

3.2.2 Functionalization of Partially Oxidized Alginate

Covalent coupling to the aldehyde units created by partial oxidation of alginate can be done using reductive amination, where an amine can react with the introduced carbonyl units [33,72], see Figure 2. For a reaction to take place between a primary amine and an aldehyde, the carbonyl group should be protonated while the amine group should be deprotonated [72]. Thus, the pH chosen for the reaction is an important parameter. An intermediate imine is formed, which with the help of a reducing agent can form a stable N-C linkage. Previously this reaction was performed using $NaCNBH_3$ as the reducing agent [73], which can produce hydrogen cyanide. An alternative non-toxic reducing agent is the 2-methylpyridine borane complex [74,75].

A grafting procedure for alginate using partial oxidation and reductive amination with this reducing agent was recently developed [33]. The amine can be linked to either of the two aldehyde units created by the partial oxidation [33]. The remaining non-grafted carbon can exist as either an aldehyde- or hydroxyl-group after the reductive amination with 2-methylpyridine borane complex, as the reducing agent does not exclusively reduce the imine [33,71,74].

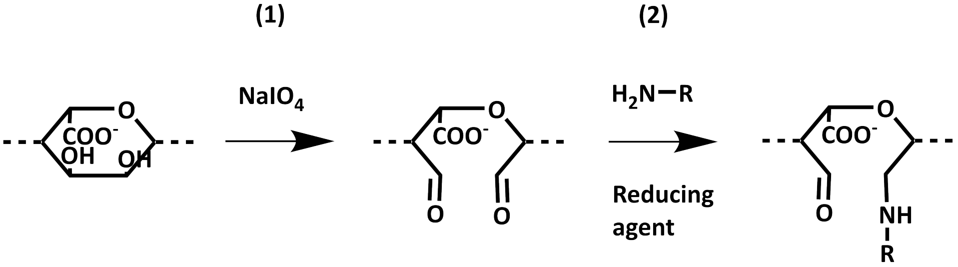

Figure 2. Overview of (1) partial oxidation of alginate with sodium (meta)periodate, followed by (2) covalent coupling of an amine using reductive amination. Adapted from *Dalheim et al. 2016* [33].

The reductive amination-reaction described can be used to tailor the functionality of the alginate by for example adding peptides to the biopolymer, or by adding “linker molecules” with the purpose for further modification using other types of reactions. Reductive amination can also be used to covalently bind molecules to the reducing end of polysaccharides such as alginate [76].

3.2.3 Cu(I)-catalyzed azide/alkyne cycloaddition reaction

Azide- and alkyne moieties can react giving 1,4 or 1,5 disubstituted triazoles in the classical Huigsen reaction where high temperature is often needed [77,78]. By using Cu(I) as a catalyst, strictly 1,4 disubstituted 1,2,3-triazoles are made [78,79]. Furthermore, the reaction is also possible at much lower temperature, and can be used at various pH and with various solvents, including water [78]. This reaction is called the Cu(I)-catalyzed azide/alkyne cycloaddition reaction [78,79], abbreviated CuAAC, and is an example of what is known as click-chemistry. An overview of the reaction is illustrated in Figure 3. Click-reactions are a term denoted to various reactions characterized by their quick, easy, and robust method of synthesis resulting in molecules with carbon-heteroatom linkages that are stable at physiological conditions [80]. Furthermore, click-chemistry is ideally stereospecific and give products with high yield that are easy to isolate. Other parameters include a non-hazardous solvent such as water or a solvent easily isolated after the reaction is done.

The Cu(I) can be introduced into the Cu(I)-catalyzed azide/alkyne cycloaddition reaction in many different ways, for example by using $CuSO_4$/sodium ascorbate [78]. This ensures that the Cu(II) is reduced to Cu(I) during the reaction. To further enhance the efficiency of the reaction ligands such as tris(benzyltriazolyl)methyl amine (TBTA) can be used to stabilize the Cu(I) [81,82]. The success of the reaction can easily be determined with ^{1}H-NMR as it results in an easily distinguishable peak at about 8 ppm of the formed triazole [83]. The 1,2,3-triazole created in the final product is very stable, and the triazole linker will not be degraded easily [84,85]. Metal independent click-chemistry also exist, which is an attractive alternative for biological systems. Cu-free click chemistry has for example been used to modify alginate with RGD-peptide [86] and to make a covalent cross-linked alginate hydrogel [87].

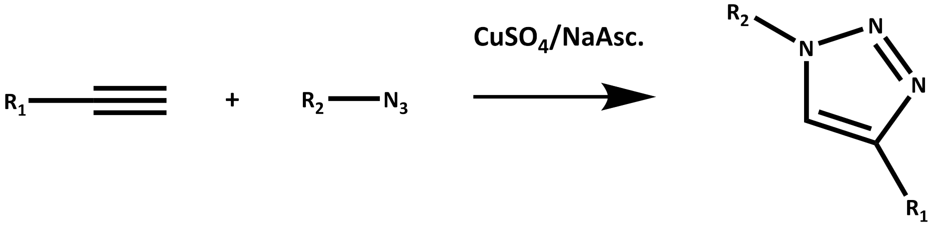

Figure 3. Overview of the Cu(I)-catalyzed azide/alkyne cycloaddition (CuAAC) reaction, using $CuSO_4$/sodium ascorbate system as the Cu(I)-source. Adapted from *Hein and Fokin 2010* [82].

3.2.4 Enzymatic Modification of Alginate

Both bacteria such as *Pseudomonas aeruginosa* and *Azotobacter vinelandii*, and brown seaweed produces alginate. Alginate is first polymerized as M-units, and then epimerases can introduce G-units into the polymer chain [88–91]. By isolating pure mannuronan (no G-units) from genetically modified bacteria, one can thereafter use specific mannuronan C-5 epimerases to tailor the sequence of the alginate [35,92,93]. Based on the bacterial synthesis of alginate, seven different mannuronan C-5 epimerases were found, cloned, and isolated from *A. vinelandii* that can be used to introduce G-monomers into the mannuronan chain [94]. The epimerases are named AlgE1-7. These enzymes are based on two modules; A and R, where the A-module is thought to bind to the substrate while the R-module helps regulate activity and product formation [95]. The epimerases have distinct epimerization patterns. For example, AlgE4 can be used to introduce alternating MG-units [96] whereas AlgE1 would introduce long

G-blocks [93]. Hence, specific block structures can be made by using the different epimerases, that allows for the tailoring of functional properties such as gel stiffness, syneresis and stability [92,93,97]. For example, by introducing alginates containing only MG- and long G-blocks by using the epimerases AlgE4 and secondly the epimerase AlgE1, alginates with excellent properties for the formation of crosslinks with calcium can be made as calcium is known to crosslink both G- and MG-blocks [93,98]. The epimerase AlgE64 is a recombinant enzyme made from a combination of AlgE4- and AlgE6-modules, but smaller in size, and providing both MG- and G-blocks [99]. The epimerases are not yet commercially available and hence detailed knowledge on their production is needed for their use.

3.3 The Alginate Hydrogel

A hydrophilic polymer network able to absorb and retain water is classified as a hydrogel [100]. They are advantageous to use as biomaterial due to their resemblance to living tissue. Examples include contact lenses, wound dressings, drug delivery systems and artificial scaffolding for tissue engineering [10,101]. Alginates can form hydrogels at physiological conditions due to their ability to form crosslinks with certain divalent cations [19,102,103]. The crosslinking sections are often described with the "egg-box" model, due to the space formed between two block-structures where the divalent cation can be bound [102,103]. This is illustrated in panel A, Figure 4. The crosslinking mechanism is a cooperative process where for example G-blocks in two different alginate chains can bind Ca^{2+} [103,104]. The difference in the cavity formed between block structures due to variance in axial and equatorial linkages between the M- and G-monomers is considered to play a role in addition to the electrostatic interactions [103,105,106].

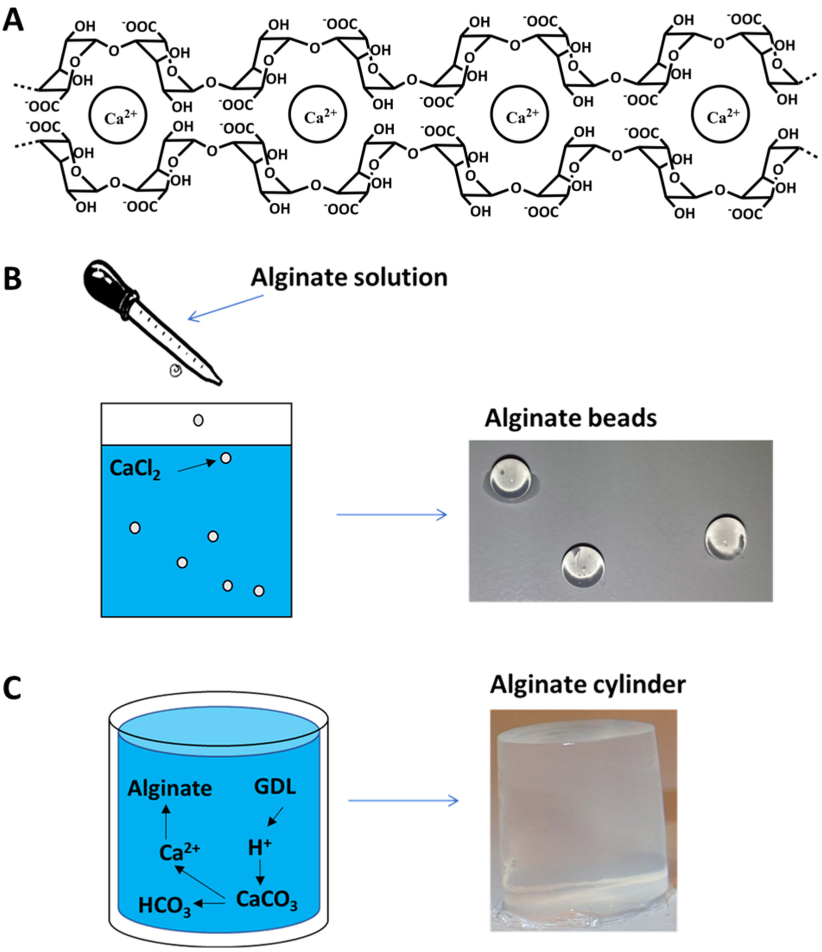

Figure 4. Alginate hydrogel formation with Ca^{2+} based on [24,32]. A: Alginate eggbox model showing a section of G-block binding Ca^{2+}. B: External gelation of alginate done by dripping dissolved alginate into a solution with Ca^{2+}. C: Internal gelation of alginate; Ca^{2+} is slowly released from an inert form.

The biopolymer shows distinct affinities towards divalent cations which largely depends on the guluronate content [105–107]; where for example the affinity for the following divalent cations is ranged as $Ca^{2+} < Sr^{2+} < Ba^{2+} < Cu^{2+} < Pb^{2+}$. The G-blocks are largely responsible for the crosslinks [108], but MG-blocks are also able to contribute to the crosslink network by binding calcium-ions [98,109]. M-blocks have also been found to bind Ba^{2+} [98]. The divalent cations chosen as the crosslinking ion can influence properties such as the strength, stability and permeability of the alginate hydrogel. An alginate hydrogel made with barium-ions will for example be stronger than a gel made with calcium-ions [98]. Consideration of the toxicity profile of the divalent cations must also be taken into account when choosing a gelling ion [18,110]. Ca^{2+} and Sr^{2+} are for example non-toxic, while Ba^{2+} is toxic at certain concentrations. The concentration of Ba^{2+} that can be utilized in hydrogels for biomedical purposes is thus limited by its toxicity.

The gelling ions can be introduced to the alginate using different methods [24]. Alginate hydrogels can be made by dripping dissolved alginate into a solution containing the gelling ion, for example a solution of $CaCl_2$ (Figure 4). The gelling ion will thus diffuse into the alginate and introduce crosslinks. However, this can create an inhomogeneous hydrogel where there is a larger concentration of alginate and gelling ion at the exterior layer of the gel compared to the middle of the gel [111]. Certain factors such as using a combination of Na^+ and Ca^{2+} in the gelling bath can decrease the heterogeneity of the hydrogel [111,112].

To make a more homogenous gel, internal gelation can be used instead. In this instance an inert form of the gelling ion is mixed with the dissolved alginate, whereby an activator can then be mixed into the solution releasing the inert gelling ions. The gelling ion will then slowly be released throughout the alginate solution. A common way to do this is to use D-glucono-δ-lactone (GDL) and $CaCO_3$ [55] (Figure 4). In this instance, protons are released when the GDL is slowly hydrolyzed, and this will react with the $CaCO_3$ ensuring the calcium-ions to be released and bind to the alginate. In other words, the GDL acts as a 1-proton donor while the $CaCO_3$ acts as a 2-proton acceptor. The hydrogel pH can be controlled by the molar ratio of GDL/$CaCO_3$, where a 2:1 ratio gives gels with a neutral pH [113]. Other factors are also important for creating homogenous gels such as the size of $CaCO_3$ particles [55]. Saturating the Ca-alginate hydrogel with Ca-ions can be done by placing the gel in a Ca-bath, and generally increases the gel strength for Ca-limited gels with available gelling zones [113,114].

Recently, a new system for the gelation of alginate was introduced named competitive ligand exchange crosslinking (CLEX) [115]. Here, an alginate solution with Ca-EDTA is mixed with an alginate solution containing an ion that has a higher affinity towards EDTA compared to the Ca-ions. Thus, Ca^{2+} is released and is free to act as a crosslinker ion. The principle is also applicable for chelator-ion combinations. This method gives good control over the gelation time in addition to being biocompatible.

3.3.1 Mechanical Properties

Chemical and enzymatic modification of alginate changes the properties of the alginate hydrogel. Such changes should be taken into consideration when tailoring the hydrogel for use in drug delivery as these changes can alter viscosity, gelation time, structural integrity, and stability. If the purpose of the hydrogel is to act as a scaffolding for tissue regeneration it might be beneficial for the gel to disintegrate in a timely manner so that it can be replaced by the desired tissue [116]. Acquiring knowledge about the mechanical properties of the alginate hydrogel is therefore very important.

One way to study the mechanical properties of hydrogels is to perform compression studies on the gel and examine how the gel is deformed when force is applied [32]. Initially when compressing a material, the stress (σ) is proportional to the strain (ε). From this, the Young's modulus or Elastic modulus (E) can be determined ($\sigma = E \cdot \varepsilon$) [38,117]. If the force is applied until the gel breaks this can give additional information about how much force the hydrogel can withstand before the gel network breaks (stress at rupture) [32].

From literature, Young's modulus was measured for both alginate beads made by the diffusion method (external gelation) and alginate hydrogel cylinders made by internal gelation [98]. For the studies done on alginate beads, the hydrogels were found to be inhomogeneous and therefore not well suited to compression measurements. Alginate hydrogel cylinders made by internal gelation were however found to be suitable due to homogeneity and reproducible results.

The type and concentration of both alginate and crosslinking ion can affect the mechanical properties of the alginate hydrogel, as well as the rate of deformation [24,32,52,97,98,117,118]. In other words, the number, length, and type of crosslinks can influence the mechanical properties of alginate hydrogels. An alginate hydrogel made from chains rich in G-blocks will generally have higher Young's modulus values compared to a gel made of alginate chains with fewer G-blocks [52].

For alginates characterized by a high content of G-residues ($F_G = 0.7$), Ba^{2+} and Sr^{2+} increased Young's modulus [98]. In contrast, for alginates with a high content of M-residues ($F_G = 0.4$) only Ba^{2+} increased Young's modulus. Concerning the concentration of alginate, decreasing the polymer concentration was previously reported to decrease the gel strength [118]. Young's modulus for alginate hydrogels can be dependent on the molecular weight up to a certain point. This cut-off point is reported to depend on the method for which the alginate hydrogels has been made. For Ca-alginate gels made by diffusion, Young's modulus generally drops with decreasing molecular weight starting from about 240 kDa [118]. For Ca-limited gels made by internal gelation using GDL/$CaCO_3$, the Young's modulus is reported to be dependent on the molecular weight up to about 350 kDa [114].

Rheology measurements can also be used to examine the transition from solution to gel state and give information about the storage modulus (G') of the hydrogel. The storage modulus can be related to Young's modulus ($G = E/3$) [32]. For Ca-alginate gels made by internal gelation with GDL/$CaCO_3$ the ratio of these compounds will influence the gelation time [119], as well as the particle size of $CaCO_3$ [55]. The gelling kinetics and mechanical properties can also be influenced by addition of G-blocks [120].

3.3.2 Syneresis

During the transition from solution to gel the alginate chains form junction zones with the divalent ions, realigning the chains and forming a more orderly network [121]. The formation of the network may expel water from the hydrogel; the polymer concentration will be higher in the alginate hydrogel than the starting liquid volume [32]. This loss of water is called syneresis and will be different depending on the type of alginate used to make the hydrogel. Increased syneresis was observed when increasing the amounts of MG-blocks, Ca^{2+}-ions and molecular weight [93,97,118,121]. On the other hand, syneresis decreases with G-block length due to a less flexible network that cannot easily be reorganized [118].

3.3.3 Degradation of Alginate

The glycosidic bonds in alginate can be cleaved by alkaline β-elimination or acid hydrolysis [122]. Degradation at neutral pH is slow and the molecular size used is often larger than what can be cleared with the renal system, about 50 kDa [123]. As alginate above this size limit was found to remain in the body, it can be assumed that no enzymatic degradation of alginate takes place in the human body. Enzymes with the ability to degrade alginate were however found in various microorganisms, marine algae, and molluscs (an important phylum of invertebrate animals) [124].

Modification of alginate has shown to change the degradation rate of alginate in both alkaline and acidic medium, via β-elimination and acid hydrolysis, respectively [71,116,125]. Partially oxidized alginate is more susceptible to β-elimination, while grafted partially oxidized alginate, using the reductive amination reaction, show similar degradation in alkaline media compared to non-modified alginate. In acidic conditions, grafted partially oxidized alginate displayed an increase in degradation compared to alginate [71].

3.3.4 Swelling and Stability

When the objective of an alginate hydrogel is to be placed inside the body, the stability of the hydrogel against swelling and dissolution is an important factor to consider [32]. A Ca-alginate hydrogel placed in the body may be subjected to shear forces, exchange of gelling ions with sodium ions and subsequent swelling due to influx of water [118,126]. Thus, swelling is largely dependent upon the ability of the gel network to counteract the osmotic pressure [93,117]. Swelling of the hydrogel can increase the pore size in the gel, and thus its permeability [126].

Both the type of alginate and gelling-ion used can affect the stability of the gel [98,118,127]. Higher G-content generally increases the stability of the Ca-alginate hydrogel [118]. Furthermore, Ba^{2+} and Sr^{2+} decrease swelling of alginate beads with a high G-content due to their strong crosslinking of G-blocks, which was not seen for high-M alginate [98]. It has also been shown that alginate chains with low molecular weight and high in M-content tends to leak out of the gel first [128]. Stability of alginate hydrogel were improved by elongating the MG-segments in the polymer chain by using enzymatically modified alginate [93,127].

3.4 Alginate hydrogels as Drug Delivery Vehicles

Bioactive agents usually need to be delivered by an appropriate vehicle to avoid issues such as low solubility, degradation, and clearance from the body before reaching the target site [2,5]. Delivery of bioactive molecules to the body is done for a vast number of reasons, and the bioactive agents consequently differ largely in physical and chemical properties. As such, it follows that there is no universal delivery vehicle. When considering an appropriate delivery vehicle there are many factors which are important [2,5]. Some of the more important factors are: How the pharmaceutical agent can be loaded into the vehicle, how the vehicle should be delivered and the body's response to the drug delivery system. In the following, some general considerations of hydrogels and alginate hydrogels as drug delivery systems are given before examples of the use of alginate in drug delivery is further outlined.

The alginate hydrogel is generally considered biocompatible and inert, although immune activation was observed for soluble alginates with a high content of mannuronate [129–132]. The size of alginate microspheres and grafting with specific moieties have also been shown to influence how the immune system responds to the hydrogel and reduced fibrosis can be obtained by increasing the size of the microbeads to about 1.5 mm [133,134]. Fibrosis surrounding the alginate hydrogels may hinder diffusion in and out of the gel and can be detrimental when the purpose of the gel is to deliver biotherapeutic agents to the body. Factors such as the choice of alginate and size/shape of the formed hydrogel should therefore also be considered when using alginate as an implantable or injectable delivery vehicle.

3.4.1 Systemic or Local Delivery

When designing a delivery system, it must be decided whether the delivery should be systemic (circulated throughout the entire body) or local (to a specific place in the body) [9]. Compared to systemic delivery, localized delivery can be advantageous due to less elimination/degradation of the drug before it reaches the target site, fewer detrimental side effects caused by the drug being delivered to the wrong place and a possibility of lowering the administered dose.

For hydrogels local delivery can be done by placing or injecting the gel at the appropriate site [135]. Injection as opposed to surgically placing the set gel in the body has certain advantages; a pre-gel solution will be able to fill up empty spaces and will in most cases be less invasive [9,136]. For injectable *in situ* gelling hydrogels the transition from solution to gel state is important to consider [137]. Ideally, the gelation time should be long enough for effortless injection, and short enough that the hydrogel is set at the appropriate place in the body (and not diluted by body fluids so that no gel forms) [9].

3.4.2 Load and Release of Bioactive Compounds

Loading water-soluble molecules and cells into the alginate hydrogel can be done by mixing the aqueous alginate solution with the appropriate agent to be loaded, and thereafter initiate gelation (see section 3.2.4) [47]. Alternatively, small water-soluble molecules can be loaded in the gel by diffusion from a solution into the hydrogel [138]. However, for molecules which are not easily dissolved in water, loading can be problematic. In addition, release of both hydrophilic and hydrophobic compounds from the alginate hydrogel can be challenging. Depending on the problem to be solved, optimal release may be over a short or long time period [9]. It is important that a therapeutic concentration is reached, meaning that the concentration of the drug is high enough to achieve the wanted effect (but not so high as to be toxic).

For poorly water-soluble molecules it may only be possible to load the hydrogel with a very low concentration of drug or it might precipitate or crystallize once loaded into the gel and not be released [139]. Small hydrophilic molecules on the other hand, may be released too fast [20]. As a vast majority of drugs are poorly soluble in water [2,140], it would be very beneficial to be able to both load and deliver hydrophobic drugs from the alginate hydrogel. In this way the gel could function as a depot of drugs, ideally giving controlled localized release of the drug over time [10].

The alginate hydrogel is an aqueous network where components can move into, through and out of the gel. The transport of molecules out of/into the alginate gel will depend on the network structure, and the physical and chemical properties of the molecule [118,138,141,142]. The compound can either diffuse out of the gel or be released from the gel network due to a change in the polymer network (for example increased pore size), destruction of the hydrogel or degradation of the polymer itself [9,143]. Controlled destruction of the hydrogel is also interesting for other applications, for example in tissue engineering where new tissue should replace the hydrogel matrix [116]. The release characteristics are further complicated if the compound to be released can interact with the hydrogel network [9].

Tanaka *et al.* [138] reported that for alginate Ca-beads (2 or 4 %) made by external gelation (Figure 4) molecules with Mw below ~20 kDa were found to freely diffuse in and out of the gel similar to their diffusion in water. The proteins albumin, γ-globulin and fibrinogen with Mw ranging from 69 – 341 kDa were not able to diffuse into the gel beads and were hindered when diffusing out of the beads as seen in a separate experiment. The diffusion of the proteins was further reduced by increasing alginate concentration, indicating that the increase in alginate concentration reduced the pore sizes of the hydrogel. The smallest Immunoglobulin (Ig), IgG with Mw of 150 kDa has been found to diffuse into 2% (w/v) Ca- or Ca/Ba-alginate gel beads [93,142,144]. However, Ca-beads made of alginate with a high-M fraction as well as epimerized alginate (introduction of MG by AlgE4, then G-residues by AlgE1) were found to be less permeable towards IgG compared to alginate beads made with alginate with a high-G fraction [93]. This indicates that not only the crosslinking zones formed by G-block crosslinked with calcium ions determine the permeability of the hydrogel. Changing the gelling ion can also affect the permeability of the alginate gel, as the calcium ions are known to crosslink both MG- and G-blocks, barium ions crosslink both G- and M-blocks and strontium ions G-blocks only [98,104]. The gelling ions as well as the presence of non-gelling ions also influence the distribution of alginate in the hydrogels [24,98]. Another study showed that bovine serum albumin (BSA, Mw ~ 70 kDa) diffused quicker out of homogenous Ca-alginate beads compared to inhomogeneous beads with alginate concentrations above 1.9% [141]. The charge on BSA also influenced the release, where increased negative charge on the protein gave faster diffusion out of the gel. The study also showed that BSA diffused faster out of gels with alginate with high G-content, indicating that both the gel structure and crosslinking as well as the molecular charge influence the permeability.

3.4.3 Examples of alginates in drug delivery systems

Alginates are commonly used in food as stabilizer or thickener, and in oral formulations of drugs, hence oral administration is considered as safe [16,17,24,145]. In biomedical applications, alginate hydrogels are commercially available as wound dressings, also with the delivery of nanosilver as antimicrobial agent [9]. Furthermore, injectable alginate hydrogels have been used for the restoration of heart tissue after ischemic heart failure with positive effects in large animals and have been evaluated positively for safety and efficacy in dilated cardiomyopathy in clinical trials [146,147].

As soluble formulations, small molecular weight alginates in the form of G-blocks of 80 - 95 % G and mean DP 10 – 12, has been shown to have activity by itself towards mucus barrier penetration allowing increased uptake of drugs via mucus membranes [148,149]. This has allowed for the development of OligoG (tradename of G-blocks by Algipharma) as a treatment towards cystic fibrosis, with currently finished Phase 2b clinical trials [150]. Oligomers of G-blocks also interfere with bacterial biofilm formation [151]. This is also relevant for cystic fibrosis where the establishment of the alginate producing bacteria *Pseudomonas aeruginosa*, together with other bacteria in the lungs of the patients is a major cause of the problems associated with the disease [152]. Hence, G-blocks have been suggested to also make an impact on the biofilm formation in cystic fibrosis [153,154].

Alginate hydrogels have been proposed as relevant drug delivery systems as is also shown by the many reviews on the topic [9,10,17,145,155–157]. The general biocompatibility, gentle gel-formation and tunable properties of alginates and alginate hydrogels makes the hydrogels popular for use in drug delivery systems, giving the possibility of targeted delivery by implantation close to the place of delivery without adverse side-effects or destruction of the drug to be delivered [9,10,17,145,155–157]. However, the hydrophilic environment of the hydrogels can make it problematic for load and release of hydrophobic drugs [10]. In addition, hydrophilic drugs may be released too fast, and macromolecules may be too large in size for release without destruction of the hydrogel network.

Ca-alginate hydrogels have for example been suggested for the local delivery of SiRNA for the silencing of genes [158]. The amount and kinetics of SiRNA released was reduced with the incorporation of polycations (chitosan or polyethyleneimine) into the alginate and increasing amounts of SiRNA was released with a photo-crosslinked alginate hydrogel. One newer example includes injectable alginate hydrogels that were studied for delivery of the hydrophilic drug taurine with the purpose of inducing regeneration of retinal pigment epithelium cells for the treatment of age-related macular degeneration [159]. Although positive results were obtained in mice and rabbits, it is difficult to extract the results since both dry and wet gels were used, and also in co-encapsulation systems with retinal pigment epithelial cells [159].

As the specifications of a drug delivery vehicle largely depends on the active pharmaceutical ingredient and where it should be delivered, it is often necessary to chemically modify the alginate or to combine it with other polymers to tailor the alginate hydrogel for specific needs. Bouhadir and coworkers used low molecular weight alginate that was oxidized and subsequently grafted with adipic dihydrazide to incorporate a drug and to cross-link the polymers into hydrogels [36]. The drug, daunomycin, an antineoplastic agent, was then released from the hydrogels after the hydrolysis of the covalent linkage between the drug and the polymer. By using this strategy, the release profile of daunomycin could be varied from 2 days to 6 weeks [36]. Jeon and coworkers reported the engineering of photocrosslinked and biodegradable alginate hydrogels [160]. In this study, alginate macromers of methacrylated alginate was tuned with different degree of methacrylation to yield hydrogels with controlled swelling behavior, elastic moduli, and degradation rates. The gels were suggested for delivery of bioactive factors, but the follow-up studies included rather encapsulated cells than smaller molecules [160,161].

Alginate microparticles and nanoparticles are also promising candidates for delivery systems [162,163]. Alginate microparticles have been designed for release of the anti-cancer drug paclitaxel for the use by inhalation to combat lung cancer [162]. The alginate microparticles (3.0 ± 0.7 µm) were fabricated by an emulsification technique with an encapsulation efficiency of paclitaxel of 61 ± 4 %. The in vitro release profile showed a slower release rate for microparticles compared to pure paclitaxel and the paclitaxel loaded microparticles were shown to inhibit the growth of cancer cell lines in vitro [162]. Another strategy was used for the preparation of nano-sized drug carriers for the co-delivery of multiple types of drugs [163]: Inorganic/organic hybrid alginate/$CaCO_3$ nanoparticles were prepared by co-precipitation with drugs, allowing the co-encapsulation of the hydrophilic drug doxorubicin hydrochloride and the hydrophobic drug paclitaxel. The nanoparticles showed sustained release of the drugs, and tumor cell inhibitory effects in vitro [163].

The ionic crosslinking of alginate is the main feature accounting for the popularity for the alginate hydrogel as immobilization matrix for cells and drugs. As alginate forms ionically crosslinked hydrogels under physiological conditions, immobilized cells retain their viability and function after encapsulation. The porous hydrogel network allows for the exchange of oxygen, nutrients and waste products, maintaining the cell viability and function in vitro and in vivo over prolonged periods [47]. Alginate hydrogels have throughout the last three decades been investigated as an immune protective membrane in cell therapy for the treatment of Type 1 diabetes [164–166] and also for the treatment of acute liver failure [167]. The use of alginate hydrogels in cell therapy has been hampered by an immune mediated fibrotic response to the alginate hydrogel resulting in fibrotic tissue surrounding alginate microbeads [134,168]. However, chemical modification of alginate by grafting with triazole or zwitterions has also shown a reduction of fibrotic responses to the alginate microcapsules in mice [169] and monkeys [170].

3.5 Cyclodextrins

The ability of cyclodextrins (CyDs) to form inclusion complexes with hydrophobic molecules and moieties makes them attractive and potent molecules for drug delivery purposes. The CyDs are for example used to enhance the solubility of hydrophobic molecules, protect drugs from degradation, give control over release and mask unpleasant taste [140,171]. Thus, the CyDs are not only popular in the pharmaceutical industry but are also utilized in for example food industry. Cyclodextrins are a group of cyclic oligosaccharides prepared from starch consisting of (1→4) linked α-D-glucopyranose units [23]. The most common cyclodextrins are α-, β- and γ-CyD, which differ due to the different number of monomers they are made from (6, 7 and 8, respectively), see Figure 5. Many different CyDs derivatives have also been made. To enhance the water solubility of β-CyD for example (18.5 mg/ml at 25°C [172]), the hydroxyl-groups can be substituted with 2-hydroxypropyl. The resulting HP-β-CyD has a much higher water solubility at >1200 mg/ml.

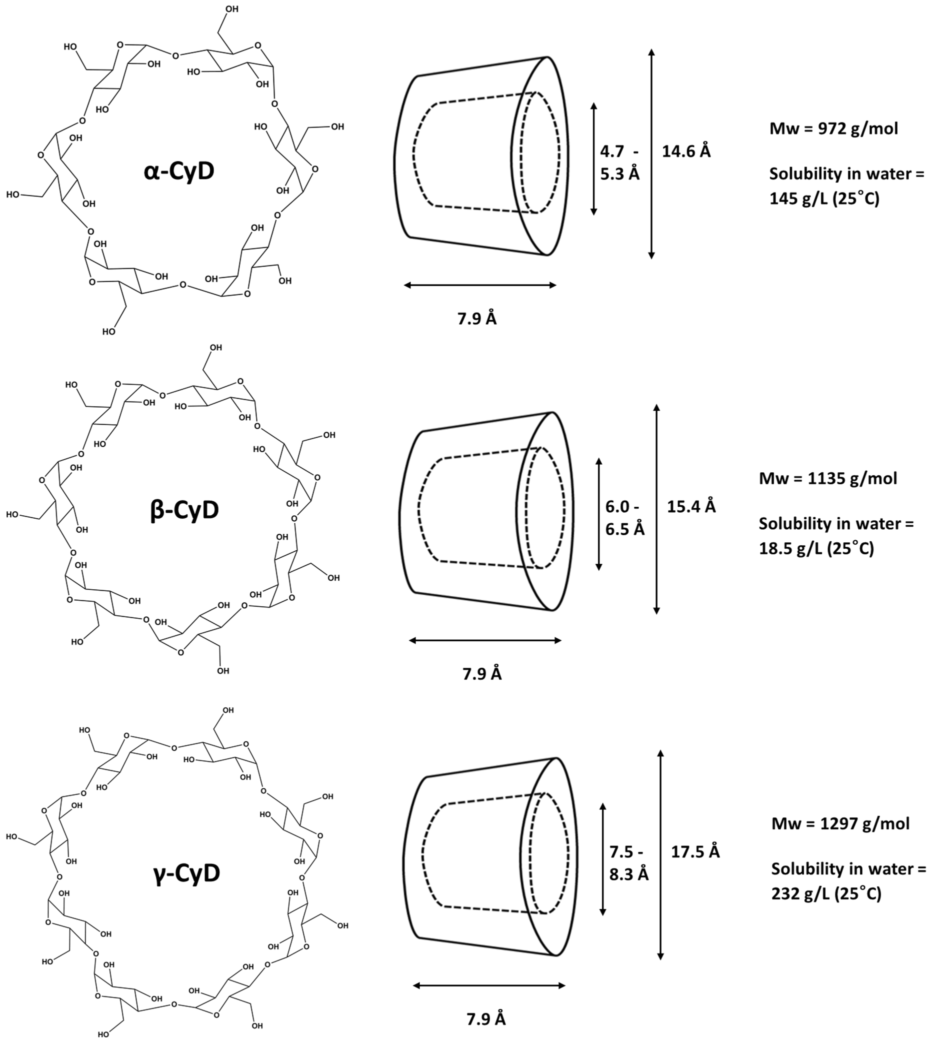

Figure 5. The most common cyclodextrins; α-, β- and γ-CyD. Structures were obtained from ChemDraw and values from reference [140].

The CyDs are shaped like a cone, where the cavity inside the cone is hydrophobic compared to the hydrophilic exterior [23,172]. This is due to the orientation of the molecule where the hydroxyl-groups are oriented at both ends of the cone, where the primary hydroxyl groups form a narrow end, and the secondary hydroxyl-groups form a wide frame at the opposite end [23]. This enables the CyDs to incorporate hydrophobic groups or molecules inside their cavity, and thus masking them from a hydrophilic bulk phase. The complex between CyD and the molecule in the cavity is called an inclusion complex, where the CyD is referred to as the host molecule and the entity located in the CyD cavity is denoted the guest molecule [23,173]. The inclusion complex can be formed by one cyclodextrin and one guest molecule (1:1 inclusion complex), or several cyclodextrins and one guest molecule. Other cyclodextrin:host ratios are also possible, for example a 2:1 inclusion complex where two cyclodextrins form a complex with one guest molecule, for instance with two different moieties on one compound. This is illustrated in Figure 6. Often, only one part of a molecule will fit in the cyclodextrin cavity. This is for example seen with the anticancer drug doxorubicin as shown in reference [174].

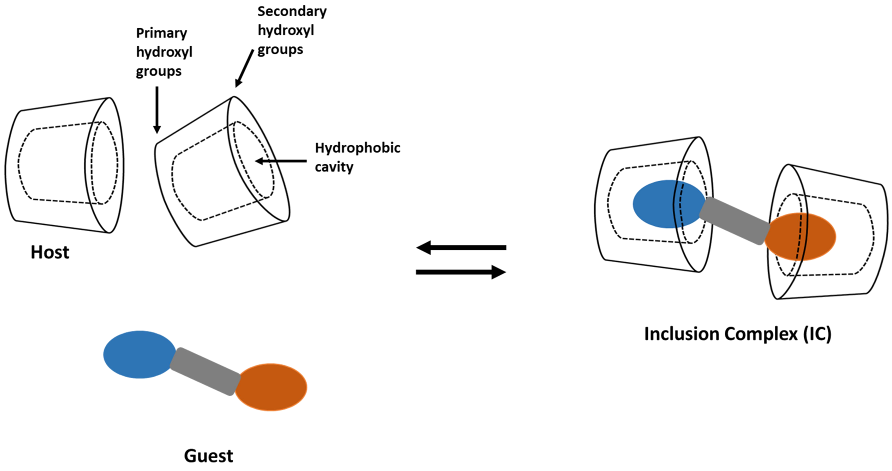

Figure 6. Inclusion complex with two CyDs (host) and one guest molecule (host:guest ratio 2:1) containing two moieties suitable for interacting with the CyD cavity. Based on [140,174].

The inclusion complex between the cyclodextrin and the guest molecule is dynamic; the guest can both associate and dissociate with the host, as seen in eq. 3, where G denotes the guest molecule, CyD the cyclodextrin and CyD*G the inclusion complex formed between the two. The stability constant Ka is used to describe this equilibrium. The equilibrium between a 1:1 inclusion complex can thus be written as seen in eq. 4, where K is the association constant, [G] denotes the concentration of guest molecule, [CyD] the concentration of cyclodextrin and [CyD*G] the concentration of the inclusion complex formed between the two.

$$CyD + G \rightleftharpoons CyD * G \qquad (3)$$

$$K_{1:1} = \frac{[CyD*G]}{[CyD][G]} \qquad (4)$$

Many factors are considered to drive the formation of the inclusion complex [140,171,174,175]. For example, the size of the cavity and how well it fits with the guest molecule can help to determine which cyclodextrin to use for a certain guest molecule. Release of water from the cavity into the bulk water-phase in exchange for a more hydrophobic compound sequestered in the cavity is considered to be the main driving force for complex formation. The guest molecule can be stabilized in the cavity by dipole-dipole forces, dispersive forces, van der Waals interaction, charge-transfer interactions, electrostatic interactions, and hydrogen bonding.

The different CyDs naturally have affinities for different types of molecules. The cavity of the β-CyDs is for example well suited to aromatic- and heterocyclic-moieties [140]. For efficient complex formation between the CyDs and guest molecule, their concentration should be such that they are easily dissolved [140]. On the other hand, a highly diluted mixture will make it more difficult for the guest molecule and CyDs to be close enough to form an inclusion complex. Dissolving a hydrophobic drug in water so that it might form an inclusion complex with CyDs (and thus enhancing its solubility) is not always straightforward. A more suitable solvent for the drug may be used to first dissolve the drug [140], before mixing it with an aqueous CyD-solution. Ideally, the drug-solvent should then not compete for the CyD cavity or otherwise be detrimental. Such a co-solvent could for example be ethanol.

For enteral use β-CyDs are considered safe [140]. However, for parenteral use β-CyDs are toxic. Modification of β-CyDs can give a non-toxic version of the molecule, for example by substituting hydroxyl-groups with 2-hydroxy-propyl (HP-β-CyDs) suitable for parenteral administration. The toxicology profile of new modifications of β-CyDs must therefore be investigated for both enteral and parenteral use.

4. Results and Discussion

In this chapter the main findings in the four papers included in this thesis will be summarized and discussed. The papers are listed in the section named “List of Papers”. Paper I, II and III are published, while Paper IV is a manuscript under preparation that will be included as a part of a larger story of ongoing work at NTNU on the chemical modification of reducing ends of block polysaccharides.

4.1 Summary of papers

Paper I, “*Efficient Grafting of Cyclodextrin to Alginate and Performance of the Hydrogel for Release of Model Drug*”, investigates the grafting of β-cyclodextrins (β-CyD) to partially oxidized alginate (POA), combining the gelation ability of the alginate with the inclusion complex ability of the cyclodextrins. Successful grafting was achieved in a three-step synthesis using periodate oxidation, reductive amination and copper(I)-catalyzed azide-alkyne cycloaddition, shown by ^{1}H-NMR and DOSY. The obtained degree of grafting ranged from 1.6 – 4.7% mol β-CyD/mol uronic acid residues, depending on the applied reaction parameters. The chosen synthesis methodology allows the degree of grafting to be regulated, resulting in a material that has tunable properties. The final degree of grafting was shown to depend largely on the amount of linker (4-pentyn-1-amine) grafted to periodate oxidized alginate, hence depending on the degree of oxidation and also the efficiency of the binding of the linker to the aldehyde of the oxidized alginate upon reduction. A proof-of-concept study was performed to examine if the CyD-grafted alginate could alter the binding and release of a model molecule loaded into the alginate hydrogel. Ca-alginate gel beads made from a mixture of β-CyD-grafted alginate and unmodified alginate showed higher initial binding and had an increased and prolonged release of methyl orange compared to non-grafted beads. The stability of the Ca-alginate gel beads was also affected by varying the amounts of the grafted and unmodified alginates, which was further explored in Paper II.

In Paper II, "*Mechanical Properties of Ca Saturated Hydrogels with Functionalized Alginate*", mechanical properties and stability of chemically and enzymatically modified alginate hydrogels were investigated, including the CyD-grafted alginate made with the strategy from Paper I. The other functionalized alginates used were grafted with either the RGD-peptide GRGDSP commonly used for cell attachment, or L-Tyrosine methyl ester (MeOTyr) used as a model small-size substitute. Furthermore, a chemoenzymatic method was also used to graft partially oxidized alginate with L-Tyrosine methyl ester, to investigate if this would alter the gel-forming abilities of grafted alginate. Functionalization was achieved in this study via periodate oxidation followed by reductive amination, previously shown to give a high and controllable degree of substitution, with an additional third step for the CyD-grafted alginate as investigated in Paper I. Young's modulus and the stress at rupture of the Ca-hydrogels were in general lowered when exchanging non-grafted alginate with the functionalized alginate. Still, the gel strength could be adjusted by the fraction of modified alginate in the mixed hydrogels as well as by the degree of oxidation. No notable difference in deformation at rupture was observed while syneresis was influenced by the degree of oxidation and possibly by the nature and amount of the grafted molecules. Grafted epimerized alginate showed better gelling properties in higher Young's modulus and higher resistance to deformation at rupture than the corresponding grafted stipe alginate. The mixed hydrogels were less stable than hydrogels with only non-grafted alginate, and functionalized alginate was released from the hydrogels. Furthermore, the hydrogels in general rather disintegrated than swelled upon saline treatments. It is evident that functionalization via periodate oxidation and subsequent grafting has considerable effect on alginates gelling properties with reducing the ability to form stable and strong gels upon crosslinking with calcium.

In Paper III, "*Alginate hydrogels functionalized with β-cyclodextrin as a local paclitaxel delivery system*", the CyD-grafted alginate was examined for its use as an injectable drug delivery hydrogel system with the poorly water-soluble anticancer drug paclitaxel which has the ability to form inclusion complexes with cyclodextrins. The rheological and mechanical properties of the prepared hydrogels were characterized, as well as in vitro release of the paclitaxel and in vitro activity on PC-3 prostate cancer cells. Introduction of β-CyD-moieties into the hydrogel reduced the mechanical properties of the gels compared to nonmodified gels, in line with the observations in paper II. However, the gelation kinetics were not markedly different. The β-CyD-modified alginate helped to reduce undesired crystallization of the paclitaxel seen as absence of crystals in the gels with β-CyD-modified alginate compared to gels with non-modified alginate. Also, the β-CyD-modified alginate facilitated paclitaxel diffusion out of the gel network. Remarkably, the β-CyD grafted alginate showed increased capacity to complex paclitaxel compared to free HPβ-CyD. Although the paclitaxel is not an ideal payload for β-CyD-based systems because of its relatively poor retention within β-CyD hydrophobic cavity, and because it is difficult to quantify due to rapid degradation, our findings support that the β-CyD-grafted alginate can modulate release of the paclitaxel from the gels. Release of both paclitaxel and degradation products were measured from the gels and were shown to have cytotoxic effects on prostate cancer cells (PC-3) in in vitro cultures. The results indicate that functionalized alginate with β-CyDs has potential as a hydrogel for drug delivery. The hydrogel system could also be applied in future work for delivery of other hydrophobic drugs and molecules that can form inclusion complexes with β-CyD.

Lastly, in Paper IV, *"Alginate Oligomers Terminally Functionalized with β- and γ-Cyclodextrins"*, both β- and γ-CyDs were attached to the reducing ends of M- and MG-blocks. A two-step reaction was performed to functionalize the reducing end of 14-mer M-, G- or MG-oligosaccharide block structures using 1) hydrazide chemistry followed by 2) Cu(I)-catalyzed azide-alkyne cycloaddition (CuAAC) with β- and γ-CyDs. Based on 1D ^{1}H-NMR spectra, 32, 42 and 58 % of the reducing end of the 14-mer MG-, M- or G-block structures, respectively, were coupled with alkyne hydrazide. Furthermore, 27-28 % and 37-45% of the reducing ends of the MG- and M-oligomers were coupled with CyDs, respectively. G-blocks were not successfully modified with CyDs, likely due to the block structures high affinity for the Cu-catalyst, reducing the efficiency in the Cu-catalyzed click reaction. In addition, alkyne hydrazide was covalently bound to partially oxidized alginate, giving a grafting degree of 7.2 % (mol linker/mol monomer), indicating higher grafting degree with this linker compared to the 4-pentyn-1-amine linker used in paper I.

Hence, three main topics can be withdrawn from the four papers: Grafting of cyclodextrins to alginate/alginate oligomers (section 4.2), mechanical properties of modified alginate hydrogels (section 4.3) and drug delivery abilities of the cyclodextrin grafted alginate (section 4.4). These topics will be examined consecutively in the following sections.

4.2 Chemical and Enzymatic Modification of Alginates

In Paper I, the purpose was to combine the hydrogel forming ability of alginates with the ability of the cyclodextrins to form inclusion complexes. The easiest way of combining these aspects may at first seem to be to simply mix CyDs into an alginate solution before starting gelation. However, when mixing β-CyDs with alginate and letting the gel set by external gelation in Ca^{2+}, we showed that the free β-CyDs quickly diffused out of the hydrogel (Paper 1). Furthermore, the non-bound cyclodextrins did not alter the load and release of the color compound methyl orange, which is known to form inclusion complexes with CyDs [176]. The other option is then to covalently attach the CyDs to the alginate network, ensuring that they do not diffuse out of the hydrogel in an untimely manner. Traditional methods of grafting molecules to alginate by carbodiimide chemistry have suffered from low grafting degrees and the formation of by-products [18,35,177].

Higher grafting degrees of compounds with an amine-functional group is possible to obtain, as was previously shown by *Dalheim et al.* [33] for peptides and for the model molecule L-Tyrosine methyl ester (Figure 7): The alginate is first partially oxidized creating reactive dialdehyde units in the alginate chain. The oxidized monomers can then react with an amine-functional group using reductive amination. Cyclodextrins have previously been grafted to dextran using Cu(I)-catalyzed click chemistry (CuAAC)

[83]. A strategy combining these synthesis pathways was therefore chosen to graft CyDs to alginate. The hypothesis was that this would give a straightforward grafting procedure with high controllable grafting degrees and without unwanted by-products. A schematic of the synthesis is given in Figure 7. The use of Cu-free click reactions are further discussed later in this chapter and in section 4.5.

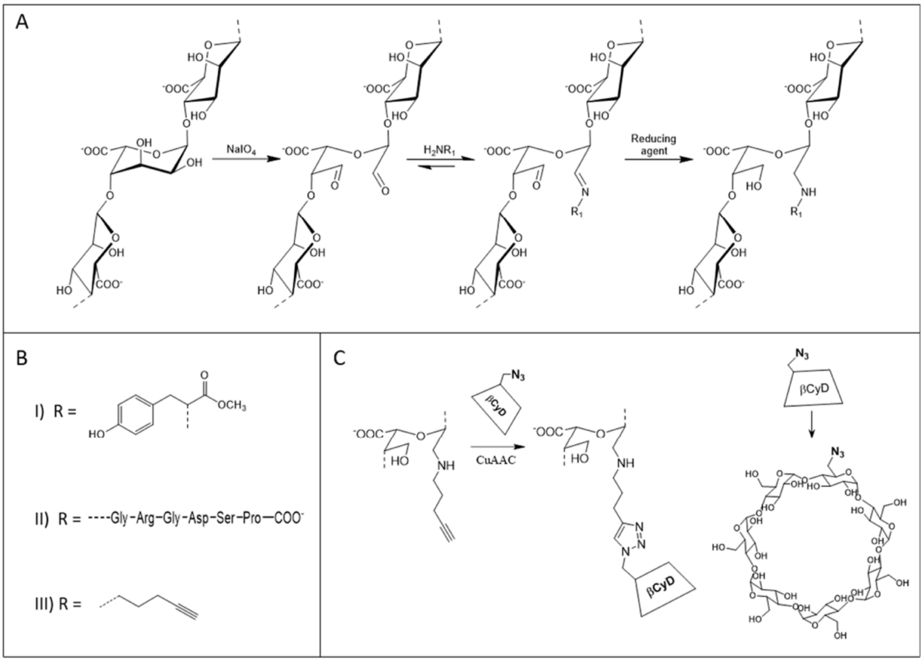

Figure 7. Schematic of the synthesis of partially oxidized alginate grafted with β-CyDs, RGD-peptide GRGDSP or L-Tyrosine methyl ester. The alginate first underwent partial oxidation and reductive amination (A) to attach either the linker 4-pentyn-1-amine, RGD peptide or L-Tyrosine methyl ester (B). β-CyD was then covalently bound to the linker via Cu(I)-catalyzed click chemistry (C). Cyclodextrin is not scaled properly in comparison to the alginate residues.

The degree of grafting was tunable based on several parameters. As the linker attaches to the aldehyde unit of the alginate, the degree of oxidation of the alginate is important and influences the final grafting degree. However, the cleaved ring-structure of oxidized alginate monomers is detrimental to the overall hydrogel forming ability of the alginate [50,68]. Thus, the oxidation should be high enough to ensure a high grafting degree giving desired effect of the functionalization, while being low enough so that the partially oxidized alginate still is able to form a hydrogel. The molar ratio between the periodate used to oxidize the alginate and the alginate monomers were therefore set to 0.08, giving a theoretical oxidation degree of 8% oxidized monomers. To indirectly confirm that the reactions had run to completion (all IO_4 consumed), a titration test was performed: 0.5 ml of the reaction mixture was mixed with 5 ml 0.5 M cold phosphate buffer (NaH_2PO_4), pH 7.0 and 0.75 ml 60% (w/v) potassium iodide (KI). If unreacted periodate was present, this would result in yellow coloration (no color change is observed if all periodate has been consumed). Direct verification of oxidization degree with 1D ^{1}H-NMR is difficult due to the complex peak pattern [50]. The same authors showed that reduction of the partially oxidized alginate (using P_0 between 2-8%) with sodium borohydride gives a distinguishable peak for unoxidized monomers with a neighboring oxidized and reduced unit, making it possible to calculate the oxidation degree, which showed similar values as the theoretical oxidation degrees.

Originally, 4-pentyn-1-amine was chosen as the linker molecule between the alginate chain and cyclodextrins due to the belief that it would be long enough for easy attachment of CyDs, while short enough to not be detrimental to the hydrogel [83]. This gave a grafting degree between 1.6 – 5.6% mol linker/mol monomer. The amount of linker added to the reaction was based on the theoretical oxidation degree. By increasing the linker added to the reaction from 5 molar equivalents to 20 equivalents, while the reaction time was lowered from 96 to 48 hours, the grafting degree was calculated to be 2.2%. Thereafter the reaction time was again increased to 84 hours using 20 molar equivalents linker, giving a grafting degree of 5.6%. These results showed that both the amount of linker and reaction time influence the grafting degree. Nevertheless, the linker was successfully attached to the partially oxidized alginate making it possible to go forward with grafting the cyclodextrins to the chemically modified alginate.

An attempt was also made to attach the linker 4-pentyn-1-amine to the reducing end of alginate oligomers. However, successfully reacting this linker with the reducing end was not achieved. In contrast to this, it was recently shown in literature that adipic acid dihydrazide can efficiently be conjugated to oligosaccharides derived from chitosan [62]. Grafting of the reducing end of alginate oligomers is still ongoing work at NTNU [64]. Based on this, a hydrazide linker with an alkyne functionality (alkyne hydrazide) was then chosen to act as the linker between alginate oligomers and CyDs in the hope that the hydrazide linker would be more efficient in reacting with the reducing end. The linker alkyne hydrazide was successfully grafted to different oligomers derived from alginate (DP = 14). For the different MG, M or G-block structures, 32, 42 or 58 % of the reducing ends of the blocks, respectively, reacted with the linker. Hence, this indicates that the reaction also depends on the type of alginate oligomer used in the reaction. The better reactivity of alkyne hydrazide compared to 4-pentyn-1-amine may be due to higher nucleophilicity of the alkyne hydrazide [62].

An experiment with partially oxidized alginate and alkyne hydrazide was also performed to examine if this linker attached with a higher grafting degree than 4-pentyn-1-amine. This experiment is reported in Paper IV. This worked very well and gave a degree of substitution of 7.2% (mol linker/mol monomer). Hence, for future work alkyne hydrazide should be further explored for attachment to both partially oxidized alginate and alginate oligomers, for example if the alkyne moiety on the linker is needed for CuAAC. This, however, was outside the scope of the work presented in this thesis.

The same method of partial oxidation and reductive amination was also used to functionalize alginate with the RGD-peptide GRGDSP (for cell attachment) and L-Tyrosine methyl ester (as model small size substitute, MeOTyr). The grafting degree was again determined by ^{1}H-NMR to be 3.9 and 7.0% (mole substituent per mole uronic acid residue), respectively. Furthermore, a chemoenzymatic method was also used for grafting to examine if hydrogels made from both enzymatically and chemically modified alginate would behave differently compared to hydrogels made from only chemically modified alginate. Here, mannuronan was partially oxidized and grafted with L-Tyrosine methyl ester. This was followed by epimerization of the grafted mannuronan with the mannuronan C-5 epimerase AlgE64 that convert M- to G-units in the unmodified part of the chain, specifically introducing MG- and G-blocks. The grafting degree of the epimerized sample (EpimPOAMeOTyr) was determined to be 7.9% while the G-content was determined to be 49%, as reported in Paper II.

The size of the β-CyD cavity fits well with the size of the aromatic ring and heterocyclic moieties which many drug molecules contain [140,178–180], and therefore this was the chosen type of CyD for modifying the alginate polymer. β-CyD was introduced in the last step of the synthesis strategy, the CuAAC-reaction [80]. This step showed robust and high substitution degrees when using N_3-β-CyD and the linker 4-pentyn-1-amine attached to partially oxidized alginate, see Paper I. Furthermore, the reaction results in a distinguishable peak at 7.8 ppm in the ^{1}H-NMR spectrum, due to the formation of a triazole unit after a successful reaction between the alkyne moiety and azide group [83]. ^{1}H-NMR was used to confirm and calculate the degree of grafting. Diffusion ordered spectroscopy (DOSY) was also initially used to confirm that the CyDs were covalently attached to the alginate; if the CyDs are grafted to the alginate, the diffusion of the CyDs and alginate are expected to be the same. A DOSY and ^{1}H-NMR spectrum of one sample of partially oxidized alginate grafted with β-CyD is shown in Figure 8. A full range 1-8 ppm spectra are given in supplementary file S1 in paper II. For non-successful grafting, the diffusion of CyD would be lower than for the alginate sample, as shown for MeOTyr by Dalheim et al. [33]. The highest achieved grafting was 4.7% mol β-CyD/mol sugar residues.

Grafting of other types of CyDs could also be interesting for future investigation. HP-β-CyD is for example safe for parenteral use and is more water-soluble compared to β-CyD [140,172]. CyDs with a larger or smaller cavity may be better suited to certain drugs compared to β-CyDs. There is also potential for tailoring the release of different drugs loaded into the same hydrogel if the drugs have different affinities for the grafted CyDs. Furthermore, other molecules than CyDs can also potentially be attached to the alginate using the aforementioned reaction steps, if the reactive group needed for the click reaction is possible to attach to the alternative compound.

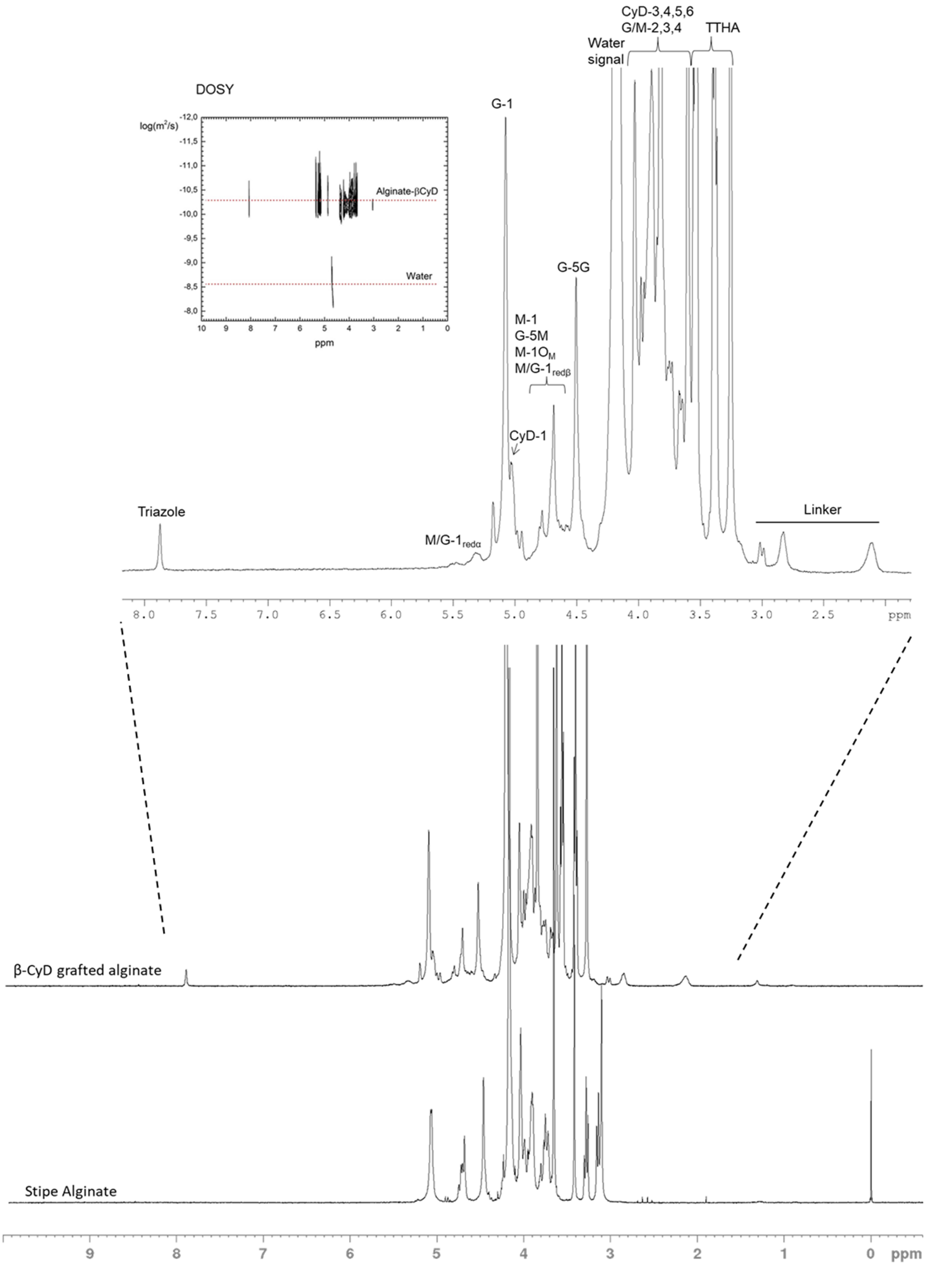

Figure 8. ^{1}H NMR of stipe alginate and partially oxidized alginate grafted with β-CyD are shown. In addition, a closer look is shown of the interesting region of the grafted alginate with an assignment of the protons of the different chemical groups, as well as DOSY (upper left corner).

With regards to the alginate oligomers (Paper IV), CuAAC was also used to attach either β-CyDs or γ-CyDs to the reducing ends of the oligomers, by reacting them with the alkyne moiety of the alkyne hydrazide linker. Even though all block structures were successfully conjugated with alkyne hydrazide, only M- and MG-oligomers successfully attached to the CyDs. Here, the M- and MG-oligomers had both β-CyD and γ-CyD attached to them. The amount of oligomers that were attached with CyDs was calculated to be 45% for the M-βCyD block, 37% for the M-γCyD block, 27% for the MG-βCyD block and 28% for the MG-γCyD block based on the ^{1}H-NMR spectrum. In other words, most of the available alkyne hydrazide reacted with the CyDs.

^{1}H-NMR showed no triazole peak when analyzing the G-oligomers, giving evidence that the CyDs had not reacted with the alkyne linker. Since the catalyst (Cu(I)) for the CuAAC-reaction is supplied as Cu^{2+}-ions, a likely explanation is that the G-oligomers forms an ionic complex with the Cu^{2+}-ions before Na-ascorbate can reduce it. Previously, it was shown that G-oligomers have a higher affinity towards Ca^{2+}-ions compared to alginate [120]. Thus, this seems to be the case also for Cu^{2+}-ions, where we hypothesize that for grafting of alginate enough Cu^{1+} is free to act as catalyst in the CuAAC-reaction, while for G-oligomers the Cu-ions are complexed so fast by the oligomers that not enough Cu^{1+} is available to catalyze the reaction. Successful reaction with G-oligomers might be done by first reacting the linker with CyDs, and thereafter reacting the oligomer with the CyD-linker. Cu-free click-reactions also exist [86,181,182] and are viable options for modifying both the alginate and its oligomers.

4.3 Mechanical Properties of Modified Alginate

The mechanical properties of alginate gels are highly dependent on type of alginate and crosslinking ion. Due to partial destruction of the gelling units when partially oxidizing the alginate, it was expected that the modified alginate would have reduced ability to gel with divalent ions [50,68]. The results presented in Papers I, II and III showed the modified alginate still contributed to the hydrogel network, although to a lesser degree compared to non-modified alginate (Alg). Furthermore, the mechanical properties of the alginate hydrogels could be tailored using a mix of modified and non-modified alginate, for example by using a mix of Alg/POA with a mix ratio of 1:1.

Compression measurements were used to find the Young's modulus and stress and deformation at rupture for gels made by internal gelation, where gels were either saturated or unsaturated with Ca^{2+} (Paper II and III). Syneresis (loss of water) and stability of the gels were also studied. The Ca-saturated hydrogels, as presented in Paper II, made from solely partially oxidized alginate (POA) or mixtures of POA/Alg were studied to examine the effect of oxidation and the subsequent destruction of the gelling segments. Further studies were then done on grafted alginate, to determine if the functional groups would further alter the properties of the hydrogel. The functionalized alginates were grafted with either:

- β-cyclodextrin for help with load and release of bioactive molecules
- the RGD-peptide GRGDSP for cell attachment
- L-Tyrosine methyl ester as model small-size substitute (MeOTyr)

In Paper III, comparison of Alg/POA and Alg gels showed that the transition time from solution to gelation was similar at ~25 minutes, indicating that the introduction of oxidized alginate does not affect how fast the alginate converts from a solution to a gel. However, the storage modulus stabilized quicker for alginate gels compared to Alg/POA gels with different mix ratios of oxidized and non-modified alginate. The alginate gel reached plateau levels at 4-6 hours compared to 8-12 hours for the Alg/POA gels (Paper II). Based on this it seems that it requires a longer time to arrange the alginate chains into a stable gel network for the Alg/POA gels compared to non-modified alginate gels. This could be because it is more difficult to form stable junction zones due to less or shorter G-blocks available for crosslinking caused by the oxidation reaction. In addition, as the POA chains are more flexible, it could also be easier for the polymer chains to rearrange, giving a longer network rearrangement time [24]. On the other hand, the POA chains could be disrupting the existing G-blocks from forming crosslinks, and thus ensuring a longer time before plateau levels are reached for Alg/POA gels.

It was possible to make hydrogels from the modified alginate by either dripping dissolved alginate into a $CaCl_2$ solution (Paper I) or by internal gelation using GDL/$CaCO_3$. Properly shaped Ca-saturated hydrogel cylinders made with internal gelation were possible to make from the 2 and 4% partially oxidized alginate, while hydrogel cylinders made purely from 8% oxidized alginate were deformed upon completion and very difficult to handle. This is in agreement with previous work on partially oxidized alginate and was expected due to the destruction of gelling units and increased chain flexibility caused by the ring opening of oxidized sugar units [50,68,116]. Partial oxidation of alginate can thus lead to reduced G-block length, and it has already been established that a block length of at least eight G-units is needed for crosslinking with Ca^{2+} [128,183]. Interestingly, Ca-alginate gels made purely of epimerized 8% oxidized alginate grafted with L-Tyrosine methyl ester (epimPOAMeOTyr) were able to form intact gel cylinders. Hydrogel cylinders made of differently modified alginates, as well as non-modified stipe alginate, are depicted in Figure 9.

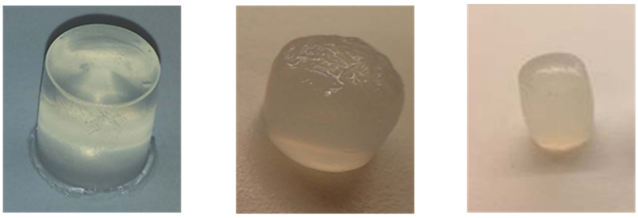

Stipe alginate **POA-βCyD** **Epim POA-MeOTyr**

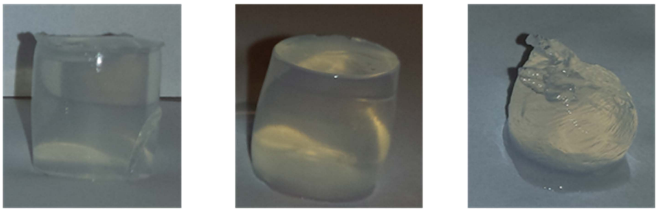

POA (P_0 = 2%) **POA (P_0 = 4%)** **POA (P_0 = 8%)**

Figure 9. Hydrogel cylinders made by internal gelation using GDL/$CaCO_3$ with 1% (w/V) alginate. Stipe alginate = non-modified alginate reference. Abbreviations: POA = partially oxidized alginate. P_0 = degree of oxidation. POA-βCyD = POA grafted with β-cyclodextrin. Epim POA-MeOTyr = epimerized mannuronan grafted with MeOTyr.

Furthermore, Young's modulus was also measured for Ca-saturated gels of 8% oxidized material, gels made of 8% oxidized material grafted with MeOTyr or β-CyD, and the epimerized 8% oxidized POA-MeOTyr sample. Here, Young's modulus was very low for all gels (0.7 – 2.5 kPa). It is also important to note that the molecular weight of the different modified alginates were not the same after undergoing the partial oxidation and grafting procedures, and lowering the molecular weight can decrease Young's modulus when the molecular weight is below 240 - 350 kDa [114,118]. As the molecular weight for the modified alginate samples were between 65 - 126 kDa this could also have had an impact on the measured values. However, variation in molecular weight is not believed to play a large role in these gels. Rather, it is the oxidation and grafting procedure which is responsible for the altered mechanical properties of these gels. Gels made of 2 or 4% oxidized alginate for instance, gave a Young's modulus of about 9 kPa, and had a molecular weight of 99 and 93 kDa, respectively. In contrast, the 8% oxidized alginate had a molecular weight of 97 kDa, similar to the 2 and 4% POA, but a Young's modulus of about 1 kPa.

Alginate hydrogels often undergo syneresis upon ionic crosslinking, that is to say they shrink and release water, giving a higher polymer concentration in the gel [32]. The main driving force for syneresis is considered to be the formation of junction zones [121]. Generally, syneresis is decreased by increased G-block length due to a less flexible network that cannot easily be reorganized [118]. For the gels made of purely 8% oxidized material, as well as the POA grafted with MeOTyr or β-CyD, and the epimerized 8% oxidized POA-MeOTyr, the syneresis was higher (46 – 67%) than the 1.0% w/v stipe alginate reference gel (30%). In comparison, the syneresis of the 0.5% w/v stipe alginate reference sample was 46%. Again, these results indicate that more rearrangement of the gel network is possible for hydrogels made of 8% oxidized alginate compared to non-modified alginate, likely due to both decreased G-block length as well as more flexible polymer chains [50,56,68]. Interestingly, gels made of solely 2% oxidized alginate showed similar syneresis compared to the 1.0% (w/v) reference sample, showing the large scope varying the oxidation degree can give over the properties of the alginate gel.

It is also important to note that, as the same Ca^{2+} concentration was used for all POA hydrogels, the modified alginate gels would have more Ca^{2+} present compared to G-units in comparison to the non-modified alginate gels, which may have contributed to a higher syneresis [55].

Syneresis also increases with increasing molecular weight [121]. No correlation of this was found for the gels made of purely modified alginate. For example, 2 and 8% oxidized samples had very similar molecular weights at 99 and 97 kDa, respectively, but showed very different syneresis. In contrast, the stipe alginate sample (Mw = 133 kDa) had about the same amount of syneresis of approximately 30% as the 2% POA sample (Mw = 99 kDa). Overall, this shows that the mechanical properties of the Ca-alginate hydrogels examined here were determined largely by the chemical and enzymatic modification of alginate as opposed to the variation seen in molecular weight. More experiments of modified Ca-gels with different Ca/G-ratios should be done to fully understand the impact of modified alginate on the syneresis.

A distinguishable difference in the stress needed to rupture the epimerized gels were observed, with a value of 3 kg as opposed to 0.1 – 0.6 kg for the gels made of solely modified alginate (P_0 = 8%). Overall, this shows that there is an effect when using a chemoenzymatic strategy where the G-units are introduced into the chain after grafting. In this way, only M-units are oxidized. However, the epimerized hydrogels still showed a large decrease in mechanical properties compared to non-modified alginate, showing that the gelling segments have been compromised even after converting M- to G-units after the grafting procedure.

For possible future work it should be kept in mind that divalent cations, such as Ba^{2+} and Sr^{2+}, can contribute to create stronger and more stable gels [98,110]. Furthermore, as the viscosity for the modified alginate is decreased, the concentration used to make the gels can be increased without leading to problems handling the liquid gel mix. This could likely give hydrogels with both increased mechanical properties and functionality. Lastly, it would also be interesting to mix block-structures and alginate with and without modification, to see if this has any effect on the mechanical properties of the formed hydrogels, since G-blocks for instance may help alter gelling kinetics and mechanical properties [120].

For the Ca-alginate hydrogels made from a mix of modified and non-modified alginate, the compression studies also showed that the tailored alginate generally lowered the mechanical properties of the gels, see Figure 10. Young's modulus, stress at rupture and syneresis was here largely influenced by both the oxidation degree and ratio of modified and non-modified alginate.

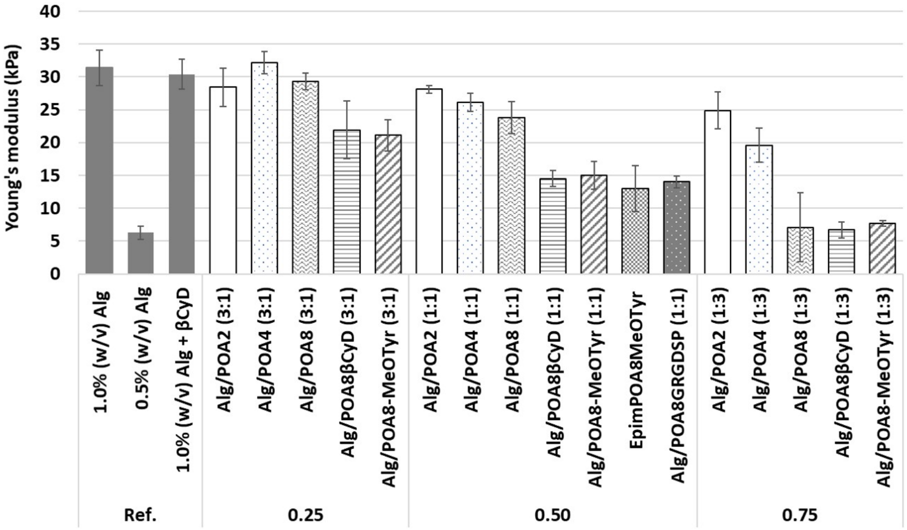

Figure 10. Young's modulus measured for different types of 1.0% w/v Ca-saturated alginate hydrogels (n= 4-10). One reference sample with 0.5% w/v alginate is also shown. Abbreviations: Ref. = reference gels. 0.25 / 0.50 / 0.75 = Weight fraction of oxidized or grafted alginate in the gel compared to total amount of alginate in hydrogel. POA2/4/8 = partially oxidized alginate with theoretical oxidation degree of 2, 4 or 8%. Alg = Stipe alginate. βCyD = β-cyclodextrin. POA-MeOTyr = POA grafted with L-Tyrosine methyl ester. POAβCyD = POA grafted with β-cyclodextrin. POA-GRGDSP = POA grafted with peptide GRGDSP. EpimPOA-MeOTyr = epimerized mannuronan grafted with MeOTyr.

Regarding the mixed hydrogels containing both POA and alginate, the syneresis for the 4% and 8% oxidized samples were lower (15 – 23 %) compared to the reference samples. This is in contrast with the gels made of solely modified alginate ($P_0 = 0.08$). Even though the mixed gel system gains more flexibility to rearrange due to the oxidized units, it seems that the network is less compact compared to non-modified alginate gels due to lessened ability to form junction zones. There may be an incompatibility between the oxidized and non-modified alginate, both decreasing the effective formation of junction zones seen in the reference gels and the flexibility of the POA chains seen in the pure modified gels ($P_0 = 0.08$). In other words, there may be less junction zones formed, and thus less syneresis.

Comparing the 1% (w/v) alginate hydrogels were the ratio between non-modified and oxidized alginate (Alg/POA) was 1:1 with the 0.5% (w/v) unmodified stipe alginate gels gives valuable information to examine if the modified alginate can contribute to the gel network. If the mechanical properties of the Alg/POA (1:1) gels would be similar to the 0.5% (w/v) reference sample, it could be assumed that the oxidized alginate did not take part in the network formation. However, the Alg/POA (1:1) gels all gave a higher Young's modulus (24-28 kPa) compared to the 0.5% (w/v) reference sample ($E = 6$ kPa). With regards to the stress at rupture, gels with $P_0 = 2\%$ showed a higher resistance to stress before rupturing, while the 4% and 8% POA gels showed similar or lower stress at rupture, respectively. The stress needed to rupture the hydrogels depends on the energy needed to fracture the junction zones, while Young's modulus depends on the amount, size, and stability of junction zones [24,32]. In addition, the length and flexibility of the segments between the junction zones also influence Young's modulus. Overall, this indicates that the oxidized alginate is still able to take part in the gel network, but the junction zones in POA/alginate gels are easier to destroy compared to non-modified alginate. This is likely due to shorter and/or fewer junction zones due to ring opening of the oxidized monomers.

A further decrease in Young's modulus was seen for calcium saturated gels when 8% oxidized alginate was grafted with either β-CyD, MeOTyr or GRGDSP and mixed with stipe alginate so that the amount of modified alginate was 25 or 50%, see Figure 10. No difference was observed for mixed gels were 75% of the alginate was grafted. The further decrease in Young's modulus for the Ca-saturated gels may be due to steric hindrance of gel network formation/rearrangement caused by the grafted substituents, and thus impeding optimized interaction with the Ca-ions. Most of the mixed gels containing grafted alginate (either with β-CyD, MeOTyr or GRGDSP) showed similar values as the mixed gels with 8% oxidized alginate when measuring the stress and deformation needed to rupture the mixed gels.

For the mixed gels containing grafted POAMeOTyr and POA-GRGDSP an increase in syneresis compared to the mixed partially oxidized alginate gels were observed, while POAβCyD showed similar syneresis compared to POA gels. This may be due to the bulky CyD-group contributing to a less flexible network compared to the two other less bulky substituents. Overall, the oxidation degree seems to be the more prevalent modification giving decreased mechanical properties, while some effect may also be attributed to grafting substituents on the partially oxidized alginate. Tailoring the functionality of alginate hydrogels using the oxidation and grafting procedure will therefore be a balance between achieving the desired functionality while still retaining good mechanical properties.

All the previously described gels were made by internal gelation using GDL/$CaCO_3$, followed by saturating the gel system with Ca^{2+} by placing the gels in a Ca-bath for 24 hours. In addition to this, some Ca-unsaturated alginate hydrogels were also examined. Generally, the same trend was seen where substituting non-modified alginate with POA reduced Young's modulus and stress at rupture. The effect of calcium increase was clearly seen, as the saturated alginate hydrogels gave a Young's modulus of about 30 kPa compared to 8 kPa for the Ca-unsaturated alginate gel. This was expected as the hydrogel network is formed on the basis of crosslinking with Ca^{2+}. The effect of Ca-concentration has previously been shown in literature [55,114,121]. Furthermore, the unsaturated gels showed no large difference in Young's modulus when comparing Alg/POA and Alg/POAβCyD.

In addition to these results, the hydrogels in this work that were unsaturated in Ca^{2+} were much less syneretic compared to the Ca-saturated gels, as was expected as Ca^{2+} is needed in the formation of junction zones. This concurs with previous work where

Ca-saturation has been shown to give more syneretic gels [121]. While the deformation the Ca-saturated hydrogels could undergo before rupture was largely similar to the reference gel, this was not the case for the gels that were unsaturated with Ca^{2+}. Interestingly, the Ca-unsaturated Alg/POA (1:1 w/v) and Alg/POA (1:3 w/v) showed about 40% and 20% deformation at rupture, respectively, compared to about 60% for both the Ca-unsaturated and Ca-saturated reference sample. Again, this points to a less stable network when more oxidized alginate is mixed in.

To better understand how the functionalizes hydrogels could be used within drug delivery it was also important to study the stability of these gels in aqueous medium. Low-molecular weight alginate rich in M-content is already known to leak out of Ca-alginate hydrogels, and when placed in a saline bath (0.15 M NaCl) gels tend to dissolve due to exchange of Ca^{2+} with Na^{+} [128,184]. In this work it was also shown that grafted alginate leaked out of gels made of a mixture of non-modified and grafted alginate (mixed gels). The fraction of grafted alginate, in this case grafted with MeOTyr, decreased with the number of saline baths, see Figure 11A. This shows that not only is low-molecular weight alginate rich in M-content leaked out initially, but grafted material is also released in the initial stages. Furthermore, the mixed hydrogels lost more material in the NaCl treatments compared to the stipe alginate gels. The most drastic difference was seen for the mixed gels where 75% of the alginate was; the mixed partially oxidized alginate gel lost 49 wt% and the POAMeOTyr gels lost 40 wt% after the two first NaCl treatments. The stipe alginate only lost 4 wt% after all four treatments.

Generally, Young's modulus decreased for all gels after each NaCl treatment. The mixed gels were always easier to destroy than the stipe alginate reference gels (it was not possible to work with the mixed gels after 2-4 treatments). Swelling (relative weight gain) happened in the same manner for all hydrogels, except for the Alg/POA (1:3, P_0 = 0.08) hydrogel. This gel system disintegrated (observed as a decrease in weight). For the remaining hydrogels, swelling increased after the initial treatments followed by dissolution of the gels. The swelling data are shown in Figure 11B. Pictures of alginate and Alg/POAβCyD beads, and their stability in NaCl-solution is also shown in Figure 13

P3. Previous work has shown continued swelling of Ca-alginate beads, by measuring the diameter of the beads, for seven consecutive NaCl treatments [93,98]. The exchange of Ca^{2+} with Na^{+} and the ability of the gel network to counteract the osmotic pressure effects the swelling of the alginate hydrogel [93,117]. Both the fast disintegration of the mixed hydrogels compared to the reference gels, as well as the higher amount of leaked material is likely due to the formation of shorter or fewer junction zones, due to the reduced number of gelling units in the modified alginate. Thus, the mixed gels are less able to withstand swelling.

As it was evident that grafted material could leak out quickly from the hydrogels, toxicity studies with PC-3 cells were performed. Here, the cells were exposed to solutions of both partially oxidized alginate mixed with free β-CyD and POAβCyD. This was done due to the knowledge that β-CyD can give hemolysis and cytotoxicity (dependent on dose) [185]. For POAβCyD solutions, cell viability was ≥ 90 for concentrations up to 5 mg/ml (1 mM β-CyD), see Figure 11C. Above this threshold, cell viability decreased in a concentration dependent manner. Furthermore, the POAβCyD polymers gave two times higher cytotoxicity compared to free β-CyD mixed with partially oxidized alginate. As substituent on CyDs are known to alter the complexation capability of the CyDs, and complexation with cellular cholesterol is linked to cytotoxicity, these results may indicate that POAβCyD is more effective in complexing the cholesterol in the cell wall compared to non-modified β-CyD [185,186]. For hydrogels made of alginate and POAβCyD, cells exposed to hydrogels left in cell medium for 72 hours did not show a substantial toxicity, indicating that while a POAβCyD showed higher toxicity compared to free β-CyD, the gels made with POAβCyD did not leak out enough grafted material to give the same effect on toxicity.

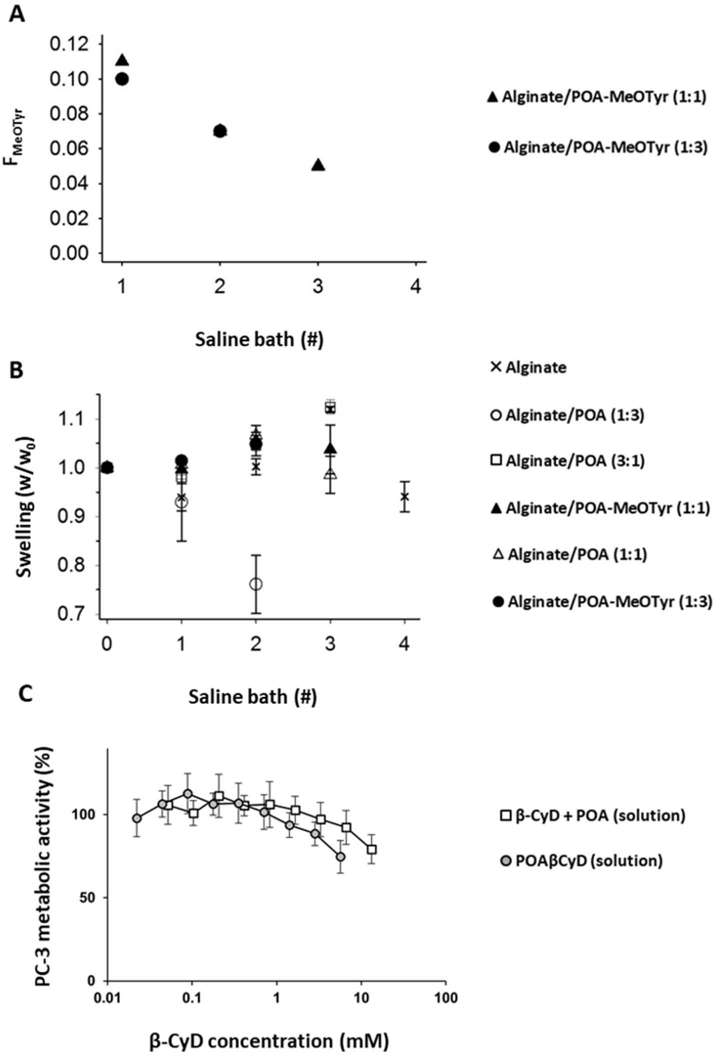

Figure 11. Leakage and swelling studies of grafted alginate hydrogels. A: Fraction of alginate grafted with L-Tyrosine methyl ester (F_{MeoTyr}) leaked out from 1.0% w/v alginate/POA-MeOTyr (P_0 = 0.08) mixed hydrogels (n = 5) after immersing the gels in consecutive baths of 0.15 M NaCl. B: Swelling (w/w$_0$) of 1.0% w/v alginate/POA (P_0 = 0.08) and alginate/POA-MeOTyr (P_0 = 0.08, DS = 7.0%) mixed hydrogels (*n* = 5) after consecutive NaCl treatments. One NaCl treatment: immersing the gels in 0.15 M NaCl for 24 hours. C: Cells were incubated with alginate functionalized with β-CyD (POAβCyD) solution and free β-CyD mixed with POA solution. Abbreviations: POA = partially oxidized alginate. P_0 = degree of oxidation. βCyD = β-cyclodextrin. POA-MeOTyr = POA grafted with L-Tyrosine methyl ester. POAβCyD = POA grafted with β-cyclodextrin.

4.4 Load and Release of Compounds from Alginate Hydrogels Functionalized with CyD

The benefit of the alginate hydrogel is its easy and gentle gelation, as well as its general biocompatibility [18]. However, the aqueous hydrogel also gives certain limitations on the load and release of different compounds. In this work, load and release of two different compounds were studied, methyl orange (presented in Paper I) and paclitaxel (presented in Paper III). Structures and molecular weight of these two compounds are given in Figure 12. The two compounds were selected to represent different extremes: Methyl orange is a smaller and more water-soluble molecule (water solubility ~15 mM at 20°C [187]) compared to paclitaxel (0.35 - 12 µM at 37°C in PBS-buffer [188]). Methyl orange is a color compound known to form an inclusion complex with CyDs [176,189] and was used as a preliminary test to examine if the β-CyD-grafted alginate (POAβCyD) was able to retain the functionality of the non-modified CyDs. It was possible to study the release both by visual inspection of the alginate beads and release medium, as well as quantify the amount of methyl orange released. Thereafter, it was interesting to examine the load and release of an actual drug, and paclitaxel was chosen as it also has the ability to form an inclusion complex with CyDs [190,191]. Furthermore, it is a highly hydrophobic anticancer drug and therefore difficult to load into an aqueous delivery system (such as a hydrogel).

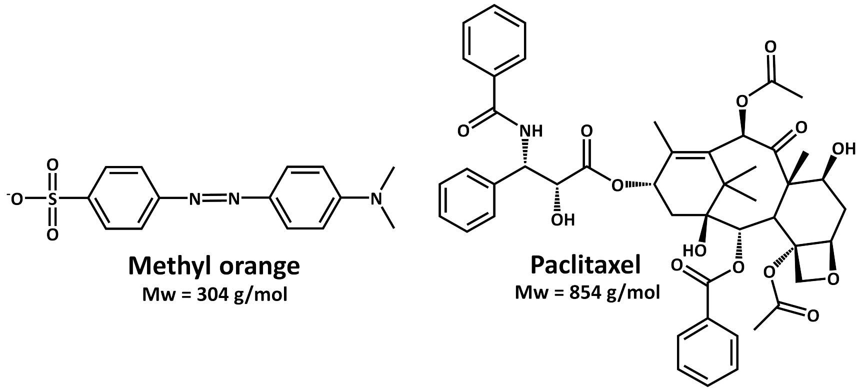

Figure 12. Structure and molecular weight of methyl orange and paclitaxel. Structures and molecular weights were obtained from ChemDraw. See also [176,192].

The two molecules methyl orange and paclitaxel thus gave insight into how the CyD-grafted alginate would handle load and release of both a small, relatively water-soluble compound and a larger hydrophobic molecule. As molecules with molecular weight below ~20 kDa are shown in literature to freely diffuse out of alginate hydrogels [138], the permeability of the gel is not expected to contribute to slowing down the release of either methyl orange or paclitaxel, and thus differences in load and release can be contributed to the CyDs.

For methyl orange, loading of the compound into the gel was done by dripping an alginate solution into a bath containing gelling ions and the color compound. Methyl orange could then simply diffuse into the beads. The concentration of methyl orange in the release medium was measured for each treatment.

The gel beads containing POAβCyD gave a higher release of methyl orange in the release medium (Figure 13, P1-2). For the first treatment POAβCyD-gels released 0.5 – 0.6 µmol compared to 0.3 µmol for the non-modified alginate gels. From the second treatment, release of methyl orange was only measured from POAβCyD-gels, ranging from 0.5 – 0.6 µmol for the second treatment and 0.1 – 0.4 µmol for the two last treatments. In addition, by visually inspecting the gel beads and release medium it was clear that gel beads containing POAβCyD gave both a higher and longer release over time as seen in

Figure 13, P3. This also strongly indicated that the load of methyl orange in grafted gel beads were higher compared to non-modified alginate (Alg) beads.

The concentration of methyl orange in the load solutions after the hydrogel beads were removed after loading was not possible to determine, possibly due to too high concentration of methyl orange. Even so, assuming a homogeneous distribution of methyl orange in the loading solution containing the alginate beads (140 µmol/L), the amount of methyl orange in the gel volume (3 mL) would be 0.4 µmol. The released methyl orange from the grafted beads (Figure 13) are 6.3 and 4.5 times higher than this for the beads containing 50% or 25% β-CyD-grafted alginate, respectively. This again indicates an accumulation of methyl orange in the beads with β-CyD-grafted alginate.

The study made with methyl orange and POAβCyD suggests that the modified hydrogel is a good system for slowing down the release of small water-soluble molecules if there is sufficient affinity for the CyDs, and also for loading more of the compound into the gel. The affinity the compound shows for the CyD cavity is an important factor and will influence the CyD-drug complex association and dissociation and subsequently the migration of the compound out of the hydrogel.

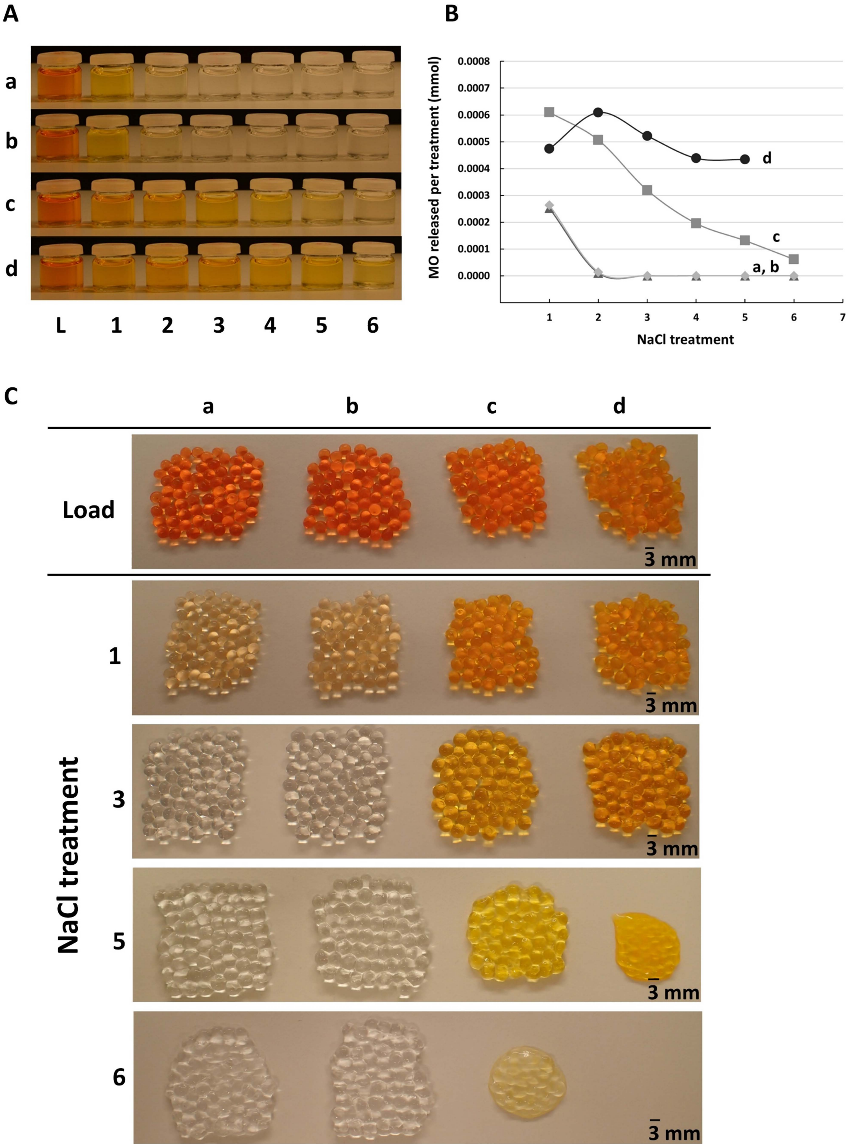

Figure 13. Release of methyl orange (MO) from Ca-alginate beads in consecutive NaCl treatments (0.9% (w/v) NaCl, one hour). A: Picture of loading solutions (L) and NaCl treatments (numbers 1–6) after removal of the beads. B: Quantified amount of MO in the treatment solutions. Lines are drawn to guide the eye. C: Beads after removal from the load-solution containing methyl orange (load) and gelling ions, and after consecutive immersion in the indicated number of 0.9% (w/v) NaCl treatment. Beads made of alginate (a), alginate + free β-CyD (b), alginate/β-CyD-grafted alginate (3:1 w/w) (c) and alginate/ β-CyD-grafted alginate (1:1 w/w) (d).

For paclitaxel the process of loading the drug into the hydrogel was more complicated due to the hydrophobic nature of the drug. A preliminary test was done to examine if the grafted alginate would help dissolve the paclitaxel. Paclitaxel was dissolved in ethanol before mixing with the alginate solution, and final paclitaxel and ethanol concentration in the alginate solutions were 28 µM and 3.7 % (v/v), respectively. The solutions consisted of either 1.5 % (w/v) Alg, 1.5 % (w/v) Alg/POAβCyD (1:1 w/w) or 2.0 % (w/v) Alg/POAβCyD (1:1 w/w). Initially, none of the samples showed signs of aggregation of the paclitaxel. After 20 hours of gentle mixing at ambient temperature all samples showed signs of paclitaxel crystallization. However, a much higher amount of paclitaxel crystals was observed in the non-modified alginate solution compared to the POAβCyD containing samples as seen in Figure 14. This strongly indicated that the grafted CyDs were able to form an inclusion complex with paclitaxel, thereby improving the solubility of the drug. Paclitaxel crystals can be stable for several months and are generally seen as detrimental for drug release [139].

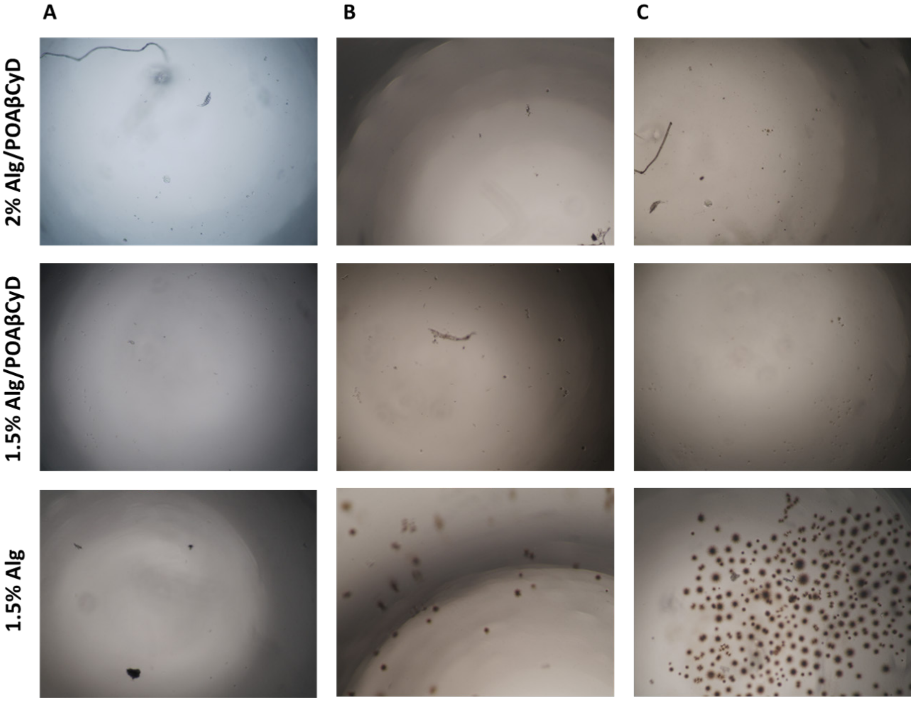

Figure 14. Light microscopy pictures (40x) of paclitaxel mixed into different alginate solutions (1.5% w/v or 2.0 % w/v polymer) immediately (A), after 2 ± 1 hours (B) and after 20 ± 1 hours (C). Solutions consisting of both alginate and β-CyD grafted alginate had a ratio of 1:1 (w/w). Abbreviations: Alg = stipe alginate. POAβCyD = β-CyD grafted alginate.

After the initial assessment had shown that the POAβCyD increased the solubility of paclitaxel in aqueous medium, the next step was to examine the load and release of the drug from alginate hydrogels. Here, the alginate hydrogels were made by internal gelation using the $CaCO_3$/GDL system. Paclitaxel was first dissolved in ethanol before the drug was mixed into the alginate solution, on the basis that this would give the most homogenous distribution of the drug throughout the gel. Thus, it could be of interest to see if the paclitaxel could be dissolved directly with the POAβCyD polymer in aqueous solution. However, as the amount of ethanol used here (up to 5.4% v/v) did not give precipitation of alginate and should not be detrimental to the inclusion complex between paclitaxel and cyclodextrin [140], no large issues with using ethanol as co-solvent is presumed for this work. Instead, the co-solvent should help dissolve the paclitaxel so that the drug is more readily available to interact with the grafted CyDs.

Alginate was mixed with paclitaxel, and thereafter gelation was started using the internal gelation method. The same amount of paclitaxel was added to the alginate samples before gelation start, and thus the final concentration of paclitaxel in the hydrogels were 25 µM. The gels were made of either alginate, Alg/POAβCyD (1:1 or 1:3 w/w) or alginate mixed with free HP-β-CyD or β-CyD. Crystal formation of paclitaxel was easily visible under a microscope (see Figure 15) and was also here used as a visual guide for determining the effect of CyDs on solubilizing the drug. As was the case with methyl orange, the Alg/POAβCyD hydrogels had a different effect on load capacity of the paclitaxel compared to hydrogels mixed with free CyDs. Very small amounts of crystals were observed for the Alg/POAβCyD hydrogels (1:3, 1.1 mM β-CyD), compared to the other hydrogels. As this included the Alg/POAβCyD hydrogels (1:1, 0.8 mM β-CyD), it seems that a paclitaxel:β-CyD molar ratio of 0.02 or lower should be used to deter paclitaxel crystallization for this particular system.

Interestingly, even though the concentration of CyDs in the gels mixed with HP-β-CyD (7.2 mM) was much higher compared to the Alg/POAβCyD hydrogels, more paclitaxel crystals were found in these gels. Again, this indicates that the POAβCyD is more efficient at dissolving paclitaxel. This could be due to a more effective paclitaxel:POAβCyD complex compared to paclitaxel:βCyD complex. Substitution β-CyDs with methyl groups for example, are shown to influence the solubility of cholesterol [185]. Furthermore, addition of water-soluble polymers to a drug/cyclodextrin solution can enhance the solubility of the drug, depending on the type and concentration of the polymer [193,194]. Even so, this would be interesting to investigate for the Alg + HPβCyD and Alg/POAβCyD systems used here. The enhanced efficacy of the Alg/POAβCyD gel may be due to an ability of the alginate to further stabilize the paclitaxel:βCyD complex since the polymer is already associated with the βCyDs. An increase in paclitaxel solubility has also been observed when comparing β-CyD-grafted hyaluronic acid with non-modified β-CyDs [195]. However, other effects such as differences in viscosity cannot be ruled out either. Initially, the Alg + HPβCyD solution had a higher viscosity compared to the Alg/POAβCyD solution, which may make it more difficult for the paclitaxel to find and interact with the cyclodextrin cavity.

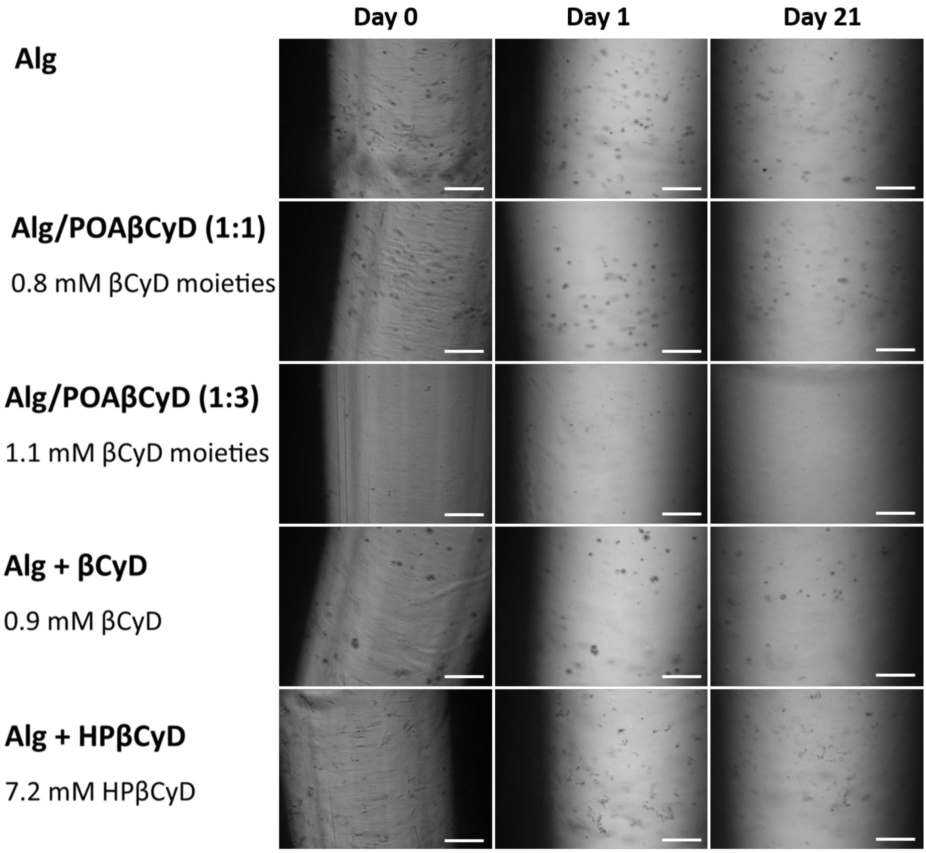

Figure 15. Paclitaxel crystals in alginate hydrogels. Gels shown at days 0 = one day after gelation start, but before addition of release medium, 1 = one day after the initial release medium was added to the system, and 21 = 21 days after the initial release medium was added to the system. The scalebar (white line) is equivalent to 500 µm. Abbreviations: Alg = alginate. POAβCyD = β-CyD grafted alginate. βCyD = β-cyclodextrin. HPβCyD = 2-hydroxypropyl β-cyclodextrin.

Release of paclitaxel from the different hydrogel systems were also done to examine if there was a difference in release from POAβCyD hydrogels and non-modified alginate hydrogels, and also to see if the released paclitaxel would affect cell viability. First, the hydrogels used to examine loading capability of paclitaxel were immersed in physiologically relevant medium at 37°C, where 200 µl of the release medium was examined after 1, 3, 6, 9, 15 and 21 days. Paclitaxel was released from all the gel systems, as is shown in Figure 16 A. In addition, the degradation products 7-epitaxol, 10-deacetyltaxol and baccatin III were also found [196], see Figure 16 B-D. In addition to paclitaxel, 7-epitaxol is also known to have anti-cancer properties [196]. To get a complete picture of the amount the drug released, all of its degradation products should ideally be quantified as well. However, these degradation products were not possible to quantify here due to lack of standards. Furthermore, paclitaxel can result in even more degradation products than found here [197]. In addition, the release medium and presence of CyDs can affect the type and amount of degradation product formed [196]. A further limitation for this experiment was that of the 300 µl release medium added to the gel samples at the start of the study, 200 µl were removed and replaced with fresh medium at each outtake. This means that some paclitaxel from the previous time-point was carried over to the next step. Hence, quantifying the precise amount of paclitaxel released from the hydrogels is not straightforward.

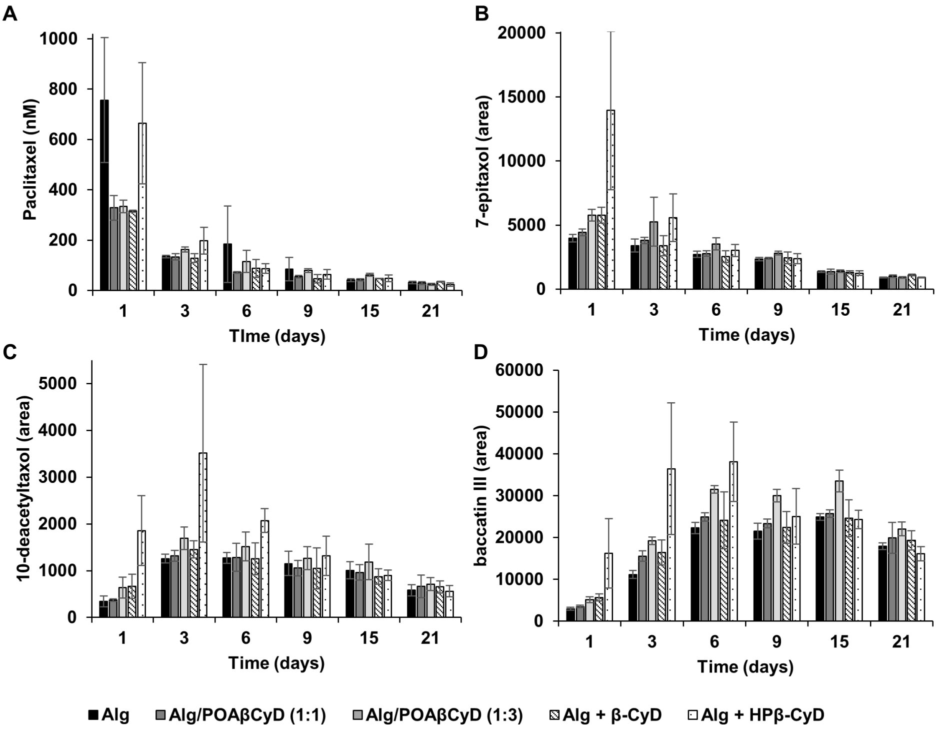

Figure 16. Drug release from hydrogels into physiologically relevant release medium at 37°C for 21 days. The concentration of paclitaxel (A) and integrals of the paclitaxel degradation products 7-epi-taxol (B), 10-deacetylytaxol (C) and baccatin III (D) found in release medium (mean +/- SD, n=3). Abbreviations: Alg = alginate. POAβCyD = β-CyD grafted alginate. βCyD = β-cyclodextrin. HPβCyD = 2-hydroxypropyl β-cyclodextrin.

Ideally, release studies should be done under sink conditions: The release medium should not limit the release of compounds from the gel due to saturation of the released drug compound, and thus the volume of the release medium should be three times higher than the volume required to solubilize the drug [188,198]. For PBS buffer, the solubility of paclitaxel is within the range of 0.35 - 12 µM at 37°C [188]. As the concentration of paclitaxel in the release medium would be 10 µM if everything was released at once, true sink conditions are not present. However, the solubility may be different in the release medium used, especially as the medium contained ethanol (< 1% v/v) since the gels were loaded with paclitaxel dissolved in ethanol.

Even so, a difference was seen in the amount of paclitaxel and degradation products released from the POAβCyD hydrogels compared to the other alginate gels. At day one, more paclitaxel was found in the release medium from the Alg gels (756 ± 248 nM) compared to the POAβCyD hydrogels (328 ± 49 and 333 ± 25 nM). After 21 days, on average 5% paclitaxel was found in the gels with highest amount of grafted alginate (Alg/POAβCyD, 1:3), and 18% paclitaxel was found in the Alg/POAβCyD (1:1) gels, see Figure 17. In comparison, 24% paclitaxel was found in the alginate gels. Small amounts of the degradation products were also found in most of the gels. As less drug was found in the POAβCyD gels compared to the alginate gels, this again suggests that the POAβCyD polymer helps to dissolve and transport paclitaxel out of the hydrogel.

For the HP-β-CyD gels more paclitaxel was also found in the release medium at day one, as well as higher amount of degradation products up to day six. This supports the conclusion that more drug is released from the gels containing free HP-β-CyD compared to the other samples, including the hydrogels mixed with free β-CyD. As both the concentration and water solubility of HP-β-CyD was higher (7.2 mM, water solubility > 860 mM) compared to that of β-CyD (0.9 mM, water solubility = 16 mM) [172], it was expected that HP-β-CyD would be more helpful in facilitating release of paclitaxel. When looking at the paclitaxel present in the hydrogels with either free HP-β-CyD or β-CyD, a large variation was seen in the leftover paclitaxel. This implies that there is a large variation in the amount of β-CyD or HP-β-CyD that diffuses out of the gel, and for more reproducible and predictable release the POAβCyD should be used instead.

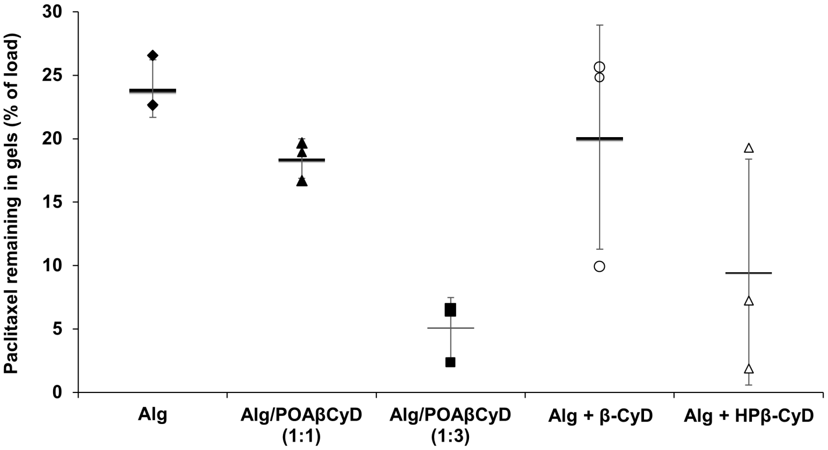

Figure 17. Paclitaxel remaining in the alginate hydrogels after being exposed to physiologically relevant medium for 21 days. Values shows amount of paclitaxel found in dissolved gels relative to the amount of the paclitaxel loaded into the hydrogels. Mean +/- SD, n=3. Abbreviations: Alg = alginate. POAβCyD = β-CyD grafted alginate. Β-CyD = β-cyclodextrin. HPβ-CyD = 2-hydroxypropyl β-cyclodextrin.

Release of the anticancer drug was examined in in vitro cell culture using prostate cancer cell line PC-3, as is shown in Figure 18. Based on the previous observations with regards to the mechanical integrity of the hydrogels, as well as the drug:CyD ratio that gave the most benefit in previous experiments, alginate hydrogels were made with a concentration of 2% (w/w) polymer and a ratio of Alg/POAβCyD of 1:1.

Alg/POAβCyD (1:1 w/w) and Alg hydrogels were loaded with 25 µM paclitaxel and immersed in culture medium. Cells were then exposed to the culture medium to determine how much paclitaxel was released from the gels. The paclitaxel release was 6.2 ± 2.7% for the alginate hydrogel and 11.2 ± 2.5% for the Alg/POAβCyD gel. The higher release from the Alg/POAβCyD gel can be explained by the visible formation of drug crystals in the Alg gels; due to increasing the solubility of paclitaxel in the POAβCyD gels the initial release was higher for these gels compared to the non-modified gels.

To determine how the release would look over a longer time, hydrogels loaded with paclitaxel (0.9, 7.2 and 25 µM), drug-free hydrogels and paclitaxel itself was exposed to PC3-cells for 72 hours. Neither Alg/POAβCyD or Alg hydrogels without paclitaxel gave an effect on the cell metabolic activity, while paclitaxel gave a decrease in metabolic activity dependent on the drug concentration. For the gels containing 0.9 and 7.2 µM paclitaxel, crystals were not visible in either type of hydrogel and release was comparable between the two systems. However, for gels loaded with 25 µM, paclitaxel crystals were again observed in the Alg gels but not in the Alg/POAβCyD gels. The Alg/POAβCyD gels gave a cell metabolic activity of 51.1 ± 19% compared to 71.8 ± 14.3% for the Alg gels. Even though the difference in release between the two gel systems were not statistically significant, when considering the other experiments, this is likely due to the help from the POAβCyD to dissolve the drug and facilitate release of paclitaxel, while the release form the Alg gels are hindered by paclitaxel crystal formation.

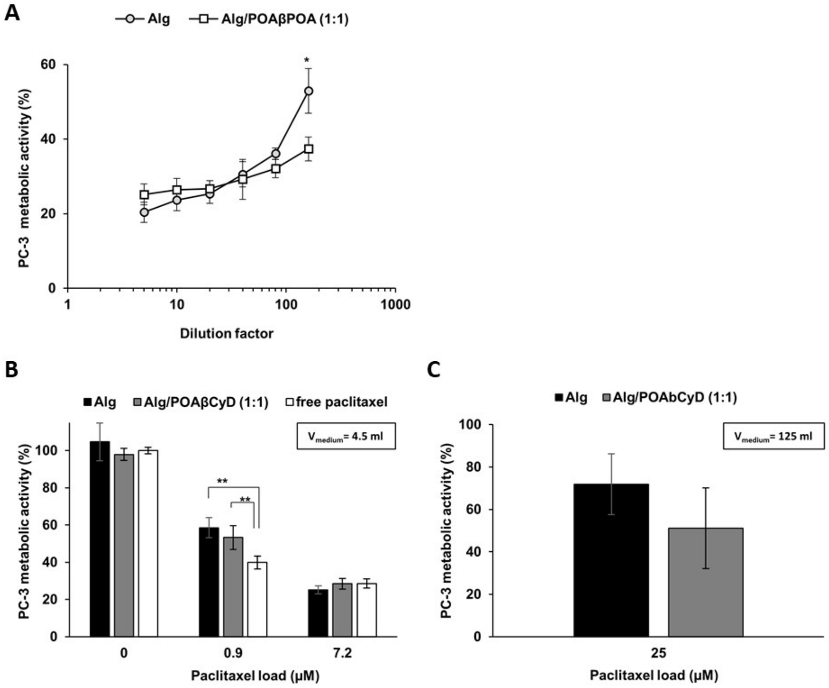

Figure 18. Metabolic activity of PC-3 cells. A: Cells were exposed to serial dilutions of 1-hour release media for paclitaxel loaded gels (25 µM) for 72 hours. B: Cells were exposed to the 50 µl gels loaded with 0, 0.9 and 7.2 µM paclitaxel for 72 hours (total volume of medium 4.5 ml). C: cells were exposed to 50 µl gels loaded with 25 µM paclitaxel for 72 hours (total volume of medium 125 ml). Cell metabolic activity is expressed as fluorescent intensities relative to a control (cells not exposed to paclitaxel were defined as 100%) after subtraction of non-cell-derived background. Data are expressed as mean ± SD, n = 2-8.

4.5 General considerations of alginate-CyD as drug delivery system

Alginate grafted with CyD can be attractive materials for the use in drug delivery systems, combining the activity of the alginate as an ionic crosslinking material or active oligomer with the ability of CyD to form inclusion complexes with drugs. Some examples of previously published alginate-CyD systems suggested for drug delivery is shown in Table 1. The formulations and applications span widely from hydrogels and nanoparticles, and topical applications to anti-cancer-treatment, respectively.

Different strategies of forming alginate-CyD systems include grafting of β-CyD to the carboxyl group of the uronic acids in the alginate polymers or oligomers [199–204], and by mixing alginate with HP-β-CyD for topical applications [205]. Further studies include grafting hydrophobic molecules onto the alginate chain and mixing it with HP-β-CyDs or polymeric β-CyDs which have been done for the formation of inclusion complexes with the hydrophobic moiety [206]. Crosslinking β-CyDs and alginate have been performed using epichlorohydrin [207] and substitution of alginate hydroxyl-groups with α-CyDs by activating the OH-groups with CNBr has also been performed [208]. For the direct covalent coupling of β-CyD to alginate, grafting of β-CyD to the carboxyl group of the alginate residues [199–204], or to G-blocks [209] has been investigated.

Table 1. Examples of different CyD-Alginate drug delivery systems.

Overview of System	**Drug**	**Ref.**
Nanosystem. Alginate + piperazine NPs conjugated with ptx:β-CyD complexes and trastuzumab (monoclonal antibody that binds to HER2). Targeted for cancer cells that overexpress human epidermal growth factor receptor-2 (HER2), internalized by endocytosis. Tested in vitro.	Paclitaxel	[210]
Compact polyelectrolyte complex (CoPECs). β-CyD-functionalized chitosan/alginate CoPEC. Drug delivery with anti-inflammatory properties. Load and release of hydrophobic drug piroxicam possible, but concentration of drug too low to increase the intrinsic inflammatory properties of the β-CyD-chitosan/alginate CoPEC. For inflammatory chronic diseases. Tested in vitro.	Piroxicam	[211]
***in situ* gel-system.** Alginate + HP-β-CyD for ocular delivery of the anti-inflammatory drug nepafenac. Tested *ex vivo*.	Nepafenac	[212]
Hydrogel. Alginate hydrogel mixed with HP-β-CyD/drug for topical alopecia treatment. Tested in vitro + ex vivo.	Minoxidil	[205]
Nanoparticles. Alginate-β-CyD NPs for release of anticancer drug. Tested in vitro.	5-fluorouracil	[213]
Nanoflowers. Cationic β-CyDs/alginate/chitosan polyelectrolyte complex. Tested in vitro.	5-fluorouracil	[214]
Micro- and nanoparticles. Alginate-chitosan-β-CyD MPs and NPs loaded with anti-tuberculosis compounds. Tested in vitro.	Isoniazid and Isoconazole nitrate	[215]
Hydrogel. Release of anti-emetic drug by mechanical compression of β-CyD-crosslinked alginate gel. Tested in vitro.	Ondansetron	[201]

It has previously been shown that grafting of alginate using reductive oxidation and subsequent reductive amination results in higher degree of grafting than using carbodiimide chemistry [33]. Hence, in this thesis we aimed at investigating the chemical modification of alginate with CyD and increasing the degree of grafting from previous studies by using a strategy of grafting linker and using click-chemistry on oxidized alginate (Paper I). Furthermore, we performed grafting of CyD to the reducing end of block oligomers (Paper IV). The study presented here on the CyD-grafted alginate are in the beginning phases, and as such several challenges still needs to be examined or optimized. First of all, even though the grafting procedure worked well, it could potentially be optimized further by choosing another linker such as the alkyne hydrazide linker detailed in section 4.2. In addition, Cu-free click chemistry would also be interesting to explore as this eliminates the problems with Cu/alginate oligomers interaction, as well as ensuring no toxic Cu-ions remain in the finished product [86,182,216]. The CyD-grafted alginate made here was treated with Ambersep GT74 resin to remove residual copper-ions, but for future use an ICP-MS element test of the sample could be beneficial to characterize if any copper-ions remained in the sample after this step to further verify the purification. As long as the copper-ions are removed before placing the material in the body, the CuAAC-reaction poses no problem for attaching CyDs to alginate polymers.

For the CyD-grafted alginate hydrogels, further optimization of the loading process of paclitaxel into the hydrogel could be beneficial. Here, factors such as mixing time before gelation, temperature and viscosity could possibly influence the amount and homogeneity of dissolved paclitaxel loaded into the CyD-grafted alginate hydrogel. Viscosity of the system can for example be largely controlled by the mix ratio used of non-modified alginate and CyD-grafted alginate. For ease of mixing and delivery, it is important to control the starting viscosity of the material. A high viscosity could potentially help hinder settling of the drug but also make mixing and injection difficult. The CyD-grafted alginate showed a lower viscosity compared to the non-modified alginate used here, likely due to being partially depolymerized during the synthesis, and as such a higher concentration of grafted alginate could be used compared to non-modified alginate which again would lead to a higher amount of CyD present in the gel. Partially depolymerization of the non-modified alginate could also be explored so that even more grafted material potentially could be included in the hydrogel system. However, it is extremely important that the effect of these changes on the mechanical properties of the hydrogels is also controlled, as is outlined in section 3.3.

The delivery method of the hydrogel should also be further assessed. For use as an injectable system, it is necessary to verify that the gelation time is so that the hydrogel solution can be injected with ease, but it is also important that the gel forms and stays where it is injected, e.g. the gel should not be washed away by bodily fluids or by moving parts, but be able to stay and settle at the injection site.

The degradation of the hydrogel in vivo is also an important parameter to control for controlled delivery of drugs. In this study, we investigated the in vitro stability of the hydrogels, showing that the gels would release grafted materials and disintegrate upon exposure to physiological saline solution (Paper I and II). It is not obvious how this compares to in vivo stability, as small concentrations of calcium (1-2 mM) in vivo would stabilize the ionic crosslinks of the hydrogel [118]. Hence, the disintegration of the gel in vivo needs further investigations, but can be tailored by the fraction of oxidized and grafted alginate as shown in Paper II, as well as the selection of gelling ions [98].

For a drug delivery system related to multiple injections, it may be desirable to have a system that can be cleared from the body over time, firstly by disintegration of the gel and secondly by the clearance of the polymers. For the clearance of the alginate or grafted alginates from the body, no enzymatic degradation in humans is known [123]. Hence, the degradation of the polymers will be by natural hydrolysis and potentially by the exposure to radicals. Hydrolysis of alginate is slow at physiological pH, and recent work has shown that despite increased degradation rate of oxidized alginates, the reduction upon grafting results in polymers with similar degradation rates as native alginate for hydrolysis [71]. Alginates with a low molecular weight, about 50 kDa, is naturally removed from the body by renal clearance [123], hence degradation of the polymer will increase the clearance of alginate. Also, by using oligomers for the grafting as shown in paper IV these could potentially be used for modulation of drug solubility by themselves or by implementing in the hydrogel systems to control both drug loading, release and disintegration of the hydrogels [52,217]. However, the influence of the CyDs on the clearance of alginate oligomers is not known and needs further investigation.

Paclitaxel was the only drug tested in the CyD-grafted alginate hydrogels created here. However, as was also shown with the molecule methyl orange, other substances or drugs that are able to form inclusion complexes with β-CyD may be interesting to test with this system. β-CyD is capable of forming inclusion complexes with aromatics and heterocycles and is commonly used in the pharmaceutical industry [140]. Some examples of other alginate-CyD systems are summarized in Table 1, demonstrating the many different drugs that can complex with CyDs. Anti-cancer drugs other than paclitaxel that are able to form an inclusion complex with CyDs, such as doxorubicin, cisplatin and zerumbone, are for example interesting [218].

By using other CyDs than β-CyD, the system can be tailored to other drugs and release profiles, enhancing the versatility of the system even further. It would also be interesting for future work to take a closer look at the release profile of paclitaxel (or other relevant drugs) from the CyD-grafted alginate and use different release models [219] to determine the kinetics of release the CyD-functionalized hydrogel gives. Eventually, the CyD-grafted alginate/paclitaxel system should also be benchmarked against commercially available delivery systems of paclitaxel, such as Taxol [2,220]. Previous literature has already shown that hydrogels can be made by crosslinking polymers using CyDs and appropriate guest molecule attached to different polymers [221,222]. This could also be interesting to examine using alginate hydrogels, and to study whether this can be used to alter for example gel strength or stability. Potentially the ratio between CyDs and guest molecule could be adjusted so that also drug molecules could interact with the gel. Furthermore, the CyD-grafted alginate could potentially be used for other purposes than drug delivery, for example for waste cleanup where both the CyDs and alginate may help sequester hazardous substances [223,224].

5. Conclusion

The scope of this work was to understand if CyD could be grafted to alginate while still preserving the functionality of both molecules, and to further test the material properties in a drug delivery system. Alginate was grafted with CyD in a three-step reaction with oxidation (1) followed by linker attachment using reductive amination (2) and finally attachment of CyD to the linker via click chemistry (3). This resulted in a grafting degree of 1.6 – 4.7% mol CyD/mol sugar residues for lateral substitution. In addition, terminal functionalization of M- and MG-oligomers was achieved using alkyne hydrazide and click-chemistry with a coupling degree ranging from 27 – 45% of the reducing ends. The grafting of G-oligomers was not successful as the Cu^{2+} necessary for the click reaction complexed with the G-oligomers and was therefore not available for the reaction. Although the synthesis can be further optimized, the grafting is tunable and results in none or minimal byproducts. Additionally, alginate was functionalized with either the RGD-peptide GRGDSP commonly used for cell attachment, or L-Tyrosine methyl ester (MeOTyr) used as a model small-size substitute.

The grafted alginates, including CyD and peptide-grafted alginates, were still able to form calcium-crosslinked hydrogels. Gels made with a chemoenzymatic method, functionalized with MeOTyr, were visually more well maintained and needed a higher stress to rupture compared to the gels consisting of only chemically modified alginate. Even so, all grafted alginates still showed a large decrease in mechanical strength and stability compared to non-modified alginate. For gels made with a mixture of non-modified and grafted alginates, increasing the oxidation degree or fraction of modified alginate in the gel systems decreased the mechanical strength, giving Young's modulus in the range of 1-31 kPa. Furthermore, grafted material was found to leak out of the gels. Overall, the mechanical properties and stability were possible to tune by mixing different ratios and type of functionalized alginate and non-modified alginate.

The CyD-functionalized alginate hydrogels were able to interact with the hydrophobic anticancer drug paclitaxel and the more water-soluble color compound methyl orange, likely by CyD forming inclusion complexes with these compounds. For methyl orange, the grafted CyDs helped retain the compound in the hydrogel and gave a higher and longer release compared to non-modified gels. With regards to paclitaxel, the CyD-grafted alginate helped stabilize the drug and hinder crystal formation, which is important for facilitating release of the drug. In addition, the CyD-functionalized hydrogels showed a greater impact on cell metabolic activity and had less drug remaining in gels after end of release studies when compared to non-modified alginate gels, depending on paclitaxel concentration.

Overall, it was shown that CyD grafted alginates could be synthesized and retain their initial properties of ionic gelation and drug inclusion, and impact on drug loading and release was demonstrated for both methyl orange and paclitaxel. Albeit showing effects on paclitaxel crystal formation and release, the limited retention of paclitaxel in the β-CyD hydrophobic cavity and rapid degradation of paclitaxel makes other CyD-drug combinations relevant to test. Future work should also include in vivo studies (e.g. tumor models in mice) of the materials and relevant drugs as in vitro effectiveness of drug release gives limited information on in vivo performance. Furthermore, the compatibility of the material with the host tissue and immune system as well as the in vivo degradation and potential accumulation and toxicity of the grafted polymers needs to be determined before relevant clinical testing.

References

1. Senapati S, Mahanta AK, Kumar S, Maiti P. Controlled drug delivery vehicles for cancer treatment and their performance. Signal Transduction and Targeted Therapy. 2018;3: 7. doi:10.1038/s41392-017-0004-3

2. Ezrahi S, Aserin A, Garti N. Basic principles of drug delivery systems – the case of paclitaxel. Advances in Colloid and Interface Science. 2019;263: 95–130. doi:10.1016/J.CIS.2018.11.004

3. van der Merwe J, Steenekamp J, Steyn D, Hamman J. The Role of Functional Excipients in Solid Oral Dosage Forms to Overcome Poor Drug Dissolution and Bioavailability. Pharmaceutics. 2020;12: 393. doi:10.3390/pharmaceutics12050393

4. Li C, Wang J, Wang Y, Gao H, Wei G, Huang Y, et al. Recent progress in drug delivery. Acta Pharmaceutica Sinica B. 2019;9: 1145–1162. doi:10.1016/J.APSB.2019.08.003

5. Fenton OS, Olafson KN, Pillai PS, Mitchell MJ, Langer R. Advances in Biomaterials for Drug Delivery. Advanced Materials. 2018;30: 1705328. doi:10.1002/adma.201705328

6. Webber MJ, Langer R. Drug delivery by supramolecular design. Chemical Society Reviews. 2017;46: 6600–6620. doi:10.1039/C7CS00391A

7. Hennenfent KL, Govindan R. Novel formulations of taxanes: a review. Old wine in a new bottle? Annals of Oncology. 2006;17: 735–749. doi:10.1093/ANNONC/MDJ100

8. Park K. Controlled drug delivery systems: Past forward and future back. Journal of Controlled Release. Elsevier B.V.; 2014. pp. 3–8. doi:10.1016/j.jconrel.2014.03.054

9. Li J, Mooney DJ. Designing hydrogels for controlled drug delivery. Nature reviews Materials. 2016/10/18. 2016;1: 16071. doi:10.1038/natrevmats.2016.71

10. Hoare TR, Kohane DS. Hydrogels in drug delivery: Progress and challenges. Polymer. 2008;49: 1993–2007. doi:10.1016/J.POLYMER.2008.01.027

11. Hoffman AS. Drug Delivery Systems. In: Hoffman AS, editor. Biomaterials Science. 2013. pp. 1024–1027. doi:10.1016/B978-0-08-087780-8.00088-7

12. Dimatteo R, Darling NJ, Segura T. In situ forming injectable hydrogels for drug delivery and wound repair. Advanced Drug Delivery Reviews. 2018;127: 167–184. doi:10.1016/J.ADDR.2018.03.007

13. Tibbitt MW, Dahlman JE, Langer R. Emerging Frontiers in Drug Delivery. Journal of the American Chemical Society. 2016;138: 704–717. doi:10.1021/jacs.5b09974

14. Vargason AM, Anselmo AC, Mitragotri S. The evolution of commercial drug delivery technologies. Nature Biomedical Engineering. 2021. doi:10.1038/s41551-021-00698-w

15. García-Astrain C, Avérous L. Synthesis and evaluation of functional alginate hydrogels based on click chemistry for drug delivery applications. Carbohydrate Polymers. 2018;190: 271–280. doi:10.1016/J.CARBPOL.2018.02.086

16. Lee KY, Mooney DJ. Alginate: properties and biomedical applications. Progress in polymer science. 2012;37: 106–126. doi:10.1016/j.progpolymsci.2011.06.003

17. Tønnesen HH, Karlsen J. Alginate in drug delivery systems. Drug Development and Industrial Pharmacy. 2002;28: 621–630.

18. Andersen T, Strand BL, Formo K, Alsberg E, Christensen BE. Alginates as biomaterials in tissue engineering. In: Rauter AP, Lindhorst TK, editors. Carbohydrate Chemistry Chemical and Biological Approaches. Cambridge: The Royal Society of Chemistry; 2012. pp. 227–258.

19. Espevik T, Skjåk-Bræk G. Application of alginate gels in biotechnology and biomedicine. Carbohydrates in Europe. 1996;14: 19–25.

20. Nielsen AL, Madsen F, Larsen KL. Cyclodextrin modified hydrogels of PVP/PEG for sustained drug release. Drug Deliv. 2009;16: 92–101.

21. Woldum HS, Larsen KL, Madsen F. Cyclodextrin controlled release of poorly water-soluble drugs from hydrogels. Drug Deliv. 2008;15: 69–80.

22. Loftsson T, Magnúsdóttir A, Másson M, Sigurjónsdóttir JF. Self-Association and Cyclodextrin Solubilization of Drugs. Journal of Pharmaceutical Sciences. 2002;91: 2307–2316. doi:10.1002/jps.10226

23. Szejtli J. Introduction and general overview of cyclodextrin chemistry. Chemical Reviews. 1998;98: 1743–1753.

24. Draget KI, Moe ST, Skjåk-Bræk G, Smidsrød O. Alginates. In: Stephen AM, Phillips GO, Williams PA, editors. Food Polysaccharides and Their Applications. Boca Raton: CRC Press; 2006. pp. 289–334.

25. Gorin PAJ, Spencer JFT. EXOCELLULAR ALGINIC ACID FROM AZOTOBACTER VINELANDII. Canadian Journal of Chemistry. 1966;44: 993–998. doi:10.1139/v66-147

26. Pindar DF, Bucke C. The biosynthesis of alginic acid by Azotobacter vinelandii. The Biochemical journal. 1975;152: 617–622. doi:10.1042/bj1520617

27. Ramsey DM, Wozniak DJ. Understanding the control of Pseudomonas aeruginosa alginate synthesis and the prospects for management of chronic infections in cystic fibrosis. Molecular microbiology. 2005;56: 309–322. doi:10.1111/j.1365-2958.2005.04552.x

28. Stanford ECC. Algin: A New Substance Obtained from Some of the Commoner Species of Marine Algæ. Scientific American. 1883;16: 6323–6324.

29. Augst AD, Kong HJ, Mooney DJ. Alginate hydrogels as biomaterials. Macromolecular bioscience. 2006;6: 623–633.

30. Draget KI, Taylor C. Chemical, physical and biological properties of alginates and their biomedical implications. Food Hydrocolloids. 2011;25: 251–256. doi:10.1016/j.foodhyd.2009.10.007

31. Mouritsen OG. Tang Grøntsager fra havet. 1. udgave,. Hansen S, editor. København: Nyt Nordisk Forlag; 2015. pp. 210–224.

32. Skjåk-Bræk G, Donati I, Paoletti S. Alginate Hydrogels: Properties and Applications. Polysaccharide Hydrogels Characterization and Biomedical Applications. Singapore: Pan Stanford; 2016. pp. 449–498. doi:doi:10.1201/b19751-14

33. Dalheim MØ, Vanacker J, Najmi MA, Aachmann FL, Strand BL, Christensen BE. Efficient functionalization of alginate biomaterials. Biomaterials. 2016;80: 146–156. doi:10.1016/j.biomaterials.2015.11.043

34. Rowley JA, Mooney DJ. Alginate type and RGD density control myoblast phenotype. Journal of Biomedical Materials Research. 2002;60: 217–223. doi:10.1002/jbm.1287

35. Sandvig I, Karstensen K, Rokstad AM, Aachmann FL, Formo K, Sandvig A, et al. RGD-peptide modified alginate by a chemoenzymatic strategy for tissue engineering applications. Journal of Biomedical Materials Research Part A. 2015;103: 896–906. doi:https://doi.org/10.1002/jbm.a.35230

36. Bouhadir KH, Kruger GM, Lee KY, Mooney DJ. Sustained and Controlled Release of Daunomycin from Cross-Linked Poly(aldehyde guluronate) Hydrogels. Journal of Pharmaceutical Sciences. 2000;89: 910–919. doi:10.1002/1520-6017(200007)89:7<910::AID-JPS8>3.0.CO;2-#

37. Vegas AJ, Veiseh O, Gurtler M, Millman JR, Pagliuca FW, Bader AR, et al. Long-term glycemic control using polymer-encapsulated human stem cell-derived beta cells in immune-competent mice. Nat Med. 2016;22: 306–311. Available: http://dx.doi.org/10.1038/nm.4030

38. Smidsrød O, Moe ST. Biopolymer chemistry. Postmyr L, editor. Trondheim: Tapir Academic Press, (Chapter 11): Tapir Academic Press; 2008. pp. 86–385.

39. Grasdalen H. High-field, 1H-n.m.r. spectroscopy of alginate: sequential structure and linkage conformations. Carbohydrate Research. 1983;118: 255–260. doi:10.1016/0008-6215(83)88053-7

40. Grasdalen H, Larsen B, Smidsrød O. 13C-N.M.R. studies of monomeric composition and sequence in alginate. Carbohydrate Research. 1981;89: 179–191.

41. Haug A, Larsen B, Smidsrød O. Studies on the Sequence of Uronic Acid Residues in Alginic Acid. Acta Chemica Scandinavica. 1967;21: 691–704. doi:10.3891/acta.chem.scand.21-0691

42. Haug A, Larsen B, Smidsrød O. A Study of the Constitution of Alginic Acid by Partial Acid Hydrolysis. Acta Chemica Scandinavica. 1966;20: 183–190. Available: http://actachemscand.dk/pdf/acta_vol_20_p0183-0190.pdf

43. Atkins EDT, Mackie W, Smolko EE. Crystalline Structures of Alginic Acids. Nature. 1970;225: 626–628. doi:10.1038/225626a0

44. Grasdalen H, Larsen B, Smidsrød O. 13C-N.m.r. studies of alginate. Carbohydrate Research. 1977;56: C11–C15. doi:10.1016/S0008-6215(00)83369-8

45. Haug A. Composition and Properties of Alginates. Norwegian Institute of Seaweed Research. 1964;30.

46. Haug A, Larsen B, Smidsrød O. Uronic acid sequence in alginate from different sources. Carbohydrate Research. 1974;32: 217–225. doi:https://doi.org/10.1016/S0008-6215(00)82100-X

47. Smidsrød O, Skjåk-Bræk G. Alginate as immobilization matrix for cells. Trends in Biotechnology. 1990;8: 71–78. doi:http://dx.doi.org/10.1016/0167-7799(90)90139-O

48. Skjåk-Bræk G, Grasdalen H, Larsen B. Monomer sequence and acetylation pattern in some bacterial alginates. Carbohydrate Research. 1986;154: 239–250. doi:10.1016/S0008-6215(00)90036-3

49. Grasdalen H, Larsen B, Smidsrød O. A p.m.r. study of the composition and sequence of uronate residues in alginates. Carbohydrate Research. 1979;68: 23–31. doi:10.1016/S0008-6215(00)84051-3

50. Kristiansen KA, Schirmer BC, Aachmann FL, Skjåk-Bræk G, Draget KI, Christensen BE. Novel alginates prepared by independent control of chain stiffness and distribution of G-residues: Structure and gelling properties. Carbohydrate Polymers. 2009;77: 725–735. doi:https://doi.org/10.1016/j.carbpol.2009.02.018

51. Aarstad OA, Stanisci A, Sætrom GI, Tøndervik A, Sletta H, Aachmann FL, et al. Biosynthesis and Function of Long Guluronic Acid-Blocks in Alginate Produced by Azotobacter vinelandii. Biomacromolecules. 2019;20: 1613–1622. doi:10.1021/acs.biomac.8b01796

52. Aarstad O, Strand BL, Klepp-Andersen LM, Skjåk-Bræk G. Analysis of G-Block Distributions and Their Impact on Gel Properties of in Vitro Epimerized Mannuronan. Biomacromolecules. 2013;14: 3409–3416. doi:10.1021/bm400658k

53. Aarstad OA, Tøndervik A, Sletta H, Skjåk-Bræk G. Alginate sequencing: an analysis of block distribution in alginates using specific alginate degrading enzymes. Biomacromolecules. 2012;13: 106–116.

54. Bidarra SJ, Barrias CC, Granja PL. Injectable alginate hydrogels for cell delivery in tissue engineering. Acta Biomaterialia. 2014;10: 1646–1662. doi:10.1016/J.ACTBIO.2013.12.006

55. Draget KI, Østgaard K, Smidsrød O. Homogeneous alginate gels: A technical approach. Carbohydrate Polymers. 1990;14: 159–178. doi:10.1016/0144-8617(90)90028-Q

56. Vold IM, Kristiansen KA, Christensen BE. A study of the chain stiffness and extension of alginates, in vitro epimerized alginates, and periodate-oxidized alginates using size-exclusion chromatography combined with light scattering and viscosity detectors. Biomacromolecules. 2006;7: 2136–2146. doi:10.1021/bm060099n

57. Haug A, Smidsrød O. Determination of Intrinsic Viscosity of Alginates. Acta Chemica Scandinavica. 1962;16: 1569–1578.

58. Smidsrød O. Solution properties of alginate. Carbohydrate Research. 1970;13: 359–372. doi:https://doi.org/10.1016/S0008-6215(00)80593-5

59. Broderick E, Lyons H, Pembroke T, Byrne H, Murray B, Hall M. The characterisation of a novel, covalently modified, amphiphilic alginate derivative, which retains gelling and non-toxic properties. Journal of Colloid and Interface Science. 2006;298: 154–161. doi:10.1016/J.JCIS.2005.12.026

60. Arlov O, Aachmann FL, Sundan A, Espevik T, Skjåk-Bræk G. Heparin-Like Properties of Sulfated Alginates with Defined Sequences and Sulfation Degrees. Biomacromolecules. 2014;15: 2744–2750. doi:Doi 10.1021/Bm500602w

61. Bayer EA, Ben-Hur H, Wilchek M. Biocytin hydrazide—A selective label for sialic acids, galactose, and other sugars in glycoconjugates using avidin-biotin technology. Analytical Biochemistry. 1988;170: 271–281. doi:https://doi.org/10.1016/0003-2697(88)90631-8

62. Mo IV, Feng Y, Øksnes Dalheim M, Solberg A, Aachmann FL, Schatz C, et al. Activation of enzymatically produced chitooligosaccharides by dioxyamines and dihydrazides. Carbohydrate Polymers. 2020;232: 115748. doi:10.1016/J.CARBPOL.2019.115748

63. Zhang H, Li X, Martin DB, Aebersold R. Identification and quantification of N-linked glycoproteins using hydrazide chemistry, stable isotope labeling and mass spectrometry. Nature Biotechnology. 2003;21: 660–666. doi:10.1038/nbt827

64. Solberg et al. Manuscript in Preparation. 2021.

65. Bouhadir KH, Kruger GM, Mooney DJ. Hydrogels and water soluble polymeric carriers for drug delivery. United States Patent - US 7,186,413 B2. 2007.

66. Smidsrød O, Painter T. Effect of periodate oxidation upon the stiffness of the alginate molecule in solution. Carbohydrate Research. 1973;26: 125–132. doi:https://doi.org/10.1016/S0008-6215(00)85029-6

67. Kristiansen KA, Potthast A, Christensen BE. Periodate oxidation of polysaccharides for modification of chemical and physical properties. Carbohydrate Research. 2010;345: 1264–1271.

68. Gomez CG, Rinaudo M, Villar MA. Oxidation of sodium alginate and characterization of the oxidized derivatives. Carbohydrate Polymers. 2007;67: 296–304. doi:https://doi.org/10.1016/j.carbpol.2006.05.025

69. Painter T, Larsen B. Formation of Hemiacetals between Neighbouring Hexuronic Acid Residues during the Periodate Oxidation of Alginate. Acta Chemica Scandinavica. 1970;24: 813–833. doi:10.3891/acta.chem.scand.24-0813

70. Boontheekul T, Kong H-J, Mooney DJ. Controlling alginate gel degradation utilizing partial oxidation and bimodal molecular weight distribution. Biomaterials. 2005;26: 2455–2465. doi:10.1016/J.BIOMATERIALS.2004.06.044

71. Dalheim MØ, Ulset A-ST, Jenssen IB, Christensen BE. Degradation kinetics of peptide-coupled alginates prepared via the periodate oxidation reductive amination route. Carbohydrate Polymers. 2017;157: 1844–1852. doi:10.1016/J.CARBPOL.2016.11.068

72. Sun Z, Wei Z, Wei K. A model for predicting the optimal conditions for labeling the carbohydrates with the amine derivatives by reductive amination. Letters in Organic Chemistry. 2009;6: 549–551.

73. Yang J-S, Xie Y-J, He W. Research progress on chemical modification of alginate: A review. Carbohydrate Polymers. 2011;84: 33–39. doi:10.1016/J.CARBPOL.2010.11.048

74. Ruhaak LR, Steenvoorden E, Koeleman CAM, Deelder AM, Wuhrer M. 2-picoline-borane: a non-toxic reducing agent for oligosaccharide labeling by reductive amination. Proteomics. 2010;10: 2330–2336. doi:10.1002/pmic.200900804

75. Sato S, Sakamoto T, Miyazawa E, Kikugawa Y. One-pot reductive amination of aldehydes and ketones with α-picoline-borane in methanol, in water, and in neat conditions. Tetrahedron. 2004;60: 7899–7906. doi:10.1016/J.TET.2004.06.045

76. Schatz C, Lecommandoux S. Polysaccharide-containing block copolymers: synthesis, properties and applications of an emerging family of glycoconjugates. Macromolecular rapid communications. 2010;31: 1664–1684. doi:10.1002/marc.201000267

77. Liang L, Astruc D. The copper(I)-catalyzed alkyne-azide cycloaddition (CuAAC) “click” reaction and its applications. An overview. Coordination Chemistry Reviews. 2011;255: 2933–2945. doi:10.1016/J.CCR.2011.06.028

78. Rostovtsev V v, Green LG, Fokin V v, Sharpless KB. A Stepwise Huisgen Cycloaddition Process: Copper(I)-Catalyzed Regioselective “Ligation” of Azides and Terminal Alkynes. Angewandte Chemie International Edition. 2002;41: 2596–2599.

79. Tornøe CW, Christensen C, Meldal M. Peptidotriazoles on Solid Phase: [1,2,3]-Triazoles by Regiospecific Copper(I)-Catalyzed 1,3-Dipolar Cycloadditions of Terminal Alkynes to Azides. The Journal of Organic Chemistry. 2002;67: 3057–3064. doi:10.1021/jo011148j

80. Kolb HC, Finn MG, Sharpless KB. Click Chemistry: Diverse Chemical Function from a Few Good Reactions. Angewandte Chemie International Edition. 2001;40: 2004–2021. doi:10.1002/1521-3773(20010601)40:11<2004::AID-ANIE2004>3.0.CO;2-5

81. Chan TR, Hilgraf R, Sharpless KB, Fokin V v. Polytriazoles as Copper(I)-Stabilizing Ligands in Catalysis. Organic Letters. 2004;6: 2853–2855. doi:10.1021/ol0493094

82. Hein JE, Fokin V v. Copper-catalyzed azide-alkyne cycloaddition (CuAAC) and beyond: new reactivity of copper(I) acetylides. Chemical Society Reviews. 2010;39: 1302–1315. doi:Doi 10.1039/B904091a

83. Nielsen TT, Wintgens V, Amiel C, Wimmer R, Larsen KL. Facile Synthesis of beta-Cyclodextrin-Dextran Polymers by “Click” Chemistry. Biomacromolecules. 2010;11: 1710–1715. doi:10.1021/bm9013233

84. Agalave SG, Maujan SR, Pore VS. Click Chemistry: 1,2,3-Triazoles as Pharmacophores. Chemistry – An Asian Journal. 2011;6: 2696–2718. doi:10.1002/asia.201100432

85. Meldal M, Tornøe CW. Cu-catalyzed azide-alkyne cycloaddition. Chemical reviews. 2008;108: 2952–3015.

86. Krause A, Kirschning A, Dräger G. Bioorthogonal metal-free click-ligation of cRGD-pentapeptide to alginate. Organic & Biomolecular Chemistry. 2012;10: 5547–5553. doi:10.1039/C2OB25604E

87. Lueckgen A, Garske DS, Ellinghaus A, Desai RM, Stafford AG, Mooney DJ, et al. Hydrolytically-degradable click-crosslinked alginate hydrogels. Biomaterials. 2018;181: 189–198. doi:10.1016/J.BIOMATERIALS.2018.07.031

88. Campa C, Holtan S, Nilsen N, Bjerkan TM, Stokke BT, Skjåk-Bræk G. Biochemical analysis of the processive mechanism for epimerization of alginate by mannuronan C-5 epimerase AlgE4. The Biochemical journal. 2004;381: 155–164. doi:10.1042/BJ20031265

89. Chitnis CE, Ohman DE. Cloning of Pseudomonas-Aeruginosa AlgG, Which Controls Alginate Structure. J Bacteriol. 1990;172: 2894–2900.

90. Ertesvåg H, Doseth B, Larsen B, Skjåk-Bræk G, Valla S. Cloning and Expression of an Azotobacter-Vinelandii Mannuronan C-5-Epimerase Gene. J Bacteriol. 1994;176: 2846–2853. Available: <Go to ISI>://WOS:A1994NL83800010

91. Haug A, Larsen B. Biosynthesis of alginate. Epimerisation of D-mannuronic to L-guluronic acid residues in the polymer chain. Biochimica et Biophysica Acta (BBA) - General Subjects. 1969;192: 557–559. doi:10.1016/0304-4165(69)90414-0

92. Donati I, Draget KI, Borgogna M, Paoletti S, Skjåk-Bræk G. Tailor-made alginate bearing galactose moieties on mannuronic residues: selective modification achieved by a chemoenzymatic strategy. Biomacromolecules. 2005;6: 88–98.

93. Strand BL, Mørch YA, Syvertsen KR, Espevik T, Skjåk-Bræk G. Molecular Engineering as an Approach to Design New Functional Properties of Alginate. Biomacromolecules. 2007;8: 2809–2814. doi:10.1021/bm700502b

94. Ertesvåg H. Alginate-modifying enzymes: biological roles and biotechnological uses. Frontiers in microbiology. 2015;6: 523. doi:10.3389/fmicb.2015.00523

95. Sletmoen M, Skjåk-Bræk G, Stokke BT. Mapping enzymatic functionalities of mannuronan C-5 epimerases and their modular units by dynamic force spectroscopy. Carbohydrate Research. 2005;340: 2782–2795. doi:10.1016/J.CARRES.2005.09.020

96. Høidal HK, Ertesvåg H, Skjåk-Bræk G, Stokke BT, Valla S. The recombinant Azotobacter vinelandii mannuronan C-5-epimerase AlgE4 epimerizes alginate by a nonrandom attack mechanism. Journal of Biological Chemistry. 1999;274: 12316–12322. doi:10.1074/jbc.274.18.12316

97. Mørch ÝA, Holtan S, Donati I, Strand BL, Skjåk-Bræk G. Mechanical Properties of C-5 Epimerized Alginates. Biomacromolecules. 2008;9: 2360–2368. doi:10.1021/bm8003572

98. Mørch YA, Donati I, Strand BL, Skjåk-Bræk G. Effect of Ca2+, Ba2+, and Sr2+ on alginate microbeads. Biomacromolecules. 2006;7: 1471–1480. doi:10.1021/bm060010d

99. Stanisci A, Aarstad OA, Tøndervik A, Sletta H, Dypås LB, Skjåk-Bræk G, et al. Overall size of mannuronan C5-Epimerases influences their ability to epimerize modified alginates and alginate gels. Carbohydrate Polymers. 2018;180: 256–263. doi:10.1016/J.CARBPOL.2017.09.094

100. Peppas NA, Bures P, Leobandung W, Ichikawa H. Hydrogels in pharmaceutical formulations. European Journal of Pharmaceutics and Biopharmaceutics. 2000;50: 27–46. doi:10.1016/S0939-6411(00)00090-4

101. Hoffman AS. Hydrogels for biomedical applications. Advanced Drug Delivery Reviews. 2012;64: 18–23. doi:10.1016/J.ADDR.2012.09.010

102. Morris ER, Rees DA, Thom D. Characterization of polysaccharide structure and interactions by circular dichroism: order–disorder transition in the calcium alginate system. Journal of the Chemical Society, Chemical Communications. 1973; 245–246. doi:10.1039/C39730000245

103. Grant GT, Morris ER, Rees DA, Smith PJC, Thom D. Biological interactions between polysaccharides and divalent cations: The egg-box model. FEBS Letters. 1973;32: 195–198. doi:10.1016/0014-5793(73)80770-7

104. Smidsrød O. Molecular basis for some physical properties of alginates in the gel state. Faraday Discussions of the Chemical Society. 1974;57: 263–274. doi:10.1039/DC9745700263

105. Smidsrød O, Haug A. Dependence upon Uronic Acid Composition of Some Ion-Exchange Properties of Alginates. Acta Chemica Scandinavica. 1968;22: 1989–1997. doi:10.3891/acta.chem.scand.22-1989

106. Haug A, Smidsrød O. Selectivity of Some Anionic Polymers for Divalent Metal Ions. Acta Chemica Scandinavica. 1970;24: 843–854. doi:10.3891/acta.chem.scand.24-0843

107. Haug A. The Affinity of Some Divalent Metals for Different Types of Alginates. Acta Chemica Scandinavica. 1961;15: 1794–1795.

108. Morris ER, Rees DA, Thom D, Boyd J. Chiroptical and stoichiometric evidence of a specific, primary dimerisation process in alginate gelation. Carbohydrate Research. 1978;66: 145–154. doi:10.1016/S0008-6215(00)83247-4

109. Donati I, Holtan S, Mørch YA, Borgogna M, Dentini M, Skjåk-Bræk G. New hypothesis on the role of alternating sequences in calcium-alginate gels. Biomacromolecules. 2005/03/15. 2005;6: 1031–1040. doi:10.1021/bm049306e

110. Zimmermann U, Mimietz S, Zimmermann H, Hillgärtner M, Schneider H, Ludwig J, et al. Hydrogel-Based Non-Autologous Cell and Tissue Therapy. BioTechniques. 2000;29: 564–581. doi:10.2144/00293rv01

111. Skjåk-Bræk G, Grasdalen H, Smidsrød O. Inhomogeneous polysaccharide ionic gels. Carbohydrate Polymers. 1989;10: 31–54. doi:10.1016/0144-8617(89)90030-1

112. Strand BL, Mørch YA, Espevik T, Skjåk-Bræk G. Visualization of alginate–poly-L-lysine–alginate microcapsules by confocal laser scanning microscopy. Biotechnology and Bioengineering. 2003;82: 386–394. doi:10.1002/bit.10577

113. Draget KI, Østgaard K, Smidsrød O. Alginate-based solid media for plant tissue culture. Applied Microbiology and Biotechnology. 1989;31: 79–83. doi:10.1007/BF00252532

114. Draget KI, Simensen MK, Onsoyen E, Smidsrød O. Gel Strength of Ca-Limited Alginate Gels Made in-Situ. Hydrobiologia. 1993;261: 563–569. Available: https://link.springer.com/article/10.1007/BF00049071

115. Bassett DC, Håti AG, Melø TB, Stokke BT, Sikorski P. Competitive ligand exchange of crosslinking ions for ionotropic hydrogel formation. Journal of Materials Chemistry B. 2016;4: 6175–6182. doi:10.1039/C6TB01812B

116. Bouhadir KH, Lee KY, Alsberg E, Damm KL, Anderson KW, Mooney DJ. Degradation of partially oxidized alginate and its potential application for tissue engineering. Biotechnol Prog. 2001;17: 945–950. doi:10.1021/bp010070p

117. Donati I, Paoletti S. Material Properties of Alginates. In: Rehm BHA, editor. Alginates: Biology and Applications. Berlin, Heidelberg: Springer Berlin Heidelberg; 2009. pp. 1–53. doi:10.1007/978-3-540-92679-5_1

118. Martinsen A, Skjåk-Bræk G, Smidsrød O. Alginate as immobilization material: I. Correlation between chemical and physical properties of alginate gel beads. Biotechnology and bioengineering. 1989;33: 79–89. doi:10.1002/bit.260330111

119. Growney Kalaf EA, Pendyala M, Bledsoe JG, Sell SA. Characterization and restoration of degenerated IVD function with an injectable, in situ gelling alginate hydrogel: An in vitro and ex vivo study. Journal of the Mechanical Behavior of Biomedical Materials. 2017;72: 229–240. doi:10.1016/J.JMBBM.2017.05.014

120. Simensen M, Onsøyen E, Draget KI, Smidsrød O, Fjæreide T. Use of G-block Polysaccharides. Int Pat Application PCT/NO97/00176. 1997.

121. Draget KI, Gåserød O, Aune I, Andersen PO, Storbakken B, Stokke BT, et al. Effects of molecular weight and elastic segment flexibility on syneresis in Ca-alginate gels. Food Hydrocolloids. 2001;15: 485–490. doi:10.1016/S0268-005X(01)00046-7

122. Haug A, Larsen B, Smidsrød O. The Degradation of Alginates at Different pH Values. Acta Chemica Scandinavica. 1963;17: 1466–1468. doi:10.3891/acta.chem.scand.17-1466

123. Al-Shamkhani A, Duncan R. Radioiodination of alginate via covalently-bound tyrosinamide allows monitoring of its fate in-vivo. Journal of Bioactive and Compatible Polymers. 1995;10: 4–13.

124. Gacesa P. Enzymic degradation of alginates. International Journal of Biochemistry. 1992;24: 545–552. doi:https://doi.org/10.1016/0020-711X(92)90325-U

125. Kristiansen KA, Tomren HB, Christensen BE. Periodate oxidized alginates: Depolymerization kinetics. Carbohydrate Polymers. 2011;86: 1595–1601. doi:https://doi.org/10.1016/j.carbpol.2011.06.069

126. Thu B, Bruheim P, Espevik T, Smidsrød O, Soon-Shiong P, Skjåk-Bræk G. Alginate polycation microcapsules: II. Some functional properties. Biomaterials. 1996;17: 1069–1079. doi:10.1016/0142-9612(96)85907-2

127. Donati I, Mørch YA, Strand BL, Skjåk-Bræk G, Paoletti S. Effect of Elongation of Alternating Sequences on Swelling Behavior and Large Deformation Properties of Natural Alginate Gels. The Journal of Physical Chemistry B. 2009;113: 12916–12922. doi:10.1021/jp905488u

128. Stokke BT, Smidsrød O, Zanetti F, Strand W, Skjåk-Bræk G. Distribution of uronate residues in alginate chains in relation to alginate gelling properties — 2: Enrichment of β-d-mannuronic acid and depletion of α-l-guluronic acid in sol fraction. Carbohydrate Polymers. 1993;21: 39–46. doi:10.1016/0144-8617(93)90115-K

129. Flo TH, Ryan L, Latz E, Takeuchi O, Monks BG, Lien E, et al. Involvement of toll-like receptor (TLR) 2 and TLR4 in cell activation by mannuronic acid polymers. The Journal of biological chemistry. 2002;277: 35489–95. doi:10.1074/jbc.M201366200

130. Otterlei M, Sundan A, Skjåk-Bræk G, Ryan L, Smidsrød O, Espevik T. Similar mechanisms of action of defined polysaccharides and lipopolysaccharides: characterization of binding and tumor necrosis factor alpha induction. Infection and immunity. 1993;61: 1917–1925. Available: https://www.ncbi.nlm.nih.gov/pubmed/8478081

131. Otterlei M, Ostgaard K, Skjåk-Bræk G, Smidsrod O, Soon-Shiong P, Espevik T. Induction of cytokine production from human monocytes stimulated with alginate. Journal of immunotherapy : official journal of the Society for Biological Therapy. 1991;10: 286–291. doi:10.1097/00002371-199108000-00007

132. Suzuki S, Christensen BE, Kitamura S. Effect of mannuronate content and molecular weight of alginates on intestinal immunological activity through Peyer's patch cells of C3H/HeJ mice. Carbohydrate Polymers. 2011;83: 629–634. doi:https://doi.org/10.1016/j.carbpol.2010.08.032

133. Veiseh O, Doloff JC, Ma M, Vegas AJ, Tam HH, Bader AR, et al. Size- and shape-dependent foreign body immune response to materials implanted in rodents and non-human primates. Nature materials. 2015;14: 643–651. doi:10.1038/nmat4290

134. Vegas AJ, Veiseh O, Doloff JC, Ma M, Tam HH, Bratlie K, et al. Combinatorial hydrogel library enables identification of materials that mitigate the foreign body response in

primates. Nature Biotechnology. 2016;34: 345. Available: http://dx.doi.org/10.1038/nbt.3462

135. Bastiancich C, Bianco J, Vanvarenberg K, Ucakar B, Joudiou N, Gallez B, et al. Injectable nanomedicine hydrogel for local chemotherapy of glioblastoma after surgical resection. Journal of Controlled Release. 2017;264: 45–54. doi:10.1016/J.JCONREL.2017.08.019

136. Kim H-S, Yang J, Kim K, Shin US. Biodegradable and injectable hydrogels as an immunosuppressive drug delivery system. Materials Science and Engineering: C. 2019;98: 472–481. doi:10.1016/J.MSEC.2018.11.051

137. Espona-Noguera A, Ciriza J, Cañibano-Hernández A, Fernandez L, Ochoa I, Saenz del Burgo L, et al. Tunable injectable alginate-based hydrogel for cell therapy in Type 1 Diabetes Mellitus. International Journal of Biological Macromolecules. 2018;107: 1261–1269. doi:10.1016/J.IJBIOMAC.2017.09.103

138. Tanaka H, Matsumura M, Veliky IA. Diffusion characteristics of substrates in Ca-alginate gel beads. Biotechnology and Bioengineering. 1984;26: 53–58. doi:https://doi.org/10.1002/bit.260260111

139. Castro JS, Tapia L v., Silveyra RA, Martinez CA, Deymier PA. Negative Impact of Paclitaxel Crystallization on Hydrogels and Novel Approaches for Anticancer Drug Delivery Systems. In: Ozdemir O, editor. Current Cancer Treatment - Novel Beyond Conventional Approaches. Rijeka: IntechOpen; 2011. pp. 767–782. doi:10.5772/897

140. del Valle EMM. Cyclodextrins and their uses: a review. Process Biochemistry. 2004;39: 1033–1046.

141. Martinsen A, Storrø I, Skjåk-Bræk G. Alginate as immobilization material: III. Diffusional properties. Biotechnology and bioengineering. 1992;39: 186–194. doi:10.1002/bit.260390210

142. Strand BL, Mørch YA, Syvertsen KR, Espevik T, Skjak-Braek G. Microcapsules made by enzymatically tailored alginate. Journal of biomedical materials research Part A. 2003;64: 540–550. doi:10.1002/jbm.a.10337

143. O'Shea TM, Aimetti AA, Kim E, Yesilyurt V, Langer R. Synthesis and Characterization of a Library of In-Situ Curing, Nonswelling Ethoxylated Polyol Thiol-ene Hydrogels for Tailorable Macromolecule Delivery. Advanced Materials. 2015;27: 65–72. doi:10.1002/adma.201403724

144. Kulseng B, Thu B, Espevik T, Skjåk-Bræk G. Alginate polylysine microcapsules as immune barrier: Permeability of cytokines and immunoglobulins over the capsule membrane. Cell Transplantation. 1997;6: 387–394. doi:10.1016/S0963-6897(97)00002-X

145. Hariyadi DM, Islam N. Current Status of Alginate in Drug Delivery. Advances in Pharmacological and Pharmaceutical Sciences. 2020. doi:10.1155/2020/8886095

146. Choy JS, Leng S, Acevedo-Bolton G, Shaul S, Fu L, Guo X, et al. Efficacy of intramyocardial injection of Algisyl-LVR for the treatment of ischemic heart failure in

swine. International Journal of Cardiology. 2018;255: 129–135. doi:10.1016/J.IJCARD.2017.09.179

147. Lee RJ, Hinson A, Bauernschmitt R, Matschke K, Fang Q, Mann DL, et al. The feasibility and safety of Algisyl-LVR^{TM} as a method of left ventricular augmentation in patients with dilated cardiomyopathy: Initial first in man clinical results. International Journal of Cardiology. 2015;199: 18–24. doi:10.1016/J.IJCARD.2015.06.111

148. Nordgård CT, Draget KI. Oligosaccharides As Modulators of Rheology in Complex Mucous Systems. Biomacromolecules. 2011;12: 3084–3090. doi:10.1021/bm200727c

149. Nordgård CT, Nonstad U, Olderøy MØ, Espevik T, Draget KI. Alterations in Mucus Barrier Function and Matrix Structure Induced by Guluronate Oligomers. Biomacromolecules. 2014;15: 2294–2300. doi:10.1021/bm500464b

150. van Koningsbruggen-Rietschel S, Davies JC, Pressler T, Fischer R, MacGregor G, Donaldson SH, et al. Inhaled dry powder alginate oligosaccharide in cystic fibrosis: a randomised, double-blind, placebo-controlled, crossover phase 2b study. ERJ Open Research. 2020;6: 00132–02020. doi:10.1183/23120541.00132-2020

151. Powell LC, Sowedan A, Khan S, Wright CJ, Hawkins K, Onsøyen E, et al. The effect of alginate oligosaccharides on the mechanical properties of Gram-negative biofilms. Biofouling. 2013;29: 413–421. doi:10.1080/08927014.2013.777954

152. LiPuma JJ. The changing microbial epidemiology in cystic fibrosis. Clinical Microbiology Reviews. 2010. pp. 299–323. doi:10.1128/CMR.00068-09

153. Hengzhuang W, Song Z, Ciofu O, Onsøyen E, Rye PD, Høiby N. OligoG CF-5/20 disruption of mucoid Pseudomonas aeruginosa biofilm in a murine lung infection model. Antimicrobial Agents and Chemotherapy. 2016;60: 2620–2626. doi:10.1128/AAC.01721-15

154. Weiser R, Rye PD, Mahenthiralingam E. Implementation of microbiota analysis in clinical trials for cystic fibrosis lung infection: Experience from the OligoG phase 2b clinical trials. Journal of Microbiological Methods. 2021;181: 106133. doi:10.1016/J.MIMET.2021.106133

155. He L, Shang Z, Liu H, Yuan Z. Alginate-Based Platforms for Cancer-Targeted Drug Delivery. Murgia S, editor. BioMed Research International. 2020;2020: 1487259. doi:10.1155/2020/1487259

156. Abasalizadeh F, Moghaddam SV, Alizadeh E, akbari E, Kashani E, Fazljou SMB, et al. Alginate-based hydrogels as drug delivery vehicles in cancer treatment and their applications in wound dressing and 3D bioprinting. Journal of Biological Engineering. 2020;14: 8. doi:10.1186/s13036-020-0227-7

157. Uyen NTT, Hamid ZAA, Tram NXT, Ahmad N. Fabrication of alginate microspheres for drug delivery: A review. International Journal of Biological Macromolecules. 2019 [cited 10 Dec 2019]. doi:10.1016/J.IJBIOMAC.2019.10.233

158. Krebs MD, Jeon O, Alsberg E. Localized and sustained delivery of silencing RNA from macroscopic biopolymer hydrogels. Journal of the American Chemical Society. 2009;131: 9204–9206. doi:10.1021/ja9037615

159. Shin EY, Park JH, Shin ME, Song JE, Thangavelu M, Carlomagno C, et al. Injectable taurine-loaded alginate hydrogels for retinal pigment epithelium (RPE) regeneration. Materials Science and Engineering: C. 2019;103: 109787. doi:10.1016/J.MSEC.2019.109787

160. Jeon O, Bouhadir KH, Mansour JM, Alsberg E. Photocrosslinked alginate hydrogels with tunable biodegradation rates and mechanical properties. Biomaterials. 2009;30: 2724–2734. doi:10.1016/J.BIOMATERIALS.2009.01.034

161. Jeon O, Powell C, Ahmed SM, Alsberg E. Biodegradable, Photocrosslinked Alginate Hydrogels with Independently Tailorable Physical Properties and Cell Adhesivity. Tissue Engineering Part A. 2010;16: 2915–2925. doi:10.1089/ten.tea.2010.0096

162. Alipour S, Montaseri H, Tafaghodi M. Preparation and characterization of biodegradable paclitaxel loaded alginate microparticles for pulmonary delivery. Colloids and Surfaces B: Biointerfaces. 2010;81: 521–529. doi:10.1016/J.COLSURFB.2010.07.050

163. Wu J-L, Wang C-Q, Zhuo R-X, Cheng S-X. Multi-drug delivery system based on alginate/calcium carbonate hybrid nanoparticles for combination chemotherapy. Colloids and Surfaces B: Biointerfaces. 2014;123: 498–505. doi:10.1016/J.COLSURFB.2014.09.047

164. Lim F, Sun AM. Microencapsulated islets as bioartificial endocrine pancreas. Science (New York, NY). 1980;210: 908–910. doi:10.1126/science.6776628

165. Soon-Shiong P, Heintz RE, Merideth N, Yao QX, Yao Z, Zheng T, et al. Insulin independence in a type 1 diabetic patient after encapsulated islet transplantation. The Lancet. 1994;343: 950–951. doi:10.1016/S0140-6736(94)90067-1

166. Jacobs-Tulleneers-Thevissen D, Chintinne M, Ling Z, Gillard P, Schoonjans L, Delvaux G, et al. Sustained function of alginate-encapsulated human islet cell implants in the peritoneal cavity of mice leading to a pilot study in a type 1 diabetic patient. Diabetologia. 2013;56: 1605–1614. doi:DOI 10.1007/s00125-013-2906-0

167. Dhawan A, Chaijitraruch N, Fitzpatrick E, Bansal S, Filippi C, Lehec SC, et al. Alginate microencapsulated human hepatocytes for the treatment of acute liver failure in children. Journal of Hepatology. 2020;72: 877–884. doi:10.1016/J.JHEP.2019.12.002

168. Strand BL, Coron AE, Skjåk-Bræk G. Current and future perspectives on alginate encapsulated pancreatic islet. Stem Cells Translational Medicine. 2017;6: 1053–1058. doi:10.1002/sctm.16-0116

169. Liu Q, Chiu A, Wang LH, An D, Zhong M, Smink AM, et al. Zwitterionically modified alginates mitigate cellular overgrowth for cell encapsulation. Nature Communications. 2019;10: 1–14. doi:10.1038/s41467-019-13238-7

170. Bochenek MA, Veiseh O, Vegas AJ, McGarrigle JJ, Qi M, Marchese E, et al. Alginate encapsulation as long-term immune protection of allogeneic pancreatic islet cells transplanted into the omental bursa of macaques. Nature Biomedical Engineering. 2018;2: 810–821. doi:10.1038/s41551-018-0275-1

171. Steed JW, Atwood JL. Supramolecular Chemistry. 2nd ed. Supramolecular Chemistry. 2nd ed. Chichester: Wiley; 2009. pp. 307–384.

172. Saokham P, Muankaew C, Jansook P, Loftsson T. Solubility of Cyclodextrins and Drug/Cyclodextrin Complexes. Molecules (Basel, Switzerland). 2018;23: 1161. doi:10.3390/molecules23051161

173. Loftsson T, Brewster ME. Cyclodextrins as Functional Excipients: Methods to Enhance Complexation Efficiency. Journal of Pharmaceutical Sciences. 2012;101: 3019–3032. doi:10.1002/JPS.23077

174. Loftsson T, Brewster ME. Pharmaceutical Applications of Cyclodextrins. 1. Drug Solubilization and Stabilization. Journal of Pharmaceutical Sciences. 1996;85: 1017–1025. doi:10.1021/JS950534B

175. Connors KA. The Stability of Cyclodextrin Complexes in Solution. Chemical Reviews. 1997;97: 1325–1358. doi:10.1021/cr960371r

176. Carrazana J, Reija B, Cabrer PR, Al-Soufi W, Novo M, Tato J v. Complexation of methyl orange with beta-cyclodextrin: Detailed analysis and application to quantification of polymer-bound cyclodextrin. Supramolecular Chemistry. 2004;16: 549–559.

177. Hermanson GT. Bioconjugate Techniques. Bioconjugate Techniques. Burlington: Elsevier Academic Press; 2013. pp. 229–258.

178. Baumann M, Baxendale IR. An overview of the synthetic routes to the best selling drugs containing 6-membered heterocycles. Beilstein journal of organic chemistry. 2013;9: 2265–2319. doi:10.3762/bjoc.9.265

179. Polêto MD, Rusu VH, Grisci BI, Dorn M, Lins RD, Verli H. Aromatic Rings Commonly Used in Medicinal Chemistry: Force Fields Comparison and Interactions With Water Toward the Design of New Chemical Entities. Frontiers in pharmacology. 2018;9: 395. doi:10.3389/fphar.2018.00395

180. Roughley SD, Jordan AM. The Medicinal Chemist’s Toolbox: An Analysis of Reactions Used in the Pursuit of Drug Candidates. Journal of Medicinal Chemistry. 2011;54: 3451–3479. doi:10.1021/jm200187y

181. Agard NJ, Prescher JA, Bertozzi CR. A Strain-Promoted [3 + 2] Azide−Alkyne Cycloaddition for Covalent Modification of Biomolecules in Living Systems. Journal of the American Chemical Society. 2004;126: 15046–15047. doi:10.1021/ja044996f

182. Jewett JC, Sletten EM, Bertozzi CR. Rapid Cu-Free Click Chemistry with Readily Synthesized Biarylazacyclooctynones. Journal of the American Chemical Society. 2010;132: 3688–3690. doi:10.1021/ja100014q

183. Bowman KA, Aarstad OA, Nakamura M, Stokke BT, Skjåk-Bræk G, Round AN. Single molecule investigation of the onset and minimum size of the calcium-mediated junction zone in alginate. Carbohydrate Polymers. 2016;148: 52–60. doi:10.1016/J.CARBPOL.2016.04.043

184. Stokke BT, Smidsrød O, Bruheim P, Skjåk-Bræk G. Distribution of uronate residues in alginate chains in relation to alginate gelling properties. Macromolecules. 1991;24: 4637–4645. doi:10.1021/ma00016a026

185. Kiss T, Fenyvesi F, Bácskay I, Váradi J, Fenyvesi É, Iványi R, et al. Evaluation of the cytotoxicity of β-cyclodextrin derivatives: Evidence for the role of cholesterol extraction. European Journal of Pharmaceutical Sciences. 2010;40: 376–380. doi:10.1016/j.ejps.2010.04.014

186. Szente L, Singhal A, Domokos A, Song B. Cyclodextrins: Assessing the Impact of Cavity Size, Occupancy, and Substitutions on Cytotoxicity and Cholesterol Homeostasis. Molecules. 2018;23: 1228. doi:10.3390/molecules23051228

187. Merck. Safety Data Sheet Methyl Orange. In: Safety Data Sheet, No. 1907/2006. Version 9 [Internet]. 2018 [cited 17 Aug 2020]. Available: https://www.merckmillipore.com/NO/en/product/msds/MDA_CHEM-101322?ReferrerURL=https%3A%2F%2Fwww.google.com%2F

188. Abouelmagd SA, Sun B, Chang AC, Ku YJ, Yeo Y. Release Kinetics Study of Poorly Water-Soluble Drugs from Nanoparticles: Are We Doing It Right? Molecular pharmaceutics. 2015;12: 997–1003. doi:10.1021/mp500817h

189. Kompany-Zareh M, Mokhtari Z, Abdollahi H. Spectrophotometric thermodynamic study of orientational isomers formed by inclusion of methyl orange into β-cyclodextrin nanocavity. Chemometrics and Intelligent Laboratory Systems. 2012;118: 230–238. doi:10.1016/J.CHEMOLAB.2012.06.001

190. Alcaro S, Ventura CA, Paolino D, Battaglia D, Ortuso F, Cattel L, et al. Preparation, characterization, molecular modeling and In vitro activity of paclitaxel–cyclodextrin complexes. Bioorganic & Medicinal Chemistry Letters. 2002;12: 1637–1641. doi:10.1016/S0960-894X(02)00217-2

191. Sharma US, Balasubramanian S v., Straubinger RM. Pharmaceutical and Physical Properties of Paclitaxel (Taxol) Complexes with Cyclodextrins. Journal of Pharmaceutical Sciences. 1995;84: 1223–1230. doi:10.1002/JPS.2600841015

192. MacEachern-Keith GJ, Wagner Butterfield LJ, Incorvia Mattina MJ. Paclitaxel Stability in Solution. Analytical Chemistry. 1997;69: 72–77. doi:10.1021/ac9606822

193. Loftsson T, Másson M. The effects of water-soluble polymers on cyclodextrins and cyclodextrin solubilization of drugs. Journal of Drug Delivery Science and Technology. Editions de Sante; 2004. pp. 35–43. doi:10.1016/s1773-2247(04)50003-5

194. Loftsson T, Fririksdóttir H. The effect of water-soluble polymers on the aqueous solubility and complexing abilities of β-cyclodextrin. International Journal of Pharmaceutics. 1998;163: 115–121. doi:10.1016/S0378-5173(97)00371-2

195. Jing J, Szarpak-Jankowska A, Guillot R, Pignot-Paintrand I, Picart C, Auzély-Velty R. Cyclodextrin/Paclitaxel Complex in Biodegradable Capsules for Breast Cancer Treatment. Chemistry of Materials. 2013;25: 3867–3873. doi:10.1021/cm4019925

196. Amini-Fazl MS, Mobedi H, Barzin J. Investigation of aqueous stability of taxol in different release media. Drug Development and Industrial Pharmacy. 2014;40: 519–526. doi:10.3109/03639045.2013.771646

197. Tian J, Stella VJ. Degradation of paclitaxel and related compounds in aqueous solutions I: Epimerization. Journal of Pharmaceutical Sciences. 2008;97: 1224–1235. doi:10.1002/JPS.21112

198. Phillips DJ, Pygall SR, Cooper VB, Mann JC. Overcoming sink limitations in dissolution testing: a review of traditional methods and the potential utility of biphasic systems. Journal of Pharmaceutics & Pharmacology. 2012;64: 1549–1559.

199. Chiang C-Y, Chu C-C. Synthesis of photoresponsive hybrid alginate hydrogel with photo-controlled release behavior. Carbohydrate Polymers. 2015;119: 18–25. doi:10.1016/J.CARBPOL.2014.11.043

200. Gomez CG, Chambat G, Heyraud A, Villar M, Auzely-Velty R. Synthesis and characterization of a beta-CD-alginate conjugate. Polymer. 2006;47: 8509–8516.

201. Izawa H, Kawakami K, Sumita M, Tateyama Y, Hill JP, Ariga K. beta-Cyclodextrin-crosslinked alginate gel for patient-controlled drug delivery systems: regulation of host-guest interactions with mechanical stimuli. Journal of Materials Chemistry B. 2013;1: 2155–2161.

202. Miao T, Fenn SL, Charron PN, Oldinski RA. Self-Healing and Thermoresponsive Dual-Cross-Linked Alginate Hydrogels Based on Supramolecular Inclusion Complexes. Biomacromolecules. 2015;16: 3740–3750.

203. Tan L, Li J, Liu Y, Zhou H, Zhang Z, Deng L. Synthesis and characterization of β-cyclodextrin-conjugated alginate hydrogel for controlled release of hydrocortisone acetate in response to mechanical stimulation. Journal of Bioactive and Compatible Polymers. 2015;30: 584–599. doi:10.1177/0883911515590494

204. Zhang S, Qiao X, Hu B, Gong Y. Formation and controlled release of the inclusion complex of water soluble model drug neutral red with β-cyclodextrin grafted sodium alginate. Journal of Controlled Release. 2011;152: e116–e118. doi:10.1016/J.JCONREL.2011.08.161

205. Lopedota A, Denora N, Laquintana V, Cutrignelli A, Lopalco A, Tricarico D, et al. Alginate-Based Hydrogel Containing Minoxidil/Hydroxypropyl-β-Cyclodextrin Inclusion Complex for Topical Alopecia Treatment. Journal of Pharmaceutical Sciences. 2018;107: 1046–1054. doi:10.1016/J.XPHS.2017.11.016

206. Burckbuchler V, Kjøniksen A-L, Galant C, Lund R, Amiel C, Knudsen KD, et al. Rheological and Structural Characterization of the Interactions between Cyclodextrin Compounds and Hydrophobically Modified Alginate. Biomacromolecules. 2006;7: 1871–1878. doi:10.1021/bm060149o

207. Shen Y, Niu L, Yu Z, Wang M, Shang Z, Yang Y. Sodium alginate-grafted β-cyclodextrins as a matrix for immobilized Arthrobacter simplex for cortisone acetate biotransfromation. Applied Surface Science. 2018;444: 42–47. doi:10.1016/J.APSUSC.2018.03.028

208. Pluemsab W, Sakairi N, Furuike T. Synthesis and inclusion property of α-cyclodextrin-linked alginate. Polymer. 2005;46: 9778–9783. doi:10.1016/J.POLYMER.2005.08.005

209. Moncada-Basualto M, Matsuhiro B, Mansilla A, Lapier M, Maya JD, Olea-Azar C. Supramolecular hydrogels of β-cyclodextrin linked to calcium homopoly-l-guluronate for release of coumarins with trypanocidal activity. Carbohydrate Polymers. 2019;204: 170–181. doi:10.1016/J.CARBPOL.2018.10.010

210. Nieto C, Centa A, Rodríguez-Rodríguez JA, Pandiella A, del Valle EMM. Paclitaxel-trastuzumab mixed nanovehicle to target HER2-overexpressing tumors. Nanomaterials. 2019;9. doi:10.3390/nano9070948

211. Hardy A, Seguin C, Brion A, Lavalle P, Schaaf P, Fournel S, et al. β-Cyclodextrin-Functionalized Chitosan/Alginate Compact Polyelectrolyte Complexes (CoPECs) as Functional Biomaterials with Anti-Inflammatory Properties. ACS Applied Materials & Interfaces. 2018;10: 29347–29356. doi:10.1021/acsami.8b09733

212. Shelley H, Rodriguez-Galarza RM, Duran SH, Abarca EM, Babu RJ. In Situ Gel Formulation for Enhanced Ocular Delivery of Nepafenac. Journal of Pharmaceutical Sciences. 2018;107: 3089–3097. doi:10.1016/J.XPHS.2018.08.013

213. Hosseinifar T, Sheybani S, Abdouss M, Hassani Najafabadi SA, Shafiee Ardestani M. Pressure responsive nanogel base on Alginate-Cyclodextrin with enhanced apoptosis mechanism for colon cancer delivery. Journal of Biomedical Materials Research Part A. 2018;106: 349–359. doi:https://doi.org/10.1002/jbm.a.36242

214. Lakkakula JR, Matshaya T, Krause RWM. Cationic cyclodextrin/alginate chitosan nanoflowers as 5-fluorouracil drug delivery system. Materials Science and Engineering: C. 2017;70: 169–177. doi:10.1016/J.MSEC.2016.08.073

215. Ivancic A, Macaev F, Aksakal F, Boldescu V, Pogrebnoi S, Duca G. Preparation of alginate-chitosan-cyclodextrin micro- and nanoparticles loaded with anti-tuberculosis compounds. Beilstein journal of nanotechnology. 2016;7: 1208–1218. doi:10.3762/bjnano.7.112

216. Fan M, Ma Y, Mao J, Zhang Z, Tan H. Cytocompatible in situ forming chitosan/hyaluronan hydrogels via a metal-free click chemistry for soft tissue engineering. Acta Biomaterialia. 2015;20: 60–68. doi:https://doi.org/10.1016/j.actbio.2015.03.033

217. Jørgensen TE, Sletmoen M, Draget KI, Stokke BT. Influence of Oligoguluronates on Alginate Gelation, Kinetics, and Polymer Organization. Biomacromolecules. 2007;8: 2388–2397. doi:10.1021/bm070208d

218. Gidwani B, Vyas A. A Comprehensive Review on Cyclodextrin-Based Carriers for Delivery of Chemotherapeutic Cytotoxic Anticancer Drugs. BioMed research international. 2015. Available: doi:10.1155/2015/198268

219. Dash S., Murthy PN., Nath L., Chowdhury P. Kinetic modeling on drug release from controlled drug delivery systems. Acta Pol Pharm . 2010;67: 217–223. Available: https://pubmed.ncbi.nlm.nih.gov/20524422/

220. Bernabeu E, Cagel M, Lagomarsino E, Moretton M, Chiappetta DA. Paclitaxel: What has been done and the challenges remain ahead. International Journal of Pharmaceutics. 2017;526: 474–495. doi:10.1016/J.IJPHARM.2017.05.016

221. van de Manakker F, Vermonden T, van Nostrum CF, Hennink WE. Cyclodextrin-Based Polymeric Materials: Synthesis, Properties, and Pharmaceutical/Biomedical Applications. Biomacromolecules. 2009;10: 3157–3175. doi:10.1021/bm901065f

222. Concheiro A, Alvarez-Lorenzo C. Chemically cross-linked and grafted cyclodextrin hydrogels: From nanostructures to drug-eluting medical devices. Advanced Drug Delivery Reviews. Elsevier B.V.; 2013. pp. 1188–1203. doi:10.1016/j.addr.2013.04.015

223. Alsbaiee A, Smith BJ, Xiao L, Ling Y, Helbling DE, Dichtel WR. Rapid removal of organic micropollutants from water by a porous beta-cyclodextrin polymer. Nature. 2016;529: 190–194.

224. Qin YM, Shi BB, Liu JJ. Application of chitosan and alginate in treating waste water containing heavy metal ions. Indian Journal of Chemical Technology. 2006;13: 464–469. Available: <Go to ISI>://WOS:000241996500007

Paper I

SCIENTIFIC REPORTS

Efficient Grafting of Cyclodextrin to Alginate and Performance of the Hydrogel for Release of Model Drug

Received: 27 June 2018
Accepted: 5 June 2019

Line Aa. Omtvedt[1], Marianne Ø. Dalheim[1], Thorbjørn T. Nielsen[2], Kim L. Larsen[2], Berit L. Strand[1] & Finn L. Aachmann[1]

Controlling the rate of release of molecules from a hydrogel is of high interest for various drug delivery systems and medical devices. A strategy to alter the release profiles of soluble and poorly soluble active ingredients from hydrogels can be to combine the hydrogel forming ability of alginate with the inclusion forming ability of cyclodextrins (CyD). Here, β-CyD was grafted to alginate in a three-step synthesis using periodate oxidation, reductive amination and copper(I)-catalyzed azide-alkyne cycloaddition. A grafting degree of 4.7% mol β-CyD/mol sugar residues was obtained. The grafting degree was controlled by varying the reaction parameters where the amount of linker used in reductive amination was especially influential. Ca-alginate gel beads grafted with β-CyD showed increased uptake of the model molecule methyl orange. Release experiments showed that the grafted material had a prolonged release of methyl orange and an increased total amount of released methyl orange. These results show that the β-CyD grafted alginate is still able to form a hydrogel while the grafted cyclodextrins retain their ability to form inclusion complex with methyl orange. Further testing should be done with this system to investigate capability for drug delivery applications.

Hydrogels may be described as water molecules entrapped with in a hydrophilic polymer network (typically 1–3% dry matter) with the mechanical properties of a solid[1]. The hydrophilic nature of a hydrogel limits its applicability as carrier of a large range of active compounds (e.g. drugs) as they most often are poorly soluble in water. The use of hydrogels as a vehicle for the release of poorly soluble drugs is thus hampered by the hydrophilic nature of the hydrogel, which leads to limited drug loading and, consequently, limited drug release. In the case of hydrophilic drugs, high loading degrees and high release rates are largely governed by the diffusion rates of the drug. In alginate-based hydrogels, the permeability of the gel network limits the drug loading and release rate. In addition, the shape, charge and size of the molecule of interest also influence the loading degree and release rate[2]. CyDs are known to alter the apparent physiochemical properties of hydrophobic molecules and molecules with hydrophobic moieties due to the formation of guest-host complexes and can, for example, improve the bioavailability of drugs and change their release profiles from drug delivery devices[3]. In this context, CyD-grafted alginates could provide a system that combines the gelling properties of alginate with the ability of CyDs to form inclusion complexes with molecules presenting hydrophobic moieties (e.g. drugs).

Alginate is a linear polysaccharide that consists of (1 → 4) linked α-L-guluronic acid (G) and β-D-mannuronic acid (M), and can be isolated from brown algae and certain bacteria[4]. Specific sequences of monosaccharide in alginate are usually described as block structures: M-blocks consisting of consecutive sequences of M-residues, G-blocks consisting of consecutive sequences of G-residues, and MG-blocks describing sequences of alternating M and G-residues. The relative amounts of each block structure varies in different types of alginates[5], which, together with the molecular weight, determines the different properties of alginates[2]. The single most important property of alginates is their ability to form hydrogels by crosslinking with divalent cations, such as calcium ions. While G-blocks are largely responsible for this key trait[6], MG-blocks can also play a significant role in Ca-crosslinking[7]. Alginates are in general considered to be non-toxic and with low immunogenicity and are widely used in biomedical and pharmaceutical applications[8]. Recent studies have focused on fibrotic reactions

[1]Norwegian Biopolymer Laboratory (NOBIPOL), Department of Biotechnology and Food Science, NTNU - Norwegian University of Science and Technology, N-7491, Trondheim, Norway. [2]Department of Chemistry and Bioscience, Aalborg University (AAU), 9220, Aalborg, Denmark. Line Aa. Omtvedt and Marianne Ø. Dalheim contributed equally. Correspondence and requests for materials should be addressed to F.L.A. (email: finn.l.aachmann@ntnu.no)

towards alginate-based capsules where fibrosis is believed to be connected to early inflammatory responses, but the mechanisms are currently not understood[9,10].

CyDs are macrocycles produced from starch made up of at least six α-(1 → 4) linked glucopyranose residues[11]. Native, unmodified CyDs with 6, 7, and 8 glucopyranose units in the macrocycle (named α-, β- and γ-CyD, respectively), are commercially available as fairly cheap bulk chemicals[12]. The CyDs can be described as truncated cones with a relatively hydrophobic cavity and a hydrophilic exterior. This gives CyDs the ability to form inclusion complexes in water with various hydrophobic molecules and moieties[11,13–16]. As drug-CyD inclusions complexes usually have a higher aqueous solubility compared with the pure drug, the apparent solubility of the drug is typically increased by CyDs. This feature, together with fast dissolution rates allows CyD to increase the bioavailability of a large range of drugs. Furthermore, by forming inclusion complexes, CyDs protect drugs from being prematurely degraded and metabolized[17]. CyDs are in general considered as biocompatible in relation to their participation as functional elements in materials and devices intended for medical uses as exemplified by recent publications[18–20]. Cyclodextrins have even shown to improve the biocompatibility of e.g. drug delivery systems[21]. CyDs have for example been used to enhance the apparent solubility of poorly water-soluble drugs in a PVP/PEG crosslinked hydrogel[22]. However, in systems of synthetic polymers such as PEG, the hydrogels are formed via covalent crosslinks between the polymer chains, often under the use of harsh chemical conditions or ultra violet light[22,23]. Since alginate crosslinks with divalent cations, the hydrogels can be formed in aqueous solution and at physiological conditions[4].

Alginates have been used as excipients in drug delivery[24,25], and can be chemically modified to obtain drug delivery systems with altered release rates and profiles[25]. Grafting alginate with CyDs should enable the hydrogel to host higher concentrations of poorly soluble drugs and other active small molecules that otherwise would readily diffuse out of the gel. Furthermore, molecules capable of inclusion complex formation with CyDs should display sustained release properties (irrespective of their solubility) compared to non-modified alginate gels.

Various strategies have been used to covalently attach β-CyD to polymer chains, including photo initiated free radical polymerization for synthetic polymers[26] and carbodiimide chemistry, reductive amination, click chemistry or combinations of these for polysaccharides[27–31]. In the case of alginates, carbodiimide chemistry has been used to link CyD to its carboxyl group either via an amine functionalized CyD[28,29,32,33] or via a linker having a primary amine[27]. Carbodiimide chemistry is commonly used to conjugate various primary amines to the carboxylate groups in alginate[34]. However, the reaction gives by-products that have been shown to associate with the alginate[35]. Also, the grafting degree of alginate using carbodiimide chemistry has been limited to 0.1 to 0.2% of monomers substituted for peptides[8,35]. The secondary hydroxyl-groups on alginate have also been used to covalently graft α-CyDs on the polysaccharide backbone, by using the cyanogen bromide method[36]. In our previous work, periodate oxidation and reductive amination was shown to be an efficient alternative to carbodiimide chemistry for grafting of peptides[37]. This approach resulted in high and tunable grafting degrees without by-product formation. Hence, grafting up to the level of degree of oxidation (e.g. 8% grafting for 8% oxidized material) has been obtained[37]. The copper(I)-catalyzed azide-alkyne cycloaddition (CuAAC) reaction has been used to covalently bind β-CyD to an alkyne-linked dextran[31]. The CuAAC-reaction is a versatile click-reaction that gives 1,4-disubstituted-1,2,3-triazoles as the end product[38–40].

Despite recent developments of various methods, grafting of suitable functional moieties to alginate in aqueous solution is still far from optimal. Development of a controlled and tunable grafting method without by-product formation in aqueous solution would be highly advantageous. The aim of the present paper is to combine the latest developments in polysaccharide-grafting methods with aqueous-solution click-chemistry to graft CyDs to alginates[31,37].

Materials and Methods

Materials. Alginates from *Laminaria hyperborea* stipe ($F_G = 0.7$, $N_{G>1} = 11–14$, $\overline{\boldsymbol{M}}_w = \sim 100$ kDa) were obtained from FMC Health and Nutrition, Sandvika, Norway. 6-O-monodeoxy-6-monoazido-β-CyD (N_3-β-CyD) was synthesized as described previously[31]. Tris(benzyltriazolylmethyl)amine (TBTA) was synthesized according to literature[41] (used for sample B and C) or bought from Sigma Aldrich (used for sample A). All other chemicals were obtained from commercial sources and were of analytical grade. Deionized water (water purified with the MilliQ system from Millipore, Bedford, MA, USA) was used in all solutions.

Coupling of linker to alginate. Periodate oxidation followed by reductive amination was used to covalently bind the linker 4-pentyn-1-amine to the alginate chain (see Fig. 1, step (1) and step (2)). In step (1) the alginate was partially oxidized using periodate ions (IO_4^-), based on previously published protocols[42–44].

Alginate was dried overnight in a desiccator. The weight of the dried alginate was adjusted for water content (10% residual water)[45] and dissolved in water corresponding to a final concentration of 7.0–8.8 mg/ml, depending on the viscosity of the solution. n-propanol was added to the samples to a final concentration of 10% (v/v), followed by degassing with nitrogen gas (N_2). Henceforth, the samples were protected from light. Sodium (meta) periodate ($NaIO_4$) was added from a freshly made stock solution of 0.25 M to a periodate/monomer molar ratio (P_0) = 0.08. The samples were incubated at 4 °C under gentle mixing until the reactions had run to completion (46–72 hours). To confirm that the reactions had run to completion (all IO_4 consumed), a titration test was performed: 0.5 ml of the reaction mixture was mixed with 5 ml 0.5 M cold phosphate buffer (NaH_2PO_4), pH 7.0 and 0.75 ml 60% (w/v) potassium iodide (KI). If unreacted periodate was present, this would result in yellow coloration (no color change would be observed if all periodate has been consumed). The solutions were then titrated with 2.5 mM sodium thiosulfate ($Na_2S_2O_3$). Close to the titration end-point, a few droplets of 10 mg/ml starch was added to the samples giving a blue color. Titration was then continued until the blue color disappeared.

Finally, the samples were dialyzed against deionized water until the measured conductivity was below 4 μS. All oxidized alginates were lyophilized after dialysis and thereafter stored at −18 °C.

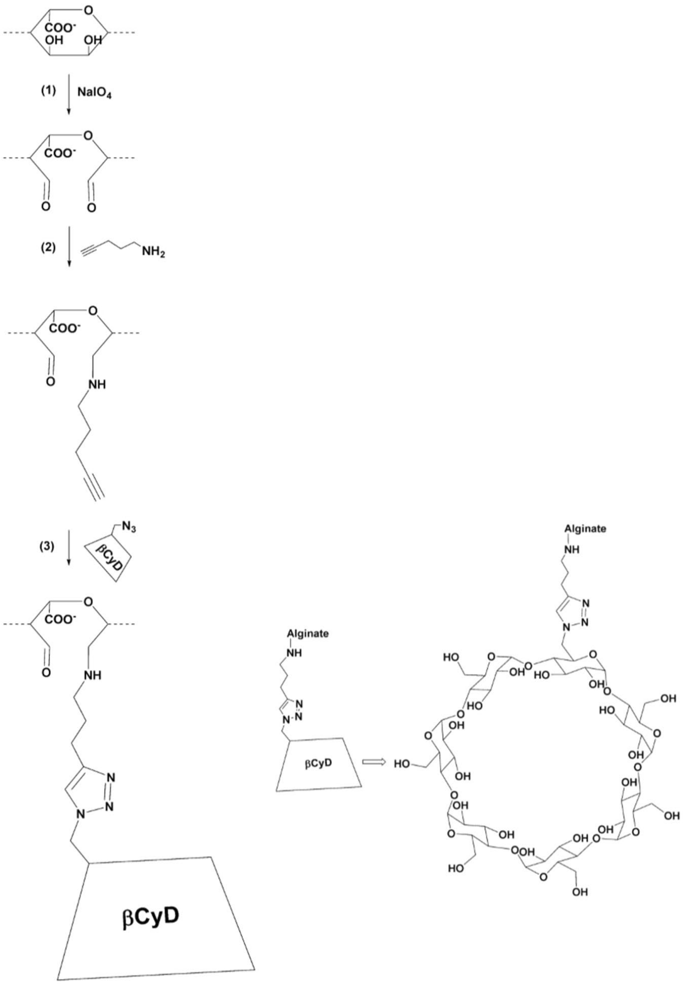

Figure 1. Scheme of the three-step synthesis of alginate (here shown for a G residue) grafted with β-CyD; (1) partial oxidation of alginate with metaperiodate, (2) grafting of the alkyne linker to either C2 or C3 of the oxidized alginate residues[37] (3) grafting of N_3-β-CyD to the alkyne linker with the Cu(I)-catalyzed azide alkyne cycloaddition click-reaction[31]. β-CyD is not appropriately scaled compared to the alginate.

In step (2) (Fig. 1) the linker, 4-pentyn-1-amine was covalently linked to the oxidized alginate by reductive amination based on the protocol developed by Dalheim *et al.*[24]. Periodate oxidized alginate (POA) was dissolved in deionized water and methanol was added according to final concentrations of 3 mg/ml and 12% (v/v) respectively. 1.2 M 4-pentyn-1-amine in MeOH was added to a concentration of 6 mM or 24 mM, corresponding to 5 and 20 molar equivalents, respectively, of the linker relative to the amount of oxidized residues ($P_0 = 0.08$). 0.25 M 2-picoline borane complex in MeOH was then added according to a final concentration of 24 mM (20 molar equivalents relative to P_0). The pH was adjusted to 5.8 with 1 M acetate buffer, pH 5.0. The reactions were incubated at room temperature under gentle mixing for 48–96 hours. The samples were dialyzed (MWCO 12–14 000 kDa) against two shifts of seven liters 50 mM NaCl and subsequently against deionized -water until the conductivity was below 4 μS. The final products were freeze dried and stored at −18 °C until further use.

Grafting of β-CyD to alginate. The grafting of β-CyD to alginate was achieved by using the Cu(I)-catalyzed azide-alkyne cycloaddition click-reaction[31], see Fig. 1, step (3). Alginate with covalently bound 4-pentyn-1-amine (product step (2)) was dissolved in deionized water to 3.5–7.4 mg/ml. In the following procedure, the amount of added reactants is given as molar equivalents relative to the theoretical oxidation degree 8%. Two equivalents of N_3-β-CyD were added into the alginate solution. Dimethyl sulfoxide (DMSO) was then added slowly to a final concentration of 40% (v/v). Freshly made 0.1 M sodium ascorbate was added to a final concentration of 0.3 equivalents and thereafter 0.11 equivalents of 0.02 M TBTA in DMSO were added. The mixture was deoxygenated with nitrogen gas for about five minutes, and subsequently 0.1 equivalents of 0.06 M $CuSO_4$ were added. Thereafter, the mixture was again deoxygenated for about three minutes. The sample vials were closed, and the reaction mixture incubated at 50 °C under gentle mixing for 40–51 hours. All samples were dialyzed first against 50 mM NaCl and then against deionized water, as described above, until conductivity was below 2 µS and freeze dried.

To remove residual copper ions, the β-CyD grafted alginate was treated with Ambersep GT74 resin. 2–15 mg/ml β-CyD grafted alginate in deionized water was added to 8 g resin per g polymer. Samples were shaken for 24–72 hours, and the resin was removed by filtration. Samples were thereafter dialyzed, lyophilized and stored at −18 °C.

NMR. All alginate samples were subjected to a mild acid hydrolysis as previously described[46] to reduce the viscosity prior to NMR analysis. Approximately 10 mg sample was dissolved in ~600 µl 99.9 atom % D_2O together with 5 µl 3-(trimethylsilyl)-propionic-2,2,3,3-*d*4 acid sodium salt (TSP; chemical shift reference) and 20 µl 0.3 M triethylene-tetra-amine hexaacetate (TTHA; chelate divalent cations). The NMR experiments were carried out on a BRUKER AVIII-HD 600 spectrometer equipped with TXI (H/C/N) probe or a BRUKER Avance DPX 400 spectrometer (Bruker, BioSpin AG, Fällanden, Switzerland) equipped with a 5 mm z-gradient DUL (C/H) probe). The amount of 4-pentyn-1-amine linker and β-CyD grafted to the alginate was determined from 1D ^1H spectra, recorded at 90 °C on the 400 MHz spectrometer for all samples.

Diffusion-Ordered SpectroscopY (DOSY) was used to measure the diffusion of the coupled products. A 2D DOSY was measured using a Bruker BioSpin stimulated echo pulse sequence with bipolar gradients (STEBPGP). Gradient pulses of 2 ms duration (δ) and 32 different strengths varying linearly from 0.03 to 0.57 $T \cdot m^{-1}$ were applied and the diffusion delay (Δ) was set to 80 ms. The DOSY spectrum was recorded at 25 °C on the 600 MHz spectrometer. The spectra were recorded using the TopSpin software versions 1.3, 2.1 or 3.2 (Bruker BioSpin AG, Fällanden, Switzerland) and processed and analyzed with the TopSpin software versions 3.0 and 3.2 (Bruker BioSpin AG, Fällanden, Switzerland).

SEC-MALS. The molecular weight of the grafted alginates was measured with Size Exclusion Chromatography with MultiAngle Light Scattering detection (SEC-MALS) according to previous published protocols[43]. The setup consisted of a mobile phase reservoir, an on-line degasser (Degasi Classic, Biotech), an HPLA isocratic pump (LC-10AD, Shimadzu), an autoinjector (SCL-10A VP, Shimadzu), a precolumn and one or two serially connected columns (TSK 6000 PW and TSK gel PWH guard column, Toso Haas, for the stipe alginate and TSK 4000 + 2500 PWXL for the modified alginates). The column outlet was connected to two serially connected detectors, a multiangle laser light scattering photometer ($\lambda_0 = 0.633$ nm) (Dawn DSP, Wyatt, USA) followed by a differential refractometer (P-10 cell) (Optilab DSP, Wyatt, USA). 0.15 M $NaNO_3$ with 0.01 M EDTA, pH 6.0 was used as the mobile phase for the stipe and partially oxidized alginate. 20% acetonitrile was added to the mobile phase for the alginate grafted with linker and β-CyD. The samples were dissolved in the mobile phase and filtered (pore size 0.8 µm) prior to injection. The analysis was carried out at ambient temperature with a flow rate of 0.5 ml/min. Injection volume and sample concentration was adjusted to obtain an optimal light scattering signal without influencing the RI profile (overloading). Astra software v. 6.1.1 (Wyatt, USA) was used to collect and process the obtained data, using a refractive index increment (dn/dc_μ) of 0.150 ml/g for alginate samples[43].

Hydrogel formation of β-CyD grafted alginate and release of methyl orange. Hydrogel formation of the β-CyD grafted alginate was performed by dripping the alginate solution into a $CaCl_2$ solution (100 mM). For the release experiment, four different samples of 1.8% (w/v) alginate solutions were made; one with only unmodified *L. hyperborea* stipe alginate, one where the unmodified alginate was mixed with free β-CyD (1.7 mg/ml), and two where unmodified alginate was mixed with 25% and 50% (w/w) β-CyD-grafted alginate, respectively). The pH of the alginate solutions was adjusted to 5.5–6.0. The weight of the β-CyD was taken into account in making the 1.8% (w/v) solutions with grafted alginates. Beads were made by dripping 3 ml of the alginate solution with a pipette into 50 ml of 100 mM $CaCl_2$ with 0.15 mM methyl orange, pH 3.5. The beads were left in this solution for 13 hours to ensure saturation of both gelling Ca^{2+} ions and methyl orange.

The release of methyl orange from the beads was evaluated through a series of saline treatments, as follows. The gel beads were immersed in 18 ml 0.9% (w/v) NaCl and left on a turn-over table for one hour (first saline treatment). The beads were then recovered from the solution and immersed in another 18 ml 0.9% (w/v) NaCl (second saline treatment). This procedure was performed for a total of six times. The concentration of methyl orange in the saline treatment solutions (after removal of the beads and adjusting the pH to 8–10) was measured as absorbance at 460 nm in a Nuncleon Flat Bottom Black Polystyrol 96-well plate (Thermo Fischer Scientific) using a multifunctional plate reader (Infinite 200 PRO, TECAN). Absorbance was converted to concentration using a calibration curve for absorbance at 460 nm as a function of the concentration of methyl orange in 0.9% (w/v) NaCl. Methyl orange can be used as an indicator due to its color change at different pH values: At acidic pH methyl orange gives a red solution, while at alkaline pH the compound gives a yellow color (the pK_a value for methyl orange is 3.49[47]. The solutions for the calibration curve were also pH-adjusted so that the predominant form of methyl orange was the same as for the saline treatment solutions.

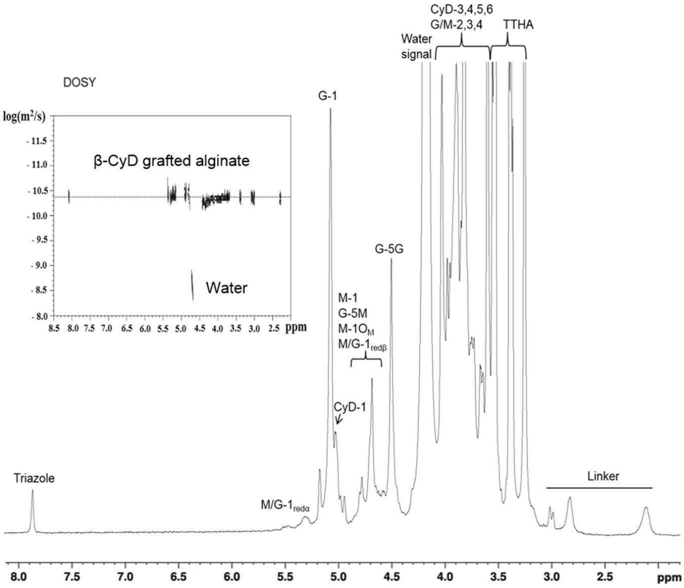

Figure 2. ^{1}H NMR and DOSY (upper left corner) of partially oxidized alginate grafted with β-CyD. The assignment of the protons of the different chemical groups are indicated. The ^{1}H NMR-spectrum was recorded at 400 MHz and 90 °C in D_2O. The DOSY spectrum was recorded at 600 MHz and 25 °C in D_2O. Dotted lines indicates the diffusion coefficient of the molecules.

Results and Discussion

β-CyD was grafted to alginate ($F_G = 0.7$) using a three-step strategy as shown in Fig. 1. The initial, (1) partial periodate oxidation, was followed by (2) grafting of a linker (4-pentyn-1-amine) by reductive amination and (3) grafting of β-CyD to the linker by the Cu(I)-catalyzed azide-alkyne cycloaddition click-reaction.

Tunable grafting of linker to alginate. The degree of oxidation can be used to tune the final degree of grafting. In step (1) of the synthesis (Fig. 1), the alginate was subjected to an amount of periodate corresponding to a degree of oxidation of 8% ($P_0 = 0.08$), which was a compromise between preserving the hydrogel formation and sufficient grafting. Higher degrees of oxidation can be obtained by adding more periodate at the expense of gelling properties[48,49]. The completeness of the reaction was checked by titration, showing that no unreacted periodate was present in the reaction mixtures. The partially oxidized alginate was also analyzed by ^{1}H NMR-spectra of *L. hyberborea* (Supplementary Information A).

The linker chosen here for grafting CyD to alginate was based on previous work done on synthesizing β-CyD-dextran polymers[31] and the grafting of amine-moieties to partially oxidized alginate[37]. In addition to using a linker to graft CyDs to alginate, an attempt to shorten the time of synthesis was also performed with partially oxidized alginate directly reacting with NH_2-CyDs using reductive amination. However, grafting NH_2-βCyDs or triazole-propylamine-βCyDs directly to partially oxidized alginate was not successful. Therefore, the linker 4-pentyn-1-amine was chosen as it had the required amine-group for use in the reductive amination reaction as well as an alkyne group which was essential for the click-reaction. Furthermore, it was hypothesized that 4-pentyn-1-amine would have long enough linker to offer easy access to the alkyne moiety during the click reaction, as well as giving sufficient accessibility to the CyD cavity after grafting without affecting the gelling properties of the alginates significantly.

The degree of grafting for the linker in step (2) was analyzed by NMR spectroscopy and calculated as % mol linker/mol uronic acid residues, by comparing the integrals of the anomeric (H-1) protons of alginate and one of the peaks originating from the linker (see Fig. 2). An overview of the results for the reductive amination is shown in Table 1.

Parameter selection for the reductive amination reaction was based on a recent study where RGD-peptides were grafted to periodate oxidized alginates using reductive amination[37]. The reductive amination reaction is pH dependent and the optimal pH is, in many cases, a compromise to achieve efficient protonation of the carbonyl group and simultaneous deprotonation of the amino group[50]. In our recent work, the optimal pH for coupling of amino acids and peptides to periodate oxidized alginates was found to be 5.8[37]. However, the pK_a values of the terminal amino group in peptides is in the range 6.8–8.0 while the pK_a value of the amino group on many aliphatic primary amines is similar to the pK_a of 4-pentyn-1-amine,10.6[51], thus affecting the optimal pH of the reaction.

	Sample	A	B	C
Reductive amination	Linker (molar equivalents relative to P_0)	5	20	20
	$W_{(POA)}$ (g)	3.0	0.14	0.10
	Reaction time (hours)	96	48	84
	Substitution (% mol linker/mol monomer)	1.6	2.2	5.6
	Yield (g)	2.9	0.14	0.11
Click-reaction	Reaction time (hours)	51	48	40
	$W_{(POA\text{-}linker)}$ (g)	2.0	0.14	0.070
	Concentration of alginate (mg/ml)	7.2	7.4	3.5
	Substitution (% mol CyD/mol linker)	100	90	84
	Yield (g)	2.5	0.097	0.067
	Final grafting degree (% mol CyD/mol uronic acid residues)	1.6	2.0	4.7

Table 1. Degree of grafting for the reductive amination and click-chemistry reactions with varying reaction parameters. The influence of the amount of linker and reaction time was investigated for the reductive amination reaction and concentration of alginate and reaction times for the click-reaction. The final degree of CyD grafted to the partially oxidized alginate is given.

Nevertheless, pH 5.8 was also used in this study as it has been observed that protonation of the carbonyl oxygen is more important to the reductive amination reaction than deprotonation of the amino group[37]. To compensate for the suboptimal pH, a higher molar equivalent of the linker relative to the concentration of oxidized residues, as well as a prolonged reaction time, were used. Increasing the concentration of 4-pentyn-1-amine to 20 molar equivalents resulted in a grafting degree of 5.6%. This demonstrates that the amount of alkyne linker grafted to the alginate chains can be tuned by varying the concentration of the substituent. Increasing the reaction time from 48 to 84 hours (using 20 molar equivalents of substituent) also resulted in a higher degree of grafting.

Efficient click-chemistry for the grafting of β-CyD to alginate. Figure 2 shows a typical ^{1}H NMR-spectra of β-CyD grafted alginate (product of step (3)). The linker, (4-pentyn-1-amine) gives rise to signals in the region 2.0–3.0 ppm and the click reaction between 4-pentyn-1-amine and N_3-β-CyD results in a triazole unit (see Fig. 1, step (3)) which gives a distinguishable singlet peak at 7.8 ppm. The presence of this peak clearly indicates that the click reaction was successful. Furthermore, the β-CyD grafted alginate was analyzed by DOSY to indirectly verify that β-CyD was covalently linked to the partially oxidized alginate[37]. As can be seen in Fig. 2 (insert), signals from both the linker and the triazole group appear to have the same diffusion coefficient as the alginate, indicating that they are covalently coupled. DOSY also confirms that non-reacted components were removed.

The amount of β-CyD bound to the linker was calculated as % mol β-CyD/mol linker based on the ^{1}H NMR-spectra recorded for the samples after complete synthesis, using the integral of one peak for the linker and the integral of the triazole singlet peak. The concentration of alginate and reaction time were varied to study the effect on the click-reaction (Table 1). Increasing the reaction time from 40 to 48 hours and the concentration of 4-pentyn-1-amine linked alginate from 3.5 to 7.4 mg/ml increased the grafting degree from 84% (sample C) to 90% (sample B). Further increasing the reaction time in step (3) from 48 hours to 51 hours, using a concentration of 7.2 mg/ml alginate (sample A), gave full substitution of CyD on the linker (100% (mol CyD/mol linker). Taking into account the starting degree of grafting of the linker (see Table 1), this corresponded to a final degree of grafting (% mol β-CyD/mol uronic acid residues) of 1.6% for sample A, 2.0% for sample B, and of 4.7% for sample C. These results show that the copper-catalyzed click-reaction is very efficient and robust, which is in line with observations reported in literature[40]. Consequently, the most important factor for determining the final degree of grafting is the amount of alkyne linker grafted to the alginate chain.

Molecular weight. The weight- and number-average molar mass for the unmodified stipe alginate, periodate oxidized stipe alginate (POA), linker grafted POA (POA-linker; product of step (2)) and βCyD grafted POA (POA-βCyD; product of step (3)) are presented in Table 2. The concentration profiles and molecular weights are given in Supplementary Information B.

As seen in Table 2 both the oxidation and the reductive amination reaction was accompanied with some degradation of the alginate. Similar results have also been observed[37] previously. Partial periodate oxidation gives the alginate polymer a more flexible nature due to the ring opening of the oxidized residues[42,43,52]. The ring opening further enhances the susceptibility to degradation of the alginate[53]. However, after the reduction has taken place, the stability of the polymer at physiological pH is expected to be comparable to that of native alginate[54]. Degradation caused by the click-reaction is not apparent from the weight-average molar mass as seen in Table 2. Indeed, an increase in molar mass is observed for the β-CyD-grafted alginate. If no degradation occurs during the click-reaction, an increase in molar mass is expected as a result of the grafting of CyDs on the alginate.

Hydrogel formation of β-CyD grafted alginate and release of methyl orange. The objective of this study was to combine the gelation ability of the alginate with the capability of CyDs to form inclusion complexes. Therefore, a proof-of-concept study was carried out to evaluate whether the new grafted material retained

Sample	$\overline{M}_w$ (kDa)	$\overline{M}_n$ (kDa)
L. hyperborea Alginate	135	79
POA	89	48
POA-linker	63	36
POA-βCyD	70	42

Table 2. Molecular weight data derived from SEC-MALS data: weight- and number-average molar mass ($\overline{M}_w$ and $\overline{M}_n$). POA: partially oxidized alginate. POA-linker: POA coupled with 4-pentyn-1-amine. POA-βCyD: β-CyD-grafted alginate.

the intrinsic properties of both the alginate and the CyD. The β-CyD-grafted alginate was by itself able to form Ca-alginate beads. However, the gel was very labile and easily deformed upon handling. The disruption of the alginates' gelling ability can largely be ascribed to the structural changes in the alginate molecule upon periodate oxidation, namely opening of the sugar ring between C2 and C3, which forms flexible "hinges" in the polymer chain[42,43,52]. This basically disrupts the G-blocks sequences and, consequently, the polymers' potential for ionic crosslinking. Furthermore, the oxidation of G-units have previously been found to occur faster than the oxidation of M-units in the alginate chain[55], underlining that the effective length of the ion-binding G-blocks is most likely shortened due to the oxidation. Therefore, Ca-alginate beads in this study were made from a mixture of the β-CyD-grafted alginate and a strong gelling alginate (unmodified *L. hyperborea* stipe alginate). This resulted in gel beads with good initial integrity suitable for release studies.

The stability of the gel beads was evaluated by visual inspection of the beads after immersing them in consecutive saline solutions. The beads containing β-CyD-grafted alginate were more labile and dissolved faster compared to pure alginate beads (Fig. 3). Disintegration was visible for beads with 50% (w/w) β-CyD-grafted alginate after the fourth saline treatment, while beads made of 25% (w/w) were more stable. In contrast, the beads made from only unmodified alginate with or without free β-CyD remained largely intact after all six saline treatments. This clearly shows that the content of grafted material influences the stability of the beads. Swelling and disruption of the Ca-alginate gel beads when placed in saline solutions was expected, as calcium-ions are exchanged by sodium-ions, leading to a weakening of the gel network followed by swelling[56]. Both reduction of G-block sequence length and numbers upon grafting and reduced molecular weight of the polymer can reduce gel strength of the grafted material[2], resulting in weaker and less stable gels compared to the unmodified alginate. The bulky nature of the CyD may also destabilize the gel network by preventing the formation of junction zones due to steric hindrance[27]. Swelling of alginate drug delivery systems have been shown to depend on which body fluid they come into contact with[24]. A destabilized gel may be favorable in a system where clearance of the gel over time is wanted. However, in order to stabilize by the alginate gel, other gelling ions (e.g. Ba^{2+} or Sr^{2+}) could be used, which are known to form stronger crosslinks and depend on shorter G-blocks[57,58]. In addition, using a chemo-enzymatic strategy and introducing the G-blocks after the chemical modification may lead to a more stable gel[35,59]. Degradation of the alginate or the grafted alginate is expected to be negligible since alginate hydrolysis is slow at neutral pH and so is the hydrolysis of grafted alginates[54].

The ability of β-CyD-grafted alginates to form inclusion complexes was studied using methyl orange as a model compound. β-CyDs can form inclusion complexes with methyl orange where the inclusion complex in neutral/basic media can be both 1:1 ($K_a = \sim 3000\,M^{-1}$) and 1:2 ($K_a < 100\,M^{-1}$)[60]. The association constant for the 1:2 inclusion complex is low compared to the 1:1 inclusion complex and can therefore be neglected. Visual inspection of the beads after each saline treatment revealed that the beads containing the β-CyD-grafted alginate retained their color longer than both reference beads (unmodified alginate with and without free β-CyD, Fig. 3). After the third saline treatment, there was no observable color left in the reference beads, while the β-CyD-grafted alginate beads retained their color until dissolution of the beads. This strongly suggests β-CyD retain the ability to form inclusion complexes with methyl orange is upon grafting to alginates.

The release of methyl orange from the beads was assessed by the content in the saline solutions (Fig. 4). Visual inspection clearly showed a continued discoloration from the beads with β-CyD-grafted alginate. In contrast to this, saline solutions from beads not containing β-CyD or free β-CyD were near to colorless after the first saline treatment. The concentration of methyl orange in the saline solutions was quantified by measuring the absorbance at 460 nm. The quantitative measurements confirmed the observations that the release of methyl orange continued throughout the saline treatments for the beads with β-CyD-grafted alginate. More methyl orange was released from beads with 50% β-CyD-grafted alginate than beads with 25% β-CyD-grafted alginate. However, the beads with 50% β-CyD-grafted alginate were largely destabilized by extensive saline treatment and were fully dissolved in the last treatment solution, as discussed previously. Hence, it cannot be excluded that some of the methyl orange in the treatment solution was still bound to the β-CyD-grafted alginate that dissolved from the gel bead.

Earlier studies have shown that the inclusion complex between β-CyD and methyl orange has a different absorbance than pure methyl orange[60], which could influence the results when quantifying the methyl orange in the saline solutions. However, in this study no significant changes in absorbance were observed. The association constants of polymer-bound CyD towards various guest molecules has previously been shown to change compared to free CyD and guest molecule alone[31,61]. This has not yet been tested with the β-CyD-grafted alginates.

The data indicate that the beads containing β-CyD-grafted alginate were able to absorb significantly more methyl orange compared to the beads made of only alginate and alginate with free β-CyD. Assuming a homogeneous distribution of methyl orange in the loading solution containing the alginate beads (140 μmol/L), the amount of methyl orange in the gel volume (3 mL) would be 0.4 μmol. As seen in Fig. 4, the released methyl

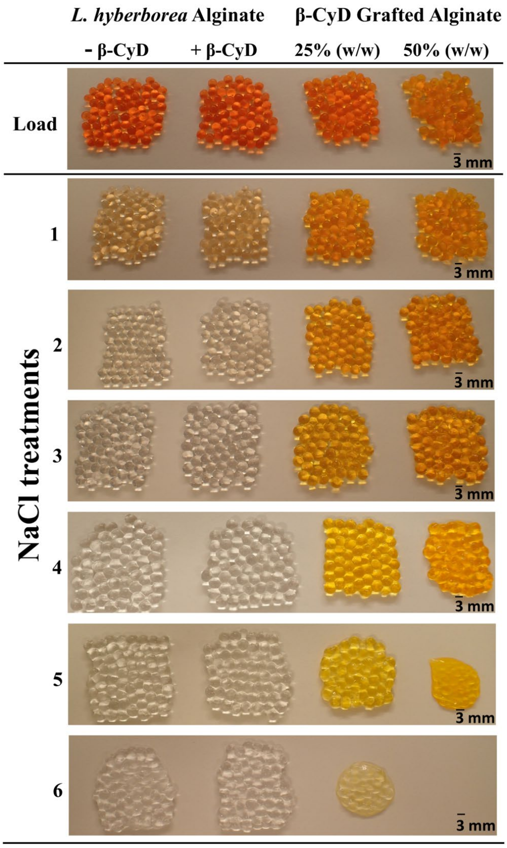

Figure 3. Ca-alginate beads made of unmodified *L. hyberborea* stipe alginate (−/+free β-CyD), and beads containing β-CyD grafted alginate mixed with unmodified *L. hyberborea* stipe alginate in two different ratios. The pictures were taken after removal of all the beads from the load-solution containing methyl orange (load) and gelling ions, and after immersion in consecutive solutions of 0.9% (w/v) NaCl (treatment 1–6).

orange from beads with 50% β-CyD-grafted and 25% β-CyD-grafted alginate is 6.3 and 4.5 times higher, respectively, indicating an accumulation of methyl orange in the beads with β-CyD-grafted alginate proportional to the amount of grafted material.

The ratio of methyl orange released from the beads and the amount of grafted β-CyD in the modified alginate beads can give further information on the release system. The amount of grafted β-CyD was 1.0 and 2.0 µmol for the beads with 25% and 50% β-CyD-grafted alginate, respectively. The total amount of methyl orange released from the 25% modified alginate beads was 1.8 µmol. This gives a ratio between the cyclodextrin and methyl orange of approximately 1:2. In the beads where 50% of the alginate was modified, 2.5 µmol is released and hence closer to 1:1 ratio between β-CyD and methyl orange.

The gel beads with unmodified alginate and free β-CyD displayed a similar release profile of methyl orange as those made of unmodified alginate only (Fig. 4), indicating that the free β-CyD did not retain methyl orange in the gel network as observed for the grafted β-CyD. NMR analysis of the methyl orange load solution for the beads made from alginate and free β-CyD showed that β-CyD (1135 Da) had leaked out of the beads and into the surrounding solution (data not shown). Previously, IgG (150 kDa) has been shown to diffuse into Ca-alginate microbeads[62]. Hence, the alginate gel by itself has limited ability to immobilize smaller molecules as also demonstrated in this study. However, via grafting of β-CyD, methyl orange could be retained in the beads before being released upon treatments with saline solution. This system could be interesting for different fields and further studies are needed to understand its full potential, such as drug delivery, tissue engineering and water treatment with alginate binding divalent ions and CyD binding smaller non-polar molecules[63].

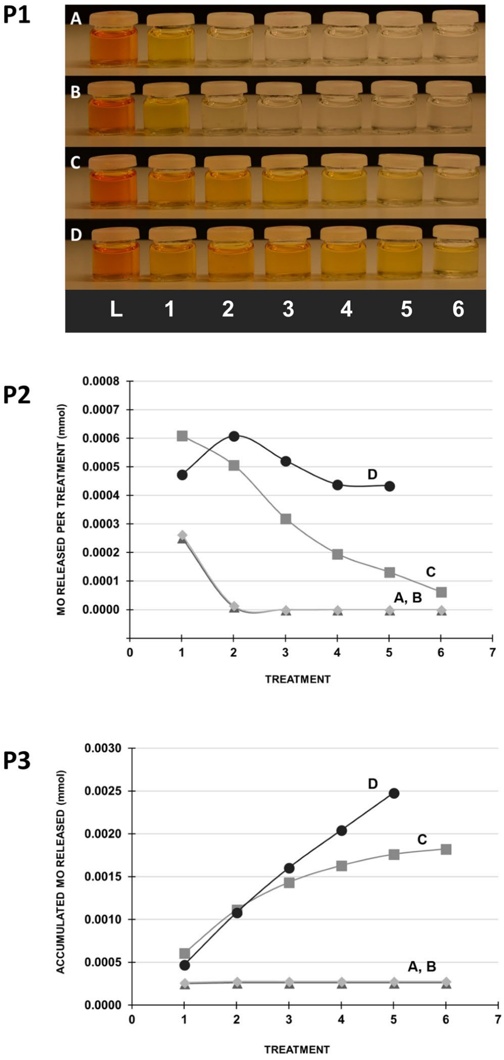

Figure 4. Release of methyl orange (MO) from Ca-alginate beads in consecutive saline treatments (0.9% (w/v) NaCl, one hour). Upper panel (P1): Picture of loading solutions (L) and saline treatment solutions (numbers 1–6) after removal of the beads. Middle panel (P2): Quantified amount of MO in the treatment solutions. Lower panel (P3): Accumulated release of MO. Beads made of unmodified alginate (A), unmodified alginate + free β-CyD (B), 75% (w/w) unmodified alginate +25% (w/w) β-CyD-grafted alginate (C) and 50% (w/w) unmodified alginate +50% (w/w) β-CyD-grafted alginate (D). Guidelines are drawn between the measurements.

Conclusion

Alginate was successfully grafted with β-CyD through a three-step synthesis, combining the gelation ability of the alginate with the inclusion complex ability of the cyclodextrins. The obtained degree of grafting ranged from 1.6–4.7% mol β-CyD/mol uronic acid residues, depending on the applied reaction parameters. The chosen synthesis methodology allows the degree of grafting to be regulated, resulting in a material that has tunable properties. The final degree of grafting was shown to depend largely on the amount of linker (4-pentyn-1-amine) grafted to periodate oxidized alginate. A reduction in molecular weight was observed during the oxidation and reductive amination step. The proof-of-concept study showed that the grafted CyDs retained their ability to form inclusion complex with methyl orange. Gel beads made from a mixture of β-CyD-grafted alginate and unmodified alginate had an increased and prolonged release of methyl orange compared to non-modified beads. The stability of the Ca-alginate gel beads was also affected by varying the amounts of the grafted and unmodified alginates. Altogether, the β-CyD grafted alginate can potentially be used as an adaptable release system and further investigating is being done on the use of β-CyD-grafted alginate for controlled drug release.

References

1. Hoffman, A. S. Hydrogels for biomedical applications. *Adv. Drug Deliv. Rev.* **64**, 18–23 (2012).
2. Martinsen, A., Skjåk-Bræk, G. & Smidsrød, O. Alginate as immobilization material: I. Correlation between chemical and physical properties of alginate gel beads. *Biotechnol. Bioeng.* **33**, 79–89 (1989).
3. Alvarez-Lorenzo, C., Moya-Ortega, M. D., Loftsson, T., Concheiro, A. & Torres-Labandeira, J. J. Cyclodextrin-Based Hydrogels. In *Cyclodextrins in Pharmaceutics, Cosmetics, and Biomedicine: Current and Future Industrial Applications* (ed. Bilensoy, E.) 297–321 (Wiley, 2011).
4. Smidsrød, O. & Skjåk-Bræk, G. Alginate as immobilization matrix for cells. *Trends Biotechnol.* **8**, 71–78 (1990).
5. Aarstad, O. A., Tøndervik, A., Sletta, H. & Skjåk-Bræk, G. Alginate sequencing: an analysis of block distribution in alginates using specific alginate degrading enzymes. *Biomacromolecules* **13**, 106–116 (2012).
6. Draget, K. I., Moe, S. T., Skjåk-Bræk, G. & Smidsrød, O. Alginates. In *Food Polysaccharides and Their Applications* (eds Stephen, A. M., Phillips, G. O. & Williams, P. A.) 289–334 (CRC Press, 2006).
7. Donati, I., Mørch, Y. A., Strand, B. L., Skjåk-Bræk, G. & Paoletti, S. Effect of Elongation of Alternating Sequences on Swelling Behavior and Large Deformation Properties of Natural Alginate Gels. *J. Phys. Chem. B* **113**, 12916–12922 (2009).
8. Andersen, T., Strand, B. L., Formo, K., Alsberg, E. & Christensen, B. E. Alginates as biomaterials in tissue engineering. In *Carbohydrate Chemistry Chemical and Biological Approaches* (eds Rauter, A. P. & Lindhorst, T. K.) **37**, 227–258 (The Royal Society of Chemistry, 2012).
9. Bochenek, M. A. *et al*. Alginate encapsulation as long-term immune protection of allogeneic pancreatic islet cells transplanted into the omental bursa of macaques. *Nat. Biomed. Eng.* **2**, 810–821 (2018).
10. Rokstad, A. M. A., Lacík, I. & Strand, B. L. Advances in biocompatibility and physico-chemical characterization of microspheres for cell encapsulation. *Adv. Drug Deliv. Rev.* **67–68**, 111–130 (2014).
11. Szejtli, J. Introduction and general overview of cyclodextrin chemistry. *Chem. Rev.* **98**, 1743–1753 (1998).
12. Larsen, K. L. Large Cyclodextrins. *J. Incl. Phenom. Macrocycl. Chem.* **43**, 1–13 (2002).
13. Wimmer, R., Aachmann, F. L., Larsen, K. L. & Petersen, S. B. NMR diffusion as a novel tool for measuring the association constant between cyclodextrin and guest molecules. *Carbohydr. Res.* **337**, 841–849 (2002).
14. Otzen, D. E., Knudsen, B. R., Aachmann, F., Larsen, K. L. & Wimmer, R. Structural basis for cyclodextrins' suppression of human growth hormone aggregation. *Protein Sci.* **11**, 1779–1787 (2002).
15. Aachmann, F. L., Otzen, D. E., Larsen, K. L. & Wimmer, R. Structural background of cyclodextrin-protein interactions. *Protein Eng.* **16**, 905–912 (2003).
16. Larsen, K. L., Aachmann, F. L., Wimmer, R., Stella, V. J. & Kjolner, U. M. Phase solubility and structure of the inclusion complexes of prednisolone and 6 alpha-methyl prednisolone with various cyclodextrins. *J. Pharm. Sci.* **94**, 507–515 (2005).
17. Steed, J. W. & Atwood, J. L. Supramolecular Chemistry. In *Supramolecular Chemistry* 307–384 (Wiley, 2009).
18. Datz, S. *et al*. Biocompatible crosslinked β-cyclodextrin nanoparticles as multifunctional carriers for cellular delivery. *Nanoscale* **10**, 16284–16292 (2018).
19. Jiang, Y., Liang, Y., Zhang, H., Zhang, W. & Tu, S. Preparation and biocompatibility of grafted functional β-cyclodextrin copolymers from the surface of PET films. *Mater. Sci. Eng. C* **41**, 1–7 (2014).
20. Klempaiová, M. *et al*. Cytotoxicity testing of a polyurethane nanofiber membrane modified with chitosan/β-cyclodextrin/berberine suitable for wound dressing application: evaluation of biocompatibility. *Cell Tissue Bank.* **17**, 665–675 (2016).
21. Hu, L.-Z. *et al*. Enhanced gene transfection performance and biocompatibility of polyethylenimine through pseudopolyrotaxane formation with α-cyclodextrin. *Nanotechnology* **28**, 125102 (2017).
22. Woldum, H. S., Larsen, K. L. & Madsen, F. Cyclodextrin controlled release of poorly water-soluble drugs from hydrogels. *Drug Deliv* **15**, 69–80 (2008).
23. Marcelo, G. *et al*. Lignin inspired PEG hydrogels for drug delivery. *Mater. Today Commun.* **7**, 73–80 (2016).
24. Tønnesen, H. H. & Karlsen, J. Alginate in drug delivery systems. *Drug Dev. Ind. Pharm.* **28**, 621–630 (2002).
25. Augst, A. D., Kong, H. J. & Mooney, D. J. Alginate hydrogels as biomaterials. *Macromol. Biosci.* **6**, 623–633 (2006).
26. Nielsen, A. L., Madsen, F. & Larsen, K. L. Cyclodextrin modified hydrogels of PVP/PEG for sustained drug release. *Drug Deliv* **16**, 92–101 (2009).
27. Gomez, C. G., Chambat, G., Heyraud, A., Villar, M. & Auzely-Velty, R. Synthesis and characterization of a beta-CD-alginate conjugate. *Polymer (Guildf).* **47**, 8509–8516 (2006).
28. Izawa, H. *et al*. Beta-Cyclodextrin-crosslinked alginate gel for patient-controlled drug delivery systems: regulation of host-guest interactions with mechanical stimuli. *J. Mater. Chem. B* **1**, 2155–2161 (2013).
29. Miao, T., Fenn, S. L., Charron, P. N. & Oldinski, R. A. Self-Healing and Thermoresponsive Dual-Cross-Linked Alginate Hydrogels Based on Supramolecular Inclusion Complexes. *Biomacromolecules* **16**, 3740–3750 (2015).
30. Ramirez, H. L. *et al*. Cyclodextrin-grafted polysaccharides as supramolecular carrier systems for naproxen. *Bioorg. Med. Chem. Lett.* **16**, 1499–1501 (2006).
31. Nielsen, T. T., Wintgens, V., Amiel, C., Wimmer, R. & Larsen, K. L. Facile Synthesis of beta-Cyclodextrin-Dextran Polymers by 'Click' Chemistry. *Biomacromolecules* **11**, 1710–1715 (2010).
32. Chiang, C.-Y. & Chu, C.-C. Synthesis of photoresponsive hybrid alginate hydrogel with photo-controlled release behavior. *Carbohydr. Polym.* **119**, 18–25 (2015).
33. Han, X.-J. *et al*. pH-induced shape-memory polymers. *Macromol. Rapid Commun.* **33**, 1055–1060 (2012).
34. Hermanson, G. T. Bioconjugate Techniques. In *Bioconjugate Techniques* 229–258 (Elsevier Academic Press, 2013).
35. Sandvig, I. *et al*. RGD-peptide modified alginate by a chemoenzymatic strategy for tissue engineering applications. *J. Biomed. Mater. Res. Part A* **103**, 896–906 (2015).
36. Pluemsab, W., Sakairi, N. & Furuike, T. Synthesis and inclusion property of alpha-cyclodextrin-linked alginate. *Polymer (Guildf).* **46**, 9778–9783 (2005).
37. Dalheim, M. Ø. *et al*. Efficient functionalization of alginate biomaterials. *Biomaterials* **80**, 146–156 (2016).
38. Rostovtsev, V. V., Green, L. G., Fokin, V. V. & Sharpless, K. B. A Stepwise Huisgen Cycloaddition Process: Copper(I)-Catalyzed Regioselective "Ligation" of Azides and Terminal Alkynes. *Angew. Chemie Int. Ed.* **41**, 2596–2599 (2002).
39. Tornøe, C. W., Christensen, C. & Meldal, M. Peptidotriazoles on solid phase: [1,2,3]-triazoles by regiospecific copper(I)-catalyzed 1,3-dipolar cycloadditions of terminal alkynes to azides. *J. Org. Chem.* **67**, 3057–3064 (2002).
40. Meldal, M. & Tornøe, C. W. Cu-catalyzed azide-alkyne cycloaddition. *Chem. Rev.* **108**, 2952–3015 (2008).
41. Chan, T. R., Hilgraf, R., Sharpless, K. B. & Fokin, V. V. Polytriazoles as Copper(I)-Stabilizing Ligands in Catalysis. *Org. Lett.* **6**, 2853–2855 (2004).

42. Smidsrød, O. & Painter, T. Effect of periodate oxidation upon the stiffness of the alginate molecule in solution. *Carbohydr. Res.* **26**, 125–132 (1973).
43. Vold, I. M., Kristiansen, K. A. & Christensen, B. E. A study of the chain stiffness and extension of alginates, *in vitro* epimerized alginates, and periodate-oxidized alginates using size-exclusion chromatography combined with light scattering and viscosity detectors. *Biomacromolecules* **7**, 2136–2146 (2006).
44. Kristiansen, K. A., Potthast, A. & Christensen, B. E. Periodate oxidation of polysaccharides for modification of chemical and physical properties. *Carbohydr. Res.* **345**, 1264–1271 (2010).
45. Haug, A. Composition and Properties of Alginates. *Nor. Inst. Seaweed Res.* **30** (1964).
46. Ertesvåg, H. & Skjåk-Bræk, G. *Modification of Alginate Using Mannuronan C-5-Epimerases*. *Carbohydrate Biotechnology Protocols* (Humana Press, 1999).
47. Reeves, R. L. The Protonation and Indicator Behavior of Some Ionic Azobenzenes in Aqueous Sulfuric Acid. *J. Am. Chem. Soc.* **88**, 2240–2247 (1966).
48. Gomez, C. G., Rinaudo, M. & Villar, M. A. Oxidation of sodium alginate and characterization of the oxidized derivatives. *Carbohydr. Polym.* **67**, 296–304 (2007).
49. Kristiansen, K. A. *et al.* Novel alginates prepared by independent control of chain stiffness and distribution of G-residues: Structure and gelling properties. *Carbohydr. Polym.* **77**, 725–735 (2009).
50. Sun, Z., Wei, Z. & Wei, K. A model for predicting the optimal conditions for labeling the carbohydrates with the amine derivatives by reductive amination. *Lett. Org. Chem.* **6**, 549–551 (2009).
51. Solomons, T. W. G. & Fryhle, C. B. *Organic chemistry*. (Wiley, 2008).
52. Lee, K. Y., Bouhadir, K. H. & Mooney, D. J. Evaluation of chain stiffness of partially oxidized polyguluronate. *Biomacromolecules* **3**, 1129–1134 (2002).
53. Kristiansen, K. A., Tomren, H. B. & Christensen, B. E. Periodate oxidized alginates: Depolymerization kinetics. *Carbohydr. Polym.* **86**, 1595–1601 (2011).
54. Dalheim, M. Ø., Ulset, A.-S. T., Jenssen, I. B. & Christensen, B. E. Degradation kinetics of peptide-coupled alginates prepared via the periodate oxidation reductive amination route. *Carbohydr. Polym.* **157**, 1844–1852 (2017).
55. Painter, T. & Larsen, B. Formation of Hemiacetals between Neighbouring Hexuronic Acid Residues during the Periodate Oxidation of Alginate. *Acta Chem. Scand.* **24**, 813–833 (1970).
56. Strand, B. L. *Alginate microcapsules for cell therapy - a study of functional properties of capsules made of native and enzymatically tailored alginates* (2002).
57. Mørch, Y. A., Donati, I., Strand, B. L. & Skjåk-Bræk, G. Effect of Ca^{2+}, Ba^{2+}, and Sr^{2+} on alginate microbeads. *Biomacromolecules* **7**, 1471–1480 (2006).
58. Stokke, B. T., Smidsrød, O., Zanetti, F., Strand, W. & Skjåk-Bræk, G. Distribution of uronate residues in alginate chains in relation to alginate gelling properties — 2: Enrichment of β-d-mannuronic acid and depletion of α-l-guluronic acid in sol fraction. *Carbohydr. Polym.* **21**, 39–46 (1993).
59. Donati, I., Draget, K. I., Borgogna, M., Paoletti, S. & Skjåk-Bræk, G. Tailor-made alginate bearing galactose moieties on mannuronic residues: selective modification achieved by a chemoenzymatic strategy. *Biomacromolecules* **6**, 88–98 (2005).
60. Carrazana, J. *et al.* Complexation of methyl orange with beta-cyclodextrin: Detailed analysis and application to quantification of polymer-bound cyclodextrin. *Supramol. Chem.* **16**, 549–559 (2004).
61. Nielsen, T. T., Wintgens, V., Larsen, K. L. & Amiel, C. Synthesis and characterization of poly(ethylene glycol) based β-cyclodextrin polymers. *J. Incl. Phenom. Macrocycl. Chem.* **65**, 341 (2009).
62. Stanisci, A. *et al.* Overall size of mannuronan C5-Epimerases influences their ability to epimerize modified alginates and alginate gels. *Carbohydr. Polym.* **180**, 256–263 (2018).
63. Alsbaiee, A. *et al.* Rapid removal of organic micropollutants from water by a porous beta-cyclodextrin polymer. *Nature* **529**, 190–194 (2016).

Acknowledgements

This work was financed by the MARPOL project 221576 funded by the Research Council of Norway. Ann-Sissel Ulset (Department of Biotechnology and Food Science, NTNU) is thanked for SEC-MALS analysis and Reinhard Wimmer (Department of Chemistry and Bioscience, Aalborg University) is credited for running DOSY and advise on the manuscript. Wenche Iren Strand is thanked for excellent technical assistance.

Author Contributions

M.Ø.D., F.L.A., B.L.S., K.L.L. and T.T.N. planned and supervised the research. L.A.O. performed most of the practical laboratory experiments. All authors have participated in writing and reviewing the manuscript, as well as analyzing the data.

Additional Information

Supplementary information accompanies this paper at https://doi.org/10.1038/s41598-019-45761-4.

Competing Interests: The authors declare no competing interests.

Publisher's note: Springer Nature remains neutral with regard to jurisdictional claims in published maps and institutional affiliations.

Supplementary Paper I

Efficient Grafting of Cyclodextrin to Alginate and Performance of the Hydrogel for Release of Model Drug.

Line Aa. Omtvedt[1,#], Marianne Ø. Dalheim[1#], Thorbjørn T. Nielsen[2], Kim L. Larsen[2], Berit L. Strand[1], and Finn L. Aachmann[1]*

[1]Norwegian Biopolymer Laboratory (NOBIPOL), Department of Biotechnology and Food Science, NTNU - Norwegian University of Science and Technology, N-7491 Trondheim, Norway.

[2]Department of Chemistry and Bioscience, Aalborg University (AAU), 9220 Aalborg, Denmark.

[#]Shared authorship

*Corresponding author Finn L. Aachmann – finn.l.aachmann@ntnu.no

Supplementary Information A – ^{1}H-NMR of *L. hyperborea* and partially oxidized alginate

The ^{1}H NMR-spectra of partially oxidized alginate and *L. hyperborea* stipe alginate are shown in figure S1. Peaks are assigned according to literature[1].

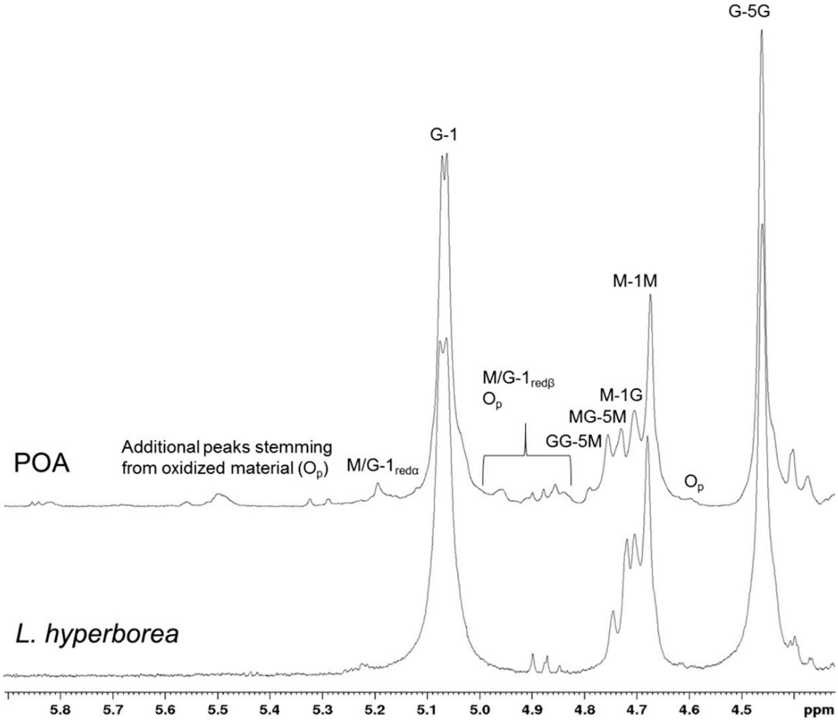

Supplementary figure S1. ^{1}H NMR-spectra of partially oxidized alginate (POA, 400 MHz, 90°C) and *L. hyperborea* (300 MHz, 90°C). Peaks denoted with an “O” refers only to the oxidized material.

(1) Kristiansen, K. A.; Schirmer, B. C.; Aachmann, F. L.; Skjåk-Bræk, G.; Draget, K. I.; Christensen, B. E. *Carbohydr. Polym.* **2009**, *77* (4), 725–735.

Supplementary Information B: SEC-MALS data

The concentration profiles and slice molecular weights are shown in figure S2 for one sample of unmodified alginate, partially oxidized alginate, partially oxidized alginate coupled with linker, and β-CyD-grafted alginate.

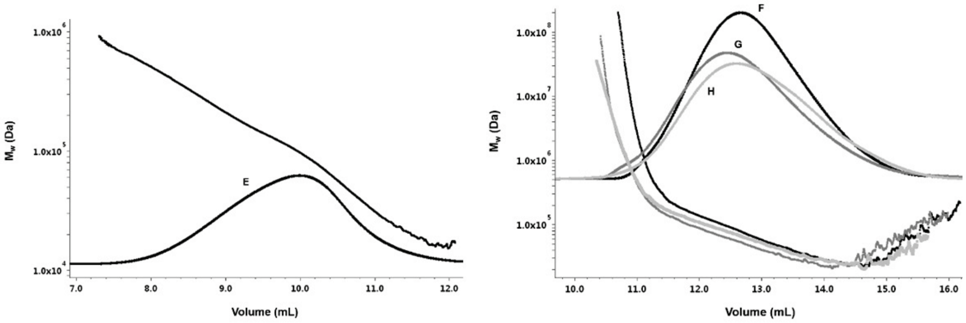

Supplementary figure S2: SEC-MALS data. Concentration profiles (solid lines) and slice molecular weights (dotted lines). Data at peak ends were removed due to noise or large deviations possibly due to aggregates prior to analysis. E: unmodified alginate. F: partially oxidized alginate. G: POA coupled with 4-pentyn-1-amine. H: β-CyD-grafted alginate.

Paper II

gels

Article

Mechanical Properties of Ca-Saturated Hydrogels with Functionalized Alginate

Marianne Ø. Dalheim [1,†], Line Aa. Omtvedt [1,†], Isabel M. Bjørge [2], Anita Akbarzadeh [1], João F. Mano [2], Finn L. Aachmann [1] and Berit L. Strand [1,*]

[1] NOBIPOL, Department of Biotechnology and Food Science, NTNU Norwegian University of Science and Technology, N-7491 Trondheim, Norway; marianne.dalheim@ntnu.no (M.Ø.D.); line.a.omtvedt@ntnu.no (L.A.O.); anita.akbarzadeh@ntnu.no (A.A.); finn.l.aachmann@ntnu.no (F.L.A.)
[2] Department of Chemistry, CICECO, Aveiro Institute of Materials, University of Aveiro, 3810-193 Aveiro, Portugal; isabel.bjorge1@gmail.com (I.M.B.); jmano@ua.pt (J.F.M.)
* Correspondence: berit.l.strand@ntnu.no; Tel.: +47-7359-4069
† These authors contributed equally to this work.

Received: 19 February 2019; Accepted: 17 April 2019; Published: 19 April 2019

Abstract: In this work, the mechanical properties and stability of alginate hydrogels containing functionalized alginates (peptide and β-cyclodextrin) were studied. There is an increasing interest in the modification of alginates to add functions such as cell attachment and increased solubility of hydrophobic drugs, for better performance in tissue engineering and drug release, respectively. Functionalization was achieved in this study via periodate oxidation followed by reductive amination, previously shown to give a high and controllable degree of substitution. Young's modulus and the stress at rupture of the hydrogels were in general lowered when exchanging native alginate with the modified alginate. Still, the gel strength could be adjusted by the fraction of modified alginate in the mixed hydrogels as well as the degree of oxidation. No notable difference in deformation at rupture was observed while syneresis was influenced by the degree of oxidation and possibly by the nature and amount of the grafted molecules. The mixed hydrogels were less stable than hydrogels with only native alginate, and modified alginate was released from the hydrogels. Furthermore, the hydrogels in general rather disintegrated than swelled upon saline treatments.

Keywords: Alginate hydrogels; periodate oxidation; reductive amination; mechanical properties; stability; cyclodextrin; peptide

1. Introduction

Hydrogels are 3D-structured water-swollen polymer networks that have been used as scaffold materials in tissue engineering, drug delivery vehicles and in the encapsulation of cells. They are considered suitable biomaterial candidates in these fields as they share many properties with biological tissue [1]. The elastic moduli of biological tissues dependent on the type of tissue [2], and it is, therefore, important to have control over the mechanical properties of the hydrogels used in the various biomaterial applications. Furthermore, the degradability of the hydrogels should also be adjustable. A degradable hydrogel may for example be beneficial if used in tissue engineering, where the goal is tissue regeneration and, hence, replacement of the hydrogel [3]. Alginates form hydrogels by ionic cross-linking of the polymer chains by certain divalent cations such as calcium and barium ions. The gelation can be done at very gentle conditions, e.g., under physiological conditions [4]. Also, alginates show low toxicity and are in general considered as highly biocompatible [5,6], which makes them suitable for in vivo applications.

Alginates are linear polysaccharides that consist of two monomers; β-D-mannuronic acid (M) and its C-5 epimer α-L-guluronic acid (G). It can be isolated from brown algae and certain bacteria. The monomers are 1→4 linked, and can be arranged as stretches of M-units (M-blocks), stretches of G-units (G-blocks), and stretches with alternating M- and G-units (MG-blocks) [4]. The G-blocks are very important for ionic gelation [7,8] and was originally thought to be solely responsible for the selective binding of certain divalent cations ($Mg^{2+} << Ca^{2+} < Sr^{2+} < Ba^{2+}$ [9]). More recent research has shown that also MG-blocks and M-blocks display ion selectivity for Ca^{2+} and Ba^{2+}, respectively [10]. Furthermore, the MG-blocks are involved in formation of junction zones upon gelation, either as MG/MG junctions or GG/MG junctions [11]. The composition of the alginate (M/G ratio) and the sequence of M and G residues is important for the mechanical and stability properties of alginate hydrogels. A high G-content is shown to result in mechanically stronger hydrogels compared to alginates with lower G-content [12]. Furthermore, increasing amount and length of MG-blocks have been found to increase both the mechanical strength [11,13] and the stability [12,13] of alginate hydrogels. Recent work has also demonstrated that long G-blocks found in algal alginates (DP > 100) account for their high mechanical strength, in comparison to engineered alginates with similar G content and average length of G-blocks [14]. Alginates varying in composition and sequential structure may be obtained from different sources [15], e.g., different algae or bacteria and different parts of the algae such as stipe and leaf. Furthermore, alginates with defined composition and sequence may be engineered in vitro from mannuronan [16] using a set of isolated bacterial epimerases [12,17].

Alginates may be chemically modified in order to add different functionalities. For example, bioactive peptide sequences, known to bind cellular receptors and induce cellular responses are commonly attached via the carboxyl group of the alginate by carbodiimide chemistry [18–20]. We have recently developed an alternative protocol for functionalization, using partial periodate oxidation and reductive amination with 2-methylpyridine borane complex [21] which gives high and controllable degrees of substitution. Previous work has also shown the use of partial periodate oxidation and reductive amination on alginate, but with the use of the toxic reducing agents sodium cyanoborohydride ($NaBH_3CN$) or sodium borohydride ($NaBH_4$) [22–24]. Periodate ions will react with vicinal diols, and in alginates this results in cleavage of the bond between C2 and C3 in the uronic acid residues (ring opening) and formation of an aldehyde group on both C2 and C3 [25]. Various substituents containing primary amines may further be covalently attached to the oxidized residues by reductive amination. Due to the ring opening, the alginate molecule becomes more flexible [26–28] and more prone to depolymerization [29] than non-oxidized alginates. The gel-forming properties as well as the mechanical properties of alginate hydrogels is much affected upon partial periodate oxidation (typically 1–8% oxidized residues) [30,31], which is thought to be a combined effect of the above mentioned altered properties as well as disruption of G-blocks and MG-blocks by the oxidized residues. In studies of cell attachment [21] and release of hydrophobic molecules [32] using peptide-grafted and β-cyclodextrin grafted alginates, respectively, prepared via this strategy, the hydrogels were made using a mixture of unmodified and modified alginates. The objective of this study is to further investigate the mechanical properties and stability of hydrogels containing oxidized and functionalized alginates alone and in combination with a strong gel-forming unmodified alginate. Three different substituents varying in size (Figure 1B) as well as in field of application were applied: methyl tyrosine ester as a small size substituent used as a model molecule, the bioactive hexapeptide GRGDSP as a larger substituent relevant for cell attachment and the bulky β-cyclodextrin substituent relevant for drug release. It was hypothesized that the mechanical properties and stability can be adjusted for different applications by varying the fraction of modified and unmodified alginate.

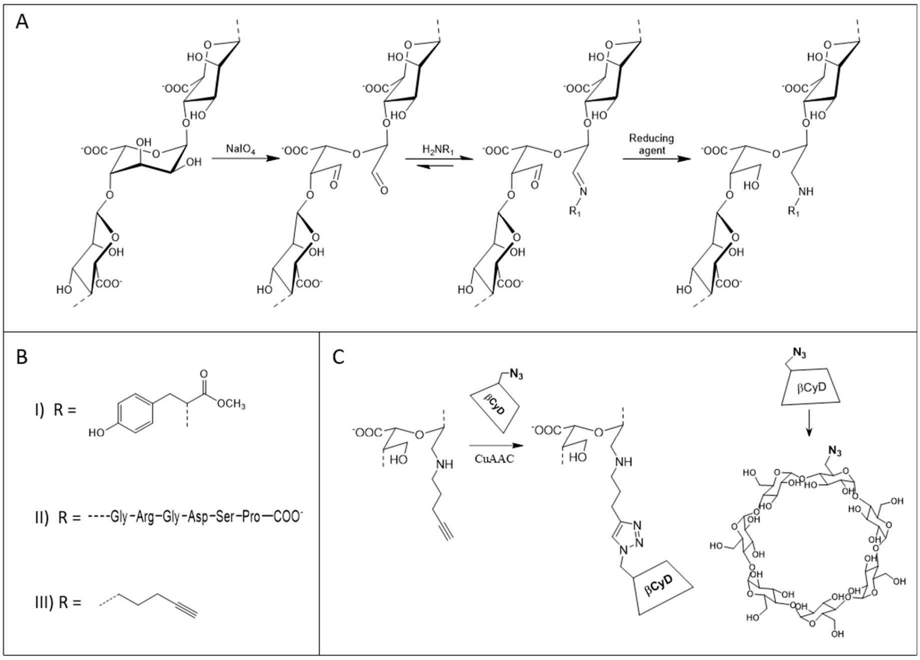

Figure 1. (**A**): General reaction scheme for periodate oxidation (step 1) followed by reductive amination (step 2 and 3) of alginate (here represented by an MGM-fragment). (**B**): Structure of the different substituents grafted onto alginate by reductive amination. I: L-methyl tyrosine ester (MeOTyr), II: the hexapeptide GRGDSP, III: 4-pentyn-amine, used as a linker for further grafting of β-cyclodextrin (β-CyD). (**C**): Grafting of β-CyD to pentyn-amine linked alginate via the copper catalyzed azide alkyne cycloaddition click-reaction. The scaling of alginate and β-CyD is not similar.

2. Results

2.1. Preparation and Characterization of the Functionalized Alginates

L. hyperborea stipe alginate (hereafter denoted stipe alginate, 65% G, 133 kDa) was used throughout the study as the starting material for modification based on its strong gel-forming properties. The stipe alginate was oxidized using periodate ions according to a final periodate/uronic acid molar ratio (P_0) = 0.02, 0.04 and 0.08 (reaction scheme in Figure 1A). Periodate oxidation is shown to be stoichiometric for P_0 up to at least 0.08 [31,33] and a final degree of oxidation corresponding to P_0 is, therefore, assumed (Table 1). An 8% periodate oxidized stipe alginate (POA, P_0 = 0.08) was further grafted with methyl tyrosine ester (POA-MeOTyr) and GRGDSP peptide (POA-GRGDSP) obtaining a degree of substitution of 7.0% and 3.9% mole substituent per mole uronic acid residues, respectively (Figure 1B). The general reaction scheme of periodate oxidation followed by reductive amination and the structure of the different substituents is shown in Figure 1A,B, respectively. Furthermore, an 8% oxidized mannuronan was grafted with MeOTyr, giving a degree of substitution of 7.9%. Thereafter, the grafted mannuronan was epimerized (epim POA-MeOTyr) with AlgE64, giving a G content of 49%. The obtained G-content is similar to a previous study were AlgE64 was used to epimerize partially oxidized (P_0 = 0.08) and reduced mannuronan [34].

β-CyD was grafted to POA (P_0 = 0.08) in two steps. First, a linker (4-pentyn-amine) was coupled to the oxidized alginate by reductive amination (Figure 1A,B) giving a degree of substitution of 1.6%, upon which pentyn amine coupled POA was fully grafted with β-CyD via the copper catalyzed click-reaction (Figure 1C) giving a final degree of substitution of 1.6%.

Table 1. Characterization of the functionalized alginates in this study: P_0 = mole periodate per mole uronate residue), degree of substitution (DS, mole substituent per mole uronate residue%), average molecular weight (M_w). POA: Oxidized alginate. POA-MeOTyr: Oxidized alginate grafted with methyl tyrosine ester. POA-β-CyD: Oxidized alginate grafted with beta cyclodextrin, POA-GRGDSP: Oxidized alginate grafted with the hexapeptide GRGDSP. Epim POA-MeOTyr: oxidized mannuronan grafted with methyl tyrosine ester and, thereafter, epimerized to a G-content of 49%.

Material	P_0	DS (%)	M_w (kDa)
L. hyperborea stipe alginate	0.00	-	133
POA	0.02	-	99
POA	0.04	-	93
POA	0.08	-	97
POA-MeOTyr	0.08	7.0	114
POA-β-CyD	0.08	1.6	65
POA-GRGDSP	0.08	3.9	134
Epim POA-MeOTyr	0.08	7.9	126

The degree of substitution was throughout this work analyzed by ^{1}H NMR spectroscopy (Supplementary file 1, S1) and calculated as mole substituent per mole uronic acid residues as previously described [21,32]. The calculations are based on earlier annotations of the proton NMR spectra of alginates [35,36], periodate oxidized alginates [31], MeOTyr grafted alginates [21], GRGDSP grafted alginates [20] and β-CyD grafted alginates [32]. The degree of substitution obtained here is in well accordance with what we have previously reported using the same methods for grafting of stipe alginate [21,32].

The molar mass of the materials was analyzed using SEC-MALS (Supplementary file 2, S2) and the obtained average molecular weights (M_w) are summarized in Table 1. The opening of the sugar ring makes oxidized alginates more prone to degradation via β-elimination and as previously observed, the oxidation was accompanied by some degradation [21,29]. A slight increase in M_w was observed upon grafting of MeOTyr and the peptide GRGDSP that, taking into account the added weight of the substituents, indicate minimal degradation during grafting. Grafting of β-CyD was, on the other hand accompanied with a reduction of M_w from 97 to 65 kDa, despite the high molecular weight substituent. Depolymerization was predominantly happening during grafting of the pentyn-amine linker [32], which can be attributed to the low degree of substitution. Grafting has been shown to reverse the degradability of the oxidized alginate back to that of unmodified alginate [37] and degradation is therefore, more pronounced during grafting of pentyn-amine compared to the more efficient reactions with MeOTyr and GRGDSP.

2.2. Ca-Saturated Alginate Hydrogels of Functionalized Alginates

Alginate hydrogels were prepared from the different modified alginates (Figure 2A–F). The hydrogels were saturated with calcium ions by dialysis, implying that maximum crosslinking of the alginate within the hydrogel was obtained. Oxidized alginates having 2% and 4% oxidized residues formed nice gels that maintained their shape upon handling. For the 8% oxidized material, on the other hand, the gel cylinders were largely affected by the oxidation and only very weak and largely deformed hydrogels could be formed. Ca-hydrogels of the epimerized POA-MeOTyr formed highly syneretic gels that showed a higher degree of shape stability after gel formation (Figure 2E) compared to the other hydrogels made of only 8% periodate oxidized alginate.

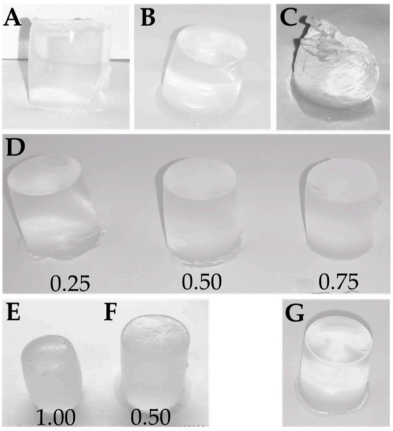

Figure 2. Ca-saturated alginate hydrogels (1.0% *w*/*v*). (**A**): POA (P_0 = 0.02), (**B**): POA (P_0 = 0.04), (**C**): POA (P_0 = 0.08), (**D**): Mixed hydrogels of POA (P_0 = 0.08) and stipe alginate in fractions of W_{POA} = 0.25, 0.50 and 0.75. (**E**): Epim POA-MeOTyr solely, (**F**): Mixed hydrogels of Epim POA-MeOTyr and stipe alginate (W_{POA^*} = 0.50). (**G**): Hydrogels of solely stipe alginate. Abbreviations: POA: Partially periodate oxidized alginate. P_0: Fraction of oxidized residues (degree of oxidation). Epim POA-MeOTyr: Mannuronan grafted with L-Tyrosine methyl ester and thereafter epimerized.

Young's modulus, syneresis, stress and deformation at rupture were measured on the oxidized and grafted materials by uniaxial compression measurements (Table 2, Supplementary file 3). In general, the syneresis was high, but less for oxidized and grafted materials than for the only oxidized material. However, Young's modulus was low for all the hydrogels. This was also the case for the stress and deformation at rupture, i.e., for the highest deformation before the gels failed and at the force at the same deformation (see example in Supplementary file 3). However, both Youngs modulus and stress at rupture increased when MeOTyr was grafted to the alginate, in contrast to β-CyD that resulted in decreased gel strength. The epimerized alginate showed a slightly higher Young's modulus than the corresponding hydrogels of oxidized and grafted alginates of stipe alginate. However, the stress at rupture for the epimerized alginate gels were 5–6 times higher than for the corresponding gels of POA-MeOTyr made from stipe alginate.

Table 2. Mechanical properties of Ca-saturated alginate hydrogels (1.0% *w*/*v*) of modified material solely, based on 8% oxidized stipe alginate (POA), grafted with MeOTyr (POA-MeOTyr), β-CyD (POA-β-CyD) or epimerized alginate grafted with MeOTyr (EpimPOA-MeOTyr).

Alginate	POA	POA-MeOTyr	POA-β-CyD	Epim POA-MeOTyr
Young's modulus, E (kPa)	1.2 ± 0.5	1.9 ± 0.7	0.7 ± 0.1	2.5 ± 0.3
Syneresis (%)	67 ± 7	46 ± 6	59 ± 3	54 ± 1
Stress at rupture (kg)	0.29 ± 0.06	0.55 ± 0.04	0.13 ± 0.01	3.01 ± 0.04
Deformation at rupture (%)	52 ± 3	60 ± 2	46 ± 3	63 ± 2

2.3. Mechanical Properties of Mixed Ca-Gels of Oxidized Alginate and Stipe Alginate

To investigate the effect of varying the fraction of modified alginate in the hydrogel as well as the materials' degree of oxidation, Ca-saturated hydrogels were prepared from mixtures of stipe alginate (F_G = 0.65) and oxidized alginates (POA) in different ratios. Also, Ca-limited gels were investigated for gelling kinetics and rheology. The total alginate concentration in both cases was 1.0% *w*/*v*, unless otherwise specified.

In general, the Ca-saturated hydrogels prepared from mixtures with stipe alginate resulted in nicely formed gels that maintained their shape upon handling (see Figure 2D). Oxidation of the alginate led in general to a reduction in Young's modulus (*E*) and stress at rupture, whereas syneresis and deformation at rupture were less affected by the oxidation (Figure 3). For hydrogels where the weight fraction of POA (W_{POA}) was 0.25, Young's modulus was not significantly different from the pure stipe alginate gel (see Table S4.1 in Supplementary file 4), varying around 30 kPa for all three degrees of oxidation. Mixing in oxidized alginate where 2% of the residues had been oxidized (P_0 = 0.02) did not have a large effect on E, while hydrogels prepared from this material alone (W_{POA} = 1.00) showed a substantial decrease in the Young's modulus of 9 kPa. The hydrogels containing POA prepared with P_0 = 0.04 showed a more gradually decrease in E, while for the hydrogels composed of different amounts of POA P_0 = 0.08 a substantial decrease in E was observed for gels having 50 to 75% POA (dry mass).

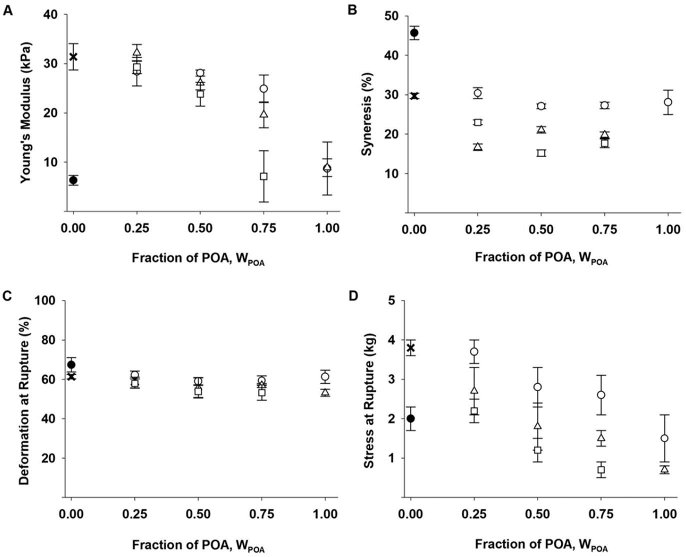

Figure 3. Mechanical characterization of 1.0% *w*/*v* mixed Ca-saturated hydrogels of stipe alginate and POA (*n* = 5–10). (**A**): Young's modulus (E), (**B**): Syneresis (%), (**C**): Deformation at rupture (%) and (**D**): Stress at rupture (kg) as a function of fraction of POA (W_{POA}) for ○: POA P_0 = 0.02, Δ: POA P_0 = 0.04 and □: POA P_0 = 0.08. Gels made of solely POA (W_{POA} = 1.00) is given for P_0 = 0.02 and P_0 = 0.04 (not syneresis for POA P_0 = 0.04). Data for P_0 = 0.08 is given in Table 2. x: 1.0% (*w*/*v*) stipe alginate gels, • 0.5% (*w*/*v*) stipe alginate gels. Abbreviations: POA = partially oxidized alginate. P_0 = degree of oxidation.

Hydrogels with various fractions of 4% and 8% oxidized alginate were in general less syneretic than the stipe alginate reference. The syneresis decreased with increasing degree of oxidation, and to a certain extent with increasing amount of oxidized alginate (W_{POA}, Figure 3B). In comparison, decreasing the total alginate concentration resulted in a higher degree of syneresis, as shown for 0.5% *w*/*v* stipe alginate hydrogels in Figure 3B. For the mixed gels with POA P_0 = 0.02, the degree of syneresis was not largely affected by the relative amount of POA.

The deformation at rupture (%) was only slightly reduced in the mixed hydrogels, relative to the stipe alginate reference hydrogel (Figure 3C). The force needed to rupture the gels (stress at rupture) was, on the other hand, highly dependent on the relative amount of POA as well as the degree of oxidation (Figure 3D). Mixing in POA resulted in a lower stress at rupture that decreased with increasing degree of oxidation and with the relative amounts of POA (Figure 3D).

Some selected mixed gels with stipe alginate and 8% oxidized alginate (Figure 4) were further studied in a rheometer where the gelling kinetics were followed over time by recording shear modulus upon release of Ca^{2+} from $CaCO_3$ following hydrolysis of glucono-δ-lactone (GDL) [38]. Ca-limited gels were chosen due to limited syneresis and, hence, good contact between the gel and the probe, as well as the general relevance of Ca-limited gels as softer gel materials than Ca-saturated gels. As expected, the shear modulus (G') decreased upon exchange of stipe alginate with oxidized alginate from 1205 to 535 Pa and 227 Pa for stipe alginate in 50% and 75% mixture with oxidized alginate, respectively. The gelling kinetics were slower for the mixed gels than for the stipe alginate alone, where 8–12 h were needed to reach plateau levels for the mixed gels versus 4–6 h for the stipe alginate.

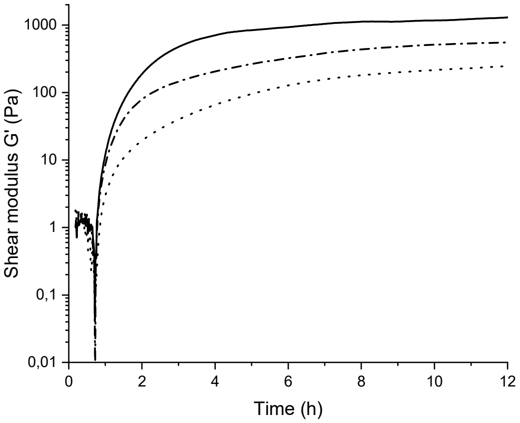

Figure 4. Shear modulus over time for 1.0% *w*/*v* mixed stipe alginate and functionalized POA (P_0 = 0.08) upon mixture with $CaCO_3$ and GDL (at 0 h, 15 mM $CaCO_3$), resulting in unsaturated Ca–alginate gels. Fraction of POA, W_{POA} = 0.00 (solid line), fraction of POA, WP_{OA} = 0.50 (-.-.-.-.-.-.-), fraction of POA, W_{POA} = 0.75 (. . . . . .). POA = partially oxidized alginate.

2.4. Mechanical Properties of Mixed Ca-Saturated Hydrogels with Functionalized Alginate

Ca-saturated hydrogels of 8% oxidized alginate as well as 8% oxidized alginate grafted with MeOTyr, β-CyD and GRGDSP were further characterized to investigate the effect of the grafted groups on the mechanical properties of the hydrogels (Figure 5). The weight fraction of functionalized POA (W_{POA^*}) was varied between 0.00 and 0.75. All materials were oxidized to 8%, but the final degree of substitution varied for the different grafted molecules (see Table 1).

Coupling of MeOTyr, β-CyD or GRGDSP to the oxidized residues resulted in a lower Young's modulus compared to hydrogels with similar amounts of POA for W_{POA^*} = 0.25 and 0.50. The different substituents showed similar effect on Young's modulus, independent of their degree of substitution. At W_{POA^*} = 0.75, no difference was observed compared to hydrogels with 75% w/w POA. Neither deformation nor stress at rupture was largely affected by grafted alginates relative to POA. With regards to the deformation at rupture, only the hydrogels grafted with MeOTyr showed a significant difference compared to the POA hydrogels at W_{POA^*} = 0.50 (see Table S4.19 in Supplementary file 4), and for the stress at rupture the hydrogels grafted with MeOTyr showed a significant difference compared to the POA hydrogels at W_{POA^*} = 0.25 (Table S4.20 in Supplementary file 4). POA-MeOTyr and POA-GRGDSP showed a higher syneresis compared to POA. This was not observed for POA-β-CyD that had lower or similar syneresis to the oxidized alginate. The epimerized alginate grafted with MeOTyr behaved similarly to the stipe alginate grafted with MeOTyr in mixture with non-modified stipe alginate (W_{POA^*} = 0.50), and no significant difference was found between the hydrogels except with regards to the deformation at rupture data assuming that *p*-values less than 0.05 are significant (see Table S4.21 Supplementary file 4 for *p*-values).

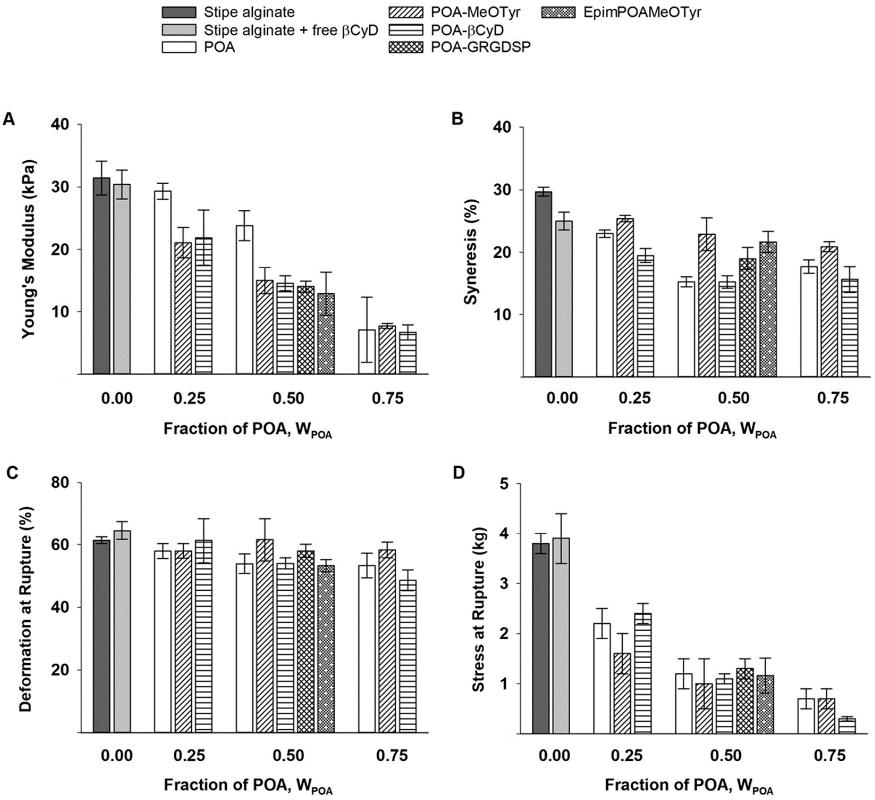

Figure 5. Mechanical characterization of 1.0% *w*/*v* mixed Ca-saturated hydrogels of stipe alginate and functionalized POA (P_0 = 0.08, *n* = 7–10). (**A**): Young's modulus (E), (**B**): Syneresis (%), (**C**): Deformation at rupture (%) and (**D**): Stress at rupture (kg) at different weight fractions of functionalized POA (W_{POA^*}). Abbreviations: POA = partially oxidized alginate. βCyD = β-cyclodextrin. POA-MeOTyr = POA grafted with L-Tyrosine methyl ester. POA-βCyD = POA grafted with β-cyclodextrin. POA-GRGDSP = POA grafted with peptide GRGDSP. EpimPOA-MeOTyr = epimerized mannuronan grafted with MeOTyr.

2.5. Stability of Mixed Hydrogels and Leakage of Material upon Saline Exposure

The stability of stipe alginate/POA (P_0 = 0.08) and stipe alginate/POA-MeOTyr mixed hydrogels was studied with regards to Young's modulus, swelling and leakage material through a series of consecutive saline treatments (0.15 M NaCl, 24 h each) (Figure 6). Young's modulus (E) was gradually reduced for every saline treatment for all hydrogels studied. For all the different mixed hydrogels, E decreased gradually with increasing number of saline treatments, approaching about 2 kPa before the gels lost their cylindrical form and hence, it was not possible to perform compression measurements (at 2–4 treatments of saline). Hydrogels with 75% POA or MeOTyr grafted POA was difficult to handle after the second treatment. At all points, the highest Young's modulus value was obtained for the stipe alginate gels, which, furthermore, showed only slightly reduced structural integrity upon the fourth saline treatment.

The swelling, which we characterized as the relative weight gain, is shown in Figure 6A. In general, minor swelling occurred upon the first saline treatment, after which it increased slightly before the hydrogel dissolved. The exception was gels containing 75% POA, for which the weight decreased upon the saline treatments due to disintegration of the gels.

As expected from the stability data, the mixed hydrogels had a higher amount of leaked material upon saline treatments than the stipe alginate gel (Figure 6C). A small amount of material leaked from the stipe alginate hydrogels upon the first four saline treatments (1–7%). In the fourth treatment, the gels started to lose their structure. In comparison, the mixed gels leaked more material and could withstand fewer saline treatments. The leakage was highest for gels with the highest content of modified alginate, e.g., 75% *w/w* POA or POA-MeOTyr with 44 and 52 wt% total leaked material in the first and second treatment for gels with POA or POA-MeOTyr, respectively.

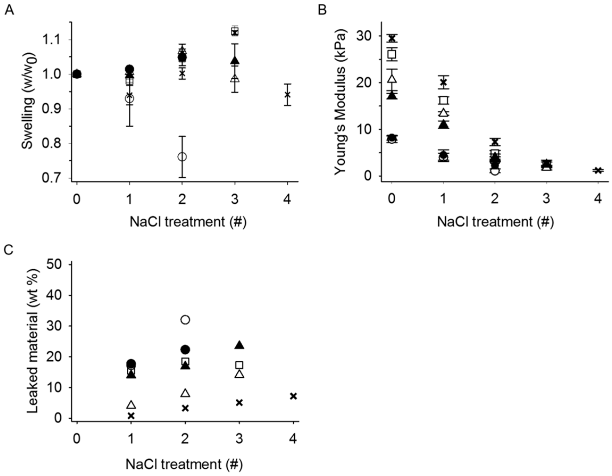

Figure 6. Stability of 1.0% *w/v* alginate/POA ($P_0 = 0.08$) and alginate/POA-MeOTyr ($P_0 = 0.08$, DS = 7.0%) mixed hydrogels ($n = 5$) after consecutive NaCl treatments. One NaCl treatment: immersing the gels in 0.15 M NaCl for 24 h. (**A**): Young's modulus (E), (**B**): Swelling (w/w_0) and (**C**): leaked material (wt%) relative to theoretical total mass of alginate in the gels. Data points at zero saline treatment represents the initial values before immersing the gels in the first saline bath. x: *L. hyperborea* stipe alginate, □: alginate/POA $W_{POA} = 0.25$, Δ: alginate/POA $W_{POA} = 0.50$ ○: alginate/POA $W_{POA} = 0.75$, ▲: alginate/POA-MeOTyr $W_{POA\text{–}MeOTyr} = 0.50$ ●: alginate/POA-MeOTyr $W_{POA\text{–}MeOTyr} = 0.75$. Abbreviations: POA = partially oxidized alginate. POA-MeOTyr = POA grafted with L-Tyrosine methyl ester.

The leaked material was further characterized using ^{1}H NMR spectroscopy and SEC-MALS in regards of composition and molecular weight, respectively (Figure 7). Initially, low molecular weight molecules leaked out of the hydrogels however, M_w increased gradually in the subsequent saline treatments approaching the M_w of the stipe alginate starting material (133 kDa). The leaked alginate from hydrogels with 75% *w/w* POA or POA-MeOTyr had a higher M_w than for the other gels (87 kDa for $W_{POA} = 0.75$ compared to 32 kDa for $W_{POA} = 0.50$ in the first saline treatment).

The alginate that leaked from the mixed hydrogels during the first saline treatment had a low guluronic acid content (F_G~0.4–0.5) compared to that of the starting material ($F_G = 0.65$ for the stipe alginate). The G-content then increased, reaching that of the starting material in the second or third treatment. Similarly, the average G-block length of the leaked alginate tended to increase upon the consecutive saline treatments. The amount of leaked material from the stipe alginate hydrogels during the first saline treatment was too small for further analysis. In the subsequent leakage materials, both the G-content and average G-block length corresponded to that of the stipe alginate.

The MeOTyr coupled alginate used in this study had a degree of substitution of 7.0%, hence, a fraction of uronic acid residues coupled to a MeOTyr molecule (F_{MeOTyr}) of 0.07. NMR analysis of the leaked material from hydrogels with $W_{POA\text{-}MeOTyr} = 0.50$ and 0.75 indicated that the leaked alginate in the first saline treatment had a higher F_{MeOTyr} than the starting material (0.11 and 0.10 for $W_{POA\text{-}MeOTyr}$

= 0.50 and 0.75, respectively). In the consecutive treatments, F_{MeoTyr} decreased, reaching 0.05 in the third saline treatment of mixed hydrogels with $W_{POA\text{-}MeOTyr}$ = 0.50.

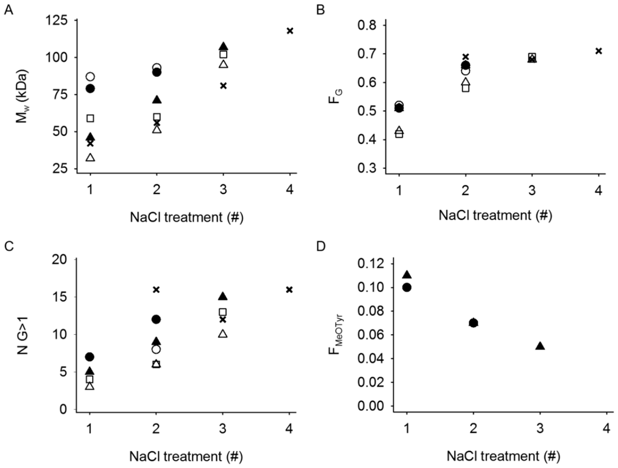

Figure 7. Characterization of leaked alginate from 1.0% *w*/*v* alginate/POA (P_0 = 0.08) and alginate/POA-MeOTyr (P_0 = 0.08) mixed hydrogels (*n* = 5) after immersing the gels in consecutive solutions of 0.15 M NaCl. (**A**): Weight average molecular weight (M_w), (**B**): Fraction of G residues (F_G), (**C**): Average G-block length larger than one ($N_{G>1}$) and (**D**): Fraction of MeOTyr (F_{MeoTyr}) x: *L. hyperborea* stipe alginate, □: alginate/POA W_{POA} = 0.25, ∆: alginate/POA W_{POA} = 0.50 ○: alginate/POA W_{POA} = 0.75, ▲: alginate/POA-MeOTyr $W_{POA\text{-}MeOTyr}$ = 0.50, ●: alginate/POA-MeOTyr $W_{POA\text{-}MeOTyr}$ = 0.75. Abbreviations: POA = partially oxidized alginate. POA-MeOTyr = POA grafted with L-Tyrosine methyl ester.

3. Discussion

The use of functionalized alginates (e.g., peptide grafted alginates) in alginate-based biomaterials is increasing and it is generally accepted that various tissue engineering- and drug release strategies will have different requirements regarding the stability and mechanical properties of the applied hydrogels. The differentiation of stem cells can for example be affected by mechanical properties [39]. The data presented here provide an increased understanding of how functionalization via periodate oxidation and subsequent grafting with peptide or cyclodextrins affect the mechanical properties and stability of alginate hydrogels. Furthermore, the data show, in principal, how mechanical properties of chemically modified alginate in mixtures with a strong gel forming alginate can be adjusted by varying the extent of modification and relative amount of functionalized alginates. Alginate with 8% oxidation was used for the grafting studies to better examine the differences between hydrogels made of both modified alginate and non-modified alginate, while also giving the benefit of a higher degree of functionality compared with a starting point of 2 or 4% oxidation.

3.1. Mechanical Properties

Rheological and mechanical studies on hydrogels composed of only periodate oxidized alginate has been performed by several groups, including ours [30,31,40]. The alginate characteristics (composition, G-block length, degree of oxidation and molecular weight) and Ca^{2+} concentration varied in the different studies, yet the general conclusion is that the ability to form hydrogels as well as the mechanical properties is highly affected upon partial oxidation (1–10%), and that increasing the degree of oxidation results in lower elastic moduli (G') [30,31]. Periodate ions are known to react faster with G-residues than M-residues (approximately 50% faster) [41], leading to a relatively larger influence on the G- and MG-blocks than on M-blocks. Previous studies have shown that the G-block length is reduced when using periodate oxidation on alginates [31]. Hence, oxidized alginates are expected to contain shorter G-blocks and consequently form shorter junction zones with the gelling ions. It is known that for alginate hydrogels, the shortest G-block length to form stable junctions with Ca^{2+} is 8 [42,43], whereas Sr^{2+} only requires a G-block length of 3 [42]. Hence, periodate oxidation may reduce the length of consecutive G units to below the critical values for crosslinking with calcium ions. A more in-depth characterization of the local hydrogel structure, in regards of size and multiplicity of the junction zones is possible by scattering techniques such as small angle X-ray scattering [44,45]. This is however beyond the scope of our work.

The mechanical properties were here characterized by Young's modulus (E), which is dependent on the number, stability and length of crosslinks (junction zones) as well as the length and flexibility of the elastic segments between junction zones [46]. Some selected materials were also characterized by rheology for Ca-limited gels, where shear modulus (G´) is proportional to E. Ca-saturated hydrogels where the weight fraction of POA (W_{POA}) was 0.25 or 0.50, showed similar or slightly reduced Young's modulus', respectively, compared to the reference stipe alginate gel for all degrees of oxidation. In comparison, reducing the total alginate concentration from 1.0% to 0.5% *w*/*v* in stipe alginate gels resulted in a large decrease in Young's modulus from 31 kPa to 6 kPa. It follows that, despite the partial disruption of G- and MG-blocks, the oxidized alginate makes a substantial contribution to the junction zones. A large decrease in Young's modulus was observed using W_{POA} = 0.75 of the 8% oxidized alginate. Mixing ratios from 0.50 to 0.75 could then be exploited to give a range of mechanical strengths. For the calcium-limited gels (unsaturated gels), mixing ratios of 0.50 and 0.75 resulted in 56% and 81% reduction in shear modulus (G´, Figure 4), respectively, that may point to a further reduction in gel strength in mixed gels when calcium is limited. The 8% oxidized alginate did not form gels under Ca-limited conditions and formed very weak gels upon Ca-saturation without the support of the non-modified alginate, further demonstrating the reduced ability to form strong junction zones upon introduction of the oxidized residues. Interestingly, coupling MeOTyr to the oxidized alginate resulted in slightly higher Youngs modulus and stress at rupture compared to the oxidized material only. This may be due to hydrophobic interactions between MeOTyr contributing to the mechanical properties of the gel.

Grafting resulted in a reduction in Young's modulus for W_{POA} 0.25 and 0.50 relative to the oxidized alginate. In the mixed gels, the potential contribution from hydrophobic interactions is probably reduced due to steric hindrance with the presence of non-modified alginate. Addition of free β-CyD did not have the same effect as grafted β-CyD (see Figure 5), suggesting that covalent coupling induce steric restrictions that negatively affect the number of junction zones formed in the mixed gels. No difference was observed for the different substituents (see Table D17 Supplementary file 4 for statistical values), despite that the degree of substitution ranged from 1.6% for POA-β-CyD to 7.0% for POA-MeOTyr (both with P_0 = 0.08). The lower molecular weight of POA-β-CyD may, however, limit its contribution to interchain junctions [47], resulting in a reduction of gel strength despite the low degree of substitution.

The stress at rupture was substantially lowered by both increasing the fraction of POA and increasing the degree of oxidation. Rupture strength is directly linked to the energy required to fracture the network junctions, and shorter junction zones in periodate oxidized alginates concomitantly result in a lower stress at rupture. Grafting of substituents to POA did not further decrease the force needed to induce rupture, suggesting that the substituents do not affect the strength of the junction zones.

The deformation at rupture, measured as the length of compression relative to the initial height of the hydrogels (%), is a measure for how much deformation the hydrogel can withstand before rupture. All the mixed hydrogels were largely compressed to the same level and was thus minimally affected by the relative amount of POA, the degree of oxidation of the incorporated oxidized alginate nor the introduction of substituents. However, as lower force was needed for them to rupture, alginates functionalized through periodate oxidation and reductive amination form more fragile hydrogels.

Using a chemoenzymatic strategy, by introducing the chemical modifications on mannuronan and secondly introducing the G-blocks by epimerization, has previously been shown to be efficient in maintaining the mechanical properties of the Ca–alginate hydrogels [12]. The same strategy has been used for the grafting of bioactive peptides to alginate using carbodiimide chemistry [20]. Mannuronan C-5 epimerases are shown to work on both oxidized alginates as well as alginate in the gel state [34]. In this work, the grafted alginate produced with a chemoenzymatic strategy (EpimPOA-MeOTyr) was hypothesized to give better mechanical properties compared to the non-epimerized POA-MeOTyr due to the grafting only taking place on the M-residues. Here, the EpimPOA-MeOTyr showed better gelling properties relative to the corresponding grafted stipe alginate (POA-MeOTyr), resulting in more defined gels and with stress at rupture close that to unmodified stipe alginate (3 versus 4 kg, respectively). However, Young's modulus was low and comparable to the corresponding POA-MeOTyr made of stipe alginate (Table 2). For mixed hydrogels, the unmodified stipe alginate dominated the mechanical properties and no significant differences were seen between the grafted epimerized alginate and the corresponding POA-MeOTyr made of stipe alginate.

3.2. Syneresis

Ionically crosslinked alginate gels are in general smaller than the starting volume of the liquid that was used to cast the gel. The negative change in volume upon gel formation is referred to as syneresis. The main driving force of syneresis is thought to be the growth of junction zones [48] and release of water. In alginates, both the length of the G-blocks and the presence of alternating sequences (MG-blocks) will affect the syneresis. Long G-blocks give little syneresis as the network is not easily reorganized [47]. Alternating sequences are, on the other hand, associated with high syneresis [12,17]. This has been attributed to the formation of MG/MG junctions leading to a partial network collapse upon Ca^{2+} saturation [13]. Hydrogels containing POA oxidized to 4 and 8% expressed less syneresis than the stipe alginate reference gel and the syneresis decreased slightly with increasing amount of the oxidized alginate. Opening of the sugar ring upon periodate oxidation increases the local flexibility, which could promote reorganization and, hence, syneresis, but reduces the effective junction zones, possibly both in number and length. Hence, it seems like oxidized alginates have a reduced ability to contribute to growth of effective junction zones that surpass the increased flexibility. An oxidation degree of 2% showed similar syneresis to the unmodified stipe alginate hydrogel, indicating that this low oxidation degree did not alter the properties of the modified alginate compared to the parent alginate markedly. A lower total concentration of alginate in the pre-gel solution gave as expected higher syneresis [49] (shown for 1.0% and 0.5% *w*/*v* stipe alginate hydrogels in 3B). Mixing-in oxidized alginate can therefore, not be seen as an effective decrease in concentration.

Grafting of molecules to the oxidized residues could possibly add steric hindrance during network reorganization and consequently reduce the syneresis. For hydrogels with 50% *w*/*w* POA or functionalized POA, the opposite was observed and syneresis increased in the order POA-β-CyD ≈ POA < POA-GRGDSP < POA-MeOTyr. This order corresponds well with the degree of substitution for the different materials (POA-β-CyD < POA-GRGDSP < POA-MeOTyr), indicating that higher level of grafting leads to a more compact hydrogel. Syneresis is known to increase with an increasing concentration of the crosslinking ion and molecular weight of the alginate [47,48]. The substituents could possibly affect the diffusion of calcium ions or exclusion of water and hence, syneresis, or there may be interactions between the substituents leading to a more compact gel network. POA-β-CyD was more degraded during preparation than the other alginates (M_w = 65 kDa, compared to 114 kDa for POA-MeOTyr), which together with the low DS (1.6%, Table 1) can account for the observed syneresis being similar to or slightly lower than POA.

3.3. Stability and Leakage

Alginate gel stability in saline solution is relevant for the use and handling of alginate gels and for the use at physiological conditions. The optimal stability of an alginate hydrogel depends on the application. For slow release of a drug from an alginate hydrogel, a robust long-lasting gel could be beneficial. On the other hand, for some tissue engineering applications, a less stable hydrogel which is more readily replaced with tissue would be better suited [3]. Ca–alginate hydrogels are vulnerable to destabilization upon exposure to saline due to the exchange of calcium with sodium ions that result in destabilization of the gelling zones and leakage of alginate. Swelling of Ca–alginate gels is previously described by the balance of exchange of Ca^{2+} with Na^{+} and influx of water and the gel network ability to withstand the osmotic pressure [17,50]. The stability of the mixed hydrogels was investigated as the change in Young's modulus and weight (swelling) and leakage of alginate upon consecutive saline treatments. A gradual decrease in Young's modulus was observed for all the different gel types, reflecting the gradual exchange of Ca^{2+} with non-crosslinking Na^{+} [17] resulting in a destabilization of the junction zones. To create more stable and long-lasting hydrogels, the gelling ions strontium or barium could be introduced as these ions bind more strongly to the G-blocks in the alginate and are depending on shorter G-blocks to form stable crosslinks [10]. In contrast, pre-treatment of the gels in saline bath could be a means for achieving faster degradation.

The mixed hydrogels were less stable than stipe alginate gels as they were able to withstand fewer saline treatments. As the total concentration of alginate was the same in all gels and, hence, also the charge density, the exchange of Ca^{2+} with Na^{+} and flux of water is expected to be approximately the same in the hydrogels. However, the reduction in G-blocks and, hence, crosslinking leads to a destabilization of the network. The mixed hydrogels and the stipe alginate gels were disintegrating rather than the typical swelling, observed as increase in volume and weight, previously seen for alginate gel beads upon consecutive saline treatments [10,17]. In addition, large amounts of alginate were released (leaked) from the mixed gels compared to the stipe alginate gels. A small amount of swelling and leakage of alginate from Ca-hydrogels from *L. hyperborea* alginate with similar composition and sequence parameters as the stipe alginate used here has been reported [13,42]. Also, the leakage material from previous studies was shown to contain shorter chains of high M containing alginate [42]. Here, an accumulation of modified alginate in the leakage material was seen, which is connected to the destruction of the crosslinking zones in the grafted alginate.

4. Conclusions

The mixed hydrogels with POA and *L. hyperborea* stipe alginate gave lower Young's modulus and stress at rupture than control gels made of unmodified *L. hyperborea* stipe alginate only, but the mechanical properties could be controlled by the fraction of modified alginate in the hydrogels as well as the degree of oxidation. Grafted epimerized alginate showed better gelling properties (higher Young's modulus and deformation at rupture) than the corresponding grafted stipe alginate. For hydrogels with a mixture of modified and unmodified stipe alginate, the mechanical properties were largely influenced by the unmodified stipe alginate. Decreased syneresis was observed upon increasing the degree of oxidation, but was only slightly affected by the relative amount of the modified alginates. Also, the data suggests that syneresis was influenced by the nature and amount of the grafted molecules. The mixed hydrogels were less stable than gels with only unmodified alginate, and the grafted chains were leaking out first. Furthermore, the mixed hydrogels were found to disintegrate rather than swell upon saline treatments. It is evident that functionalization via periodate oxidation and subsequent grafting (via reductive amination and Cu-catalyzed click-chemistry) has considerable effect on alginates gelling properties. This must be taken into account, and can be utilized upon designing alginate hydrogels as biomaterials.

5. Materials and Methods

5.1. Materials

Alginate from *Laminaria hyperborea* stipe was obtained from FMC Health and Nutrition, Drammen, Norway. Its composition obtained from NMR spectroscopy and molar mass (M_w) obtained from

SEC-MALS are given in Table 3. The hexapeptide GRGDSP was purchased from CASLO ApS, Denmark and 6-*O*-monodeoxy-6-monoazido-β-cyclodextrin (N_3-β-CyD) was synthesized in-house [51] by Thorbjørn Nielsen at Aalborg University. All other chemicals were purchased from commercial sources and were of analytical grade. Mannuronan was obtained from FMC Health and Nutrition ([η] = 1548 mL/g), F_G =0.00.

Table 3. Chemical characterization of the starting material used for chemical modification and as unmodified alginate in alginate hydrogels. Composition is described by the fraction of M and G (F_M and F_G), fraction of diad and triplet sequences (e.g., F_{GGG}: fraction of alginate consisting of guluronic triplets) and the average length of G-blocks ($N_{G>1}$).

Alginate	M_w (kDa)	F_G	F_M	F_{GG}	F_{MG}/F_{GM}	F_{MM}	F_{MGG}/F_{GGM}	F_{MGM}	F_{GGG}	$N_{G>1}$
L. hyperborea stipe alginate	133	0.65	0.35	0.53	0.12	0.23	0.05	0.10	0.48	11

5.2. Periodate Oxidation and Preparation of Functionalized Alginates

Stipe alginate and mannuronan were oxidized upon addition of sodium periodate as previously described [31]. L-Tyrosine methyl ester (MeOTyr) was grafted to both the oxidized stipe alginate and mannuronan as previously described [21]. In addition, the peptide GRGDSP was grafted to stipe alginate in the same manner. In short, the alginates were oxidized using a concentration of periodate ions that corresponded to a P_0 of 0.08. The periodate oxidized alginates were further reacted with MeOTyr or GRGDSP using 2-methylpyridine borane complex (picoline borane) as the reducing agent.

β-CyD was grafted to periodate oxidized alginate (P_0 = 0.08) in two steps, as previously described [32]. A linker, 4-pentyn-1-amine, was first grafted to the periodate oxidized alginate by reductive amination. Thereafter, β-CyD was linked to 4-pentyn-1-amine coupled alginate via the Cu(I)-catalyzed azide alkyne cycloaddition click-reaction [51].

The L-Tyrosine methyl ester grafted mannuronan was epimerized with AlgE64 [34] to obtain an alginate were the G-units were introduced into the chain after the grafting procedure. Briefly, MeOTyr grafted mannuronan was dissolved in water, and the enzyme and epimerization buffer were then added. The ratio between the enzyme and grafted alginate used was 1 mg enzyme per 25 mg grafted mannuronan. The final concentrations in the reaction mixture were 2.4 mg/mL grafted mannuronan, 50 mM MOPS, 75 mM NaCl and 2 mM $CaCl_2$. The reaction mixture was incubated at 37 °C, and after 48 h the reaction was stopped by adding 10 mL EDTA (100 mM, pH = 7). The product was dialyzed until conductivity measured below 1 µS.

5.3. Preparation of Calcium–Alginate Hydrogels

Internally set calcium alginate gel cylinders (Ca-limited or unsaturated gels) were prepared by adding $CaCO_3$ and the slowly hydrolyzing D-glucono-δ-lactone (GDL), as previously described [38]. Briefly, the release of proton from GDL and the subsequent lowering of pH destabilize the $CaCO_3$ and cause release of calcium ions that will bind to the alginate. Alginates were dried overnight in a desiccator with phosphorus pentoxide (Sicapent, Sigma-Aldrich, Oslo, Norway) and dissolved in MQ water. A dispersion of $CaCO_3$ (4 µm, ESKAL 500, KSL Staubtechnik GMBH, Lauingen, Germany) was added to the alginate solutions and the solutions were thereafter degassed, using vacuum suction. GDL was then added to the mixtures to start the gel formation. The mixtures were stirred carefully for a few seconds before they were poured into the wells of a 24-well plate (16/18 mm, Costar, Cambridge, MA, USA) and left at room temperature for 20 h. The final concentrations were 1.0% (or 0.5%) *w*/*v* alginate, 15 mM $CaCO_3$ and 30 mM GDL. The amount of calcium added is calculated to theoretically crosslink all G present, however, it is shown that the gel strength and syneresis of calcium gels further increase with calcium concentration [38]. Hence, Ca-saturated hydrogels were made by immersing the gel cylinders in 50 mM $CaCl_2$ and 0.2 M NaCl (800 mL for 8 cylinders) for 24 h at 4 °C to ensure excess of calcium in the gels.

5.4. Syneresis and Mechanical Properties

The syneresis (the volume of gels relative to the initial volume of solute) was determined as the weight reduction of the calcium-alginate hydrogels with respect to the initial weight and calculated according to $S = (1 - w/w_0) \times 100$, where w_0 and w is the initial and final weight respectively. The initial weight was calculated based on the volume of the wells, assuming no significant change in density from water for 0.5–1.0% alginate.

The mechanical properties of the alginate gel cylinders were characterized by uniaxial compression using a Stable MicroSystems, TA XT plus Texture Analyser with a P/35 probe at room temperature and a compression rate of 0.1 mm/s. The weight of the loading cell was five kg. Young's modulus (E) was calculated from the initial slope (typically 0.1–0.3 mm) of the force/deformation curves $(F/A) = E \times \Delta l/l$ (l = length of gel before measurement, Δl = change in length) and corrected for syneresis: $E_{corrected} = E_{measured} \times (C_{initial}/C_{final})^2$ [52]. All data were collected and processed with the "Texture Expert Exponent 32" software. Stress at rupture and deformation at rupture (or ultimate compression strength) was determined in experiments where the hydrogels were compressed to the point of rupture, and the reported data are the maximum value on the force-deformation curve (See Supplementary file 3).

5.5. Rheological Characterisation of Unsaturated Gels

1.0% (w/v) Ca-limited (unsaturated) alginate gels were prepared as described above (4.3) by internal gelation with final concentration of 15 mM $CaCO_3$ and 30 mM GDL. Immediately after addition of GDL and rapid and careful mixture to avoid bobble formation, 0.65 mL sample was loaded to a rheometer and recordings started 10 min after adding GDL to the alginate solution. The development of shear modulus (G´, Pa) was followed over time in room temperature by Kinexus Rheometer (Malvern instruments, Uppsala, Sweden) using a 2 cm flat probe and a flat plate geometry with 1 mm gap and recorded at a frequency of 1 Hz.

5.6. Stability

The stability of the hydrogels was analyzed through a series of consecutive saline treatments of Ca-saturated gel cylinders. For each gel type, five gels were immersed in 100 mL 0.15 M NaCl (20 mL per gel) and left for 24 h at 4 °C with gentle stirring (first saline treatment). Swelling is defined as volume increase, however, as alginate gels increase in volume by absorbing the surrounding solution that correspond to subsequent increase in weight, swelling of the gels were characterized as w/w_0, where w_0 is the initial weight before the first saline treatment and w is the weight after the respective saline treatments. Compression measurements (1 mm compression) were then performed before the hydrogels were immersed in a new 0.15 M NaCl solution (second saline treatment). This was repeated until the gels had lost their cylindrical form and it was not possible to perform mechanical measurements on them (2–4 treatments).

5.7. Analysis of the Leaked Alginate

After removing the hydrogels, the separate NaCl treatment solutions was added 2 mL of a 150 mM EDTA solution. The saline treatments solutions were further dialyzed, using a MWCO of 3.5 kDa against two shifts of 0.05 M NaCl and then MQ water until the conductivity was below 4 µS/cm. The samples were freeze dried and further prepared for NMR and SEC-MALS analysis as described below.

5.8. NMR

1D ^1H NMR spectroscopy was used to analyze the degree of substitution as well as the uronic acid composition of the alginates. The samples were subjected to mild acid hydrolysis as previously described [53] to reduce the viscosity prior to the NMR analysis. 6–10 mg of the samples were then dissolved in 600 µL D_2O (99.9%) and added 5 µL 3-(Trimethylsilyl)propionic 2,2,3,3-d_4 acid (TSP, Sigma-Aldrich, Oslo, Norway) as an internal standard and 15 µL Triethylenetetraamine-hexaacetic acid (TTHA, Sigma Aldrich) as a chelating agent for residual divalent ions. The latter was not added to samples already added EDTA (analysis of leaked alginate). 1D ^{1}H spectra were recorded at 90 °C on a Bruker Ascend 400 MHz Avance III HD spectrometer, equipped with a 5-mm SmartProbe z-gradient probe and SampleCase (Bruker BioSpin AG, Fällanden, Switzerland). The spectra were recorded using TopSpin 3.2 software (Bruker BioSpin, Fällanden, Switzerland) and processed and analyzed with TopSpin 3.5 software (Bruker BioSpin).

5.9. SEC-MALS

Size exclusion chromatography with multi angle light scattering (SEC-MALS) was used to measure the molecular weight, as previously described [28]. The system consisted of a mobile phase reservoir, an on-line degasser, an HPLC isocratic pump (LC-10ADVP, Shimadzu, Kyoto, Japan), an autoinjector (SCL-10AV, Shimadzu), a pre-column and two serially connected columns: TSK 6000 PWXL and TSK 5000 PWXL (Toso Haas, Stuttgard, Germany). The columns were followed by two serially connected detectors; a Dawn DSP laser light scattering photometer (Wyatt Technology, Santa Barbara, CA, USA) (λ_0 = 0.664 nm) and an Optilab DSP differential refractometer (Wyatt Technology, Santa Barbara, CA, USA). 0.15 M $NaNO_3$ with 0.01 M NaEDTA, pH 6 was used as the mobile phase. 20% acetonitrile was added to the mobile phase for the alginate grafted with β-CyD. All samples were dissolved in the mobile phase (0.25–7.5 mg/mL) and filtered (pore size 0.8 µm) prior to injection. The injection volume was adjusted to obtain an optimal light scattering signal and to avoid overloading. Astra software v. 6.1 (Wyatt Technology, Santa Barbara, CA, USA) was used to collect and process the obtained data, using a refractive index increment (dn/dcµ) of 0.150 mL/g for alginate samples [28].

5.10. Statistical Analysis

The Tukey honest significant differences test was done using R to examine significant differences between the hydrogels with regards to the Young's modulus, syneresis, deformation at rupture and stress at rupture measurements. For the comparison of the POA-MeOTyr gels with regards to epimerized and non-epimerized alginate the Welch *t*-test was used to compare the two sets of gels. The statistical values can be found in Supplementary file 4. Data is shown as mean ± standard deviation. Samples with *p*-values less than 0.05 were considered statistically significant.

Supplementary Materials: Supplementary materials can be found at http://www.mdpi.com/2310-2861/5/2/23/s1.

Author Contributions: Conceptualization, B.L.S. and F.L.A.; Formal analysis, M.Ø.D., L.A.O., I.M.B. and A.A.; Funding acquisition, B.L.S., F.L.A. and J.F.M.; Investigation, L.A.O., M.Ø.D., I.M.B. and A.A.; Methodology, F.L.A., B.L.S., M.Ø.D. and L.A.O.; Project administration: B.L.S., F.L.A. and J.F.M.; Supervision, F.L.A., B.L.S., M.Ø.D., L.A.O. and J.F.M.; Validation, F.L.A., B.L.S., M.Ø.D. and L.A.O.; Visualization, M.Ø.D., L.A.O., B.L.S., A.A. and I.M.B.; Writing – original draft, M.Ø.D., L.A.O. and B.L.S.; Writing – review & editing, F.L.A., B.L.S., M.Ø.D., L.A.O., I.M.B., A.A. and J.F.M.

Funding: This research was funded by the MARPOL project 221576 and 3DLife project 269273/O70, the Norwegian Research Council and NTNU (Project 81726300, Ph.D. Grant Marianne Øksnes Dalheim). We wish to thank the SINTEF Epimerase project 250875 for funding the production of the epimerase for this study. We also wish to thank the Norwegian NMR Platform 226244.

Acknowledgments: Thorbjørn T. Nielsen (Department of Chemistry and Bioscience, Aalborg University) is acknowledged for production of 6-*O*-monodeoxy-6-monoazido-β-CyD (N_3-β-CyD). We also thank Wenche I. Strand, Ann-Sissel T. Ulset and Ina S. Pedersen (Department of Biotechnolgy and Food Science, NTNU) for NMR and SEC-MALS, and for performing gel measurements on epimerized gels, respectively.

Conflicts of Interest: The authors declare no conflict of interest.

References

1. Lutolf, M.P. Biomaterials: Spotlight on hydrogels. *Nat. Mater.* **2009**, *8*, 451–453. [CrossRef]
2. Discher, D.E.; Mooney, D.J.; Zandstra, P.W. Growth Factors, Matrices, and Forces Combine and Control Stem Cells. *Science* **2009**, *324*, 1673–1677. [CrossRef] [PubMed]

3. Augst, A.D.; Kong, H.J.; Mooney, D.J. Alginate hydrogels as biomaterials. *Macromol. Biosci.* **2006**, *6*, 623–633. [CrossRef] [PubMed]
4. Draget, K.I.; Moe, S.T.; Skjåk-Bræk, G.; Smidsrød, O. Alginates. In *Food Polysaccharides and Their Applications*; Stephen, A.M., Phillips, G.O., Williams, P.A., Eds.; CRC Press: Boca Raton, FL, USA, 2006; pp. 289–334.
5. Lee, K.Y.; Mooney, D.J. Alginate: Properties and biomedical applications. *Prog. Polym. Sci.* **2012**, *37*, 106–126. [CrossRef]
6. Rokstad, A.M.; Brekke, O.-L.; Steinkjer, B.; Ryan, L.; Kolláriková, G.; Strand, B.L.; Skjåk-Bræk, G.; Lacík, I.; Espevik, T.; Mollnes, T.E. Alginate microbeads are complement compatible, in contrast to polycation containing microcapsules, as revealed in a human whole blood model. *Acta Biomater.* **2011**, *7*, 2566–2578. [CrossRef] [PubMed]
7. Smidsrød, O. Molecular basis for some physical properties of alginates in the gel state. *Faraday Discuss. Chem. Soc.* **1974**, *57*, 263–274. [CrossRef]
8. Smidsrød, O.; Haug, A. Dependence upon Uronic Acid Composition of Some Ion-Exchange Properties of Alginates. *Acta Chem. Scand.* **1968**, *22*, 1989–1997. [CrossRef]
9. Haug, A.; Smidsrød, O. Selectivity of Some Anionic Polymers for Divalent Metal Ions. *Acta Chem. Scand.* **1970**, *24*, 843–854. [CrossRef]
10. Mørch, Y.A.; Donati, I.; Strand, B.L.; Skjåk-Bræk, G. Effect of Ca^{2+}, Ba^{2+}, and Sr^{2+} on alginate microbeads. *Biomacromolecules* **2006**, *7*, 1471–1480. [CrossRef]
11. Donati, I.; Holtan, S.; Mørch, Y.A.; Borgogna, M.; Dentini, M.; Skjåk-Bræk, G. New hypothesis on the role of alternating sequences in calcium-alginate gels. *Biomacromolecules* **2005**, *6*, 1031–1040. [CrossRef]
12. Mørch, Ý.A.; Holtan, S.; Donati, I.; Strand, B.L.; Skjåk-Bræk, G. Mechanical Properties of C-5 Epimerized Alginates. *Biomacromolecules* **2008**, *9*, 2360–2368. [CrossRef]
13. Donati, I.; Mørch, Y.A.; Strand, B.L.; Skjåk-Bræk, G.; Paoletti, S. Effect of Elongation of Alternating Sequences on Swelling Behavior and Large Deformation Properties of Natural Alginate Gels. *J. Phys. Chem. B* **2009**, *113*, 12916–12922. [CrossRef] [PubMed]
14. Aarstad, O.; Strand, B.L.; Klepp-Andersen, L.M.; Skjåk-Bræk, G. Analysis of G-Block Distributions and Their Impact on Gel Properties of in Vitro Epimerized Mannuronan. *Biomacromolecules* **2013**, *14*, 3409–3416. [CrossRef] [PubMed]
15. Haug, A. Composition and Properties of Alginates. *Nor. Inst. Seaweed Res.* **1964**, *30*.
16. Gimmestad, M.; Sletta, H.; Ertesvag, H.; Bakkevig, K.; Jain, S.; Suh, S.; Skjåk-Bræk, G.; Ellingsen, T.E.; Ohman, D.E.; Valla, S. The Pseudomonas fluorescens AlgG protein, but not its mannuronan C-5-epimerase activity, is needed for alginate polymer formation. *J. Bacteriol.* **2003**, *185*, 3515–3523. [CrossRef]
17. Mørch, Ý.A.; Donati, I.; Strand, B.L.; Skjåk-Bræk, G. Molecular Engineering as an Approach to Design New Functional Properties of Alginate. *Biomacromolecules* **2007**, *8*, 2809–2814. [CrossRef]
18. Fonseca, K.B.; Bidarra, S.J.; Oliveira, M.J.; Granja, P.L.; Barrias, C.C. Molecularly designed alginate hydrogels susceptible to local proteolysis as three-dimensional cellular microenvironments. *Acta Biomater.* **2011**, *7*, 1674–1682. [CrossRef]
19. Rowley, J.A.; Madlambayan, G.; Mooney, D.J. Alginate hydrogels as synthetic extracellular matrix materials. *Biomaterials* **1999**, *20*, 45–53. [CrossRef]
20. Sandvig, I.; Karstensen, K.; Rokstad, A.M.; Aachmann, F.L.; Formo, K.; Sandvig, A.; Skjåk-Bræk, G.; Strand, B.L. RGD-peptide modified alginate by a chemoenzymatic strategy for tissue engineering applications. *J. Biomed. Mater. Res. Part A* **2015**, *103*, 896–906. [CrossRef]
21. Dalheim, M.Ø.; Vanacker, J.; Najmi, M.A.; Aachmann, F.L.; Strand, B.L.; Christensen, B.E. Efficient functionalization of alginate biomaterials. *Biomaterials* **2016**, *80*, 146–156. [CrossRef] [PubMed]
22. Carré, M.-C.; Delestre, C.; Hubert, P.; Dellacherie, E. Covalent coupling of a short polyether on sodium alginate: Synthesis and characterization of the resulting amphiphilic derivative. *Carbohydr. Polym.* **1991**, *16*, 367–379. [CrossRef]
23. Andresen, I.-L.; Painter, T.; Smidsrød, O. Concerning the effect of periodate oxidation upon the intrinsic viscosity of alginate. *Carbohydr. Res.* **1977**, *59*, 563–566. [CrossRef]
24. Kang, H.-A.; Jeon, G.-J.; Lee, M.-Y.; Yang, J.-W. Effectiveness test of alginate-derived polymeric surfactants. *J. Chem. Technol. Biotechnol.* **2002**, *77*, 205–210. [CrossRef]
25. Dryhurst, G. *Periodate Oxidation of Diol and Other Functional Groups: Analytical and Structural Applications*; Pergamon Press: Oxford, UK, 1970.

26. Lee, K.Y.; Bouhadir, K.H.; Mooney, D.J. Evaluation of chain stiffness of partially oxidized polyguluronate. *Biomacromolecules* **2002**, *3*, 1129–1134. [CrossRef] [PubMed]
27. Smidsrød, O.; Painter, T. Effect of periodate oxidation upon the stiffness of the alginate molecule in solution. *Carbohydr. Res.* **1973**, *26*, 125–132. [CrossRef]
28. Vold, I.M.; Kristiansen, K.A.; Christensen, B.E. A study of the chain stiffness and extension of alginates, in vitro epimerized alginates, and periodate-oxidized alginates using size-exclusion chromatography combined with light scattering and viscosity detectors. *Biomacromolecules* **2006**, *7*, 2136–2146. [CrossRef]
29. Kristiansen, K.A.; Tomren, H.B.; Christensen, B.E. Periodate oxidized alginates: Depolymerization kinetics. *Carbohydr. Polym.* **2011**, *86*, 1595–1601. [CrossRef]
30. Gomez, C.G.; Rinaudo, M.; Villar, M.A. Oxidation of sodium alginate and characterization of the oxidized derivatives. *Carbohydr. Polym.* **2007**, *67*, 296–304. [CrossRef]
31. Kristiansen, K.A.; Schirmer, B.C.; Aachmann, F.L.; Skjåk-Bræk, G.; Draget, K.I.; Christensen, B.E. Novel alginates prepared by independent control of chain stiffness and distribution of G-residues: Structure and gelling properties. *Carbohydr. Polym.* **2009**, *77*, 725–735. [CrossRef]
32. Omtvedt, L.A.; Dalheim, M.Ø.; Nielsen, T.T.; Larsen, K.L.; Strand, B.L.; Aachmann, F.L. Efficient Grafting of Cyclodextrin to Alginate and Performance of the Hydrogel for Release of Model Drug. *Sci. Reports* **2019**. submitted.
33. Kristiansen, K.A.; Ballance, S.; Potthast, A.; Christensen, B.E. An evaluation of tritium and fluorescence labelling combined with multi-detector SEC for the detection of carbonyl groups in polysaccharides. *Carbohydr. Polym.* **2009**, *76*, 196–205. [CrossRef]
34. Stanisci, A.; Aarstad, O.A.; Tøndervik, A.; Sletta, H.; Dypås, L.B.; Skjåk-Bræk, G.; Aachmann, F.L. Overall size of mannuronan C5-Epimerases influences their ability to epimerize modified alginates and alginate gels. *Carbohydr. Polym.* **2018**, *180*, 256–263. [CrossRef]
35. Grasdalen, H. High-field, 1H-n.m.r. spectroscopy of alginate: Sequential structure and linkage conformations. *Carbohydr. Res.* **1983**, *118*, 255–260. [CrossRef]
36. Grasdalen, H.; Larsen, B.; Smidsrød, O. A p.m.r. study of the composition and sequence of uronate residues in alginates. *Carbohydr. Res.* **1979**, *68*, 23–31. [CrossRef]
37. Dalheim, M.Ø.; Ulset, A.-S.T.; Jenssen, I.B.; Christensen, B.E. Degradation kinetics of peptide-coupled alginates prepared via the periodate oxidation reductive amination route. *Carbohydr. Polym.* **2017**, *157*, 1844–1852. [CrossRef] [PubMed]
38. Draget, K.I.; Østgaard, K.; Smidsrød, O. Homogeneous alginate gels: A technical approach. *Carbohydr. Polym.* **1990**, *14*, 159–178. [CrossRef]
39. Huebsch, N.; Arany, P.R.; Mao, A.S.; Shvartsman, D.; Ali, O.A.; Bencherif, S.A.; Rivera-Feliciano, J.; Mooney, D.J. Harnessing traction-mediated manipulation of the cell/matrix interface to control stem-cell fate. *Nat. Mater.* **2010**, *9*, 518. [CrossRef] [PubMed]
40. Bouhadir, K.H.; Lee, K.Y.; Alsberg, E.; Damm, K.L.; Anderson, K.W.; Mooney, D.J. Degradation of partially oxidized alginate and its potential application for tissue engineering. *Biotechnol. Prog.* **2001**, *17*, 945–950. [CrossRef]
41. Painter, T.; Larsen, B. Formation of Hemiacetals between Neighbouring Hexuronic Acid Residues during the Periodate Oxidation of Alginate. *Acta Chem. Scand.* **1970**, *24*, 813–833. [CrossRef]
42. Stokke, B.T.; Smidsrød, O.; Zanetti, F.; Strand, W.; Skjåk-Bræk, G. Distribution of uronate residues in alginate chains in relation to alginate gelling properties—2: Enrichment of β-d-mannuronic acid and depletion of α-l-guluronic acid in sol fraction. *Carbohydr. Polym.* **1993**, *21*, 39–46. [CrossRef]
43. Bowman, K.A.; Aarstad, O.A.; Nakamura, M.; Stokke, B.T.; Skjåk-Bræk, G.; Round, A.N. Single molecule investigation of the onset and minimum size of the calcium-mediated junction zone in alginate. *Carbohydr. Polym.* **2016**, *148*, 52–60. [CrossRef]
44. Stokke, B.T.; Draget, K.I.; Smidsrød, O.; Yuguchi, Y.; Urakawa, H.; Kajiwara, K. Small-Angle X-ray Scattering and Rheological Characterization of Alginate Gels. 1. Ca−Alginate Gels. *Macromolecules* **2000**, *33*, 1853–1863. [CrossRef]
45. Yuguchi, Y.; Hasegawa, A.; Padoł, A.M.; Draget, K.I.; Stokke, B.T. Local structure of Ca^{2+} induced hydrogels of alginate–oligoguluronate blends determined by small-angle-X-ray scattering. *Carbohydr. Polym.* **2016**, *152*, 532–540. [CrossRef] [PubMed]

46. Skjåk-Bræk, G.; Donati, I.; Paoletti, S. Alginate Hydrogels: Properties and Applications. In *Polysaccharide Hydrogels: Characterization and Biomedical Applications*; Pan Stanford: Singapore, 2015; pp. 449–498.
47. Martinsen, A.; Skjåk-Bræk, G.; Smidsrød, O. Alginate as immobilization material: I. Correlation between chemical and physical properties of alginate gel beads. *Biotechnol. Bioeng.* **1989**, *33*, 79–89. [CrossRef]
48. Draget, K.I.; Gåserød, O.; Aune, I.; Andersen, P.O.; Storbakken, B.; Stokke, B.T.; Smidsrød, O. Effects of molecular weight and elastic segment flexibility on syneresis in Ca–alginate gels. *Food Hydrocoll.* **2001**, *15*, 485–490. [CrossRef]
49. Aarstad, O.; Heggset, B.E.; Pedersen, S.I.; Bjørnøy, H.S.; Syverud, K.; Strand, L.B. Mechanical Properties of Composite Hydrogels of Alginate and Cellulose Nanofibrils. *Polymers* **2017**, *9*, 378. [CrossRef]
50. Smidsrød, O.; Moe, S.T. *Biopolymer Chemistry*; Postmyr, L., Ed.; Tapir Academic Press: Trondheim, Norway, 2008.
51. Nielsen, T.T.; Wintgens, V.; Amiel, C.; Wimmer, R.; Larsen, K.L. Facile Synthesis of beta-Cyclodextrin-Dextran Polymers by “Click” Chemistry. *Biomacromolecules* **2010**, *11*, 1710–1715. [CrossRef]
52. Smidsrød, O.; Haug, A.; Lian, B. Properties of Poly(1,4-hexuronates) in the Gel State. I. Evaluation of a Method for the Determination of Stiffness. *Acta Chem. Scand.* **1972**, *26*, 71–78. [CrossRef]
53. Ertesvåg, H.; Skjåk-Bræk, G. *Modification of Alginate Using Mannuronan C-5-Epimerases.*; Bucke, C., Ed.; Humana Press: Totowa, NJ, USA, 1999.

Supplementary Paper II

Supplementary file 1 (S1)

^{1}H NMR spectra including bulk assignment of the grafted alginates are given in Figure S1. The samples were subjected to mild acid hydrolysis as previously described [46] to reduce the viscosity prior to the NMR analysis. 6-10 mg of the samples were then dissolved in 600 µl D_2O (99.9%) and added 5 µl 3-(Trimethylsilyl)propionic 2,2,3,3-d_4 acid (TSP, Sigma Aldrich) as an internal standard and 15 µl Triethylenetetraamine-hexaacetic acid (TTHA, Sigma Aldrich) as a chelating agent for residual divalent ions. The latter was not added to samples already added EDTA (analysis of leaked alginate). 1D ^{1}H spectra were recorded at 90 °C on a Bruker Ascend 400 MHz Avance III HD spectrometer, equipped with a 5-mm SmartProbe z-gradient probe and SampleCase (Bruker BioSpin AG, Fällanden, Switzerland). The spectra were recorded using TopSpin 3.2 software (Bruker BioSpin) and processed and analyzed with TopSpin 3.5 software (Bruker BioSpin).

The degree of substitution was calculated as mole substituent per mole uronic acid residues as previously described [21,29]. The calculations are based on earlier annotations of the proton NMR spectra of alginates [32,33], periodate oxidized alginates [28], alginates grafted with methyl tyrosine ester (MeOTyr) [21], GRGDSP grafted alginates [20] and β-cyclodextrin (β-CyD) grafted alginates [29].

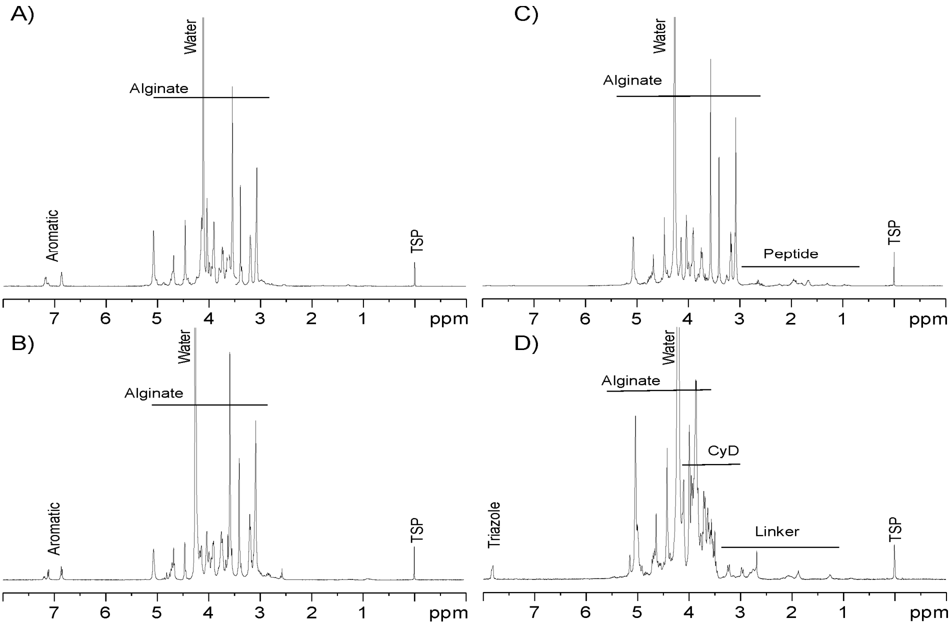

Figure S1: ^{1}H NMR of A: partially oxidized (P_0 = 0.08) *L. hyperborea* stipe alginate(65 % G) grafted with MeOTyr, B: partially oxidized (P_0 = 0.08) mannuronan grafted with MeOTyr and epimerized with AlgE64, C: partially oxidized (P_0 = 0.08) *L. hyperborea* stipe alginate grafted with GRGDSP peptide and D: partially oxidized (P_0 = 0.08) *L. hyperborea* stipe alginate grafted with β-CyD. The bulk assignment of the protons of the different chemical groups are indicated. The exact annotations of the proton NMR spectra can be found as following: alginates [32,33], periodate oxidized alginates [28], MeOTyr grafted alginates [21], GRGDSP grafted alginates [20] and β-CyD grafted alginates [29]. The 1H NMR-spectrum was recorded at 400 MHz and 90 °C in D2O.

Supplementary file 2, S2

The molar mass of the materials was analyzed using SEC-MALS, as previously described [25]. The system consisted of a mobile phase reservoir, an on-line degasser, an HPLC isocratic pump (LC-10ADVP, Shimadzu), an autoinjector (SCL-10AV, Shimadzu), a pre-column and two serially connected columns: TSK 6000 PWXL and TSK 5000 PWXL (Toso Haas). The columns were followed by two serially connected detectors; a Dawn DSP laser light scattering photometer (Wyatt, USA) ($\lambda_0 = 0.664$ nm) and an Optilab DSP differential refractometer (Wyatt, USA). 0.15 M $NaNO_3$ with 0.01 M NaEDTA, pH 6 was used as the mobile phase. 20% acetonitrile was added to the mobile phase for the alginate grafted with β-CyD. All samples were dissolved in the mobile phase (0.25-7.5 mg/mL) and filtered (pore size 0.8 μm) prior to injection. The injection volume was adjusted to obtain an optimal light scattering signal and to avoid overloading. Astra software v. 6.1 (Wyatt, USA) was used to collect and process the obtained data, using a refractive index increment (dn/dcμ) of 0.150 mL/g for alginate samples [25].

Chromatograms and slice molecular weights for the samples are given in Figure S2.1 – S2.4.

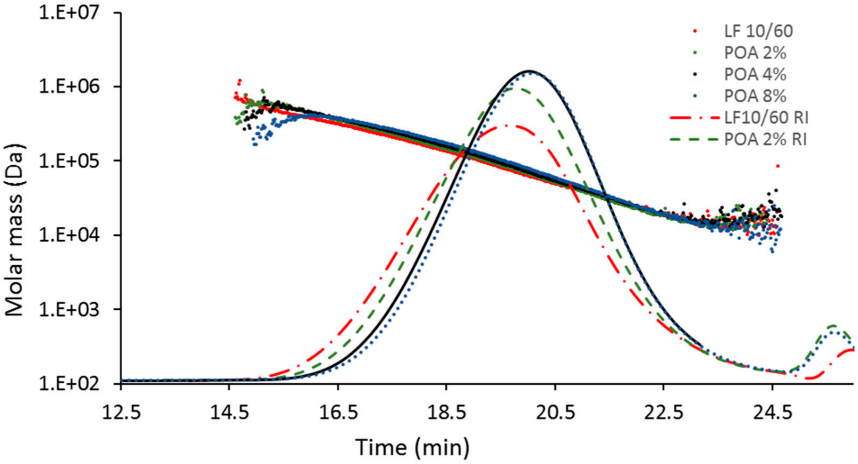

Figure S2.1: SEC-MALS data for from left to right: *Laminaria hyperborea* stipe alginate (65 %G) (red), periodate oxidized stipe alginate $P_0 = 0.02$ (green), $P_0 = 0.04$ (black), $P_0 = 0.08$ (blue). Mobile phase: 0.15 M $NaNO_3$ with 0.01 M NaEDTA, pH 6. Concentration profiles are represented with lines and slice molecular weights with dots.

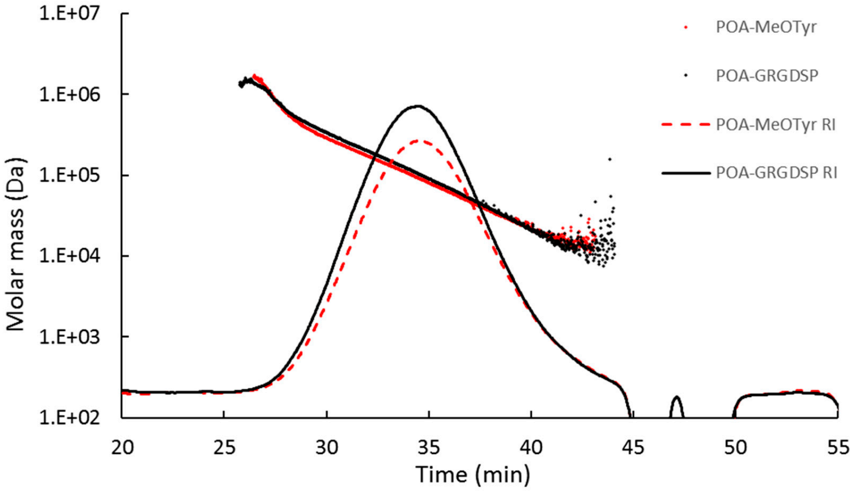

Figure S2.2: SEC-MALS data for from left to right: GRGDSP grafted stipe alginate $P_0 = 0.08$, DS = 7.0 % (POA-GRGDSP) (red) and MeOTyr grafted stipe alginate $P_0 = 0.08$, DS = 7.0 % (POA-MeOTyr) (black). Mobile phase: 0.15 M NaNO3 with 0.01 M NaEDTA, pH 6. Concentration profiles are represented with lines and slice molecular weights with dots.

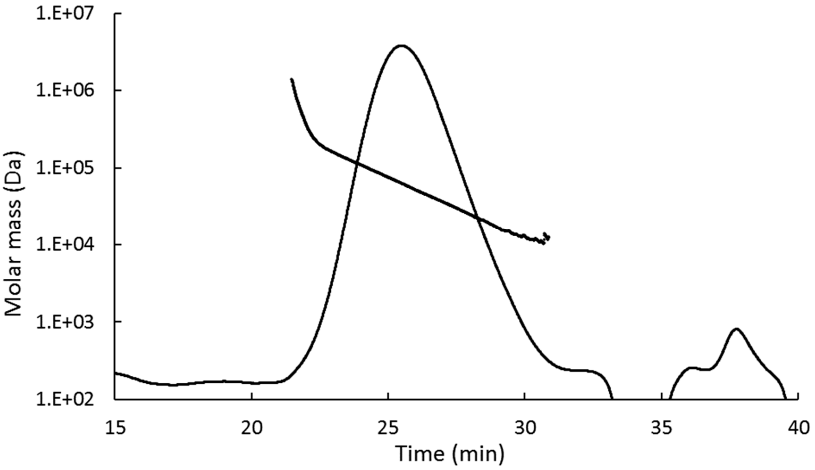

Figure S2.3: SEC-MALS data for β-CyD grafted stipe alginate $P_0 = 0.08$, DS = 1.6 % (POA-GRGDSP). Mobile phase: 0.15 M NaNO3 with 0.01 M NaEDTA, pH 6 with 20 % acetonitrile. Concentration profiles are represented with lines and slice molecular weights with dots.

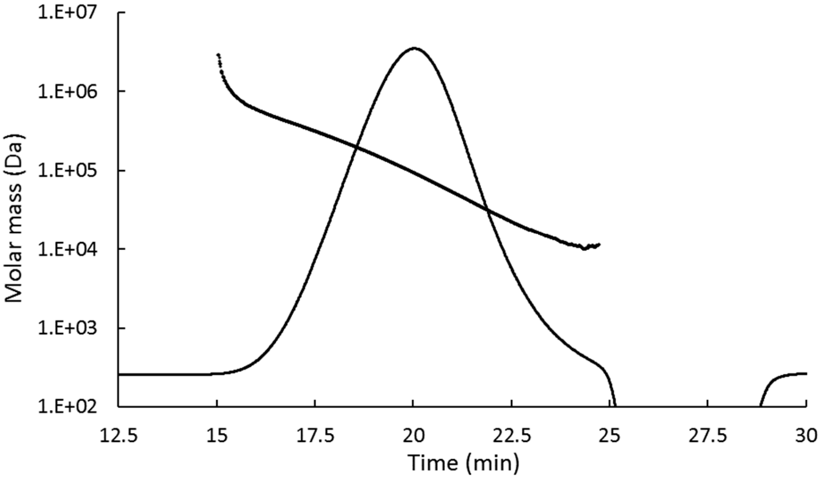

Figure S2.4: SEC-MALS data for MeOTyr grafted mannuronan, $P_0 = 0.08$, DS = 7.9 %, epimerized with AlgE64, 49 % G (epim POA-MeOTyr). Mobile phase: 0.15 M NaNO3 with 0.01 M NaEDTA, pH 6. Concentration profiles are represented with lines and slice molecular weights with dots.

Supplementary file 3

The mechanical properties of the alginate gel cylinders were characterized by uniaxial compression using a Stable MicroSystems, TA XT plus Texture Analyser with a P/35 probe at room temperature and a compression rate of 0.1 mm/s. The weight of the loading cell was five kg. Young's modulus (E) was calculated from the initial slope (typically 0.1 – 0.3 mm) of the force/deformation curves (F/A) = E x Δl/l (see figure C1) and corrected for syneresis: $E_{corrected} = E_{measured} \times (C_{initial}/C_{final})^2$ [48]. All data were collected and processed with the "Texture Expert Exponent 32" software. Strain and stress at rupture (or ultimate compression strength) was determined in experiments where the hydrogels were compressed to the point of rupture. Reported data of stress at rupture is the maximum value on the force-deformation curve (see figure S3.1), while the deformation at rupture is reported as the compression distance at the point of rupture (mm) relative to the initial gel height (mm).

Uniaxial compression curves for the different gels are given in Figure S3.2 – S3.8.

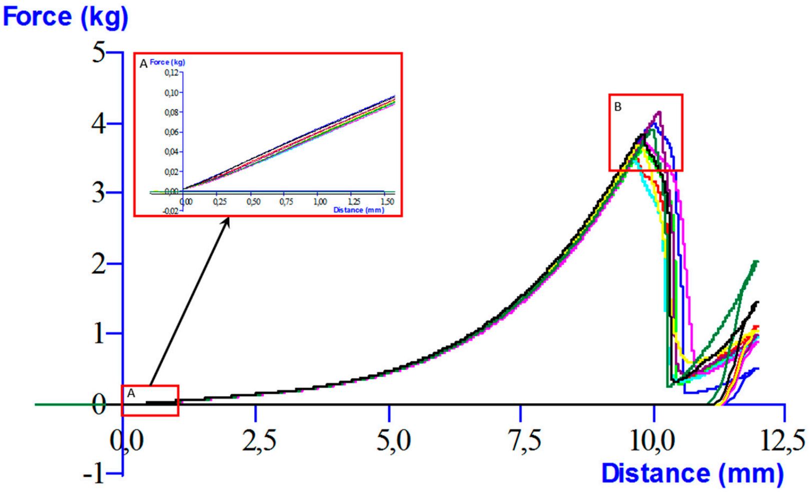

Figure S3.1: Stress (kg) – deformation (distance, mm) curves for compression of 1.0 % w/v *L. hyperborea* stipe alginate gel cylinders (n = 9). Area A shows the initial linear elastic region (typically 0.1 – 0.3 mm) used to find the initial slope from which Young's modulus is calculated. Area B shows point of rupture used to find the stress (kg) and deformation at rupture (%), calculated as the compression at rupture (mm) relative to the initial gel height (mm).

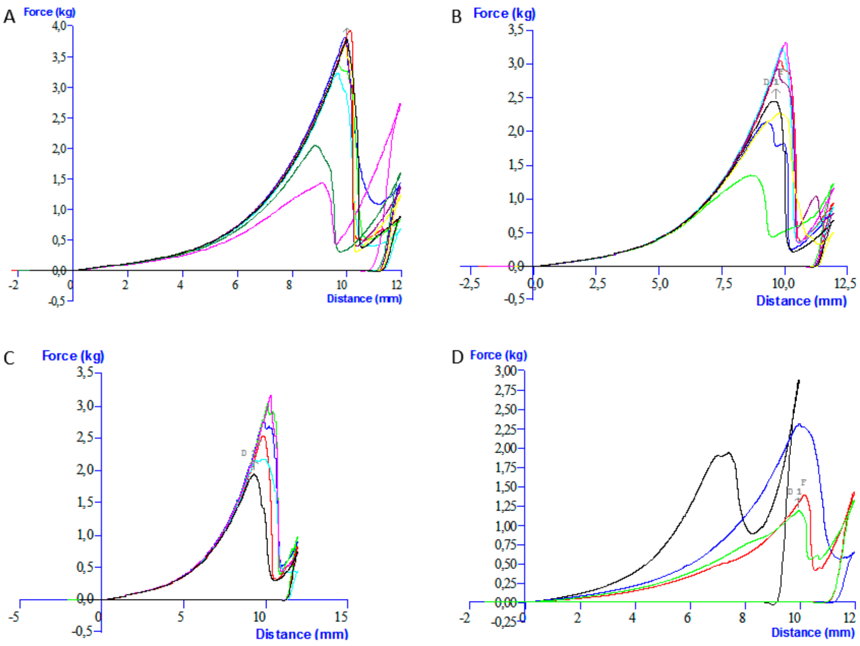

Figure S3.2: Stress (kg) – deformation (mm) curves for compression of 1.0 % w/v mixed Ca-saturated hydrogel cylinders of *L. hyperborea* stipe alginate and various fractions of POA $P_0 = 0.02$ (W_{POA}). A: $W_{POA} = 0.25$ (n= 9), B: $W_{POA} = 0.50$ (n= 9), A: $W_{POA} = 0.75$ (n= 6) and D: $W_{POA} = 1.00$ (n= 4)

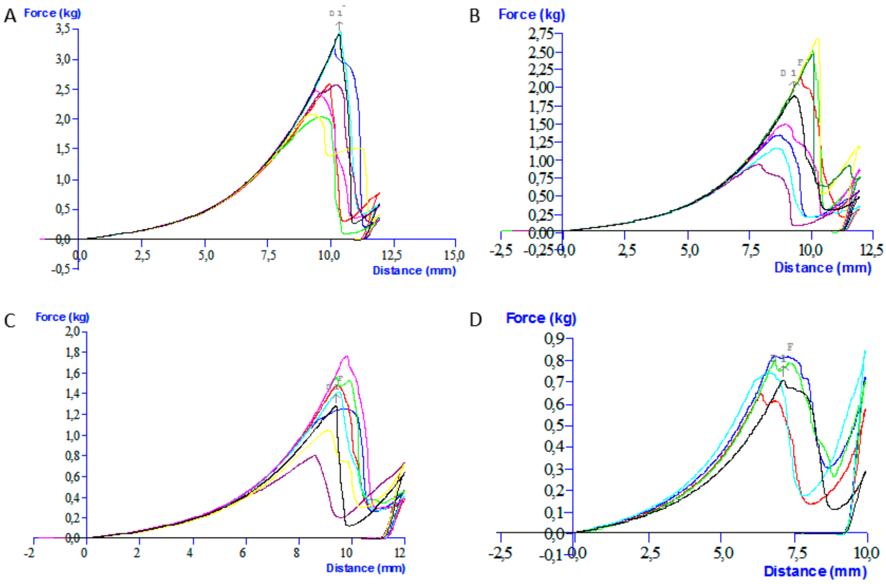

Figure S3.3: Stress (kg) – deformation (mm) curves for compression of 1.0 % w/v mixed Ca-saturated hydrogel cylinders of *L. hyperborea* stipe alginate and various fractions of POA $P_0 = 0.04$ (W_{POA}). A: $W_{POA} = 0.25$ (n= 8), B: $W_{POA} = 0.50$ (n= 9), A: $W_{POA} = 0.75$ (n= 8) and D: $W_{POA} = 1.00$ (n= 5)

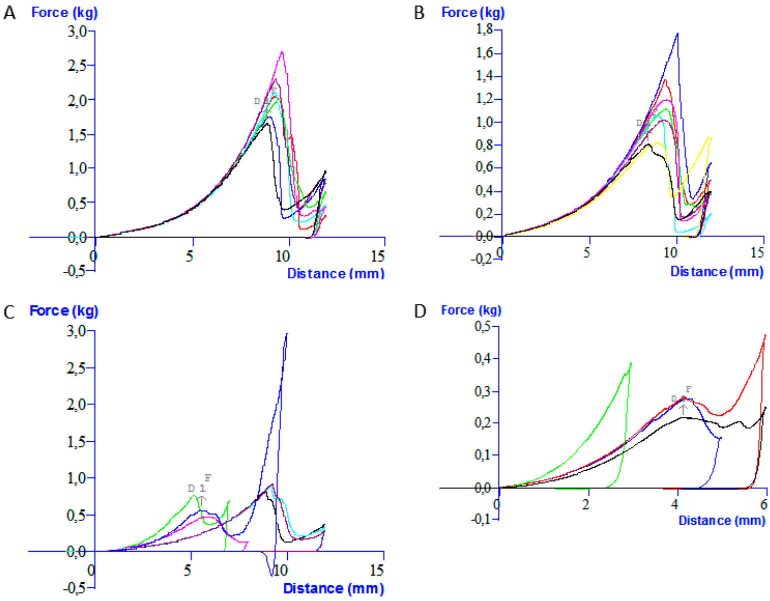

Figure S3.4: Stress (kg) – deformation (mm) curves for compression of 1.0 % w/v mixed Ca-saturated hydrogel cylinders of *L. hyperborea* stipe alginate and various fractions of POA $P_0 = 0.08$ (W_{POA}). A: $W_{POA} = 0.25$ (n= 7), B: $W_{POA} = 0.50$ (n= 8), A: $W_{POA} = 0.75$ (n= 7) and D: $W_{POA} = 1.00$ (n= 4)

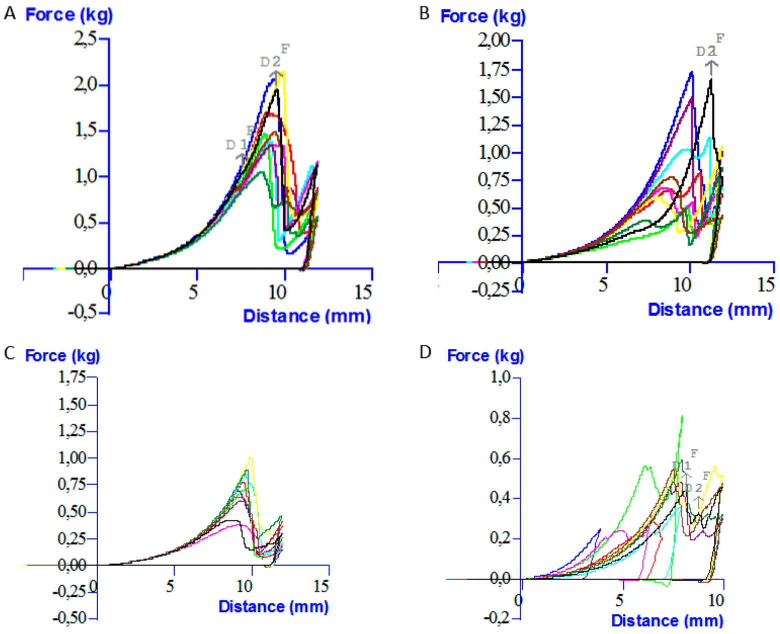

Figure S3.5: Stress (kg) – deformation (mm) curves for compression of 1.0 % w/v mixed Ca-saturated hydrogel cylinders of *L. hyperborea* stipe alginate and various fractions ($W_{POA\text{-}MeOTyr}$) of POA grafted with L-Tyrosine methyl ester (POA-MeOTyr). A: $W_{POA\text{-}MeOTyr} = 0.25$ (n= 10), B: $W_{POA\text{-}MeOTyr} = 0.50$ (n= 10), A: $W_{POA\text{-}MeOTyr} = 0.75$ (n= 10) and D: $W_{POA\text{-}MeOTyr} = 1.00$ (n= 10)

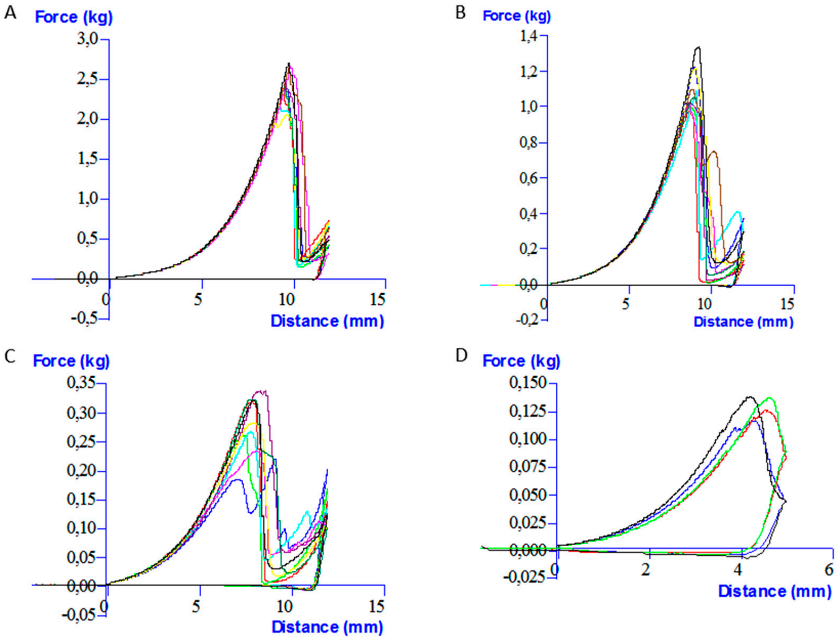

Figure S3.6: Stress (kg) – deformation (mm) curves for compression of 1.0 % w/v mixed Ca-saturated hydrogel cylinders of *L. hyperborea* stipe alginate and various fractions ($W_{POA-\beta CyD}$) of POA grafted with β-cyclodextrin (POA-βCyD). A: $W_{POA-\beta CyD} = 0.25$ (n= 10), B: $W_{POA-\beta CyD} = 0.50$ (n= 10), A: $W_{POA-\beta CyD} = 0.75$ (n= 9) and D: $W_{POA-\beta CyD} = 1.00$ (n= 4)

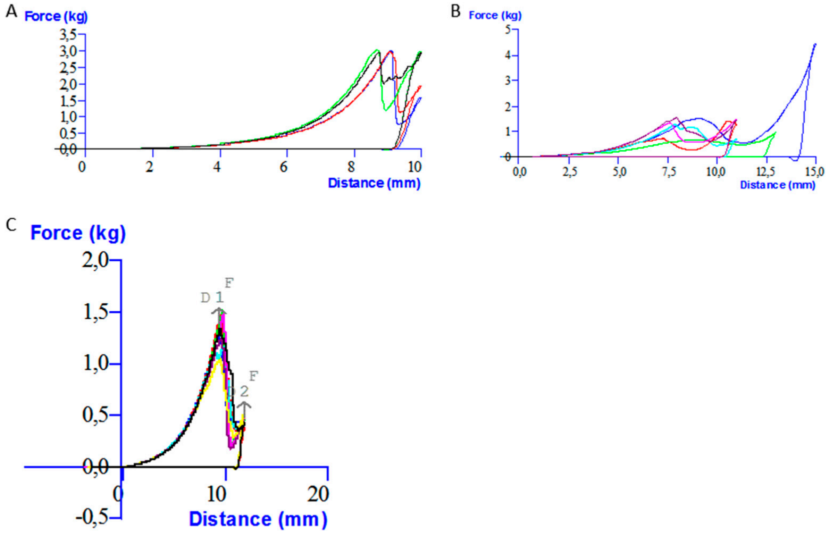

Figure S3.7: Stress (kg) – deformation (mm) curves for compression of 1.0 % w/v mixed Ca-saturated hydrogel cylinders of A: *L. hyperborea* stipe alginate and EpimPOA-MeOTyr (epimerized mannuronan grafted with MeOTyr) $W_{EpimPOA-MeOTyr} = 0.50$ (n = 5), B: *L. hyperborea* stipe alginate and EpimPOA-MeOTyr, $W_{EpimPOA-MeOTyr} = 1.00$ (n = 4) and C: *L. hyperborea* stipe alginate and POA grafted with GRGDSP (POA-GRGDSP), $W_{POA-GRGDSP} = 0.50$ (n = 8).

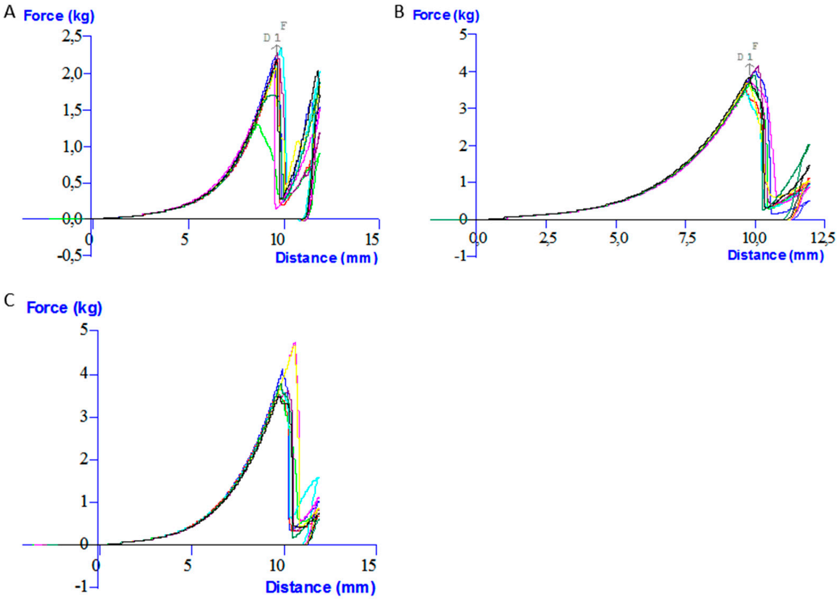

Figure S3.8: Stress (kg) – deformation (mm) curves for compression of A: 0.5 % w/v *L. hyperborea* stipe alginate gel cylinders (n = 9), B: 1.0 % w/v *L. hyperborea* stipe alginate gel cylinders (n = 9) and C: 1.0 % w/v *L. hyperborea* stipe alginate gel cylinders with free β-CyD (n = 9).

Supplementary file 4

Statistical data for the modified alginate gels are here given with regards to the Young's modulus, syneresis and compression and stress at rupture.

Table S4.1. Statistical data of the partially oxidized alginate gels with regards to the pure stipe alginate 1% gels. The values for Young's modulus and syneresis are given as the mean of the gels. Abbreviations: n = number of gels. SD = standard deviation. POA = partially oxidized alginate.

Oxidation degree (%)	Fraction of POA	Young's modulus (kPa)	SD	n	p-value	Syneresis (%)	SD	n	p-value
2	0.25	28.4	2.9	9	0.50	30.4	1.4	9	1.0
	0.50	28.1	0.6	8	0.41	27.1	0.6	8	<0.01
	0.75	24.9	2.8	6	<0.01	27.3	0.8	6	0.059
	1.00	8.7	5.4	5	<0.01	28.1	3.1	3	0.84
4	0.25	32.2	1.7	8	1.00	16.7	0.8	8	<0.01
	0.50	26.1	1.4	8	<0.01	21.1	0.8	8	<0.01
	0.75	19.6	2.6	7	<0.01	19.8	0.8	7	<0.01
	1.00	8.9	1.8	5	<0.01	39.2	3.6	5	<0.01
8	0.25	29.3	1.3	6	0.96	23.0	0.6	6	<0.01
	0.50	23.8	2.4	8	<0.01	15.2	0.8	8	<0.01
	0.75	7.1	5.2	7	<0.01	17.7	1.1	3	<0.01

Table S4.2. Statistical data of the partially oxidized alginate gels with regards to the pure stipe alginate 1% gels. The values for deformation at rupture (compression) and stress at rupture are given as the mean of the gels. Abbreviations: n = number of gels. SD = standard deviation. POA = partially oxidized alginate.

Oxidation degree (%)	**Fraction of POA**	**Deformation (%)**	**SD**	**n**	**p-value**	**Stress at rupture (N)**	**SD**	**n**	**p-value**
2	0.25	62.2	2.0	7	1.0	35.8	2.5	7	1.0
	0.50	59	1.8	7	0.94	27.3	4.7	7	<0.01
	0.75	59.4	2.4	6	0.99	25.5	4.7	6	<0.01
	1.00	61.3	3.4	5	1.0	15.1	5.5	5	<0.01
4	0.25	58.4	2.7	8	0.73	26.8	5.5	8	<0.01
	0.50	55.7	5.2	8	0.017	17.3	6.3	8	<0.01
	0.75	56.9	1.0	6	0.21	14.3	1.8	6	<0.01
	1.00	53.2	1.8	5	<0.01	7.3	0.7	5	<0.01
8	0.25	57.9	2.4	6	0.60	21.3	3.2	6	<0.01
	0.50	53.9	3.1	7	<0.01	11.3	3.3	7	<0.01
	0.75	53.3	3.9	7	<0.01	7.1	1.7	7	<0.01

Table S4.3. Statistical data of the partially oxidized alginate gels with regards to the pure stipe alginate 0.5% gels. The values for Young's modulus and syneresis are given as the mean of the gels. Abbreviations: n = number of gels. SD = standard deviation. POA = partially oxidized alginate.

Oxidation degree (%)	Fraction of POA	Young's modulus (kPa)	SD	n	p-value	Syneresis (%)	SD	n	p-value
2	0.25	28.4	2.9	9	<0.01	30.4	1.4	9	<0.01
	0.50	28.1	0.6	8	<0.01	27.1	0.6	8	<0.01
	0.75	24.9	2.8	6	<0.01	27.3	0.8	6	<0.01
	1.00	8.7	5.4	5	0.92	28.1	3.1	3	<0.01
4	0.25	32.2	1.7	8	<0.01	16.7	0.8	8	<0.01
	0.50	26.1	1.4	8	<0.01	21.1	0.8	8	<0.01
	0.75	19.6	2.6	7	<0.01	19.8	0.8	7	<0.01
	1.00	8.9	1.8	5	0.89	39.2	3.6	5	<0.01
8	0.25	29.3	1.3	6	<0.01	23.0	0.6	6	<0.01
	0.50	23.8	2.4	8	<0.01	15.2	0.8	8	<0.01
	0.75	7.1	5.2	7	1.0	17.7	1.1	3	<0.01

Table S.4.4. Statistical data of the partially oxidized alginate gels with regards to the pure stipe alginate 0.5% gels. The values for deformation at rupture (compression) and stress at rupture are given as the mean of the gels. Abbreviations: n = number of gels. SD = standard deviation. POA = partially oxidized alginate.

Oxidation degree (%)	Fraction of POA	Deformation (%)	SD	n	p-value	Stress at rupture (N)	SD	n	p-value
2	0.25	62.2	2.0	7	0.047	35.8	2.5	7	<0.01
	0.50	59	1.8	7	<0.01	27.3	4.7	7	0.021
	0.75	59.4	2.4	6	<0.01	25.5	4.7	6	0.28
	1.00	61.3	3.4	5	0.028	15.1	5.5	5	0.55
4	0.25	58.4	2.7	8	<0.01	26.8	5.5	8	0.031
	0.50	55.7	5.2	8	<0.01	17.3	6.3	8	0.96
	0.75	56.9	1.0	6	<0.01	14.3	1.8	6	0.23
	1.00	53.2	1.8	5	<0.01	7.3	0.7	5	<0.01
8	0.25	57.9	2.4	6	<0.01	21.3	3.2	6	1.0
	0.50	53.9	3.1	7	<0.01	11.3	3.3	7	<0.01
	0.75	53.3	3.9	7	<0.01	7.1	1.7	7	<0.01

Table S4.5. Statistical data comparing the partially oxidized alginate gels with regards to the oxidation degree. Data for the 1% and 0.5% pure stipe alginate gels are also given. The values for Young's modulus are given as the mean of the gels. Abbreviations: n = number of gels. SD = standard deviation. POA 0.02 = 2% partially oxidized alginate. POA 0.04 = 4% partially oxidized alginate. POA 0.08 = 8% partially oxidized alginate.

Fraction of POA	Gel A / Gel B	Young's modulus (kPa)	SD	n	p-value
0	1% gel / 0.5% gel	31.4 / 6.3	2.7 / 1.0	8 / 9	<0.01
0.25	POA 0.02 / POA 0.04	28.4 / 32.2	2.9 / 1.7	9 / 8	0.17

	POA 0.02 / POA 0.08	28.4 / 29.3	2.9 / 1.3	9 / 6	1.0
	POA 0.04 / POA 0.08	32.3 / 29.3	1.7 / 1.3	8 / 6	0.72
0.50	POA 0.02 / POA 0.04	28.1 / 26.1	0.6 / 1.4	8 / 8	0.95
	POA 0.02 / POA 0.08	28.1 / 23.8	0.6 / 2.4	8 / 8	0.084
	POA 0.04 / POA 0.08	26.1 / 23.8	1.4 / 2.4	8 / 8	0.88
0.75	POA 0.02 / POA 0.04	24.9 / 19.6	2.8 / 2.6	6 / 7	0.032
	POA 0.02 / POA 0.08	24.9 / 7.1	2.8 / 5.2	6 / 7	<0.01
	POA 0.04 / POA 0.08	19.6 / 7.1	2.6 / 5.2	7 / 7	<0.01
1.00	POA 0.02 / POA 0.04	8.7 / 8.9	5.4 / 1.8	5 / 5	1.0

Table S4.6. Statistical data comparing the partially oxidized alginate gels with regards to the oxidation degree. Data for the 1% and 0.5% pure stipe alginate gels are also given. The values for syneresis are given as the mean of the gels. Abbreviations: n = number of gels. SD = standard deviation. POA 0.02 = 2% partially oxidized alginate. POA 0.04 = 4% partially oxidized alginate. POA 0.08 = 8% partially oxidized alginate.

Fraction of POA	Gel A / Gel B	Syneresis (%)	SD	n	p-value
0	1% gel / 0.5% gel	29.7 / 45.7	0.7 / 1.7	9 / 9	<0.01
0.25	POA 0.02 / POA 0.04	30.4 / 16.7	1.4 / 0.8	9 / 8	<0.01
	POA 0.02 / POA 0.08	30.4 / 23.0	1.4 / 0.6	9 / 6	<0.01
	POA 0.04 / POA 0.08	16.7 / 23.0	0.8 / 0.6	8 / 6	<0.01
0.50	POA 0.02 / POA 0.04	27.1 / 21.1	0.6 / 0.8	8 / 8	<0.01
	POA 0.02 / POA 0.08	27.1 / 15.2	0.6 / 0.8	8 / 8	<0.01
	POA 0.04 / POA 0.08	21.1 / 15.2	0.8 / 0.8	8 / 8	<0.01
0.75	POA 0.02 / POA 0.04	27.3 / 19.8	0.8 / 0.8	6 / 7	<0.01
	POA 0.02 / POA 0.08	27.3 / 17.7	0.8 / 1.1	6 / 3	<0.01
	POA 0.04 / POA 0.08	19.8 / 17.7	0.8 / 1.1	7 / 3	0.58
1.00	POA 0.02 / POA 0.04	NA	NA	NA	NA

Table S4.7. Statistical data comparing the partially oxidized alginate gels with regards to the oxidation degree. Data for the 1% and 0.5% pure stipe alginate gels are also given. The values for deformation at rupture (compression) are given as the mean of the gels. Abbreviations: n = number of gels. SD = standard deviation. POA 0.02 = 2% partially oxidized alginate. POA 0.04 = 4% partially oxidized alginate. POA 0.08 = 8% partially oxidized alginate.

Fraction of POA	Gel A / Gel B	Deformation (%)	SD	n	p-value
0	1% gel / 0.5% gel	61.4 / 67.4	1.1 / 3.6	8 / 9	<0.01
0.25	POA 0.02 / POA 0.04	62.2 / 58.4	2.0 / 2.7	7 / 8	0.43
	POA 0.02 / POA 0.08	62.2 / 57.9	2.0 / 2.4	7 / 6	0.32
	POA 0.04 / POA 0.08	58.4 / 57.9	2.7 / 2.4	8 / 6	1.0
0.50	POA 0.02 / POA 0.04	59.0 / 55.7	1.8 / 5.2	7 / 8	0.64
	POA 0.02 / POA 0.08	59.0 / 53.9	1.8 / 3.1	7 / 7	0.088
	POA 0.04 / POA 0.08	55.7 / 53.9	5.2 / 3.1	8 / 7	1.0
0.75	POA 0.02 / POA 0.04	59.4 / 56.9	2.4 / 1.0	6 / 6	0.96

	POA 0.02 / POA 0.08	59.4 / 53.3	2.4 / 3.9	6 / 7	0.026
	POA 0.04 / POA 0.08	56.9 / 53.3	1.8 / 3.9	6 / 7	0.66
1.00	POA 0.02 / POA 0.04	61.3 / 53.2	3.4 / 1.8	5 / 5	<0.01

Table S4.8. Statistical data comparing the partially oxidized alginate gels with regards to the oxidation degree. Data for the 1% and 0.5% pure stipe alginate gels are also given. The values for stress at rupture are given as the mean of the gels. Abbreviations: n = number of gels. SD = standard deviation. POA 0.02 = 2% partially oxidized alginate. POA 0.04 = 4% partially oxidized alginate. POA 0.08 = 8% partially oxidized alginate.

Fraction of POA	Gel A / Gel B	Stress at rupture (N)	SD	n	p-value
0	1% gel / 0.5% gel	37.1 / 20.0	2.4 / 3.3	8 / 9	<0.01
0.25	POA 0.02 / POA 0.04	35.8 / 26.8	2.5 / 5.5	7 / 8	<0.01
	POA 0.02 / POA 0.08	35.8 / 21.3	2.5 / 3.2	7 / 6	<0.01
	POA 0.04 / POA 0.08	26.8 / 21.3	5.5 / 3.2	8 / 6	0.30
0.50	POA 0.02 / POA 0.04	27.3 / 17.3	4.7 / 6.3	7 / 8	<0.01
	POA 0.02 / POA 0.08	27.3 / 11.3	4.7 / 3.3	7 / 7	<0.01
	POA 0.04 / POA 0.08	17.3 / 11.3	6.3 / 3.3	8 / 7	0.16
0.75	POA 0.02 / POA 0.04	25.5 / 14.3	4.7 / 1.8	6 / 6	<0.01
	POA 0.02 / POA 0.08	25.5 / 7.1	4.7 / 1.7	6 / 7	<0.01
	POA 0.04 / POA 0.08	14.3 / 7.1	1.8 / 1.7	6 / 7	0.061
1.00	POA 0.02 / POA 0.04	15.1 / 7.3	5.5 / 0.7	5 / 5	0.093

Table S4.9. Statistical data comparing the partially oxidized alginate gels with regards to the fraction of modified alginate in the gels. The values for Young's modulus are given as the mean of the gels. Abbreviations: n = number of gels. SD = standard deviation. POA = partially oxidized alginate.

Oxidation degree (%)	Fraction of POA	Young's modulus (kPa)	SD	n	p-value
2	0.25 / 0.50	28.4 / 28.1	2.9 / 0.6	9 / 8	1.0
	0.25 / 0.75	28.4 / 24.9	2.9 / 2.8	9 / 6	0.40
	0.25 / 1.0	28.4 / 8.7	2.9 / 5.4	9 / 5	<0.01
	0.50 / 0.75	28.1 / 24.9	0.6 / 2.8	8 / 6	0.57
	0.50 / 1.0	28.1 / 8.7	0.6 / 5.4	8 / 5	<0.01
	0.75 / 1.0	24.9 / 8.7	2.8 / 5.4	6 / 5	<0.01
4	0.25 / 0.50	32.2 / 26.1	1.7 / 1.4	8 / 8	<0.01
	0.25 / 0.75	32.2 / 19.6	1.7 / 2.6	8 / 7	<0.01
	0.25 / 1.0	32.2 / 8.9	1.7 / 1.8	8 / 5	<0.01
	0.50 / 0.75	26.1 / 19.6	1.4 / 2.6	8 / 7	<0.01
	0.50 / 1.0	26.1 / 8.9	1.4 / 1.8	8 / 5	<0.01
	0.75 / 1.0	19.6 / 8.9	2.6 / 1.8	7 / 5	<0.01
8	0.25 / 0.50	29.3 / 23.8	1.3 / 2.4	6 / 8	0.02
	0.25 / 0.75	29.3 / 7.1	1.3 / 5.2	6 / 7	<0.01
	0.50 / 0.75	23.8 / 7.1	2.4 / 5.2	8 / 7	<0.01

Table S4.10. Statistical data comparing the partially oxidized alginate gels with regards to the fraction of modified alginate in the gels. The values for syneresis are given as the mean of the gels. Abbreviations: n = number of gels. SD = standard deviation. POA = partially oxidized alginate.

Oxidation degree (%)	Fraction of POA	Syneresis (%)	SD	n	p-value
2	0.25 / 0.50	30.4 / 27.1	1.4 / 0.6	9 / 8	<0.01
	0.25 / 0.75	30.4 / 27.3	1.4 / 0.8	9 / 6	<0.01
	0.25 / 1.0	30.4 / 28.1	1.4 / 3.1	9 / 3	0.34
	0.50 / 0.75	27.1 / 27.3	0.6 / 0.8	8 / 6	1.0
	0.50 / 1.0	27.1 / 28.1	0.6 / 3.1	8 / 3	1.0
	0.75 / 1.0	27.3 / 28.1	0.8 / 3.1	6 / 3	1.0
4	0.25 / 0.50	16.7 / 21.4	0.8 / 0.8	8 / 8	<0.01
	0.25 / 0.75	16.7 / 19.8	0.8 / 0.8	8 / 7	<0.01
	0.25 / 1.0	16.7 / 39.2	0.8 / 3.6	8 / 5	<0.01
	0.50 / 0.75	21.4 / 19.8	0.8 / 0.8	8 / 7	0.81
	0.50 / 1.0	21.4 / 39.2	0.8 / 3.6	8 / 5	<0.01
	0.75 / 1.0	19.8 / 39.2	0.8 / 3.6	7 / 5	<0.01
8	0.25 / 0.50	23.0 / 15.2	0.6 / 0.8	6 / 8	<0.01
	0.25 / 0.75	23.0 / 17.7	0.6 / 1.1	6 / 3	<0.01
	0.50 / 0.75	15.2 / 17.7	0.8 / 1.1	8 / 3	0.28

Table S4.11. Statistical data comparing the partially oxidized alginate gels with regards to the fraction of modified alginate in the gels. The values for deformation at rupture (compression) are given as the mean of the gels. Abbreviations: n = number of gels. SD = standard deviation. POA = partially oxidized alginate.

Oxidation degree (%)	Fraction of POA	Deformation (%)	SD	n	p-value
2	0.25 / 0.50	62.2 / 59.0	2.0 / 1.8	7 / 7	0.73
	0.25 / 0.75	62.2 / 59.4	2.0 / 2.4	7 / 6	0.89
	0.25 / 1.0	62.2 / 61.3	2.0 / 3.4	7 / 5	1.0
	0.50 / 0.75	59.0 / 59.4	1.8 / 2.4	7 / 6	1.0
	0.50 / 1.0	59.0 / 61.3	1.8 / 3.4	7 / 5	0.98
	0.75 / 1.0	59.4 / 61.3	2.4 / 3.4	6 / 5	1.0
4	0.25 / 0.50	58.4 / 55.7	2.7 / 5.2	8 / 8	0.94
	0.25 / 0.75	58.4 / 56.9	2.7 / 1.0	8 / 6	1.0
	0.25 / 1.0	58.4 / 53.2	2.7 / 1.8	8 / 5	0.12
	0.50 / 0.75	55.7 / 56.9	5.2 / 1.0	8 / 6	1.0
	0.50 / 1.0	55.7 / 53.2	5.2 / 1.8	8 / 5	0.95
	0.75 / 1.0	56.9 / 53.2	1.0 / 1.8	6 / 5	0.72
8	0.25 / 0.50	57.9 / 53.9	2.4 / 3.1	6 / 7	0.46
	0.25 / 0.75	57.9 / 53.3	2.4 / 3.9	6 / 7	0.26
	0.50 / 0.75	53.9 / 53.3	3.1 / 3.9	7 / 7	1.0

Table S4.12. Statistical data comparing the partially oxidized alginate gels with regards to the fraction of modified alginate in the gels. The values for stress at rupture are given as the mean of the gels. Abbreviations: n = number of gels. SD = standard deviation. POA = partially oxidized alginate.

Oxidation degree (%)	Fraction of POA	Stress at rupture (N)	SD	n	p-value
2	0.25 / 0.50	35.8 / 27.3	2.5 / 4.7	7 / 7	<0.01
	0.25 / 0.75	35.8 / 25.5	2.5 / 4.7	7 / 6	<0.01
	0.25 / 1.0	35.8 / 15.1	2.5 / 5.5	7 / 5	<0.01
	0.50 / 0.75	27.3 / 25.5	4.7 / 4.7	7 / 6	1.0
	0.50 / 1.0	27.3 / 15.1	4.7 / 5.5	7 / 5	<0.01
	0.75 / 1.0	25.5 / 15.1	4.7 / 5.5	6 / 5	<0.01
4	0.25 / 0.50	26.8 / 17.3	5.5 / 6.3	8 / 8	<0.01
	0.25 / 0.75	26.8 / 14.3	5.5 / 1.8	8 / 6	<0.01
	0.25 / 1.0	26.8 / 7.3	5.5 / 0.7	8 / 5	<0.01
	0.50 / 0.75	17.3 / 14.3	6.3 / 1.8	8 / 6	0.97
	0.50 / 1.0	17.3 / 7.3	6.3 / 0.7	8 / 5	<0.01
	0.75 / 1.0	14.3 / 7.3	1.8 / 0.7	6 / 5	0.15
8	0.25 / 0.50	21.3 / 11.3	3.2 / 3.3	6 / 7	<0.01
	0.25 / 0.75	21.3 / 7.1	3.2 / 1.7	6 / 7	<0.01
	0.50 / 0.75	11.3 / 7.1	3.3 / 1.7	7 / 7	0.70

Table S4.13. Statistical data of the partially oxidized alginate gels with regards to the pure stipe alginate 1% gels. The values for Young's modulus are given as the mean of the gels. Abbreviations: n = number of gels. SD = standard deviation. POA = partially oxidized alginate. βCyD = β-cyclodextrin. POA-MeOTyr = POA grafted with L-Tyrosine methyl ester. POA-βCyD = POA grafted with β-cyclodextrin. POA-GRGDSP = POA grafted with peptide GRGDSP.

Unmodified alginate mixed with:	Fraction of modified alginate	Young's modulus (kPa)	SD	n	p-value
free βCyD	NA	30.4	2.3	9	1.0
POA-MeOTyr	0.25	21.1	2.4	10	<0.01
	0.50	15.0	2.1	10	<0.01
	0.75	7.7	0.4	10	<0.01
POA-βCyD	0.25	21.9	4.4	10	<0.01
	0.50	14.5	1.2	10	<0.01
	0.75	6.7	1.2	9	<0.01
POA-GRGDSP	0.50	14.0	0.9	8	<0.01

Table S4.14. Statistical data of the partially oxidized alginate gels with regards to the pure stipe alginate 1% gels. The values for syneresis are given as the mean of the gels. Abbreviations: n = number of gels. SD = standard deviation. POA = partially oxidized alginate. βCyD = β-cyclodextrin. POA-MeOTyr = POA grafted with L-Tyrosine methyl ester. POA-βCyD = POA grafted with β-cyclodextrin. POA-GRGDSP = POA grafted with peptide GRGDSP.

Unmodified alginate mixed with:	Fraction of modified alginate	Syneresis (%)	SD	n	p-value
free βCyD	NA	25.0	1.4	9	<0.01
POA-MeOTyr	0.25	25.4	0.5	10	<0.01
	0.50	22.9	2.6	10	<0.01
	0.75	20.9	0.8	10	<0.01
POA-βCyD	0.25	19.5	1.1	10	<0.01
	0.50	15.2	1.0	10	<0.01
	0.75	15.6	2.1	9	<0.01
POA-GRGDSP	0.50	19.0	1.8	8	<0.01

Table S4.15. Statistical data of the partially oxidized alginate gels with regards to the pure stipe alginate 1% gels. The values for deformation at rupture (compression) are given as the mean of the gels. Abbreviations: n = number of gels. SD = standard deviation. POA = partially oxidized alginate. βCyD = β-cyclodextrin. POA-MeOTyr = POA grafted with L-Tyrosine methyl ester. POA-βCyD = POA grafted with β-cyclodextrin. POA-GRGDSP = POA grafted with peptide GRGDSP.

Unmodified alginate mixed with:	Fraction of modified alginate	Deformation (%)	SD	n	p-value
free βCyD	NA	64.6	2.9	9	0.87
POA-MeOTyr	0.25	58.0	2.3	10	0.78
	0.50	61.6	6.8	10	1.0
	0.75	58.3	2.5	10	0.88
POA-βCyD	0.25	61.3	7.1	10	1.0
	0.50	54.0	1.8	10	<0.01
	0.75	48.6	3.3	9	<0.01
POA-GRGDSP	0.50	58.0	2.1	8	0.85

Table S4.16. Statistical data of the partially oxidized alginate gels with regards to the pure stipe alginate 1% gels. The values for the stress at rupture are given as the mean of the gels. Abbreviations: n = number of gels. SD = standard deviation. POA = partially oxidized alginate. βCyD = β-cyclodextrin. POA-MeOTyr = POA grafted with L-Tyrosine methyl ester. POA-βCyD = POA grafted with β-cyclodextrin. POA-GRGDSP = POA grafted with peptide GRGDSP.

Unmodified alginate mixed with:	Fraction of modified alginate	Stress at rupture (N)	SD	n	p-value
free βCyD	NA	38.4	4.9	9	1.0
POA-MeOTyr	0.25	15.8	3.6	10	<0.01
	0.50	9.9	4.6	10	<0.01
	0.75	6.9	1.9	10	<0.01
POA-βCyD	0.25	24.0	2.0	10	<0.01
	0.50	10.9	1.2	10	<0.01
	0.75	2.8	0.4	9	<0.01
POA-GRGDSP	0.50	13.0	1.8	8	<0.01

Table S4.17. Statistical data comparing the partially oxidized alginate gels with regards to the fraction of modified alginate in the gels. The values for Young's modulus are given as the mean of the gels. Abbreviations: n = number of gels. SD = standard deviation. POA = partially oxidized alginate. βCyD = β-cyclodextrin. POA-MeOTyr = POA grafted with L-Tyrosine methyl ester. POA-βCyD = POA grafted with β-cyclodextrin. POA-GRGDSP = POA grafted with peptide GRGDSP.

Fraction of modified alginate	Gel A / Gel B	Young's modulus (kPa)	SD	n	p-value
0.25	POA 0.08 / POA MeOTyr	29.3 / 21.1	1.3 / 2.4	6 / 10	<0.01
	POA 0.08 / POA βCyD	29.3 / 21.9	1.3 / 4.4	6 / 10	<0.01
	POA MeOTyr / POA βCyD	21.1 / 21.9	2.4 / 4.4	10 / 10	1.0
0.50	POA 0.08 / POA MeOTyr	23.8 / 15.0	2.4 / 2.1	8 / 10	<0.01
	POA 0.08 / POA βCyD	23.8 / 14.5	2.4 / 1.2	8 / 10	<0.01
	POA 0.08 / POA GRGDSP	23.8 / 14.0	2.4 / 0.9	8 / 8	<0.01
	POA MeOTyr / POA βCyD	15.0 / 14.5	2.1 / 1.2	10 / 10	1.0
	POA MeOTyr / POA GRGDSP	15.0 / 14.0	2.1 / 0.9	10 / 8	1.0
	POA βCyD / POA GRGDSP	14.5 / 14.0	1.2 / 0.9	10 / 8	1.0
0.75	POA 0.08 / POA MeOTyr	7.1 / 7.7	5.2 / 0.4	7 / 10	1.0
	POA 0.08 / POA βCyD	7.1 / 6.7	5.2 / 1.2	7 / 9	1.0
	POA MeOTyr / POA βCyD	7.7 / 6.7	0.4 / 1.2	10 / 9	1.0

Table S4.18. Statistical data comparing the partially oxidized alginate gels with regards to the fraction of modified alginate in the gels. The values for syneresis are given as the mean of the gels. Abbreviations: n = number of gels. SD = standard deviation. POA = partially oxidized alginate. βCyD = β-cyclodextrin. POA-MeOTyr = POA grafted with L-Tyrosine methyl ester. POA-βCyD = POA grafted with β-cyclodextrin. POA-GRGDSP = POA grafted with peptide GRGDSP.

Fraction of modified alginate	Gel A / Gel B	Syneresis (%)	SD	n	p-value
0.25	POA 0.08 / POA MeOTyr	23.0 / 25.4	0.6 / 0.5	6 / 10	0.066
	POA 0.08 / POA βCyD	23.0 / 19.5	0.6 / 1.1	6 / 10	<0.01
	POA MeOTyr / POA βCyD	25.4 / 19.5	0.5 / 1.1	10 / 10	<0.01
0.50	POA 0.08 / POA MeOTyr	15.2 / 22.9	0.8 / 2.6	8 / 10	<0.01
	POA 0.08 / POA βCyD	15.2 / 15.2	0.8 / 1.0	8 / 10	1.0
	POA 0.08 / POA GRGDSP	15.2 / 19.0	0.8 / 1.8	8 / 8	<0.01
	POA MeOTyr / POA βCyD	22.9 / 15.2	2.6 / 1.0	10 / 10	<0.01
	POA MeOTyr / POA GRGDSP	22.9 / 19.0	2.6 / 1.8	10 / 8	<0.01
	POA βCyD / POA GRGDSP	15.2 / 19.0	1.0 / 1.8	10 / 8	<0.01
0.75	POA 0.08 / POA MeOTyr	17.7 / 20.9	1.1 / 0.8	3 / 10	0.044
	POA 0.08 / POA βCyD	17.7 / 15.6	1.1 / 3.3	3 / 9	0.50
	POA MeOTyr / POA βCyD	20.9 / 15.6	0.8 / 3.3	10 / 9	<0.01

Table S4.19. Statistical data comparing the partially oxidized alginate gels with regards to the fraction of modified alginate in the gels. The values for deformation at rupture (compression) are given as the mean of the gels. Abbreviations: n = number of gels. SD = standard deviation. POA = partially oxidized alginate. βCyD = β-cyclodextrin. POA-MeOTyr = POA grafted with L-Tyrosine methyl ester. POA-βCyD = POA grafted with β-cyclodextrin. POA-GRGDSP = POA grafted with peptide GRGDSP.

Fraction of modified alginate	**Gel A / Gel B**	**Deformation (%)**	**SD**	**n**	**p-value**
0.25	POA 0.08 / POA MeOTyr	57.9 / 58.0	2.4 / 2.3	6 / 10	1.0
	POA 0.08 / POA βCyD	57.9 / 61.3	2.4 / 7.1	6 / 10	0.86
	POA MeOTyr / POA βCyD	58.0 / 61.3	2.3 / 7.1	10 / 10	0.76
0.50	POA 0.08 / POA MeOTyr	53.9 / 61.6	3.1 / 6.8	7 / 10	<0.01
	POA 0.08 / POA βCyD	53.9 / 24.0	3.1 / 1.8	7 / 10	1.0
	POA 0.08 / POA GRGDSP	53.9 / 58.0	3.1 / 2.1	7 / 8	0.65
	POA MeOTyr / POA βCyD	61.6 / 24.0	6.8 / 1.8	10 / 10	<0.01
	POA MeOTyr / POA GRGDSP	61.6 / 58.0	6.8 / 2.1	10 / 8	0.74
	POA βCyD / POA GRGDSP	24.0 / 58.0	1.8 / 2.1	10 / 8	0.54
0.75	POA 0.08 / POA MeOTyr	53.3 / 58.3	3.9 / 2.5	7 / 10	0.28
	POA 0.08 / POA βCyD	53.3 / 48.6	3.9 / 3.3	7 / 9	0.38
	POA MeOTyr / POA βCyD	58.3 / 48.6	2.5 / 3.3	10 / 9	<0.01

Table S4.20. Statistical data comparing the partially oxidized alginate gels with regards to the fraction of modified alginate in the gels. The values for stress at rupture are given as the mean of the gels. Abbreviations: n = number of gels. SD = standard deviation. POA = partially oxidized alginate. βCyD = β-cyclodextrin. POA-MeOTyr = POA grafted with L-Tyrosine methyl ester. POA-βCyD = POA grafted with β-cyclodextrin. POA-GRGDSP = POA grafted with peptide GRGDSP.

Fraction of modified alginate	**Gel A / Gel B**	**Stress at rupture (N)**	**SD**	**n**	**p-value**
0.25	POA 0.08 / POA MeOTyr	21.3 / 15.8	3.2 / 3.6	6 / 10	0.021
	POA 0.08 / POA βCyD	21.3 / 24.0	3.2 / 2.0	6 / 10	0.80
	POA MeOTyr / POA βCyD	15.8 / 24.0	3.6 / 2.0	10 / 10	<0.01
0.50	POA 0.08 / POA MeOTyr	11.3 / 9.9	3.3 / 4.6	7 / 10	1.0
	POA 0.08 / POA βCyD	11.3 / 10.9	3.3 / 1.2	7 / 10	1.0
	POA 0.08 / POA GRGDSP	11.3 / 13.0	3.3 / 1.8	7 / 8	0.99
	POA MeOTyr / POA βCyD	9.9 / 10.9	4.6 / 1.2	10 / 10	1.0
	POA MeOTyr / POA GRGDSP	9.9 / 13.0	4.6 / 1.8	10 / 8	0.52
	POA βCyD / POA GRGDSP	10.9 / 13.0	1.2 / 1.8	10 / 8	0.93
0.75	POA 0.08 / POA MeOTyr	7.1 / 6.9	1.7 / 1.9	7 / 10	1.0
	POA 0.08 / POA βCyD	7.1 / 2.8	1.7 / 0.4	7 / 9	0.14
	POA MeOTyr / POA βCyD	6.9 / 2.8	1.9 / 0.4	10 / 9	0.091

Table S4.21. Statistical data comparing the gels with epimerized POA-MeOTyr with gels containing non-epimerized POA-MeOTyr (W_{POA^*} =0.50). The values are given as the mean and standard deviation of the data for the epimerized gels. Abbreviations: n = number of gels. POA-MeOTyr = POA grafted with L-Tyrosine methyl ester.

Young's modulus (kPa)	**p-value**	**Syneresis (%)**	**p-value**	**Deformation at rupture (%)**	**p-value**	**Stress at rupture (kg)**	**p-value**
12.9 ± 3.5, n = 6	0.21	21.7 ± 1.7, n = 6	0.27	53.3 ± 1.9, n = 6	0.0039	1.2 ± 0.4, n = 6	0.54

Statistical data for the modified alginate gels are here given with regards to the Young's modulus, syneresis and compression and stress at rupture.

Paper III

Received: 20 April 2021 | Revised: 3 June 2021 | Accepted: 4 June 2021
DOI: 10.1002/jbma.a.37255

RESEARCH ARTICLE

Alginate hydrogels functionalized with β-cyclodextrin as a local paclitaxel delivery system

Line Aanerud Omtvedt | **Kåre Andre Kristiansen** | **Wenche Iren Strand** | **Finn Lillelund Aachmann** | **Berit Løkensgard Strand** | **Daria Sergeevna Zaytseva-Zotova**

NOBIPOL, Department of Biotechnology and Food Science, NTNU Norwegian University of Science and Technology, Trondheim, Norway

Correspondence
Daria Sergeevna Zaytseva-Zotova, NOBIPOL, Department of Biotechnology and Food Science, NTNU Norwegian University of Science and Technology, Trondheim, Norway.
Email: daria.zaytseva-zotova@ntnu.no

Funding information
The Research Council of Norway, Grant/Award Numbers: 221576-MARPOL, 250875-Epimerases, 269273/O70-3Dlife

Abstract

Modification of drug delivery materials with beta-cyclodextrins (β-CyD) is known to increase solubility of poorly water-soluble drugs, protect drugs from degradation and sustain release. In this study, we developed a hydrogel drug delivery system for local paclitaxel delivery using the natural polysaccharide alginate functionalized with β-CyD-moieties. Paclitaxel was chosen due to its ability to form inclusion complexes with cyclodextrins. The rheological and mechanical properties of the prepared hydrogels were characterized, as well as in vitro release of the paclitaxel and in vitro activity on PC-3 prostate cancer cells. Introduction of β-CyD-moieties into the hydrogel reduces the mechanical properties of the gels compared to nonmodified gels. However, gelation kinetics were not markedly different. Furthermore, the β-CyD-modified alginate helped to reduce undesired crystallization of the paclitaxel in the gel and facilitated paclitaxel diffusion out of the gel network. Remarkably, the β-CyD grafted alginate showed increased capacity to complex paclitaxel compared to free HPβ-CyD. Release of both paclitaxel and degradation products were measured from the gels and were shown to have cytotoxic effects on the PC-3 cells. The results indicate that functionalized alginate with β-CyDs has potential as a material for drug delivery systems.

KEYWORDS
alginate, cytotoxicity, drug delivery system, hydrogel, paclitaxel, β-cyclodextrin

1 | INTRODUCTION

Local drug delivery gives an advantage compared to systemic therapy due to increased drug concentration at delivery site, less detrimental systemic side effects, and ease of administration.[1] Local drug delivery strategies include micro- and nanocarriers, implants, and injectable depots. Injectable systems are advantageous due to their minimally invasive delivery, capacity to fill the cavity they are placed in, and ability to form a drug-loaded depot that can protect payload from enzymatic degradation and sustain drug release over a long period of time.[2] Many injectable in situ forming hydrogels have been developed, and their superior efficacy in animal models over conventional systemic therapy has been demonstrated.[3] As an example, an injectable hydrogel has been used for local delivery of paclitaxel for the treatment of glioblastoma in mice.[4] To design an efficacious hydrogel-based injectable system many parameters should be controlled, including biocompatibility, mechanical, and viscoelastic properties.[3]

Alginate, a polysaccharide found in brown algae, is an excellent candidate for an injectable hydrogel system. The polymer has the ability to form a hydrogel by crosslinking with divalent ions at physiological conditions, and the sol/gel transition is gentle enough that cells and biomolecules will be functional after entrapment in the hydrogel.[5] Furthermore, alginate can be tailored to present different functional groups[6-10] and the mechanical properties can be adjusted.[11-13] In addition, the polymer is biocompatible and nontoxic.[14] Different approaches for using alginate as an injectable delivery system are currently being investigated, often in combination with other polymers or components in the quest to achieve optimal delivery capability.[15-20]

The hydrophilic nature of the hydrogel presents certain challenges for drug delivery.[21,22] Small water-soluble molecules will often quickly diffuse out of the hydrogel matrix, giving a high burst release. On the other hand, hydrophobic molecules can be difficult to load into the hydrogel and their release in a controlled manner also possesses a challenge. To gain better control over the loading and release of therapeutic agents from a hydrogel, cyclodextrins (CyDs) can be incorporated into the gel.[23,24]

CyDs are well known cyclic structures built from glucopyranose units produced by enzymatic treatment of starch.[25] Due to the cyclic structure of the formed CyD molecules, the cavity of the ring structure is hydrophobic while the exterior is hydrophilic. The cavity can then give a local environment in the hydrogel that is better suited for entrapment of hydrophobic molecules and moieties.[24,26,27]

Paclitaxel is a highly hydrophobic anticancer drug that can form inclusion complexes with CyDs, including β-CyD.[28,29] It should be noted however that paclitaxel has a limited penetration into the hydrophobic cavity of β-CyD and the obtained inclusion complex is characterized by a low binding constant.[29,30] Given intravenously, paclitaxel is not specifically targeted to the tumor, and thus only low therapeutic levels of the drug can be achieved at the tumor site.[31,32] Moreover, paclitaxel has been shown to have poor penetration across the blood–brain-barrier in preclinical models.[31,33] Hence, paclitaxel use in treatment of brain tumors and brain metastases is limited, although it was shown to be active against various tumor types.[33] Interestingly, it has been shown recently that in addition to the antiproliferative activity, paclitaxel has a capacity to promote antitumor immunity.[34] This makes paclitaxel a very promising candidate for drug delivery systems. To enhance the therapeutic potential of paclitaxel several delivery strategies and formulations of paclitaxel have been developed,[35,36] including only a few injectable hydrogel systems based on alginate.[37,38]

CyDs have previously been grafted to alginate by attachment to the carboxyl- or OH-group,[39-46] often for drug delivery applications. Examples include photoresponsive CyD-grafted alginate hydrogels where UV-light can be used to control the inclusion complex between CyDs and azobenzene moieties, giving control over gel morphology and subsequent release from the gel,[39] release of the antiemetic drug ondansetron by mechanical stimulation of a cyclodextrin-crosslinked alginate gel,[41] and release of the poorly soluble anti-inflammatory agent hydrocortisone acetate from β-CyD grafted alginate hydrogels.[43]

We have recently shown that functionalization of alginate hydrogels with β-CyD moieties allows to slow down the release rate of a small model compound methyl orange.[9] Based on this finding, we hypothesized that with the β-CyD-grafted alginate, it might be possible to modulate the release of paclitaxel. While numerous studies have investigated the entrapment of paclitaxel in hydrogel systems, to the best of our knowledge, this study for the first time describes a paclitaxel delivery system based on alginate hydrogels functionalized with β-CyDs. In this study, we focused on, first, the development of an injectable hydrogel system and characterized it with respect to rheological and mechanical properties. Second, in vitro release of the paclitaxel and in vitro cytotoxicity toward PC-3 prostate cancer cells was studied.

2 | MATERIAL AND METHODS

2.1 | Materials

Alginate (Alg) from *Laminaria hyperborea* stipe ($F_G = 0.7$, $N_{G>1} = 11$, $\bar{M}_w = 126\,\text{kDa}$) was obtained from FMC Health and Nutrition, Sandvika, Norway. For cell studies, ultrapure stipe alginate from Novamatrix™, Norway (UPLVG, $F_G = 0.67$, $N_{G>1} = 13$, $\bar{M}_w = 221\,\text{kDa}$) was used. 6-monoazido-6-monodeoxy-β-cyclodextrin was kindly provided from Aalborg University.[47] The oxidized and grafted alginate materials were made in-house from stipe alginate and ultrapure stipe alginate at NTNU as previously described.[9] The following materials were synthesized for this work: partially oxidized alginate (POA, $P_O = 8\%$, $\bar{M}_w = 102\,\text{kDa}$), POA grafted with β-CyD (POAβCyD, DS = 3.7% mol CyD/mol monomer, $\bar{M}_w = 55\,\text{kDa}$). For the cell studies, POA ($\bar{M}_w = 127\,\text{kDa}$) and POAβCyD (DS = 3.4% (mol/mol), $\bar{M}_w = 61\,\text{kDa}$) were produced from UPLVG. Hydroxypropyl-β-cyclodextrin (HPβ-CyD, CAVASOL® W7 HP) and β-CyD (CAVAMAX® W7) were obtained from Wacker Chemie AG (Burghausen, Germany). Physiological buffer was made according to literature,[48] without bovine serum albumin. High glucose Dulbecco's Modified Eagle Medium without sodium pyruvate (DMEM), fetal bovine serum (FBS), penicillin–streptomycin solution, phosphate buffered saline pH 7.4 (PBS), 0.25% Trypsin–EDTA solution were from Sigma-Aldrich. AlamarBlue™ cell viability reagent was from Invitrogen. All the other chemicals used were obtained from commercial sources and were analytical or high-performance liquid chromatography (HPLC) grade and were used without further purification.

2.2 | Methods

2.2.1 | Preparation of hydrogels

The calcium alginate hydrogels were prepared (with different ratios of unmodified alginate mixed with modified alginates) by internal gelation by mixing alginate solution, $CaCO_3$ ($d = 4\ \mu\text{m}$) and the slowly hydrolyzing glucono-δ-lactone (GDL, freshly prepared), as previously reported.[49] After addition of the $CaCO_3$ alginate solutions were degassed to prevent air bubbles in the hydrogel. The final concentration of components in the gelling solution was 1% (w/v) alginate, 15 mM $CaCO_3$, and 30 mM GDL. The hydrogels for the cell studies were made differently as described in the methods section detailing the cell experiments.

2.2.2 | Gelation kinetics

In addition to testing a stipe alginate sample (Alg), a 1:1 (w/w) mixture of the stipe alginate and POA (Alg/POA [1:1]) were tested. Within 3 min after dissolution of GDL (at time point zero), an aliquot of the sample was applied onto the lower plate and gelation was followed by Kinexus Rheometer (Malvern instruments, Uppsala, Sweden) using a 2 cm flat probe and a flat plate geometry with 0.1 mm gap, 0.005 strain, and 0.5 Hz frequency. The gelation kinetics was determined by repeated measurement of storage modulus G', loss modulus G'', and phase angle δ at 1-min intervals within the first 20 min and at 5 min intervals for approximately 5 hr. At least two repetitions were done for each sample.

2.2.3 | Syneresis and compression measurements

Young's modulus, stress at rupture, deformation at rupture and syneresis of the Alg, Alg/POA (1:1), a 1:3 (w/w) mixture of the stipe alginate and POA (Alg/POA [1:3]), and a 1:1 (w/w) mixture of the stipe alginate and POAβCyD (Alg/POAβCyD (1:1)) samples were assessed. Additionally, since the molecular weight of monomers with attached CyDs is higher than for ungrafted monomers, we evaluated a 1:0.8 (w/w) mixture of the stipe alginate and POA (Alg/POA [1:0.8]) sample which contained the same molar amount of alginate units as a Alg/POAβCyD (1:1) sample. Hereafter, a freshly made GDL solution was added to the alginate mixture to initiate gelation, the mixture was immediately aliquoted into silicone forms (1.5 mL/well) and left to mature for 1 day. The next day gel cylinders were carefully wiped down to remove separated water and mass measured. Syneresis was determined as $100 \times (W_0 - W)/W_0$, where W_0 and W are initial and final weights of the cylinders, respectively. Diameter and height of the cylinders were measured with digital calipers prior to compression measurements. The response of the gels to uniaxial compression was evaluated using a Stable Micro Systems TA-XT2 texture analyzer equipped with a P/35 probe, 5 kg pressure capacity load cell, and at a compression rate of 0.1 mm/s and 1 g trigger force. The stress deformation curves were recorded at room temperature.[50] Young's modulus (Pa) was calculated as $G \times (h/A)$, where G is the initial slope (N/m) of the curve, h is the height of the cylinder (m), and A is the area (m^2) of the cylinder. At least four cylinders of each gel type were measured.

2.2.4 | Release studies of paclitaxel from Ca-alginate gels into physiological buffer

The alginate hydrogels were loaded with 25 μM paclitaxel and release of paclitaxel was studied in the physiological buffer. Five different 1% (w/v) alginate solutions were prepared for gelation: Alg, Alg/POAβCyD (1:1) containing 0.8 mM β-CyD residues, Alg/POAβCyD (1:3) containing 1.1 mM β-CyD residues, Alg + free β-CyD (0.9 mM β-CyD), and Alg + free HPβ-CyD (7.2 mM HPβ-CyD). The solutions were divided into 1.5 mL polypropylene tubes. Paclitaxel dissolved in ethanol was mixed into the solutions to a final concentration of 25 μM paclitaxel, 2.5% (v/v) ethanol, and an end volume of 200 μL of gel (paclitaxel was added after mixing the solution with $CaCO_3$ and degassing but before adding GDL). Three parallels of each sample were made. Samples were left to gel at room temperature for 23 hr (day 0). Physiological buffer of 300 μL was then added, and gels were incubated at 37°C.

After 1, 3, 6, 9, 15, and 21 days, 200 μL supernatant was removed and pictures of the gels were taken with light microscopy (40× magnification). Thereafter, 200 μL fresh physiological buffer was again added to the gel-vials. The 200 μL supernatant was diluted in acetonitrile (1:1). Internal standard docetaxel in the samples was 5 μM. Gels were weighed and dissolved in 400 μL EDTA (100 mM) overnight after sample collection at day 21. The dissolved gels were then diluted with acetonitrile (1:1 the weight of the gels was taken into account), and internal standard docetaxel was added to a final concentration of 5 μM. All samples were stored at −20°C. Samples were thawed and centrifuged for 15 min at 23,000×*g* before analyzed with ultra-high performance liquid chromatography coupled to tandem quadrupole mass spectrometry using an ACQUITY I-class UPLC system coupled to a Xevo TQ-S triple quadrupole mass spectrometer (Waters, Milford, MA) (Appendix S1).

2.2.5 | Stability of paclitaxel

For the stability studies, 195 μL physiological buffer was mixed with 5 μL paclitaxel dissolved in ethanol (375 μM). This gave 9.4 μM paclitaxel aqueous solutions with 2.5% (v/v) ethanol as a starting point. This was done to mimic the making of the hydrogels were 195 μL was water containing alginate and gelling components, while 5 μL of paclitaxel dissolved in ethanol was mixed in to give a final volume of 200 μL. physiological buffer or water was used as the aqueous medium and left at 37°C for 0, 1, 3, 6, 9, 15, or 21 days. Samples were then diluted 1:1 with acetonitrile and stored in freezer. Samples with physiological buffer were then centrifuged (15 min 23,000×*g*), and the supernatant analyzed with liquid chromatography coupled to tandem quadrupole mass spectrometry (Appendix S1). Samples with water were directly analyzed without further sample preparation.

2.2.6 | Cell line and subculture

PC-3 human prostate carcinoma cell line (ATCC® CRL-1435™) was chosen as a model cells for in vitro studies. Cells were cultured in the DMEM supplemented with 10% FBS and 1% (v/v) penicillin–streptomycin at 37°C and 5% CO_2, 95% air, and complete humidity. Cells were maintained in exponential growth phase until they were detached by trypsin–EDTA solution, counted, and seeded into experimental plates/flasks.

2.2.7 | Cytotoxicity of β-CyD-grafted alginate

The test solutions of 40 mg/mL of POAβCyD and the solution of free β-CyD (13.2 mM) in 40 mg/mL POA were prepared in PBS supplemented with 1 mM $CaCl_2$ and 0.5 mM $MgCl_2$ and sterilized through 0.2 μm syringe PES filters prior use. Nine 1:1 serial dilutions of the solutions were then made in 40 mg/mL POA to ensure equal concentration of alginate in all tested solutions after serial dilutions.

PC-3 cells were seeded in a concentration of 5×10^5 cells into each well of 96-well clear bottom TC-treated black plates (100 μL/well) and incubated at 37°C overnight. After 24 hr, old medium was replaced with 50 μL/well of nine 1:1 serial dilutions of the test solutions. PC-3 cells were incubated with the test solutions for 2 hr, after which the plates were centrifuged at 150×*g* for 5 min. Then, the tested solutions were carefully aspirated and 100 μL of fresh culture medium was added. The plates were incubated for additional 48 hr and cell metabolic activity was assessed using resazurin assay. Maximal tested concentrations were 13.2 mM of free β-CyD and 40 mg/mL of POAβCyD (5.65 mM of β-CyD-moieties). The 40 mg/mL POA a solution was used as a control. All the samples and controls were run in four replicates.

2.2.8 | Hydrogels for cell studies

Hydrogels based on ultrapure Alg and on Alg/POAβCyD (1:1) were prepared for cell studies under sterile conditions. Hydrogels contained 2% (w/v) alginate, 30 mM $CaCO_3$, 60 mM GDL, and paclitaxel. Ultrapure alginate solutions and GDL solutions were sterilized through 0.2 μm syringe PES filters. $CaCO_3$ particles (0.7 μm) were autoclaved at 121°C for 30 min and then suspended in a sterile deionized water. Paclitaxel was pre-dissolved in ethanol. For burst release studies, hydrogels ($V = 200$ μL) were loaded with 25 μM paclitaxel. For the cytotoxicity studies, hydrogels ($V = 50$ μL) were loaded with 0, 0.9, 7.2, and 25 μM paclitaxel. After fabrication, the gels were left to gel at 4°C for at least 1 day.

2.2.9 | Burst release in culture medium

PC-3 cells were seeded in a concentration of 3200 cells/well into 96-well plates (50 μL/well) and incubated at 37°C overnight. Next day, the 200 μL gels containing 25 μM paclitaxel were incubated with 300 μL of DMEM supplemented with 10% FBS at 37°C for 1 hr. After 1 hr, the medium was aspirated, diluted (six 1:1 serial dilutions), and added to the PC-3 cells (50 μL/well). After 72 hr, PC-3 cells metabolic activity was assessed using resazurin assay. The obtained values of cell metabolic activity were used to determine concentration of the released drug. To generate a standard curve, 0–200 nM paclitaxel solutions in media were used (Figure A1, Supporting Information S1). All the samples and controls were run in triplicates.

2.2.10 | Cytotoxicity of paclitaxel-loaded hydrogels

PC-3 cells were seeded in a concentration of 1×10^5 cells into each well of 6-well plates (3 mL/well) and incubated at 37°C. After 24 hr, 1.45 mL of fresh medium and 50 μL hydrogels (or free paclitaxel solution) were added into each well of PC-3 seeded plates, and plates were incubated at 37°C for 72 hr. After 72 hr, cell metabolic activity was assessed using resazurin assay. Hydrogels contained 0, 0.9, and 7.2 μM of paclitaxel. Free paclitaxel (final concentrations in the plate were 1, 5, 10, 40, and 80 nM) was used as a positive control. Drug-free medium and the hydrogel without the drug were used as negative controls. All the samples and controls were run in triplicate. Gels were examined by optical microscopy before and after experiment.

For the gels loaded with 25 μM paclitaxel, 300 cm^2 tissue culture treated flasks were used and the total (volume of medium was increased up to 125 mL). PC-3 cells were seeded in a concentration of 3×10^6 cells into 300 cm^2 tissue culture treated flasks (50 mL/flask) and incubated at 37°C overnight. Next day, 75 mL of fresh medium and 50 μL of gels loaded with 25 μM paclitaxel were added into the flasks. Cells were incubated with gels at 37°C for 72 hr and cell metabolic activity was assessed using resazurin assay. Drug-free medium was used as a negative control. All the samples and controls were run in triplicates. Gels were examined by optical microscopy before and after experiment.

2.2.11 | Resazurin cell metabolic activity assay

Cells were incubated with 50% diluted AlamarBlue™ reagent at 37°C for 1–8 hr, as it is recommended by a supplier. Then, 100 μL aliquots were transferred into black 96-well plates with clear bottom and fluorescence was read with Spectra Max i3x (Molecular Devices) at 560 nm excitation and 600 nm emission wavelengths. Cell metabolic activity was expressed as percentage of fluorescent intensities relative to a control (cells not exposed to paclitaxel were defined as 100%) after subtraction of non-cell-derived background.

2.2.12 | Statistical analysis

Statistical analysis was performed using Microsoft Office Excel 365 or SigmaPlot Version 14.0 (Systat Software Inc., CA) and differences between groups were compared applying a two-tailed *t*-test. The significance level was set at 0.05. Differences between more than two groups were tested using one-way (or two-way when necessary) analysis of variance (ANOVA). After ANOVA, the Tukey's post hoc test or a two-tailed *t*-test was used for comparison. All results are expressed as means ± *SD*.

3 | RESULTS AND DISCUSSION

We have previously shown that CyDs grafted to alginate were able to interact with the model compound methyl orange, a small guest molecule that can form inclusion complexes with β-CyD.[9] This new study relies on the hypothesis that introduction of β-CyD moieties into alginate mediates the uptake of highly hydrophobic drugs like paclitaxel and their release from the alginate hydrogel. For this study the alginate was functionalized with β-CyD moieties in a three-step synthesis as previously described.[9] The partial oxidation of alginate performed in the first step is known to lead to noticeable structural changes, such as partial depolymerization and ring opening (cleavage of the C2–C3 bonds).[11,51-53] Such changes in the alginate structure have been shown to affect the gelation capability of the polymer and mechanical properties of the hydrogels fabricated from this polymer.[11,12,40,54] Therefore, we conducted a series of experiments to characterize gelation kinetics and mechanical properties of the hydrogel system based on the modified alginate.

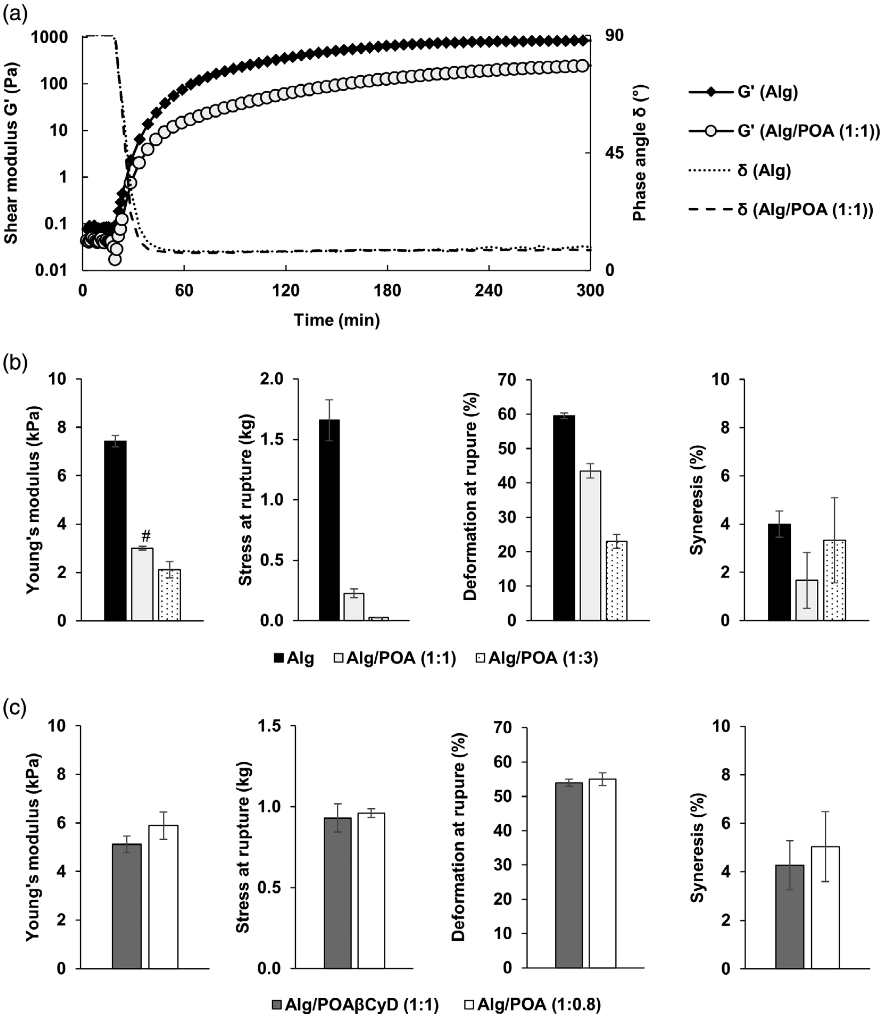

FIGURE 1 Gelation kinetics and mechanical properties of the 1% (w/v) calcium-unsaturated alginate hydrogels. (a) Gelation kinetics of Alg and Alg/POA (mean, $n = 3$). Young's modulus, rupture strength, deformation at rupture and syneresis of the Alg and Alg/POA hydrogels: (b) Effect of 1:1 and 1:3 (w/w) mix of Alg/POA on properties of the hydrogels (mean ± *SD*, $n = 4$–8); (c) Comparison of the mixed hydrogels containing equal number of unmodified alginate monomers (mean ± *SD*, $n = 4$–8). #—it was not possible to measure dimensions of the gels due to extreme softness of the Alg:POA (1:3) mixed gels, therefore theoretical area of the cylinders was used to calculate Young's modulus

3.1 | Gelation kinetics and mechanical properties of Ca-alginate hydrogels

The well-established system of alginate gelation, using slowly releasing calcium ions from $CaCO_3$ particles induced by the slow release of H^+ from GDL, was used to allow for slow gelation of alginate.[55] Using this technique, it is possible to make soft alginate gels with homogeneous and reproducible structure at physiological conditions, while the end products of the reaction, namely CO_2 and D-glucuronic acid, are nontoxic.[49] Importantly, this method allows to have control over gelation kinetics of alginate by varying the release rate of calcium ions from the calcium carbonate particles. The size of $CaCO_3$ particles have previously been shown to largely influence the gelation kinetics.[49] For an injectable hydrogel, the gelation time will influence how easy it is to inject the gel, as well as its propensity to gel at the injection site instead of leakage before the gel network can form.[56,57]

The rate of gelation was followed by oscillation rheometry showing similar values for the sol–gel transition time for the gels with stipe alginate only (Alg) and in 1:1 w/w mix with oxidized alginate (Alg/POA (1:1)) (25.1 ± 2.8 min and 24.3 ± 2.4 min, respectively) (Figure 1a). Hence the gelation kinetics seems not to be influenced when mixing in the modified alginate. The sol–gel transition time in the studied conditions was about 25 min, but it can be significantly extended/reduced by minor modification of the gelling solution composition to fulfill time-requirements for systemic administration. As expected, the storage modulus (G'_{max}) of the Alg/POA (1:1) mixed gel was significantly lower than for the Alg hydrogels: 266 ± 17 Pa for (1:1) mixture and 875 ± 108 Pa for the unmodified alginate. The pronounced difference in storage modulus reflects the reduced capacity of the oxidized material to form ionic crosslinks which has also been shown previously, where the storage modulus was measured for 12 hr.[12]

To further investigate the mechanical properties of the formed gels, the gels were cast in cylinders and mechanical properties investigated by compression measurements (Figure 1b). The Ca-unsaturated hydrogels casted from Alg maintained their shape upon handling, whereas introduction of POA resulted in softer and weaker gels. Gel elasticity (Young's elastic modulus), deformation and stress at rupture, as well as volume reduction upon gel formation (syneresis) of the formed hydrogels were measured in a series of compression tests. Increase in POA content showed a clear trend toward weaker hydrogels with lower Young's modulus, stress at rupture, deformation at rupture, and syneresis compared to the gels made from unmodified alginate alone. This trend was previously also observed for the same type of mixed Alg/POA gels for Ca-saturated hydrogels.[12] To see if introduction of β-CyD would influence the mechanical properties relative to the oxidized sample, two samples containing equal molar ratio of uronic acid residues between stipe alginate and modified alginates (POA or POAβCyD) were prepared (Figure 1c). Mechanical properties of Alg/POAβCyD (1:1) gels ($E = 5.1$ kPa, stress at rupture = 0.93 kg) were not significantly different from the Alg/POA (1:0.8) gels ($E = 5.9$ kPa, stress at rupture = 0.96 kg), indicating that introduction of linker and β-CyD moieties onto POA did not significantly change gel-forming properties of the material for the Ca-unsaturated hydrogels. When comparing the Alg/POAβCyD (1:1) gels with the Alg/POA (1:1) gels ($E = 3$ kPa, stress at rupture = 0.23 kg), the stress needed to rupture the Alg/POA gels were lower compared to the grafted gels. The opposite is observed for Ca-saturated gels[12] where Young's modulus decreased for Alg/POAβCyD gels (1:1, ~15 kPa) compared to Alg/POA gels (1:1, 24 kPa), while the stress at rupture was approximately the same (~1 kg). This was also observed for mixed hydrogels grafted with other substituents than β-CyD. This indicates that for Ca-unsaturated gels Young's modulus for mixed Alg/POAβCyD gels is not largely affected by grafting, but for Ca-saturated gels the covalent coupling of β-CyD affects the network formation/rearrangement due to steric effects, and may hinder optimal interaction with Ca-ions for the crosslinking units of the alginate.

3.2 | Loading of paclitaxel into alginate gels

To load paclitaxel into alginate hydrogels, the drug was solubilized in ethanol and mixed with alginate solution before gelation was initiated. All the loaded drugs were maintained within the gel, hence, the final concentration of paclitaxel in the gels was 25 μM. The strategy of internal gelation was chosen as this has been shown to give homogeneous distribution of polymer in the gels.[49] Similarly, it was assumed that homogenous distribution of paclitaxel within the gels would also be achieved in addition to facilitate formation of inclusion complexes between the drug and POAβCyD. Here, precipitation of paclitaxel was utilized as an indirect indicator of inclusion complex formation.

Crystallization of paclitaxel is known to occur in both aqueous solution and hydrogels[58] and was clearly observed in the alginate gels (Figure 2). The Alg/POAβCyD (1:1) and Alg/POAβCyD (1:3) hydrogels loaded with 25 μM of paclitaxel showed variable crystallization of the drug (Figures 2 and A2, Supporting Information S1): Paclitaxel crystals were present in the 1:1 hydrogels, whereas very little crystal formation was observed for the 1:3 gels. The resulted paclitaxel:β-CyD molar ratios were 0.03 and 0.02 for 1:1 and 1:3 gels, respectively. This indicates that a paclitaxel:β-CyD molar ratio of 0.02 or lower should be used to prevent paclitaxel crystallization in the alginate hydrogels. Crystals of paclitaxel were also present in the gels mixed with free β-CyD (0.9 mM) and also HPβ-CyD (7.2 mM) (Figure 2) where the drug:cyclodextrin molar ratios were 0.03 and 0.004, respectively. Interestingly, although drug:cyclodextrin molar ratio in HPβ-CyD sample was 10 times lower than in the Alg/POAβCyD (1:3) hydrogels, more crystallization was observed in the gels containing HPβ-CyD. This could indicate that the nongrafted CyDs are showing limited usefulness in helping dissolve the paclitaxel in the studied conditions or may have inferior inclusion complex ability with paclitaxel compared to POAβCyD. This is surprising, in particular for HPβ-CyD which was chosen due to its higher water solubility compared to β-CyD, as well as its more frequent use in pharmaceutics due to it being suitable for parenteral injection.[59] The phenomenon of the increase in complexation ability of β-CyD upon grafting has been also observed for β-CyD-grafted hyaluronic acid.[60] Authors reported paclitaxel:cyclodextrin

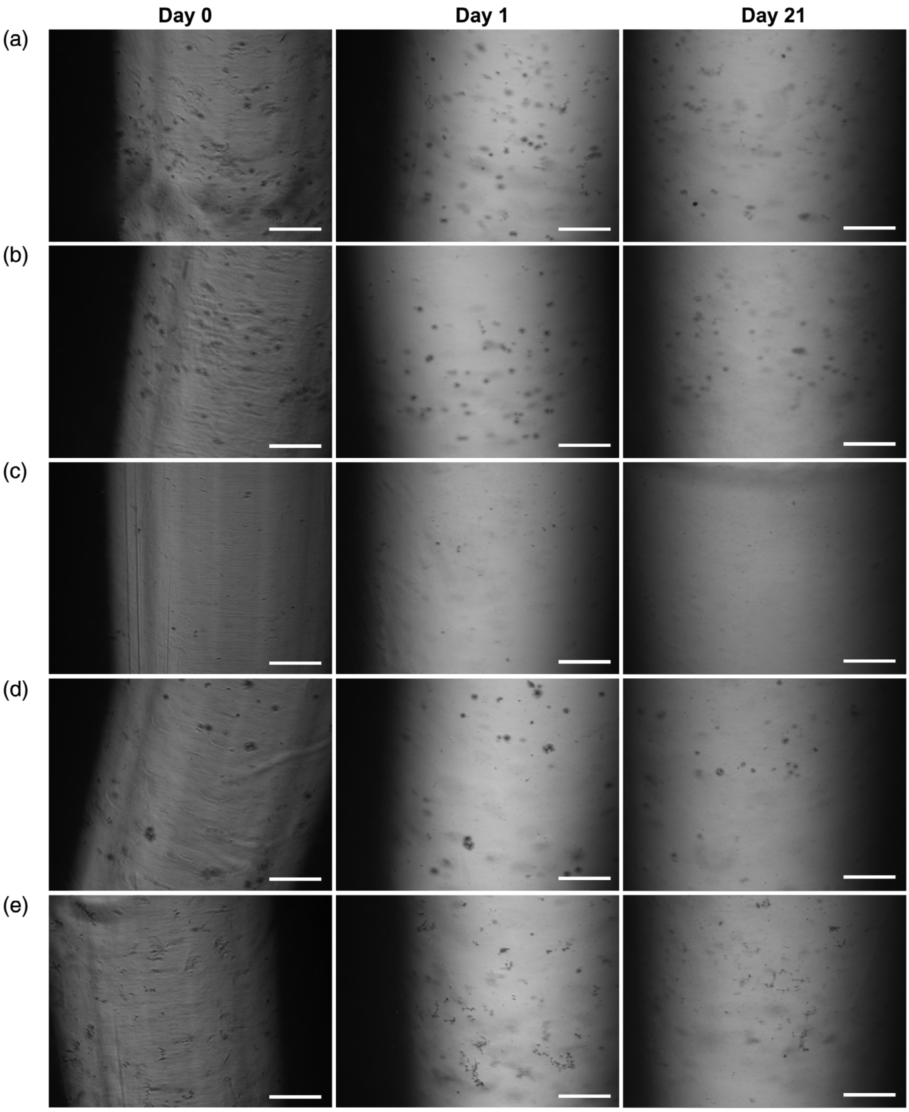

FIGURE 2 Paclitaxel crystals in alginate hydrogels loaded with 25 μM paclitaxel. Hydrogels shown at days 0 (1 day after gelation), 1 and 21. (a) Alg. (b) Alg/POAβCyD (1:1 (w/w), 0.8 mM β-CyD moieties). (c) Alg/POAβCyD (1:3 (w/w), 1.1 mM β-CyD moieties). (d) Alg + β-CyD (0.9 mM β-CyD). (e) Alg + HPβ-CyD (7.2 mM HPβ-CyD). Scale bar 500 μm

molar ratios of 0.011, 0.00026, and 0.007 for the hyaluronic acid grafted β-CyD, β-CyD, and dimethyl-β-CyD, respectively.

The paclitaxel crystals have been reported to be stable in aqueous environment up to 2 months and are seen as a limitation for achieving a therapeutic effect from the drug.[58] Therefore, the presence of crystals is not desirable, especially for controlled drug release systems. Here, paclitaxel crystals could be observed in the gels after 21 days after exposure to physiological buffer with same observations of the different gels as mentioned above (Figure 2).

3.3 | Release of paclitaxel from alginate gels

The ability of the developed hydrogel system to release paclitaxel was studied in vitro in the physiological buffer (Figure 3). Paclitaxel concentration was measured based on a standard curve of paclitaxel dissolved in extraction solvent, however the presence of paclitaxel degradation products (7-epi-taxol, 10-deacetyltaxol, and baccatin III) in the release samples was obvious throughout the time of the experiment (21 days) and was measured as areas due to lack of standards. In the experiment, 200 μL of 300 μL medium was removed at each time point and analyzed, and 200 μL new medium added. This means that measured paclitaxel and degradation products from day 3 to 21 also includes remains from previous time points, hence a mix of newly and previously released drug.

After 1 day, the concentration of paclitaxel (Figure 3a) found in physiological buffer was much lower for the samples containing β-CyD-grafted polymer (328–333 nM) than the concentration observed for Alg and Alg + HPβ-CyD samples (756 and 665 nM, respectively) and was comparable with the sample Alg + β-CyD, which contained free β-CyD (315 nM). When looking at the degradation products (Figure 3b–d), a slight increase could be seen for the Alg/POAβCyD (1:3) sample relative to the Alg gels. For baccatin III (Figure 3d) both grafted samples generally showed higher areas of this degradation product compared to Alg samples. The Alg/POAβCyD (1:3) gels showed significantly higher areas of baccatin III compared to Alg sample at days 6, 9, and 15 (p value less than 0.01 for all samples, $n = 3$). This could indicate that the grafted alginate influences the release and/or degradation of the paclitaxel. For the degradation products, no accurate quantification can be made due to the lack of standards, however, it can be seen that 7-epi-taxol largely follows the release of paclitaxel, whereas 10-deacetyltaxol and baccatin III show higher amounts at the early timepoints (day 1–6) relative to later (day 9–21). Interestingly, it has been shown previously that the epimer 7-epi-taxol still shows anti-cancer properties.[61]

At day 1, Alg and Alg + HPβ-CyD showed higher concentrations of paclitaxel in physiological buffer than other gels. For Alg samples, the observed increase cannot be explained by higher initial release from this sample, because the areas of the degradation products did not increase accordingly, and vice versa, they were not significantly different from those for Alg/POAβCyD (1:1) and Alg/POAβCyD (1:3) samples. The similar increase in paclitaxel concentration at day 1 was observed in one of the control samples that contained POA instead of grafted material (Alg/POA (1:3)) (Figure A3, Supporting Information S1).

For the Alg + HPβ-CyD sample more degradation products were found at day 1–6 compared to the other samples, indicating faster release of paclitaxel in presence of free HPβ-CyD compared to the

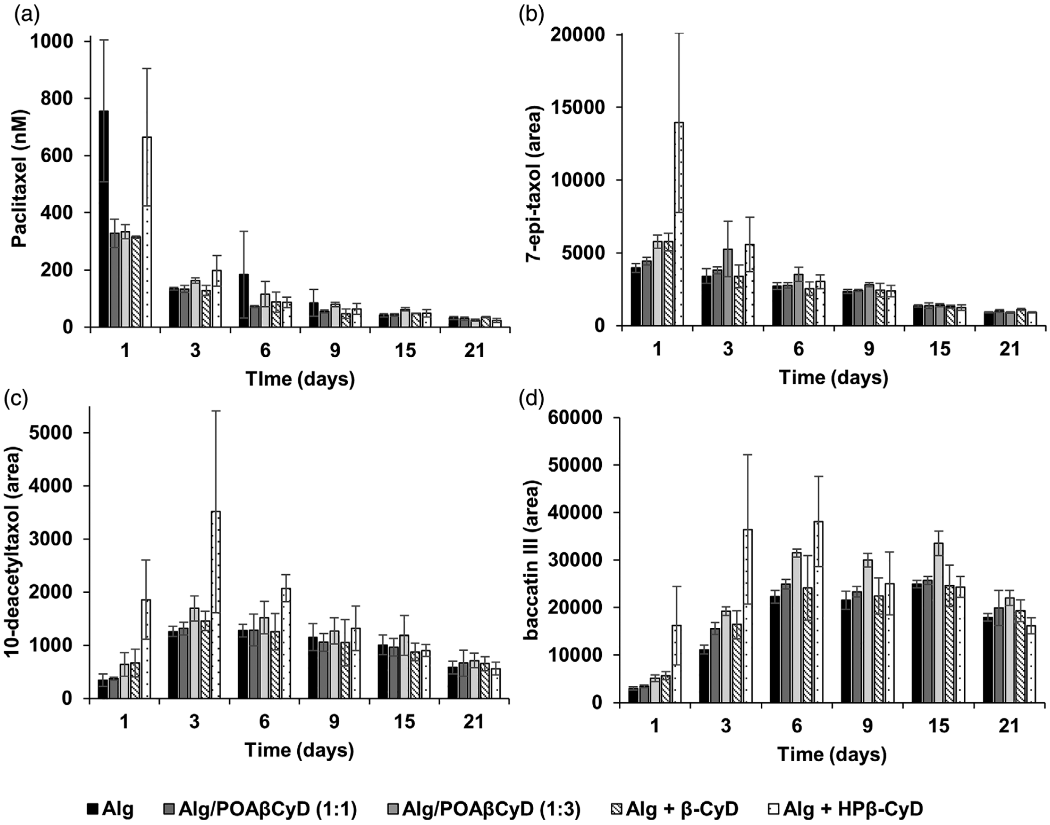

FIGURE 3 Drug release from hydrogels into physiological buffer at 37°C for 21 days. (a) Concentration of paclitaxel in release medium. (b,c) Integrals of the paclitaxel degradation products found in release medium: (b) 7-epi-taxol, (c) 10-deacetylytaxol, and (d) baccatin III. Mean ± SD, $n = 3$

other samples. Furthermore, the release of paclitaxel from Alg + HPβ-CyD was much higher compared to the gels containing free β-CyD. There are several important factors to consider here: higher concentration of HPβ-CyD than that of β-CyD (7.2 vs. 0.9 mM, respectively) and higher water solubility of HPβ-CyD (>860 mM compared to 16 mM for β-CyD).[62] It was therefore expected to be easier for HPβ-CyD to transport paclitaxel out of the gel *via* diffusion compared to the β-CyD.

At the end of the release study, the remaining paclitaxel in the gels were measured (Figure 4). All samples contained unreleased paclitaxel, with more in the Alg gels compared to grafted gels. Looking at the average values, about 5% of the loaded drug was found in the Alg/POAβCyD (1:3) hydrogels, about 18% in the Alg/POAβCyD (1:1) hydrogel and about 24% in the Alg hydrogel. For the degradation products found in these gels, only baccatin III and 10-deacetyltaxol were found in the Alg gels whereas also 7-epi-taxol was found in the Alg/POAβCyD gels (Figure A4, Supporting Information S1).

For the Alg gels mixed with free β-CyD or HPβ-CyD, the variation in the amount of remaining paclitaxel in the gels was very large, compared to the other gels. This may reflect differences in the release of free CyD from the gels and hence drug released or potential differences in initial crystallization (Figure A2, Supporting Information S1). On average, the paclitaxel remaining in the Alg gels with free β-CyD was higher (20%) than in the Alg gels with free HPβ-CyD (9%), which again indicates faster release from the gels in presence of free HPβ-CyD and agrees with the observations made in the release study. In these gels, baccatin III, 10-deacetyltaxol, and 7-epi-taxol were also found at day 21 (Figure A4, Supporting Information S1).

Taken together, our results indicate that more paclitaxel is solubilized in the gels with grafted alginate (Figure 2), and more is released over time, relative to nongrafted alginate and alginate gels with free β-CyD (Figures 3 and 4). In total, 82–95% of the paclitaxel was released into physiological buffer and/or underwent degradation at day 21 for the grafted material (Figure 4). Inclusion complexes between β-CyDs and paclitaxel are characterized by low association constants as paclitaxel molecules have a limited penetration into the hydrophobic cavity of cyclodextrin.[29,30] On the other hand, one can expect faster release rate of paclitaxel in presence of β-CyDs. Indeed, paclitaxel in vitro release from the different drug delivery systems functionalized with β-CyD moieties has been reported to be 30–100% during the first 24 hr.[60,63,64]

Other factors that may influence the release of paclitaxel from the gels could be different mechanical properties of the gels with different concentration of the grafted material (see the Section 3.1). The gels in which POAβCyD is substituted with POA can be considered as a good control for mechanical properties of the gels. For the Alg/POA (1:3), which also showed high concentrations of both paclitaxel and degradation products in physiological buffer, concentration of the remaining drug was found to be ~11%, whereas more drug (~ 26%) was found in the stiffer Alg/POA (1:1) gel (Figure A5, Supporting Information S1). Stiffer gels are recognized by a higher crosslinking density, that could influence both degradation of the gels[12] as well as gel permeability. Although no direct degradation of the gels was measured in this study, differences in stability were observed as the grafted alginate samples were more difficult to handle than the nonmodified samples. Also, slight decrease in gels weight was found at day 21 (Figure A6, Supporting Information S1). The permeability of the gels in this study is not known, although one may speculate that lower crosslinking density will lead to more permeable gels. However, for Ca-saturated alginate gels, the opposite is found, as alginates with a low content of guluronic acid were shown to be less permeable to, for example, albumin, than alginate with a higher content of guluronic acid and thus higher crosslinking density.[65] The alginate gel network as such is not expected to influence the release of paclitaxel, as Ca-saturated alginate hydrogels are open for diffusion for larger molecules such as antibodies (IgG, 150 kDa).[13] Hence, paclitaxel, as a nonpolar and small molecule (854 Da), is expected to readily diffuse through the alginate hydrogels. However, differences in release could also be caused by differences in the drug loading procedure (see the discussion above). The crystallization of paclitaxel must also be considered. For a system containing only paclitaxel dissolved in aqueous medium (no gel), only very little of the free drug (less than 10%) has

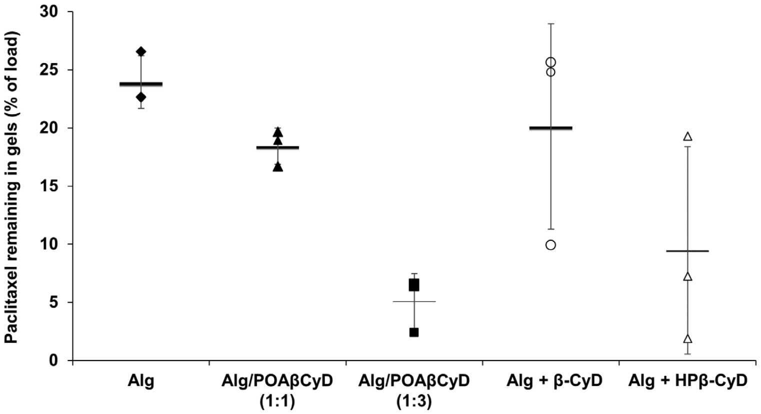

FIGURE 4 Paclitaxel remaining in the alginate hydrogels after being exposed to physiological buffer for 21 days. Values show amount of paclitaxel found in dissolved gels relative to the amount of the paclitaxel loaded into the hydrogels. Mean ± *SD*, *n* = 3

been shown to be released within 10 days in PBS pH 7.4, which is likely due to the low solubilization/crystallization of paclitaxel in water.[66]

It should also be noted that the release study was not conducted under sink conditions. The release medium used for drug release studies should ideally obtain sink conditions, that is to say the volume of the medium should be three times higher than the volume required to solubilize the drug to ensure free diffusion out of the drug delivery system.[67,68] The solubility of paclitaxel in physiological buffer has not been tested in this study. But one could expect that paclitaxel solubility in physiological buffer is comparable to the solubility in PBS buffer, which is reported[67] to be within the range of 0.3–10 μg/mL (0.35–12 μM) at 37°C. If all the paclitaxel releases at once from the tested hydrogel, the concentration in physiological buffer will reach 10 μM, which corresponds to the reported solubility limit. However, the release media used in our study also contained traces of ethanol (below 1% (v/v) from the gels), which increases the solubility of paclitaxel.

As degradation of paclitaxel seemed to be a major issue in determining release from the gels, stability studies of paclitaxel were performed in the physiological buffer and water for comparison (Figure 5). At day 1, about 90% of the paclitaxel was found in both water and physiological buffer. Thereafter, the degradation was especially prevalent in the physiological buffer where only 33%, 11%, and 2% of the initial concentration could be found after 3, 9, and 15 days, respectively. In water, about 80% of the paclitaxel remained in the solution after 3 days and to the end of the study. Hence, limited degradation was seen in water. The degradation products 10-deacetyltaxol and baccatin III[6169] were found in both solutes (Figure A7, Supporting Information S1), whereas the epimer 7-epi-taxol was found only in physiological buffer. This underlines the difficulties in determining release of paclitaxel in relevant fluids. Here, we identified three degradation products, but more degradation products of paclitaxel are reported,[69] hence illustrating the complexity in determining released paclitaxel. Since the degradation of paclitaxel was also observed in water, it was therefore decided to cast paclitaxel-loaded hydrogels at 4°C for further experiments.

3.4 | Cytotoxicity of paclitaxel-loaded hydrogels

The effect of the released drug was further studied in in vitro cell culture on the prostate cancer cell line PC-3. For the cell studies, the total concentration of alginate in the gels was increased from 1% (w/v) up to 2% (w/v) while keeping the ratio of Alg/POAβCyD 1:1 (w/w) and paclitaxel loading remained unchanged. This allowed for a drug:cyclodextrin molar ratio in the gels below 0.02 and thus to avoid crystallization of paclitaxel within the gels. Another benefit of increasing the alginate concentration was higher stiffness of the gels and their reduced vulnerability to syneresis in culture medium (Figure A8, Supporting Information S1).

The potential toxic effect of the grafted polymer by itself was first studied, followed by examining the burst release effects. Thereafter, the cytotoxicity of the paclitaxel-loaded hydrogels on metabolic activity of PC-3 cells was studied. The reasoning behind studying cytotoxicity of the functionalized polymer itself was as follows: Firstly, although cyclodextrins are widely used as excipients in pharmaceutic applications, it has been shown previously that β-CyDs can cause dose-dependent hemolysis and cytotoxicity.[70] Secondly, formation of the Alg/POAβCyD gel is not instant, meaning that upon injection in vivo the surrounding tissue and cells can interact with nongelled polymers. And lastly, possible leakage of POAβCyD from the gels over time[12] can lead to unwanted cytotoxic effects. To address this question, PC-3 cells were exposed to nongelled POAβCyD polymer. Free β-CyD dissolved in POA (β-CyD + POA sample) was used as a control. The cells exposed to nongelled POAβCyD showed viability ≥90% for concentrations up to 1 mM of β-CyD, which equals 5 mg/mL of the polymer (Figure 6a). A decrease in the cells metabolic activity was seen above this concentration in a concentration-dependent manner. The cytotoxic effect of POAβCyD was nearly two times higher than that one of free β-CyD dissolved in POA solution (β-CyD + POA sample). The half maximal inhibitory concentrations (IC50) were not obtained in this experiment, because high viscosity of the polymers (POAβCyD is highly viscous at concentrations >40 mg/mL) and low water solubility of free β-CyD (water solubility is 16.3 mM[62]) limited

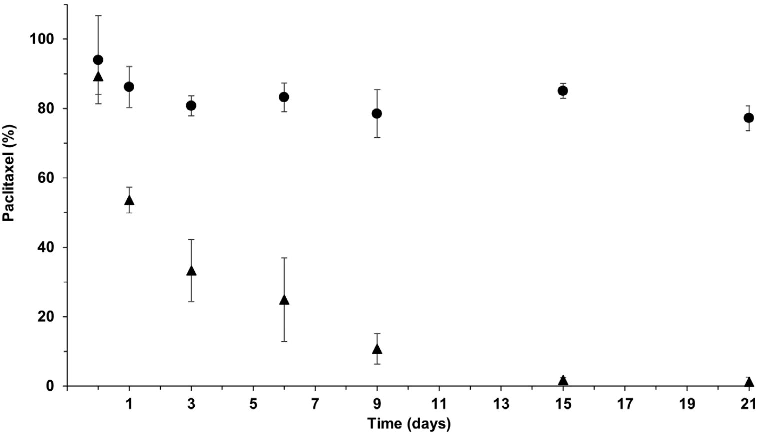

FIGURE 5 Stability of paclitaxel over time in water (circle) and physiological buffer (triangle) at 37°C

further increase of samples concentration. It has been previously reported that substituents can attenuate cytotoxicity of the native CyDs.[71,72] However, our results with POAβCyD show the opposite effect. We hypothesize that the observed effect might be connected to the difference in interaction between free βCyD and grafted βCyD moieties with the cellular cholesterol, since the cytotoxicity of various CyD derivatives is known to depend on their capacity to extract cholesterol from the cell membrane.[70]

Next, we formed alginate gels loaded with paclitaxel and studied burst release of the drug in culture media and hydrogels cytotoxicity in vitro. To study the burst release of paclitaxel, Alg and Alg/POAβCyD (1:1) hydrogels were loaded with 25 μM of paclitaxel and incubated in the culture media for 1 hr. The concentration of the released drug was then determined by exposing PC-3 cells to serial dilutions of the collected media and subsequent conversion of the obtained cytotoxicity values into the drug concentration using a standard curve. The standard curve was prepared using free paclitaxel in media (Figure A1, Supporting Information S1). The effects of the collected medium on metabolic activity of the PC-3 cells are shown on Figure 6b. The release-medium from both grafted and nongrafted alginates decreased cell metabolic activity in a concentration dependent manner. The paclitaxel burst release was found to be 6.2 ± 2.7% for Alg gel and 11.2 ± 2.5% for Alg/POAβCyD (1:1) gel. Under light microscope, the Alg/POAβCyD (1:1) mixed gels did not contain visible crystals of paclitaxel, whereas the Alg gels had clearly visible crystals. Thus, it is very likely that the Alg gels released less drug during the first hour due to crystal formation of the drug within these gels.

Next, to demonstrate efficacy of the developed delivery system in vitro, free paclitaxel, empty gels and gels loaded with paclitaxel were added to PC-3 cells and cell metabolic activity was determined after 72 hr of co-incubation (Figure 6c–d). Two gel types, namely Alg gels and Alg/POAβCyD (1:1) gels, and three different loadings (0.9, 7.2, and 25 μM) as well as placebo (without drug) were compared. The gels of both grafted and nongrafted alginate without paclitaxel showed no effect

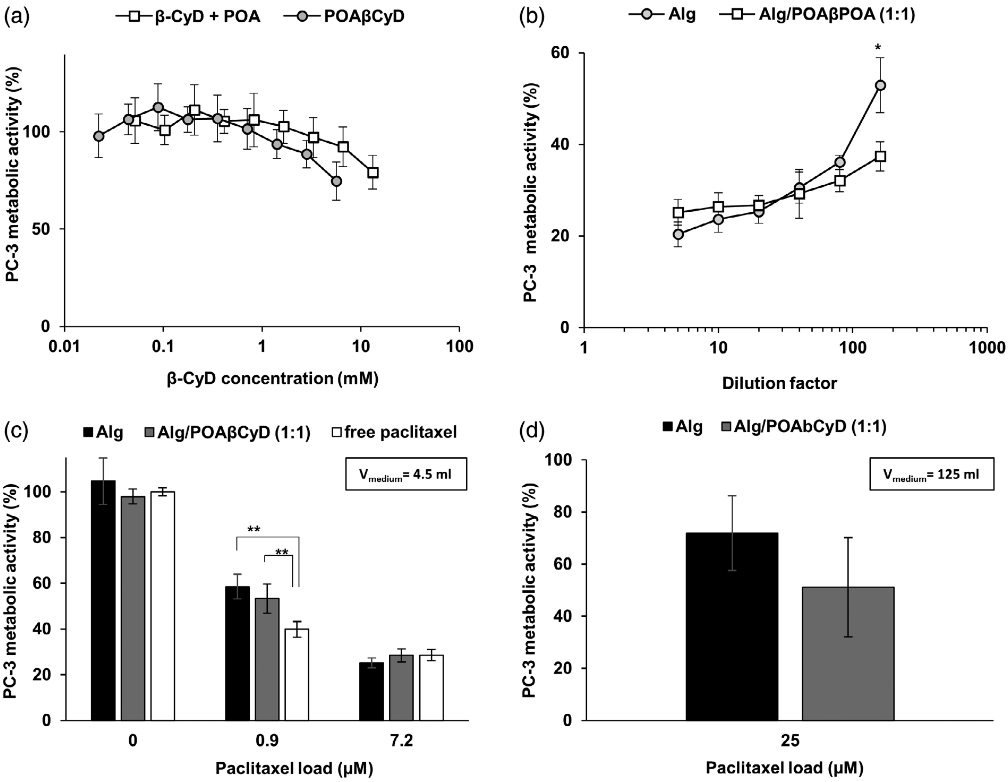

FIGURE 6 Metabolic activity of PC-3 cells. (a) Cells were incubated with alginate functionalized with β-CyD (POAβCyD) solution and free β-CyD mixed with POA solution; (b) cells were exposed to serial dilutions of 1-hr release media for paclitaxel loaded gels (25 μM) for 72 hr; (c) Cells were exposed to the 50 μL gels loaded with 0, 0.9 and 7.2 μM paclitaxel for 72 hr (total volume of medium 4.5 mL); and (d) cells were exposed to the 50 μL gels loaded with 25 μM paclitaxel for 72 hr (total volume of medium 125 mL). Cell metabolic activity is expressed as fluorescent intensities relative to a control (cells not exposed to paclitaxel were defined as 100%) after subtraction of non-cell-derived background. Data are expressed as mean ± *SD*, $n = 2–8$. * and ** denote statistically significant differences ($p < 0.05$ and $p < 0.01$, respectively) between two groups

on the metabolic activity of the cells (Figure 6c). The drug-loaded gels as expected decreased metabolic activity of PC-3 cells in dose-dependent manner relative to the loading concentration of paclitaxel. The Alg gel and Alg/POAβCyD (1:1) mixed gels loaded with 0.9 μM paclitaxel decreased cell viability down to 53.5 ± 4.8% and 60.4 ± 4%, respectively, whereas the gels loaded with 7.2 μM paclitaxel decreased cell viability down to 28.2 ± 1.9% and 24.3 ± 1.9%, respectively. Thus, the difference between two gel types (with and without POAβCyD) was not noticeable when 0.9 and 7.2 μM loadings were tested. These samples did not contain visible crystals of paclitaxel neither inside Alg nor Alg/POAβCyD (1:1) gels. In contrast, upon 25 μM paclitaxel loading, crystallization of the drug was visible inside the Alg gels, but not within the gels comprising grafted β-CyD. The mixed gels of Alg/POAβCyD (1:1) decreased cell metabolic activity to 51.1 ± 19%, whereas the Alg gels reduced it to 71.8 ± 14.3%; (Figure 6d). The Alg gels still contained undissolved paclitaxel crystals after 72 hr of incubation with cells, whereas the grafted gels remained transparent. Although the difference between Alg and Alg/POAβCyD (1:1) gels was not statistically significant ($p = 0.11$ ($n = 2$) and $p = 0.2$ ($n = 2$) for two independent experiments), we assume that the observed slightly higher cytotoxic activity of Alg/POAβCyD (1:1) gels could be related to a slightly faster paclitaxel release from these gels as well as higher burst release found in culture media.

In this work, we evaluated the in vitro biological activity of the functionalized alginate hydrogels loaded with paclitaxel on prostate cancer cells. This cell model was chosen because paclitaxel is known to be efficacious against various prostate cancer cells, including PC-3 cells.[73] At present, however, paclitaxel is only approved for the treatment of breast cancer, cancer of the ovaries, nonsmall cell lung cancer, and Kaposi's sarcoma, and is being currently used off-label for the treatment of castration-resistant prostate cancer and some other malignant tumors.[74] In situ forming hydrogel systems can serve as a local depot slowly releasing paclitaxel and may be beneficial for the treatment of patients with prostate tumors. A recent preclinical study demonstrates therapeutic efficacy of local delivery system based on an injectable polymer paste with paclitaxel in LNCaP human prostate cancer xenografts.[75] In addition, the efficacy of the developed paclitaxel delivery system would be interesting to study in models of brain tumor and brain metastases. As mentioned earlier, paclitaxel has strong anticancer activity against glioma cells and many other cancers in vitro.[33] However, paclitaxel is a substrate for the P-gp/ABCB1, and therefore has limited access to the central nervous system.[33] Since local delivery systems have already shown antitumor efficacy against glioblastoma,[4] delivery of drugs to brain tumors is a relevant follow-up of the studied gel system. In addition, other poorly water-soluble chemotherapeutic agents that can form inclusion complexes with β-CyD, for instance cisplatin, doxorubicin, curcumin, camptothecin, and so on, may be considered as potential payloads for the developed depot hydrogel.

4 | CONCLUSIONS

In this study, we developed a hydrogel-based delivery system employing β-CyD functionalized alginate, where alginate acted as the gelling material and the β-CyD moieties were responsible for formation of inclusion complexes with a poorly soluble drug (paclitaxel). The introduction of β-CyD-moieties into the delivery system generally decreased the mechanical properties of the gels (compared to nonmodified alginate hydrogels) and modulated paclitaxel behavior but did not influence gelation kinetics. The significance of the present work is that it shows increased capacity of β-CyD grafted alginate to complex paclitaxel as compared to free HPβ-CyD. Although the paclitaxel is not an ideal payload for β-CyD-based systems because of its relatively poor retention within β-CyD hydrophobic cavity, and because it is difficult to quantify due to rapid degradation, our findings support that the β-CyD-grafted alginate can modulate release of the paclitaxel from the gels. The β-CyD-grafted alginate prevented crystallization of the paclitaxel by retaining a complexed dispersion of the drug and facilitated paclitaxel diffusion out of the gel network. This effect was observed at paclitaxel:β-CyD molar ratios not exceeding 0.02. Furthermore, the paclitaxel-loaded hydrogels comprising modified alginate were shown to have cytotoxic activity. The results indicate that β-CyD functionalized alginates have potential to be used as a material for drug delivery systems. The hydrogel system could also be applied in future work for delivery of other hydrophobic drugs and molecules that can form inclusion complexes with β-CyD.

ACKNOWLEDGMENTS

Professor Anne des Rieux and Dr Fabienne Danhier at Catholic University of Louvain, Louvain-la-Neuve, Belgium for helpful input to the experimental set-up. The PC-3 cells were kindly provided by chef engineer K. Grendstad, Department of Physics, NTNU, Trondheim, Norway. The authors are grateful to Professor Kim L. Larsen and Professor Thorbjørn T. Nielsen, Department of Chemistry and Bioscience, Aalborg University (AAU), Aalborg, Denmark for the supply of modified cyclodextrins. This work has been supported by The Research Council of Norway [grant numbers 221576-MARPOL, 269273/O70-3Dlife, and 250875-Epimerases].

CONFLICT OF INTEREST

The authors declare no conflict of interest.

AUTHOR CONTRIBUTIONS

The manuscript was written through contributions of all authors. All authors have given approval to the final version of the manuscript.

DATA AVAILABILITY STATEMENT

The relevant data generated or analyzed during the current study are included within the published article (and its supplementary information) or are available from the corresponding author upon reasonable request.

ORCID

Line Aanerud Omtvedt https://orcid.org/0000-0003-1227-7907

REFERENCES

1. Darge HF, Andrgie AT, Tsai HC, Lai JY. Polysaccharide and polypeptide based injectable thermo-sensitive hydrogels for local biomedical

applications. *Int J Biol Macromol*. 2019;*133*:545-563. https://doi.org/10.1016/j.ijbiomac.2019.04.131.

2. Dimatteo R, Darling NJ, Segura T. In situ forming injectable hydrogels for drug delivery and wound repair. *Adv Drug Deliv Rev*. 2018;*127*:167-184. https://doi.org/10.1016/j.addr.2018.03.007.
3. Cirillo G, Spizzirri UG, Curcio M, Nicoletta FP, Iemma F. Injectable hydrogels for cancer therapy over the last decade. *Pharmaceutics*. 2019;*11*(9):486. https://doi.org/10.3390/pharmaceutics11090486.
4. Bastiancich C, Bianco J, Vanvarenberg K, et al. Injectable nanomedicine hydrogel for local chemotherapy of glioblastoma after surgical resection. *J Control Release*. 2017;*264*:45-54. https://doi.org/10.1016/j.jconrel.2017.08.019.
5. Draget KI, Taylor C. Chemical, physical and biological properties of alginates and their biomedical implications. *Food Hydrocoll*. 2011;*25*(2):251-256. https://doi.org/10.1016/j.foodhyd.2009.10.007.
6. Sandvig I, Karstensen K, Rokstad AM, et al. RGD-peptide modified alginate by a chemoenzymatic strategy for tissue engineering applications. *J Biomed Mater Res A*. 2015;*103*(3):896-906. https://doi.org/10.1002/jbm.a.35230.
7. Arlov Ø, Aachmann FL, Sundan A, Espevik T, Skjåk-Bræk G. Heparin-like properties of sulfated alginates with defined sequences and sulfation degrees. *Biomacromolecules*. 2014;*15*(7):2744-2750. https://doi.org/10.1021/bm500602w.
8. Donati I, Draget KI, Borgogna M, Paoletti S, Skjåk-Braek G. Tailor-made alginate bearing galactose moieties on mannuronic residues: selective modification achieved by a chemoenzymatic strategy. *Biomacromolecules*. 2005;*6*(1):88-98. https://doi.org/10.1021/bm040053z.
9. Omtvedt LA, Dalheim MØ, Nielsen TT, Larsen KL, Strand BL, Aachmann FL. Efficient grafting of cyclodextrin to alginate and performance of the hydrogel for release of model drug. *Sci Rep*. 2019;*9*(1):9325. https://doi.org/10.1038/s41598-019-45761-4.
10. Dalheim MØ, Vanacker J, Najmi MA, Aachmann FL, Strand BL, Christensen BE. Efficient functionalization of alginate biomaterials. *Biomaterials*. 2016;*80*:146-156. https://doi.org/10.1016/j.biomaterials.2015.11.043.
11. Kristiansen KA, Schirmer BC, Aachmann FL, Skjåk-Braek G, Draget KI, Christensen BE. Novel alginates prepared by independent control of chain stiffness and distribution of G-residues: structure and gelling properties. *Carbohydr Polym*. 2009;*77*(4):725-735. https://doi.org/10.1016/j.carbpol.2009.02.018.
12. Dalheim MØ, Omtvedt LA, Bjørge IM, et al. Mechanical properties of ca-saturated hydrogels with functionalized alginate. *Gels*. 2019;*5*(2):23. https://doi.org/10.3390/gels5020023.
13. Mørch YA, Donati I, Strand BL, Skjåk-Braek G. Effect of Ca2+, Ba2+, and Sr2+ on alginate microbeads. *Biomacromolecules*. 2006;*7*(5):1471-1480. https://doi.org/10.1021/bm060010d.
14. Andersen T, Strand BL, Formo K, Alsberg E, Christensen BE. Alginates as biomaterials in tissue engineering. In: Rauter AP, Lindhorst T, eds. *Carbohydrate chemistry: chemical and biological approaches*. Cambridge: The Royal Society of Chemistry; 2012:227-258. https://doi.org/10.1039/9781849732765-00227.
15. Shin EY, Park JH, Shin ME, et al. Injectable taurine-loaded alginate hydrogels for retinal pigment epithelium (RPE) regeneration. *Korean J Couns Psychother*. 2019;*103*:109787. https://doi.org/10.1016/j.msec.2019.109787.
16. Criado-Gonzalez M, Fernandez-Gutierrez M, San Roman J, Mijangos C, Hernández R. Local and controlled release of tamoxifen from multi (layer-by-layer) alginate/chitosan complex systems. *Carbohydr Polym*. 2019;*206*:428-434. https://doi.org/10.1016/j.carbpol.2018.11.007.
17. Etter JN, Oldinski RA. Synthesis of a tri-network alginate hydrogel for use as an injectable cell carrier. *Biomed Phys Eng Express*. 2018;*5*(1):015017. https://doi.org/10.1088/2057-1976/aaeb6f.
18. Ferreira NN, Caetano BL, Boni FI, et al. Alginate-based delivery systems for bevacizumab local therapy: *in vitro* structural features and release properties. *J Pharm Sci*. 2019;*108*(4):1559-1568. https://doi.org/10.1016/j.xphs.2018.11.038.
19. Brudno Y, Pezone MJ, Snyder TK, et al. Replenishable drug depot to combat post-resection cancer recurrence. *Biomaterials*. 2018;*178*:373-382. https://doi.org/10.1016/j.biomaterials.2018.05.005.
20. Zhang Y, Li X, Zhong N, Huang Y, He K, Ye X. Injectable in situ dual-crosslinking hyaluronic acid and sodium alginate based hydrogels for drug release. *J Biomater Sci Polym Ed*. 2019;*30*(12):995-1007. https://doi.org/10.1080/09205063.2019.1618546.
21. Hoare TR, Kohane DS. Hydrogels in drug delivery: progress and challenges. *Polymer*. 2008;*49*(8):1993-2007. https://doi.org/10.1016/j.polymer.2008.01.027.
22. McKenzie M, Betts D, Suh A, Bui K, Kim LD, Cho H. Hydrogel-based drug delivery systems for poorly water-soluble drugs. *Molecules*. 2015;*20*(11):20397-20408. https://doi.org/10.3390/molecules201119705.
23. Nielsen AL, Madsen F, Larsen KL. Cyclodextrin modified hydrogels of PVP/PEG for sustained drug release. *Drug Deliv*. 2009;*16*(2):92-101. https://doi.org/10.1080/10717540802605129.
24. Woldum HS, Larsen KL, Madsen F. Cyclodextrin controlled release of poorly water-soluble drugs from hydrogels. *Drug Deliv*. 2008;*15*(1):69-80. https://doi.org/10.1080/10717540701829267.
25. Szejtli J. Introduction and general overview of cyclodextrin chemistry. *Chem Rev*. 1998;*98*(5):1743-1754. https://doi.org/10.1021/cr970022c.
26. Peng K, Tomatsu I, Korobko AV, Kros A. Cyclodextrin-dextran based in situ hydrogel formation: a carrier for hydrophobic drugs. *Soft Matter*. 2010;*6*(1):85-87. https://doi.org/10.1039/B914166A.
27. Grimaudo MA, Nicoli S, Santi P, Concheiro A, Alvarez-Lorenzo C. Cyclosporine-loaded cross-linked inserts of sodium hyaluronan and hydroxypropyl-β-cyclodextrin for ocular administration. *Carbohydr Polym*. 2018;*201*:308-316. https://doi.org/10.1016/j.carbpol.2018.08.073.
28. Singla AK, Garg A, Aggarwal D. Paclitaxel and its formulations. *Int J Pharm*. 2002;*235*(1–2):179-192. https://doi.org/10.1016/s0378-5173(01)00986-3.
29. Alcaro S, Ventura CA, Paolino D, et al. Preparation, characterization, molecular modeling and *in vitro* activity of paclitaxel-cyclodextrin complexes. *Bioorg Med Chem Lett*. 2002;*12*(12):1637-1641. https://doi.org/10.1016/s0960-894x(02)00217-2.
30. Sharma US, Balasubramanian SV, Straubinger RM. Pharmaceutical and physical properties of paclitaxel (Taxol) complexes with cyclodextrins. *J Pharm Sci*. 1995;*84*(10):1223-1230. https://doi.org/10.1002/jps.2600841015.
31. Sparreboom A, van Tellingen O, Nooijen WJ, Beijnen JH. Tissue distribution, metabolism and excretion of paclitaxel in mice. *Anticancer Drugs*. 1996;*7*(1):78-86. https://doi.org/10.1097/00001813-199601000-00009.
32. Wolinsky JB, Colson YL, Grinstaff MW. Local drug delivery strategies for cancer treatment: gels, nanoparticles, polymeric films, rods, and wafers. *J Control Release*. 2012;*159*(1):14-26. https://doi.org/10.1016/j.jconrel.2011.11.031.
33. Fellner S, Bauer B, Miller DS, et al. Transport of paclitaxel (Taxol) across the blood-brain barrier *in vitro* and *in vivo*. *J Clin Invest*. 2002;*110*(9):1309-1318. https://doi.org/10.1172/JCI15451.
34. Wanderley CW, Colón DF, Luiz JPM, et al. Paclitaxel reduces tumor growth by reprogramming tumor-associated macrophages to an M1 profile in a TLR4-dependent manner. *Cancer Res*. 2018;*78*(20):5891-5900. https://doi.org/10.1158/0008-5472.CAN-17-3480.
35. Wang F, Porter M, Konstantopoulos A, Zhang P, Cui H. Preclinical development of drug delivery systems for paclitaxel-based cancer chemotherapy. *J Control Release*. 2017;*267*:100-118. https://doi.org/10.1016/j.jconrel.2017.09.026.

36. De Clercq K, Xie F, De Wever O, et al. Preclinical evaluation of local prolonged release of paclitaxel from gelatin microspheres for the prevention of recurrence of peritoneal carcinomatosis in advanced ovarian cancer. *Sci Rep*. 2019;*9*(1):14881. https://doi.org/10.1038/s41598-019-51419-y.
37. Ranganath SH, Kee I, Krantz WB, Chow PK, Wang CH. Hydrogel matrix entrapping PLGA-paclitaxel microspheres: drug delivery with near zero-order release and implantability advantages for malignant brain tumour chemotherapy. *Pharm Res*. 2009;*26*(9):2101-2114. https://doi.org/10.1007/s11095-009-9922-2.
38. Abe T, Sakane M, Ikoma T, Kobayashi M, Nakamura S, Ochiai N. Intraosseous delivery of paclitaxel-loaded hydroxyapatitealginate composite beads delaying paralysis caused by metastatic spine cancer in rats. *J Neurosurg Spine*. 2008;*9*(5):502-510. https://doi.org/10.3171/SPI.2008.9.11.502.
39. Chiang C-Y, Chu C-C. Synthesis of photoresponsive hybrid alginate hydrogel with photo-controlled release behavior. *Carbohydr Polym*. 2015;*119*:18-25. https://doi.org/10.1016/J.CARBPOL.2014.11.043.
40. Gomez CG, Chambat G, Heyraud A, Villar M, Auzely-Velty R. Synthesis and characterization of a beta-CD-alginate conjugate. *Polymer*. 2006;*47*(26):8509-8516. https://doi.org/10.1016/j.polymer.2006.10.011.
41. Izawa H, Kawakami K, Sumita M, Tateyama Y, Hill JP, Ariga K. Beta-cyclodextrin-crosslinked alginate gel for patient-controlled drug delivery systems: regulation of host-guest interactions with mechanical stimuli. *J Mater Chem B*. 2013;*1*:2155-2161. https://doi.org/10.1039/C3TB00503H.
42. Miao T, Fenn SL, Charron PN, Oldinski RA. Self-healing and Thermoresponsive dual-cross-linked alginate hydrogels based on supramolecular inclusion complexes. *Biomacromolecules*. 2015;*16*:3740-3750. https://doi.org/10.1021/acs.biomac.5b00940.
43. Tan L, Li J, Liu Y, Zhou H, Zhang Z, Deng L. Synthesis and characterization of β-cyclodextrin-conjugated alginate hydrogel for controlled release of hydrocortisone acetate in response to mechanical stimulation. *J Bioactive Compatible Polym*. 2015;*30*:584-599. https://doi.org/10.1177/0883911515590494.
44. Zhang S, Qiao X, Hu B, Gong Y. Formation and controlled release of the inclusion complex of water soluble model drug neutral red with β-cyclodextrin grafted sodium alginate. *J Control Release*. 2011;*152*:e116-e118. https://doi.org/10.1016/J.JCONREL.2011.08.161.
45. Moncada-Basualto M, Matsuhiro B, Mansilla A, Lapier M, Maya JD, Olea-Azar C. Supramolecular hydrogels of β-cyclodextrin linked to calcium homopoly-l-guluronate for release of coumarins with trypanocidal activity. *Carbohydr Polym*. 2019;*204*:170-181. https://doi.org/10.1016/J.CARBPOL.2018.10.010.
46. Pluemsab W, Sakairi N, Furuike T. Synthesis and inclusion property of α-cyclodextrin-linked alginate. *Polymer*. 2005;*46*:9778-9783. https://doi.org/10.1016/J.POLYMER.2005.08.005.
47. Nielsen TT, Wintgens V, Amiel C, Wimmer R, Larsen KL. Facile synthesis of beta-cyclodextrin-dextran polymers by "click" chemistry. *Biomacromolecules*. 2010;*11*(7):1710-1715. https://doi.org/10.1021/bm9013233.
48. Bastiancich C, Vanvarenberg K, Ucakar B, et al. Lauroyl-gemcitabine-loaded lipid nanocapsule hydrogel for the treatment of glioblastoma. *J Control Release*. 2016;*225*:283-293. https://doi.org/10.1016/j.jconrel.2016.01.054.
49. Draget KI, Østgaard K, Smidsrød O. Homogeneous alginate gels: a technical approach. *Carbohydr Polym*. 1990;*14*:159-178. https://doi.org/10.1016/0144-8617(90)90028-Q.
50. Mørch YA, Holtan S, Donati I, Strand BL, Skjåk-Braek G. Mechanical properties of C-5 epimerized alginates. *Biomacromolecules*. 2008;*9*(9):2360-2368. https://doi.org/10.1021/bm8003572.
51. Smidsrød O, Painter T. Effect of periodate oxidation upon the stiffness of the alginate molecule in solution. *Carbohydr Res*. 1973;*26*(1):125-132. https://doi.org/10.1016/S0008-6215(00)85029-6.
52. Lee KY, Bouhadir KH, Mooney DJ. Evaluation of chain stiffness of partially oxidized polyguluronate. *Biomacromolecules*. 2002;*3*(6):1129-1134. https://doi.org/10.1021/bm025567h.
53. Vold IM, Kristiansen KA, Christensen BE. A study of the chain stiffness and extension of alginates, *in vitro* epimerized alginates, and periodate-oxidized alginates using size-exclusion chromatography combined with light scattering and viscosity detectors. *Biomacromolecules*. 2006;*7*(7):2136-2146. https://doi.org/10.1021/bm060099n.
54. Gomez CG, Rinaudo M, Villar MA. Oxidation of sodium alginate and characterization of the oxidized derivatives. *Carbohydr Polym*. 2007;*67*:296-304. https://doi.org/10.1016/j.carbpol.2006.05.025.
55. Draget KI, Østgaard K, Smidsrød O. Alginate-based solid media for plant tissue culture. *Appl Microbiol Biotechnol*. 1989;*31*:79-83. https://doi.org/10.1007/BF00252532.
56. Espona-Noguera A, Ciriza J, Cañibano-Hernández A, et al. Tunable injectable alginate-based hydrogel for cell therapy in type 1 *Diabetes mellitus*. *Int J Biol Macromol*. 2018;*107*:1261-1269. https://doi.org/10.1016/j.ijbiomac.2017.09.103.
57. Li J, Mooney DJ. Designing hydrogels for controlled drug delivery. *Nat Rev Mater*. 2016;*1*(12):16071. https://doi.org/10.1038/natrevmats.2016.71.
58. Castro JS, Tapia LV, Silveyra RA, Martinez CA, Deymier PA. Negative impact of paclitaxel crystallization on hydrogels and novel approaches for anticancer drug delivery systems. In: Ozdemir O, ed. *Current cancer treatment—Novel beyond conventional approaches*. London: InTech; 2011:767-782.
59. Del Valle EMM. Cyclodextrins and their uses: a review. *Process Biochem*. 2004;*39*(9):1033-1046. https://doi.org/10.1016/S0032-9592(03)00258-9.
60. Jing J, Szarpak-Jankowska A, Guillot R, Pignot-Paintrand I, Picart C, Auzély-Velty R. Cyclodextrin/paclitaxel complex in biodegradable capsules for breast cancer treatment. *Chem Mater*. 2013;*25*(19):3867-3873. https://doi.org/10.1021/cm4019925.
61. Amini-Fazl MS, Mobedi H, Barzin J. Investigation of aqueous stability of taxol in different release media. *Drug Dev Ind Pharm*. 2014;*40*(4):519-526. https://doi.org/10.3109/03639045.2013.771646.
62. Saokham P, Muankaew C, Jansook P, Loftsson T. Solubility of cyclodextrins and drug/cyclodextrin complexes. *Molecules*. 2018;*23*(5):1161. https://doi.org/10.3390/molecules23051161.
63. Mognetti B, Barberis A, Marino S, et al. *In vitro* enhancement of anticancer activity of paclitaxel by a cremophor free cyclodextrin-based nanosponge formulation. *J Incl Phenom Macrocycl Chem*. 2012;*74*:201-210. https://doi.org/10.1007/s10847-011-0101-9.
64. Zhang X, Zhang X, Wu Z, et al. A hydrotropic β-cyclodextrin grafted hyperbranched polyglycerol co-polymer for hydrophobic drug delivery. *Acta Biomater*. 2011;*7*(2):585-592. https://doi.org/10.1016/j.actbio.2010.08.029.
65. Martinsen A, Storrø I, Skjårk-Braek G. Alginate as immobilization material: III diffusional Properties. *Biotechnol Bioeng*. 1992;*39*(2):186-194. https://doi.org/10.1002/bit.260390210.
66. Choi SG, Lee SE, Kang BS, Ng CL, Davaa E, Park JS. Thermosensitive and mucoadhesive sol-gel composites of paclitaxel/dimethyl-β-cyclodextrin for buccal delivery. *PLoS One*. 2014;*9*(9):e109090. https://doi.org/10.1371/journal.pone.0109090.
67. Abouelmagd SA, Sun B, Chang AC, Ku YJ, Yeo Y. Release kinetics study of poorly water-soluble drugs from nanoparticles: are we doing it right? *Mol Pharm*. 2015;*12*(3):997-1003. https://doi.org/10.1021/mp500817h.
68. Phillips DJ, Pygall SR, Cooper VB, Mann JC. Overcoming sink limitations in dissolution testing: a review of traditional methods and the potential utility of biphasic systems. *J Pharm Pharmacol*. 2012;*64*(11):1549-1559. https://doi.org/10.1111/j.2042-7158.2012.01523.x.
69. Tian J, Stella VJ. Degradation of paclitaxel and related compounds in aqueous solutions I: epimerization. *J Pharm Sci*. 2008;*97*(3):1224-1235. https://doi.org/10.1002/jps.21112.

70. Kiss T, Fenyvesi F, Bácskay I, et al. Evaluation of the cytotoxicity of beta-cyclodextrin derivatives: evidence for the role of cholesterol extraction. *Eur J Pharm Sci*. 2010;*40*(4):376-380. https://doi.org/10.1016/j.ejps.2010.04.014.
71. Szente L, Singhal A, Domokos A, Song B. Cyclodextrins: assessing the impact of cavity size, occupancy, and substitutions on cytotoxicity and cholesterol homeostasis. *Molecules*. 2018;*23*(5):1228. https://doi.org/10.3390/molecules23051228.
72. Wang L, Ruffner DE. Cyclodextrin grafted biocompatible amphilphilic polymer and methods of preparation and use thereof. 2001.
73. Castilla C, Flores ML, Medina R, et al. Prostate cancer cell response to paclitaxel is affected by abnormally expressed securin PTTG1. *Mol Cancer Ther*. 2014;*13*(10):2372-2383. https://doi.org/10.1158/1535-7163.MCT-13-0405.
74. Weaver BA. How taxol/paclitaxel kills cancer cells. *Mol Biol Cell*. 2014;*25*(18):2677-2681. https://doi.org/10.1091/mbc.E14-04-0916.
75. Jackson JK, Gleave ME, Yago V, Beraldi E, Hunter WL, Burt HM. The suppression of human prostate tumor growth in mice by the intratumoral injection of a slow-release polymeric paste formulation of paclitaxel. *Cancer Res*. 2000;*60*(15):4146-4151.

SUPPORTING INFORMATION

Additional supporting information may be found online in the Supporting Information section at the end of this article.

How to cite this article: Omtvedt, L. A., Kristiansen, K. A., Strand, W. I., Aachmann, F. L., Strand, B. L., & Zaytseva-Zotova, D. S. (2021). Alginate hydrogels functionalized with β-cyclodextrin as a local paclitaxel delivery system. *Journal of Biomedical Materials Research Part A*, *109*(12), 2625–2639. https://doi.org/10.1002/jbm.a.37255

Supplementary Paper III

Appendix S1

Methods

Ultra-high performance liquid chromatography (UHPLC) coupled to tandem quadrupole (TQ) mass spectrometry analysis

Samples were thawed and centrifuged for 15 min at 23 000 g before the UHPLC-TQ analysis using an ACQUITY I-class UPLC system coupled to a Xevo TQ-S triple quadrupole mass spectrometer (Waters, Milford, MA, USA).

Analytes were separated on a Waters ACQUITY UPLC® BEH C18 Column (130 Å, 50 mm ×2.1 mm L×I.D. 1.7 μm), and the column manager was set to 45°C. Mobile phase A consisted of water and mobile phase B acetonitrile, both containing 0.10% (v/v) formic acid. Flow rate was set at 0.600 ml/min. Conditions were kept constant at 99.0% A for one minute, then a linear gradient was set from 99.0% A to 1.0% A in three minutes, followed by 1.0% A constant for a half a minute, before the gradient was brought back to 99.0% A in 0.10 minute. Finally, the column was equilibrated for 0.90 minute before starting a new injection. Total run time was 4.5 minutes. Ethanol was used as needle wash, and injection volume was 5 μl.

The TQ mass spectrometer was equipped with an electrospray ionization source operating in positive mode. Capillary voltage and source offset voltages were set at 2.5 kV and 22 V, respectively. Source temperature was maintained at 150°C, desolvation gas temperature at 500°C and gas flow rate at 1000 l/h. Cone gas flow rate was fixed at 150 l/h, and the nebulizer gas flow maintained at 6.0 bar. Collision gas flow was set to 0.15 ml/min of argon. Cone voltages (CV), collision energies (CE) and MS/MS transitions (precursor and daughter ions) of paclitaxel and docetaxel were optimized using intellistart by infusing 500 nM standard solutions at 10-20 μl/min combined with 0.05mL/min with equal amounts of mobile phase A and B from the UHPLC-system.

Paclitaxel was quantified by means of one selected precursor ion-product ion transition (m/z 854.60-286.46, CV = 22 V, CE = 16 eV), and its identity confirmed by one qualifier transition (m/z 854.60-105.23, CV = 22 V and CE = 48 eV). Docetaxel was used as internal standard (m/z 808.37-226.12, CV = 20 V, CE = 12 eV). Degradation products Baccatin III (m/z 587.25-327.16, CV = 30 V, CE = 10 eV), 7-epi-taxol (identical transition as paclitaxel) and 10-deacetyltaxol (m/z 812.33-286.10, CV = 30 V, CE = 10 eV) was monitored, but not absolutely quantified. A 10-20 ms dwell time was calculated for each transition as recommended by the auto dwell function in MassLynx to ensure 20 data points across the peaks. UHPLC–MS/MS data were acquired and processed using MassLynx software (v4.1) and TargetLynx application manager.

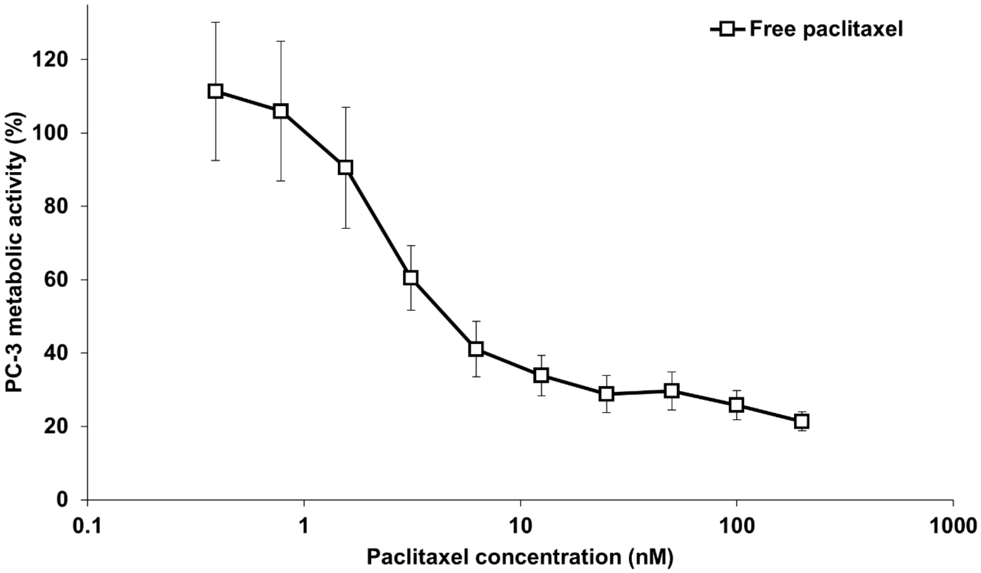

Fig. A1. Metabolic activity of PC-3 cells after incubation with paclitaxel for 72 hours. Cell metabolic activity is expressed as percentage of fluorescent intensities relative to a control (cells not exposed to paclitaxel were defined as 100%) after subtraction of non-cell-derived background. Data are expressed as Mean ± SD.

A single column fitting image

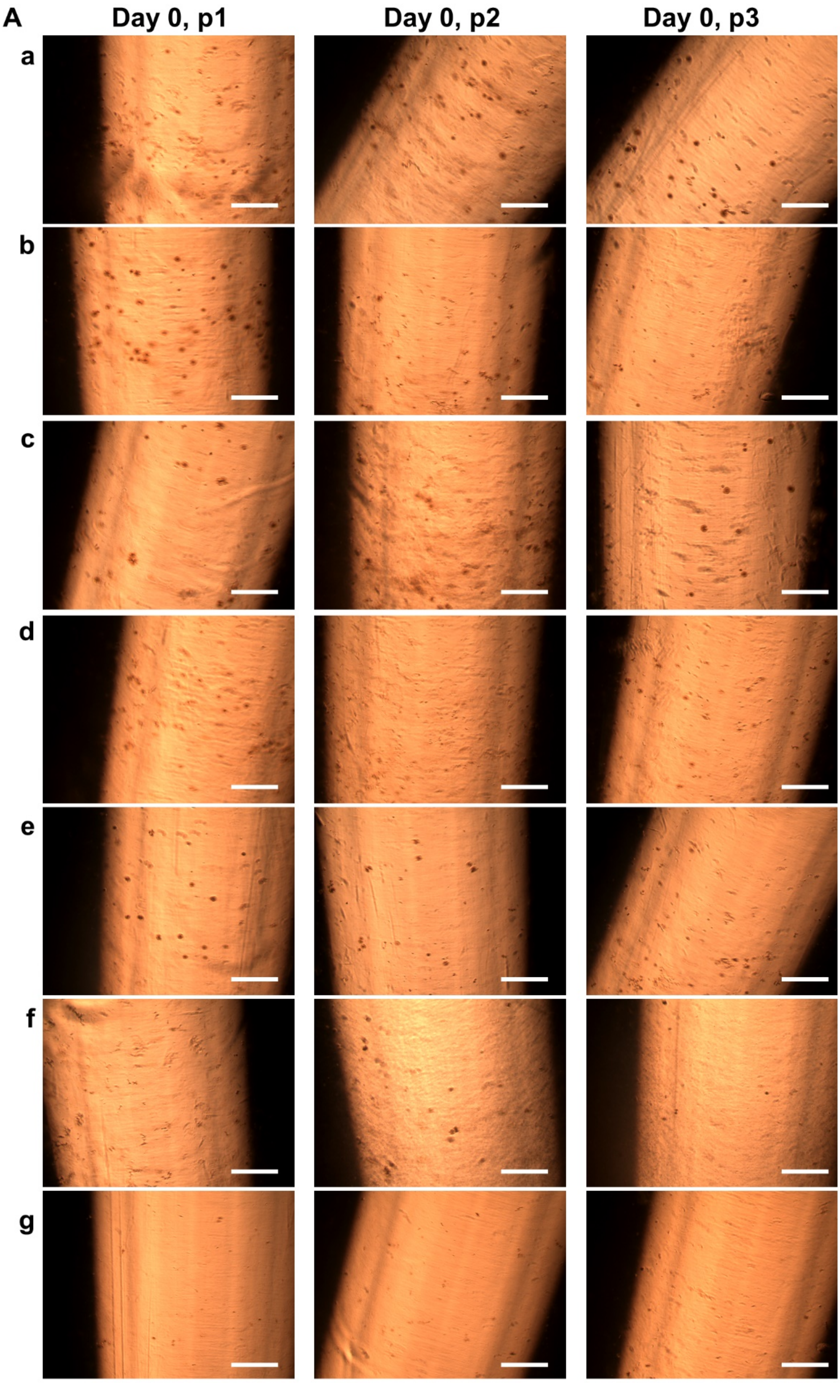

45

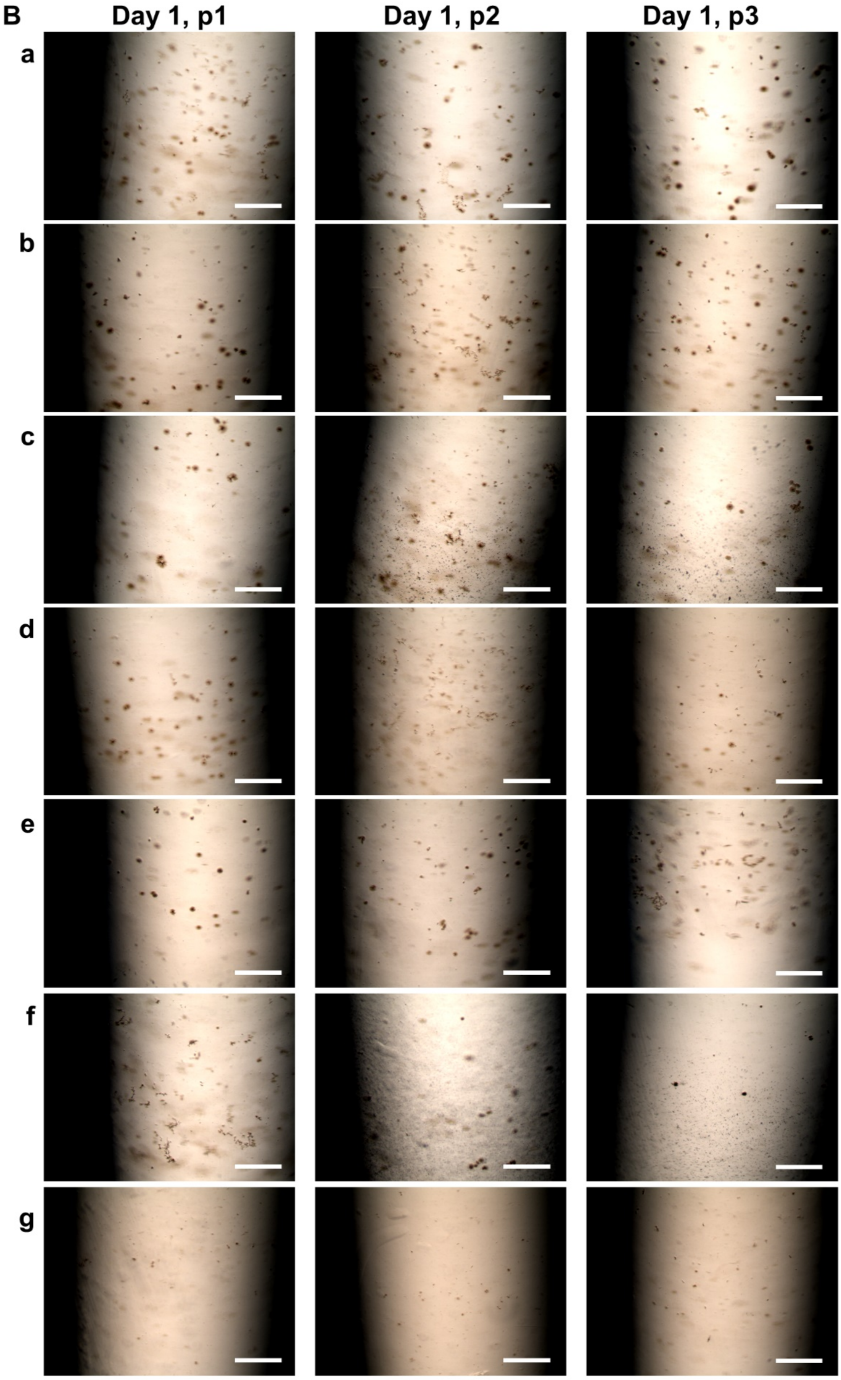

46

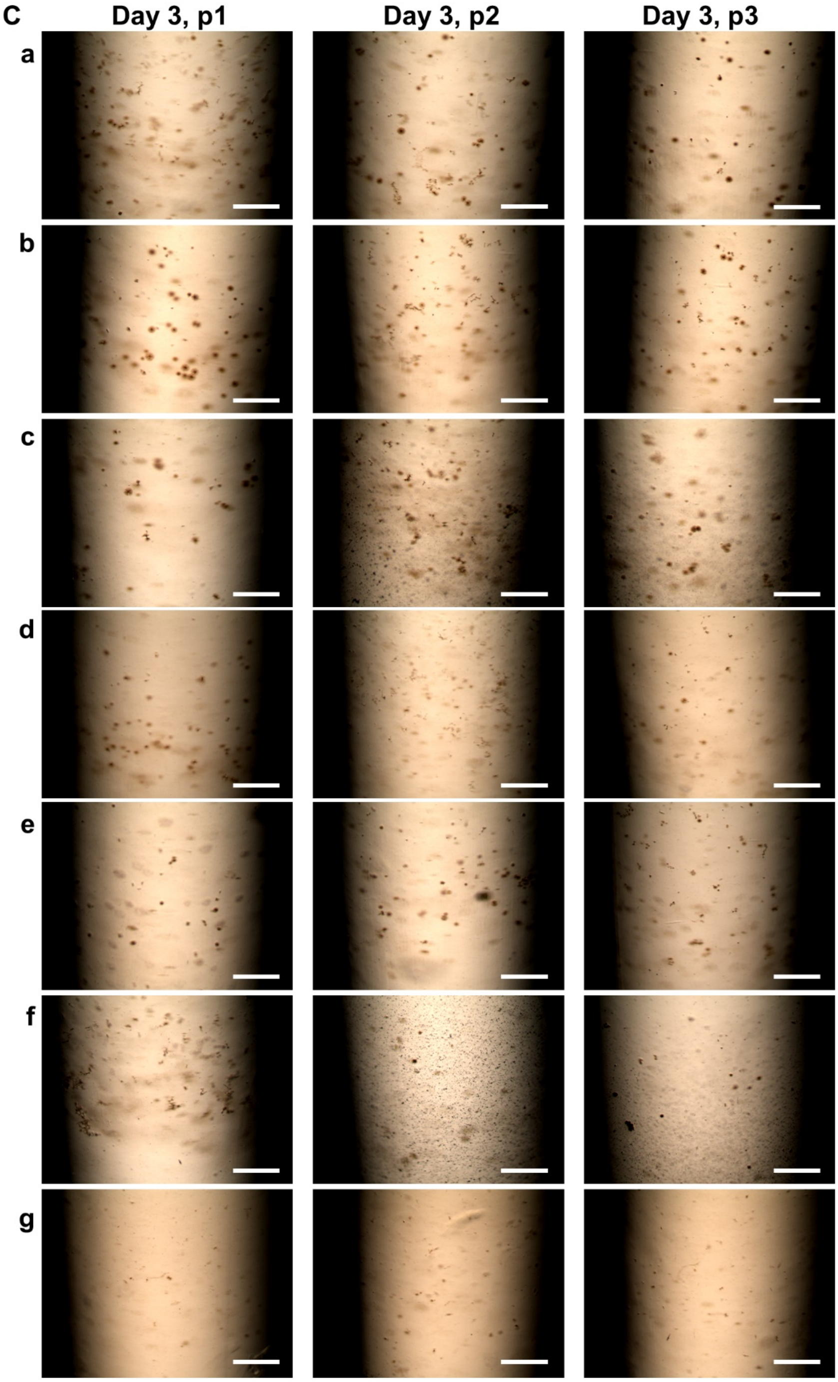

47

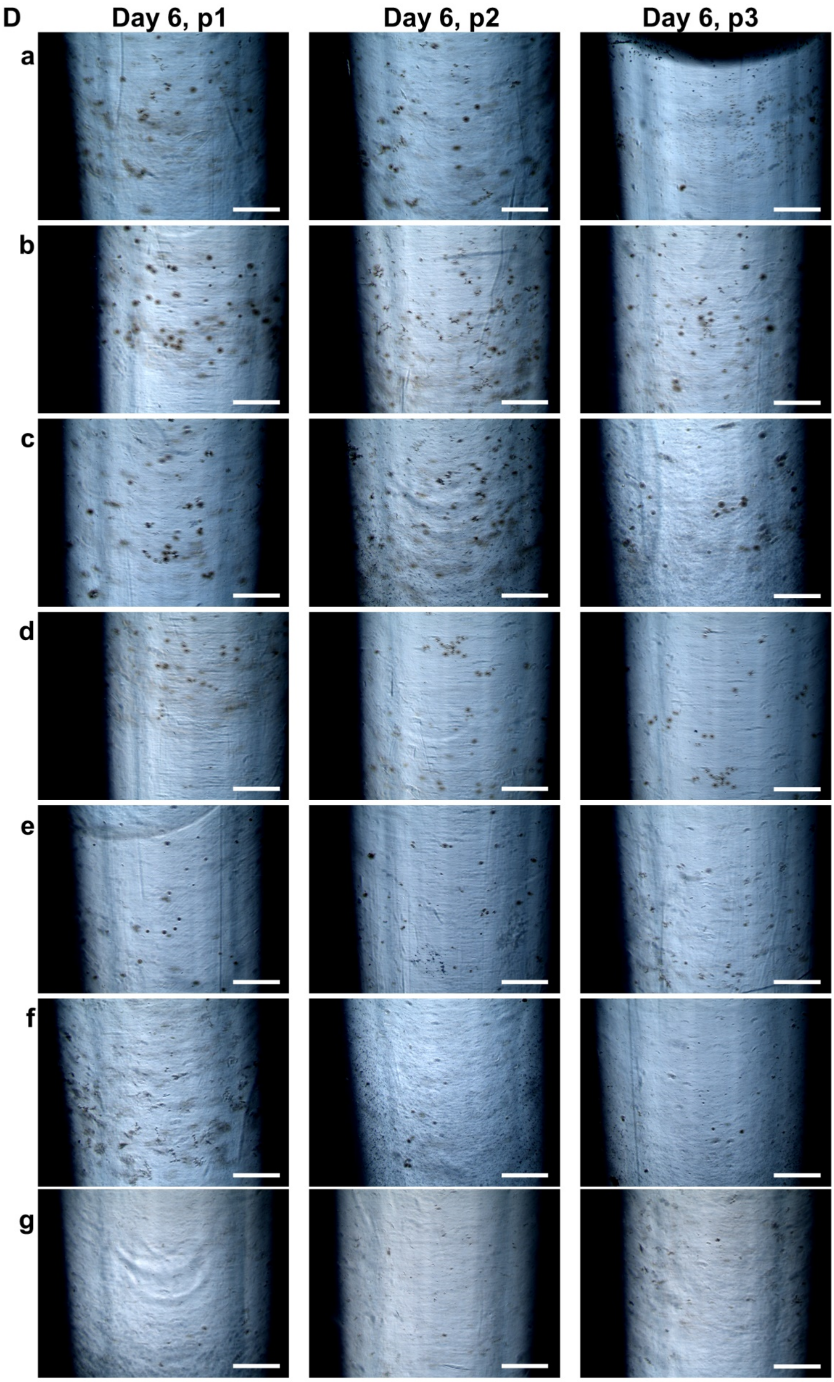
D
Day 6, p1
Day 6, p2
Day 6, p3
a
b
c
d
e
f
g

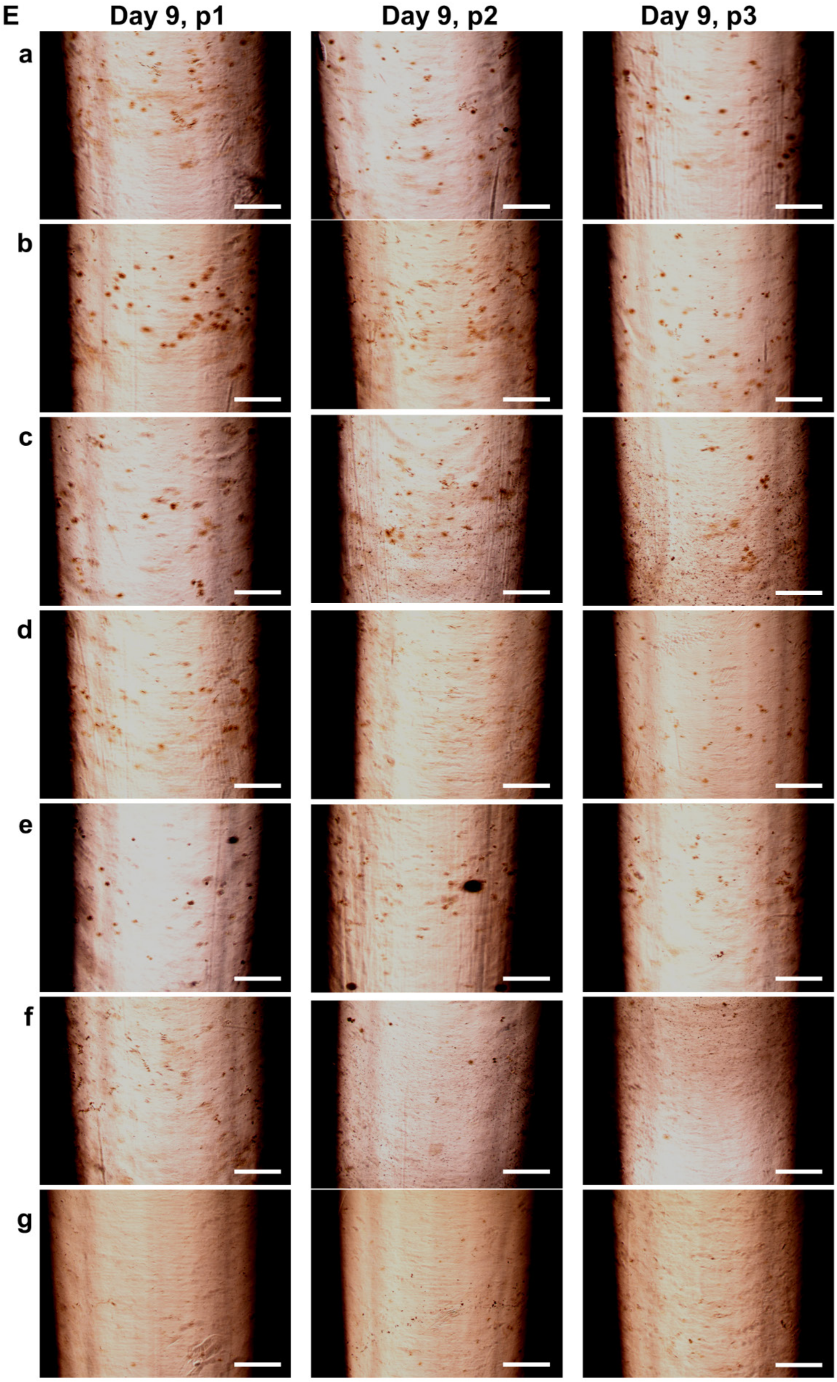
E
Day 9, p1
Day 9, p2
Day 9, p3
a
b
c
d
e
f
g

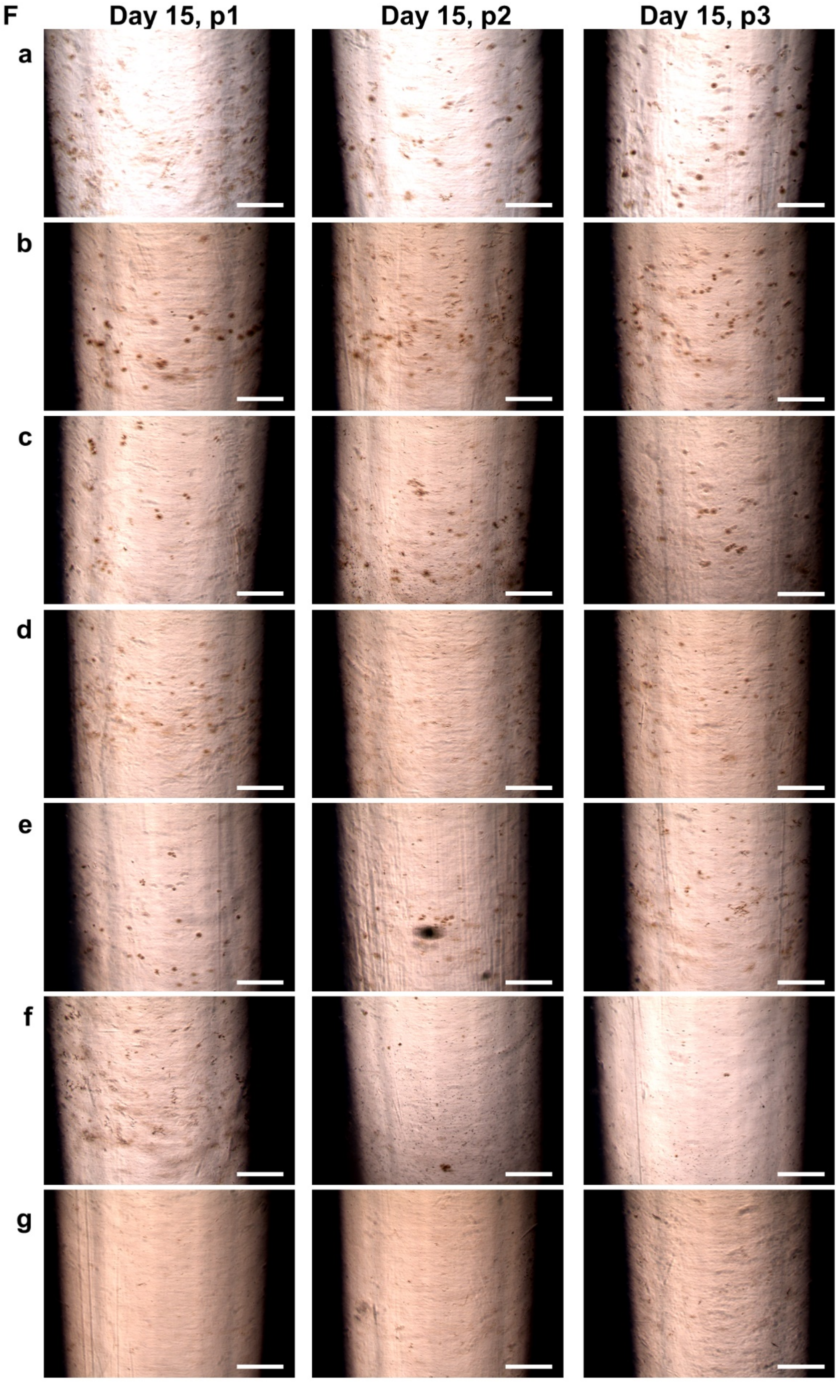

50

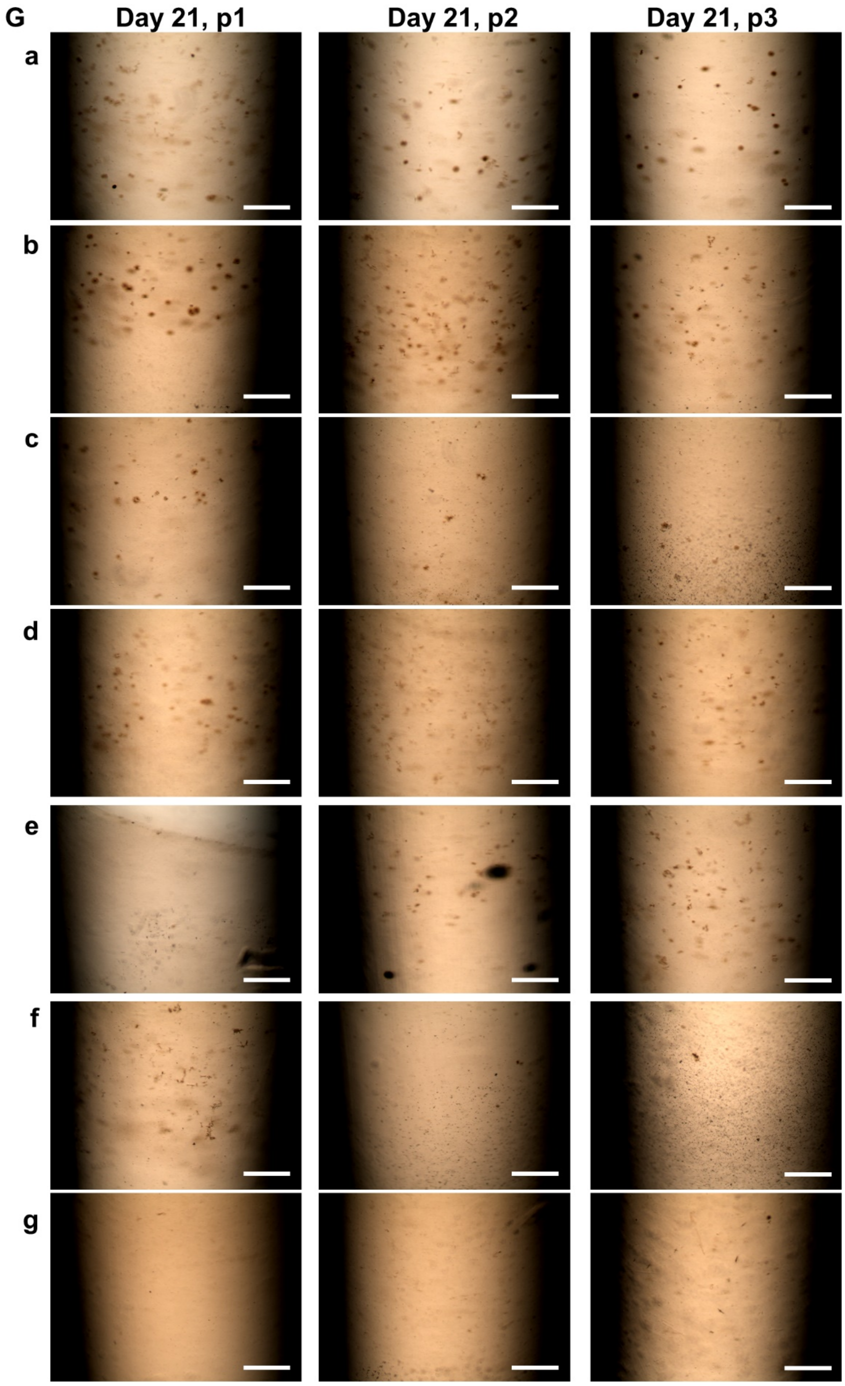

Fig. A2. Paclitaxel crystals in alginate hydrogels. Hydrogels (a) Alg, (b) Alg/POA (1:1 (w/w)), (c) Alg + β-CyD (0.9 mM β-CyD), (d) Alg/POAβCyD (1:1 (w/w), 0.8 mM β-CyD), (e)

Alg/POA (1:3 (w/w)), (f) Alg + HPβ-CyD (7.2 mM HPβ-CyD), and (g) Alg/POAβCyD (1:3 (w/w), 1.1 mM β-CyD). Gels shown at (A) day 0 (one day after gelation), (B) day 1, (C) day 3, (D) day 6, (E) day 9, (F) day 15, and (G) day 21. Three parallels: p1-3. Scale bar 500 µm.

A 2-column fitting image

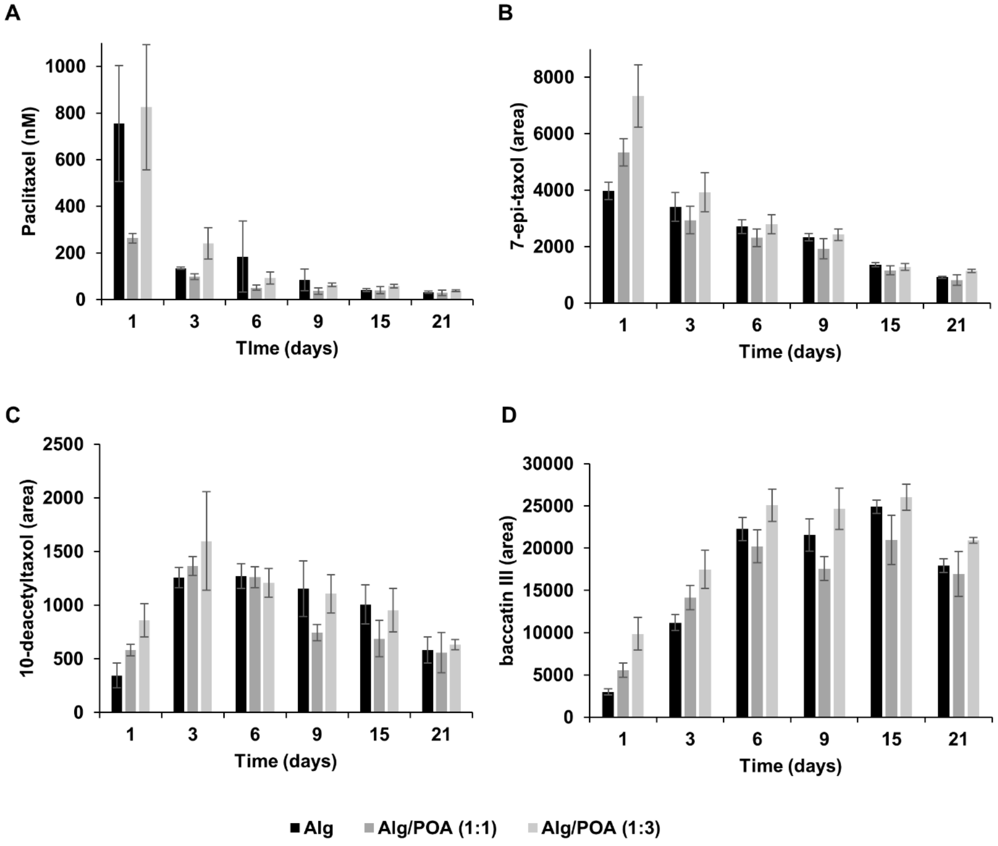

Fig. A3. Paclitaxel release from 1% (w/v) Ca-alginate hydrogels into physiological buffer at 37°C for 21 days. (A) Concentration of paclitaxel in release medium. (B-C) Integrals of the paclitaxel degradation products found in release medium: (B) 7-epi-taxol, (C) 10-deacetylytaxol, and (D) baccatin III. Mean ± SD, n=3. Alg/POA (1:3) showed high paclitaxel concentration at day 1, while another POA control sample Alg/POA (1:1) did not. The mechanism behind these effects cannot be explained by the current set of data, but we could speculate that crystallization of the drug occurs differently in Alg, Alg/POA (1:1) and

Alg/POA (1:3) gels leading to the differences seen at day 1. When looking at the light microscopy pictures taken after the gels were set there appears to be more crystals present in the Alg/POA (1:1) gels compared to the Alg/POA (1:3) gels (S2 Fig). A possible explanation could be that more paclitaxel crystals initially formed in the 1:1 mixed gels compared to the 1:3 hydrogels, and due to this less paclitaxel was initially released. This indicated that the release is not only affected by cyclodextrins, but also by the initial amount of paclitaxel crystals formed when the gels are set. Furthermore, if this is true then the solubility of the paclitaxel in the alginate hydrogels cannot be solely controlled by addition of cyclodextrins, but may be influenced by factors such as mixing, viscosity and gelation. However, it is not possible to form a conclusion on this without more extensive testing.

A 2-column fitting image

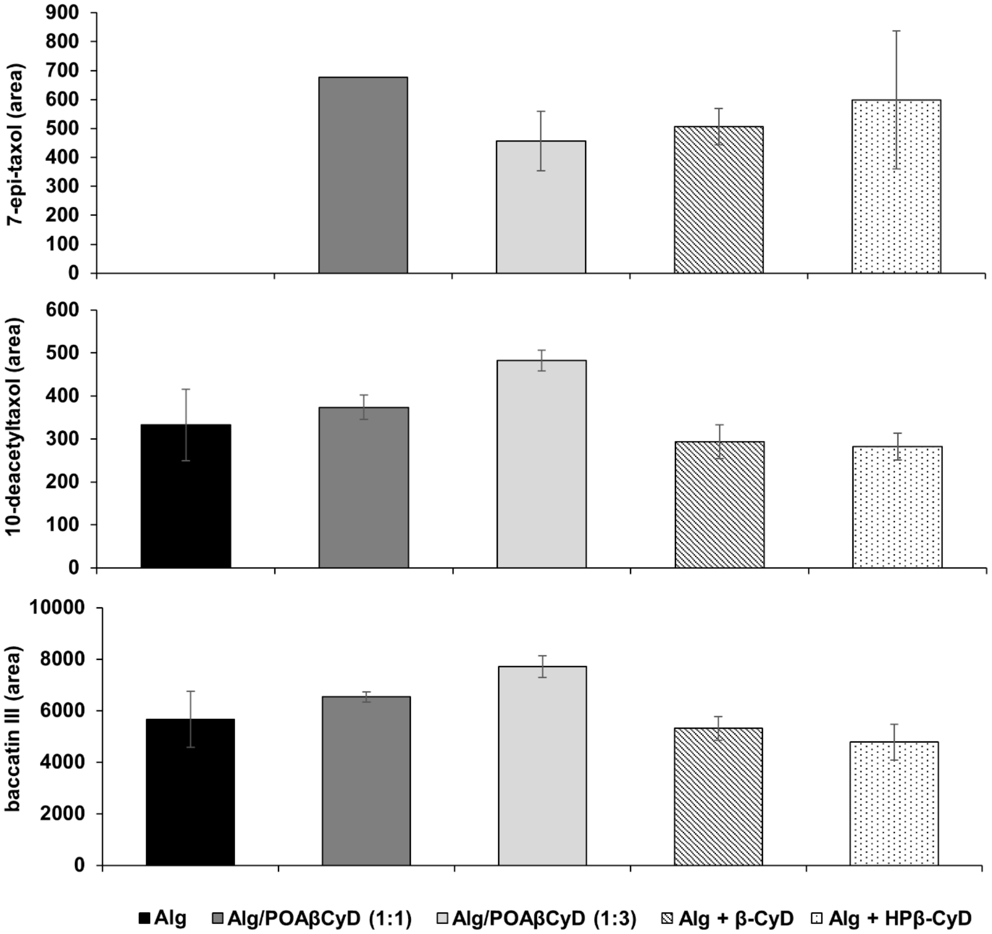

Fig. A4. Degradation products of paclitaxel found in the hydrogels at day 21 of the release study into physiological buffer at 37°C. Integrals of 7-epi-taxol, 10-deacetylytaxol, and baccatin III. Mean ± SD, n=3.

A single column fitting image

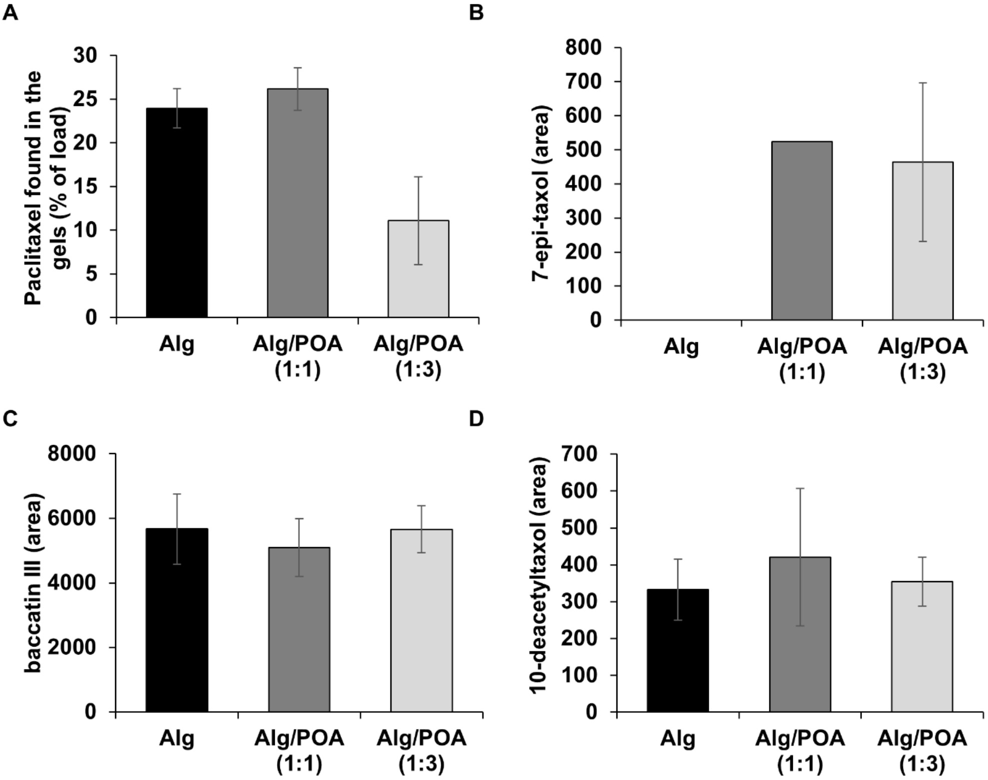

Fig. A5. Paclitaxel and paclitaxel degradation products remaining in the 1% (w/v) Ca-alginate hydrogels gels at day 21 of the release into physiological buffer at 37°C. The percentage of paclitaxel found in dissolved gels with regards to the amount of the paclitaxel loaded into the hydrogels.

A 2-column fitting image

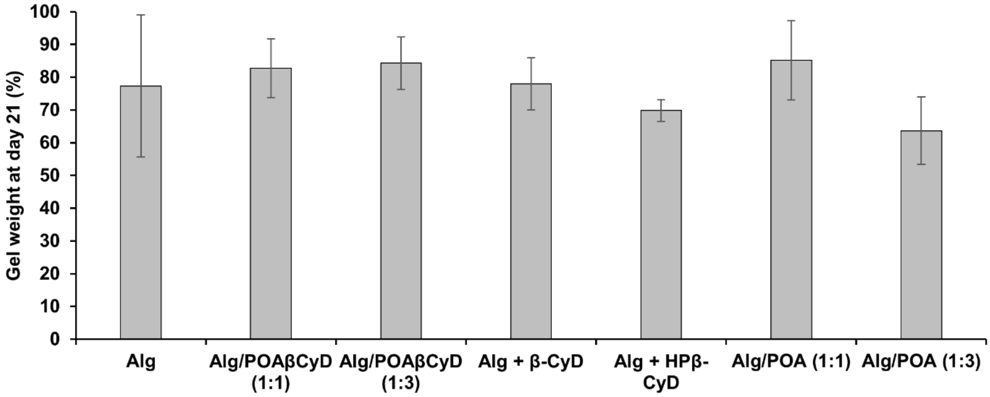

Fig. A6. Weigh of the hydrogels at day 21 of the release study in physiological buffer at 37°C. Initial weight of the gels was approximately 200 mg. Mean ± SD, n=3.

A 2-column fitting image

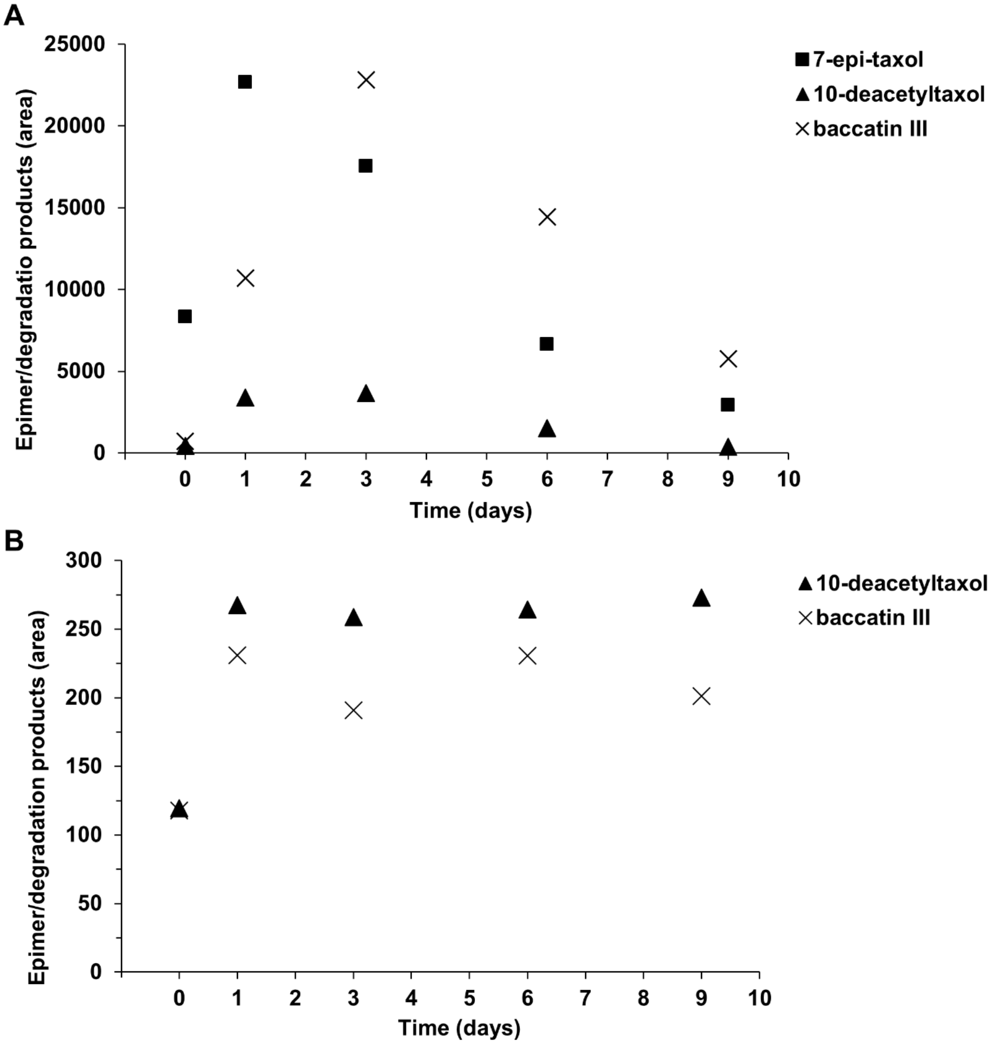

Fig. A7. Degradation products of paclitaxel in physiological buffer (A) and water (B).

Integrals of baccatin III, 10-deacetylytaxol, and 7-epi-taxol. Mean ± SD, n=3.

single column fitting image

A

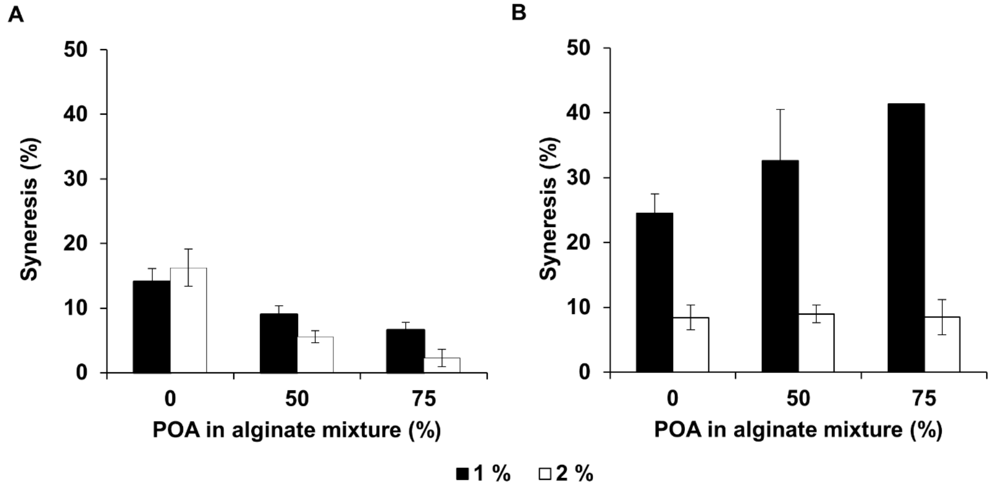

Fig. A8. Syneresis of the hydrogels. (A) Syneresis measured 24 hours after gel formation. (B) Syneresis measured 24 hours after gel formation followed by 72 hours incubation in 4.5 ml of DMEM at RT. Gels were casted from solutions of 1% (w/v) alginate, 15 mM $CaCO_3$ and 30 mM GDL and of 2% (w/v) alginate, 30 mM $CaCO_3$ and 60 mM GDL. Mean ± SD (n=4). POA = periodate oxidized alginate (Po=0.08). $CaCO_3$ particles size 4 µm.

A 2-column fitting image

Paper IV

Manuscript in preparation

ISBN 978-82-326-5704-9 (printed ver.)
ISBN 978-82-326-5681-3 (electronic ver.)
ISSN 1503-8181 (printed ver.)
ISSN 2703-8084 (online ver.)

NTNU
Norwegian University of
Science and Technology